

# **Tumour-Endothelial Interactions in Metastasis**

Aarren J. Mannion

Submitted in accordance with the requirements for the degree of  
Doctor of Philosophy

The University of Leeds  
Faculty of Medicine and Health  
School of Medicine

December 2018

The candidate confirms that the work submitted is his/her own and that appropriate credit has been given where reference has been made to the work of others. This copy has been supplied on the understanding that it is copyright material and that no quotation from the thesis may be published without proper acknowledgement.

The right of Aarren J. Mannion to be identified as Author of this work has been asserted by him in accordance with the Copyright, Designs and Patents Act 1988.

© 2018 The University of Leeds and Aarren J. Mannion

## Acknowledgments

Firstly, I would like to thank my supervisors Graham Cook and Pam Jones for their continued support and open-mindedness throughout my PhD and for allowing me to pursue my own scientific interests (despite contributions to Dr. Penny Inajar). I would also like to thank my co-supervisor Adam Odell for his extensive knowledge, guidance and companionship in the laboratory. Adam's unparalleled enthusiasm for lab work and scientific discussion was very inspiring throughout my PhD. I am also indebted to a number of collaborators who contributed in both practical and supportive capacities during this project. In this regard, I would like to thank Alison Taylor, who without which, none of the *in vivo* aspect of this project would have materialised. I am also most grateful to Andy Benest from the University of Nottingham, for his advice and guidance. I would like to thank the members past and present of the Cook group and level 5 at St James' for their support both in and out of the laboratory. In particular, I would like to thank Sarah Phillips for her light-hearted, unwavering criticism and ridicule throughout my PhD. My housemates and colleagues, Abigail Bloy, Rebecca Astley and Lewis Hammond are entirely responsible for keeping me from staying at work until the early hours and I am most grateful for this and their friendship. This project would not have been possible without the continued support of my family and friends who were always keen to show an interest in what I was doing. Finally, I would like to thank Rachel for her love and support over the last 3 years and for putting up with countless weekend and evening trips to the lab.

## Abstract

Metastatic progression of cancer occurs in a vast number of patients and accounts for 90% of cancer related deaths. Understanding metastasis therefore remains a priority for cancer research and treatment. Tumour cells need to bind to and cross endothelial cell barriers during metastasis. The aim of this work was to investigate tumour-endothelial interactions *in vitro* and *in vivo* and understand their implications on metastatic progression. The type I transmembrane receptor CD99 is expressed by leucocytes and endothelial cells (EC) and participates in inflammatory transendothelial migration (TEM). CD99 is also expressed by tumour cells and we have analysed the role of CD99 in tumour progression and cancer cell TEM. In a xenograft model, CD99 negatively regulated metastatic progression of human breast cancer. *In vitro*, tumour cell CD99 was required for adhesion to EC. However, CD99 negatively regulated post-adhesion events of tumour TEM, namely invasiveness of the endothelial barrier by metastatic cancer cells and TEM itself. Furthermore, tumour cell CD99 depletion was associated with cytoskeletal remodelling. For EC, loss of CD99 enhanced endothelial barrier function and reduced tumour cell TEM. The loss of CD99 enhanced expression and activity of the Rho GTPase Cdc42, a known cytoskeletal organiser. As a signal transduction hub, Cdc42 activity impacts upon many of the hallmarks of cancer. The functional link between CD99 and Cdc42 now implicates CD99 in these diverse functions. Further work in this thesis focussed on brain metastatic breast cancer cells. A major site for breast cancer metastasis is the brain where a specialised endothelial barrier, the blood brain barrier, operates. A surface screen of adhesion molecules revealed a role for CD146 in the adhesion and transmigration of breast cancer cells across the endothelium. Analysis of clinical data indicated that CD146 may of prognostic value in evaluating breast cancer metastasis. This work uncovers a potentially novel role for CD146 in breast cancer brain metastasis through mediating the interaction between cancer cells and the brain endothelium. The immortalised cell line hCMEC/D3 is a commonly used model of brain barrier endothelium. However, this cell line lacks key endothelial functions, for example being poorly responsive to VEGF signalling. It is shown here that p53 plays a key role in regulating the endothelial phenotype of this cell line and that stable p53 knockdown enhances the endothelial responses of this cell line thereby increasing the utility of this model system.

## Table of contents

<b>Acknowledgments</b> .....	<b>ii</b>
<b>Abstract</b> .....	<b>iii</b>
<b>Table of contents</b> .....	<b>iv</b>
<b>Figures</b> .....	<b>vii</b>
<b>Tables</b> .....	<b>viii</b>
<b>Abbreviations</b> .....	<b>ix</b>
<b>Chapter 1 Introduction</b> .....	<b>1</b>
<b>1.1 Health care burden of cancer metastasis</b> .....	<b>1</b>
<b>1.2 The metastatic cascade</b> .....	<b>1</b>
<b>1.2.1 Initiation of metastasis</b> .....	<b>3</b>
1.2.1a Epithelial to mesenchymal transition .....	3
1.2.1b The microenvironment and metastasis.....	3
<b>1.2.2 Intravasation</b> .....	<b>5</b>
<b>1.2.3 Adhesion of circulating cancer cells</b> .....	<b>6</b>
1.2.3a Receptors in cancer cell adhesion .....	8
<b>1.2.4 Endothelial cell-cell junctions</b> .....	<b>10</b>
<b>1.2.5 Extravasation and transendothelial migration</b> .....	<b>14</b>
<b>1.3 Ras and Rho family GTPases</b> .....	<b>17</b>
<b>1.3.1 GTPases in TEM</b> .....	<b>19</b>
<b>1.4 Colonisation</b> .....	<b>20</b>
<b>1.4.1 Organ-specific metastasis</b> .....	<b>20</b>
<b>1.4.2 Breast cancer brain metastasis</b> .....	<b>21</b>
<b>1.5 The blood brain barrier</b> .....	<b>23</b>
<b>1.5.1 The organotypic nature of endothelial cells in the BBB</b> .....	<b>27</b>
<b>1.6 VEGF signalling in endothelial cells</b> .....	<b>27</b>
1.6.1 Vascular development.....	27
1.6.2 VEGF family .....	28
1.6.3 VEGF receptors.....	29
1.6.4 Coreceptors of VEGFR .....	31
1.6.5 Angiogenesis in cancer .....	32
<b>1.7 p53 tumour suppressor</b> .....	<b>32</b>
<b>1.7.1 Endothelial p53</b> .....	<b>35</b>
<b>1.8 Aims</b> .....	<b>37</b>
<b>Chapter 2 Materials and Methods</b> .....	<b>39</b>
<b>2.1 Cell lines</b> .....	<b>39</b>
<b>2.1.1 Cell culture</b> .....	<b>39</b>
<b>2.1.2 Freezing and thawing cells</b> .....	<b>40</b>

2.1.3 Cell counting .....	41
2.1.4 Cell tracker green (CTG) labelling of cells .....	41
2.1.5 Adhesion assay .....	41
2.1.6 Transendothelial migration assay .....	42
2.1.7 Live cell imaging of intercalation .....	42
2.1.8 Flow cytometry .....	42
2.2 Cell lysate preparation for SDS-PAGE .....	44
2.2.1 SDS-PAGE and Western Blotting.....	44
2.2.2 Immunofluorescent confocal microscopy .....	48
2.2.3 siRNA transfection .....	50
2.2.4 Kaplan-Meier survival curves .....	50
2.2.5 Tubulogenesis assay.....	52
2.2.6 Lentiviral transduction .....	52
2.2.7 Matrigel cord formation assay.....	52
2.2.8 Electrical cell substrate impedance sensing (ECIS) barrier integrity measurement .....	53
2.2.9 RT-PCR .....	53
2.3 Cell viability assay .....	54
2.3.1 Real Time Cell Analyser (RTCA) XCELLigence .....	55
2.3.2 Scratch/Wound migration assay.....	56
2.3.3 Proliferation assay – crystal violet .....	56
2.3.4 ECM adhesion assay and immunofluorescence.....	57
2.3.5 <i>In vivo</i> experimental metastasis .....	57
2.3.6 GTP-Cdc42 immunoprecipitation.....	58
2.3.7 Statistical analysis .....	59
<b><i>Chapter 3 Investigating cancer-endothelial cell interactions using a breast cancer metastasis model.....</i></b>	<b>60</b>
3.1 Introduction.....	60
3.2 Cancer cells preferentially adhere to HUVEC cells over hCMEC.....	62
3.3 BrM shows reduced capacity to traverse endothelial barriers compared to MDA-231 cells.....	64
3.4 BrM express high levels of CD146.....	68
3.5 CD146 depletion increases adhesion and TEM of BrM .....	72
3.6 High CD146 expression negatively correlates with recurrence and metastasis free survival of ER and PR negative breast cancers .....	77
3.7 Discussion .....	82
<b><i>Chapter 4 Regulation of the endothelial cell phenotype by p53.....</i></b>	<b>89</b>
4.1 Introduction.....	89

4.2 The expression of EC surface markers by the hCMEC cell line .....	91
4.3 hCMEC express reduced VEGFR2 and exhibit greatly reduced angiogenic potential .....	93
4.5 VEGFR2 suppression in hCMEC cells is p53-dependent .....	100
4.6 CD34 expression .....	106
4.7 VEGFR2 upregulation increases hCMEC angiogenic potential .....	108
4.8 p53 depletion in hCMEC induces a more representative BBB phenotype.....	110
4.9 p53 depletion may not confer greater barrier properties to hCMEC .....	112
4.10 p53 depletion does not alter key BBB endothelial transcription factors.....	114
4.11 VEGFR2 depletion reverses the endothelial phenotype of hCMEC shp53 .....	116
4.12 Functional assessment of hCMEC shp53 line in cancer cell adhesion/TEM .....	118
4.13 Discussion .....	120
<b><i>Chapter 5 CD99 promotes adhesion and transendothelial migration of cancer cells through Cdc42 .....</i></b>	<b>128</b>
5.1 Introduction.....	128
5.2 CD99 expression correlates with increased breast cancer metastasis and is broadly expressed by breast cancer cell lines.....	130
5.4 CD99 suppresses transendothelial migration of metastatic cancer cells.....	137
5.5 CD99 regulates chemotactic migration and spreading of breast cancer <i>in vitro</i> ..	140
5.6 CD99 regulates actin dynamics upon adhesion to ECM substrates.....	144
5.7 CD99 suppresses metastatic dissemination of breast cancer <i>in vivo</i> .....	148
5.8 Endothelial CD99 regulates cancer cell transendothelial migration.....	150
5.9 CD99 modulates Cdc42 activity and expression .....	153
5.10 Endothelial CD99 regulates <i>in vitro</i> angiogenesis.....	156
5.11 Discussion .....	159
<b><i>Summary and Discussion .....</i></b>	<b>167</b>
<b><i>References .....</i></b>	<b>173</b>
<b><i>Appendix .....</i></b>	<b>200</b>

## Figures

Fig 1.1. The Metastatic Cascade. ....	2
Fig 1.2 Cancer cell adhesion and transendothelial migration.....	7
Fig 1.3 Endothelial cell-cell junctions.....	12
Fig 1.4 The blood brain barrier (BBB).....	26
Figure 1.5. p53 signaling .....	34
Fig. 3.1. MDA-BrM show similar adhesion profile to MDA-MB-231 .....	63
Fig. 3.2. BrM line show reduced capacity to transmigrate across HUVEC and hCMEC monolayers compared to MDA-231 .....	<b>Error! Bookmark not defined.</b>
Fig. 3.3. BrM show reduced capacity to intercalate into HUVEC monolayers compared to MDA-231 .....	67
Fig. 3.4. BrM express high levels of surface CD146 compared to MDA-231.....	70
Fig. 3.5. BrM express high levels of CD146 compared to MDA-231 .....	71
Fig. 3.6. CD146 siRNA depletion in MDA-231 and BrM .....	74
Fig. 3.7. CD146 depletion increases MDA-231 and BrM adhesion but not intercalation.....	<b>Error! Bookmark not defined.</b>
Fig. 3.8. CD146 depletion increases BrM migration and transendothelial migration .....	<b>Error! Bookmark not defined.</b>
Fig. 3.9. High CD146 expression in patient breast cancer correlates with poor survival and probability of metastasis .....	81
Fig. 4.1. hCMEC express a number of endothelial cell surface markers .....	92
Fig. 4.2. hCMEC lack VEGFR2 expression .....	96
Fig. 4.3. hCMEC exhibit poor angiogenic function .....	97
Fig. 4.4. hCMEC express high levels of inactive p53 and SV40 LTag .....	99
Fig. 4.5. siRNA knockdown of p53 in hCMEC induces CD31 expression .....	100
Fig. 4.6. Generation of stable p53 shRNA knockdown hCMEC .....	102
Fig. 4.7. p53 knockdown normalises expression of endothelial markers .....	103
Fig. 4.8. p53 knockdown induces expression of endothelial markers .....	104
Fig. 4.9. p53 knockdown restores VEGFR2 expression and function in hCMEC.....	105
Fig. 4.10. P53 depletion reduces CD34 expression in hCMEC.....	107
Fig. 4.11. p53 knockdown normalises hCMEC angiogenic potential in cord formation assays.....	<b>Error! Bookmark not defined.</b>
Fig. 4.12. shp53 hCMEC exhibit increased expression of tight junctional marker claudin 5 .....	111
Fig. 4.13. p53 knockdown does not alter hCMEC barrier function .....	113

Fig. 4.14. P53 depletion does not alter expression of key BBB transcription factors .....	115
Fig. 4.15. shp53 VEGFR2 depletion reduces expression of VE-Cadherin and PECAM1 .....	117
Fig. 4.16. P53 depletion in hCMEC reduces cancer cell adhesion but does not affect intercalation.....	119
Fig. 5.1. CD99 expression correlates with increased metastasis and is expressed broadly by breast cancer cell lines.....	132
Fig. 5.2. CD99 regulates breast cancer adhesion to endothelial cells.....	134
Fig. 5.3. CD99 regulates breast cancer adhesion to endothelial cells.....	136
Fig. 5.4. CD99 suppresses transendothelial migration of metastatic cancer cells.	138
Fig. 5.5. Depletion of MDA-231 CD99 enhances disruption of endothelial monolayers .....	<b>Error! Bookmark not defined.</b>
Fig. 5.6. CD99 regulates chemotactic migration and spreading of breast cancer in vitro.....	142
Fig. 5.7. Proliferation of MDA-231 is not perturbed by CD99 depletion .....	143
Fig. 5.8. Actin reorganisation upon adhesion to ECM substrates is regulated by CD99 .....	146
Fig. 5.9. CD99 suppresses spreading of PC3 metastatic prostate cancer cells.....	147
Fig. 5.10. CD99 suppresses metastatic dissemination of breast cancer in vivo .....	149
Fig. 5.11. Endothelial CD99 regulates cancer cell transendothelial migration .....	151
Fig. 5.12. Depletion of HUVEC CD99 increases endothelial barrier integrity.....	<b>Error! Bookmark not defined.</b>
Fig. 5.13. CD99 modulates Cdc42 activity and expression.....	155
Fig. 5.14. Endothelial CD99 regulates in vitro angiogenesis .....	157

## Tables

Table 1. Flow cytometry antibodies.....	43
Table 2. Western blotting antibodies .....	46
Table 3. Immunofluorescent antibodies .....	49
Table 4. siRNA sequences and product details .....	51
Table 5. Taqman qPCR gene expression probes .....	54
Table 6. Cycling protocol used for Taqman gene expression qPCR .....	54

## Abbreviations

°C	Degrees Celsius
ADAM12	Disintegrin and metalloproteinase domain-containing protein 12
AF	Alexa fluora
AJ	Adherens junction
AKT	Protein kinase B
ANG1	Angiopoietin 1
ANGPTL4	Angiopoietin-like 4
APC	Allophycocyanin
APP	Amyloid precursor protein
APS	Ammonium persulfate
ARP	Actin related protein
ATM	Ataxia-telangiectasia mutated
ATR	Ataxia-telangiectasia-related
BBB	Blood brain barrier
BCBM	breast cancer brain metastasis
bFGF	Basic fibroblastic growth factor
cANGPTL4	C-terminal fibrinogen-like domain of angiopoietin-like 4
CAR	Coxsackievirus and adenovirus receptor
CCL2	C-C Motif Chemokine Ligand 2
CCR2	C-C Motif Chemokine Receptor 2
Cdc42	Cell division control protein 42 homolog
cDNA	Complementary DNA
ChIP	Chromatin immunoprecipitation
Chk1/2	Checkpoint kinase 1/2
CIM-plate	Cell invasion and migration plate
CNS	Central nervous system
COX2	Cyclooxygenase-2
CSCs	Cancer stem cells
CTG	Cell tracker green
Da	Dalton
DC	Dendritic cell
DDR	DNA damage response
DEPC	Diethylpyrocarbonate
DMEM	Dulbecco's modified essential media
DMFS	Distance metastatic free survival

DMSO	Dimethyl sulfoxide
DR6	Death receptor 6
E-cadherin	Epithelial cadherin
E-selectin	Endothelial selectin
E2F	E2 factor
EAAT	Excitatory amino acid transporters
EC	Endothelial cell
ECACC	The European Collection of Authenticated Cell Culture
ECBM	Endothelial cell basal medium
ECIS	Electrical cell substrate impedance sensing
ECIS	Electrical cell substrate impedance sensing
ECL	Enhanced chemiluminescence
ECM	Extracellular matrix
ECs	Endothelial cells
EGFR	Epidermal growth factor receptor
EMT	Epithelial to mesenchymal transition
EndoMT	Endothelial mesenchymal transition
EPCAM	Epithelial cell adhesion molecule
ER	Eostrogen receptor
ERK	Extracellular-signal-regulated kinase
ERM	Ezrin-radixin-moesin
F-actin	Filamentous actin
FACs	Fluorescence-activated cell sorting
FAK	Focal adhesion kinase
FCS	Foetal calf serum
FITC	Fluorescein isothiocyanate
g	Gram
GAPDH	Glyceraldehyde 3-phosphate dehydrogenase
GAPs	GTPase activating proteins
GBD	GTPase binding domain
GDP	Guanosine diphosphate
GEFs	Guanine nucleotide exchange factors
GLUT1	Glucose transporter 1
GTP	Guanosine triphosphate
HBD	Heparin binding domain
HBMEC	Human brain microvascular endothelial cells
hCMEC/D3	Human cerebral microvascular endothelial cells D3

HEK293	Human embryonic kidney cells 293
HER2	Human epidermal growth factor receptor 2
HIF	Hypoxia inducible factor
HRE	Hypoxia response element
HRP	Horse radish peroxidase
HSF1	Heat shock factor 1
hTERT	Telomerase reverse transcriptase
HUVEC	Human umbilical vascular endothelial cells
ICAM1	Intercellular Adhesion Molecule 1
IFN $\gamma$	Interferon gamma
IHC	Immunohistochemistry
IP	Immunoprecipitation
JAK-STAT	Janus kinase-signal transducers and activators of transcription
JAM	Junctional adhesion molecule
KDa	Kilo Dalton
Kg	Kilogram
L	Litre
L-selectin	Leukocyte selectin
L1CAM	L1 cell adhesion molecule
LAT1	L-system for large neutral amino acids
M	Molar
MAPK	Mitogen-activated protein kinases
MCAM/CD146	Melanoma Cell Adhesion Molecule
MCF7	Michigan Cancer Foundation-7 cell line
MDM2	Mouse double minute 2 homolog
MET	Mesenchymal to epithelial transition
MFI	Median fluorescent intensity
mg	Milligram
MIC	Metastasis initiating cell
ml	Millilitre
MLC	Myosin light chain
mM	Millimolar
MMP	Matrix metalloproteinase
MRI	Magnetic resonance imaging
MT1-MMP	Membrane-type-1 matrix metalloproteinase
MUC1	Mucin 1
N-cadherin	Neural cadherin

ng	Nanogram
NHS	National health service
NRP	Neuropilin
ns	Non-significant
P-selectin	Platelet selectin
PAK1	P21 activated kinase
PBD	p21 binding domain
PBS	Phosphate buffered saline
PE	Phycoerythrin
PECAM1	Platelet and Endothelial Cell Adhesion Molecule 1
PFA	Paraformaldehyde
pg	Picogram
PI3K	Phosphatidylinositol 3-kinase
PKA	Protein kinase C
PKC	Protein kinase C
PLC $\gamma$	Phospholipase C $\gamma$
PIGF	Placental derived growth factor
PR	Progesterone receptor
PTEN	Phosphatase and tensin homolog
qPCR	Quantitative polymerase chain reaction
qRT-PCR	Quantitative real-time polymerase chain reaction
Rac1	Ras-related C3 botulinum toxin substrate 1
Rb	Retinoblastoma protein
RFS	Recurrence free survival
RNA-seq	RNA sequencing
ROCK	Rho-associated protein kinase
ROS	Reactive oxygen species
RPMI	Roswell Park Memorial Institute
RT	Room temperature
RTCA	Real time cell analyser
RTK	Receptor tyrosine kinases
SCID	Severe combined immune deficiency
Scr	Scrambled
SDS	Sodium dodecyl sulfate
Sema3E	Semaphorin 3a
SFM	Serum free media
shRNA	Short hairpin RNA

siRNA	Short interfering RNA
SLC7A1	Solute Carrier Family 7 Member 1
sLe <sup>a</sup>	Sialyl Lewis a
sLe <sup>x</sup>	Sialyl Lewis x
SV40 Tag	Simian virus 40 Large T antigen
sVEGFR1	Soluable VEGFR
TEER	Transepithelial/transendothelial electrical resistance
TEM	Transendothelial migration
TGFβ	Transforming growth factor beta
TH17	T-helper cell 17
TJ	Tight junction
TNBC	Triple negative breast cancer
TNF-α	Tumour necrosis factor alpha
UV	Ultra violet
v/v	Volume per volume
VCA	(Verprolin, cofilin, acidic) domain
VCAM1	Vascular cell adhesion molecule 1
VE-cadherin	Vascular endothelial cadherin
VEGF	Vascular endothelial growth factor
VEGFR	Vascular endothelial growth factor receptor
VLA-4	Very Late Antigen-4
w/v	Weight per volume
WASP	Wiskott–Aldrich Syndrome protein
WAVE	WASP-family verprolin-homologous protein
ZO	Zonula Occludens
μg	Microgram
μl	Microliter
μm	Micrometre
μM	Micromolar

## **Chapter 1 Introduction**

### **1.1 Health care burden of cancer metastasis**

Despite advances in treatment over the last 50 years, cancer remains a highly prevalent disease globally and a major healthcare challenge. In the UK, over a quarter of deaths are caused by cancer (Cancer Research UK 2016a). Primary tumours are not usually the main cause of mortality, whereas metastases (the spreading of cancer from a primary site to other organs) are responsible for 90% of cancer related deaths (Lambert et al., 2017). Significantly, between 2010 and 2015, £5 billion was spent on the treatment and care of patients with cancer in the UK each year, with overall costs to society totalling over £18 billion per year (Department of Health and Social Care 2015). Cancer represents a substantial social and financial burden to both the National Health Service (NHS) and society.

In England, 131,936 patients were diagnosed with late stage cancers which represents 44% of newly diagnosed cases between 2013 and 2015 (Public Health England, 2014). These cases alone are estimated to cost >£700 million in treatment and care over the next 15 years, highlighting the burden of late stage cancers to the NHS (Macmillan Cancer Support 2016). It is these later stage cancers which are often metastatic, spreading from primary to secondary organs. Currently, treatment offered to patients with metastatic cancer is very limited, resulting in poor survival rates for these patients. This highlights the need for further research in this area.

### **1.2 The metastatic cascade**

Metastasis is one of the hallmarks of cancer (Hanahan and Weinberg 2011; Hanahan and Weinberg 2000). The process of cancer metastasis is thought to occur in a sequential manner, known as the 'metastatic cascade', and describes the initiation of cancer cell invasion, dissemination into local tissues and eventual breaching of the lymphatic and haematogenous vessels (Figure 1.1) (Strilic and Offermanns, 2017). Once in the circulation, cancer cells must survive anoikis (Frisch and Ruoslahti, 1997), exposure to shear flow (Weiss, 1992), and immune cell detection (Talmadge et al., 1980), before eventual adherence to the vascular wall, and movement into secondary tissues. Once a metastatic cell has established itself in a secondary organ, it will either experience a period of dormancy or alternatively, proliferate and develop into full-blown metastatic growth (Valastyan and Weinberg 2011; Sosa, Bragado and Aguirre-Ghiso 2014).

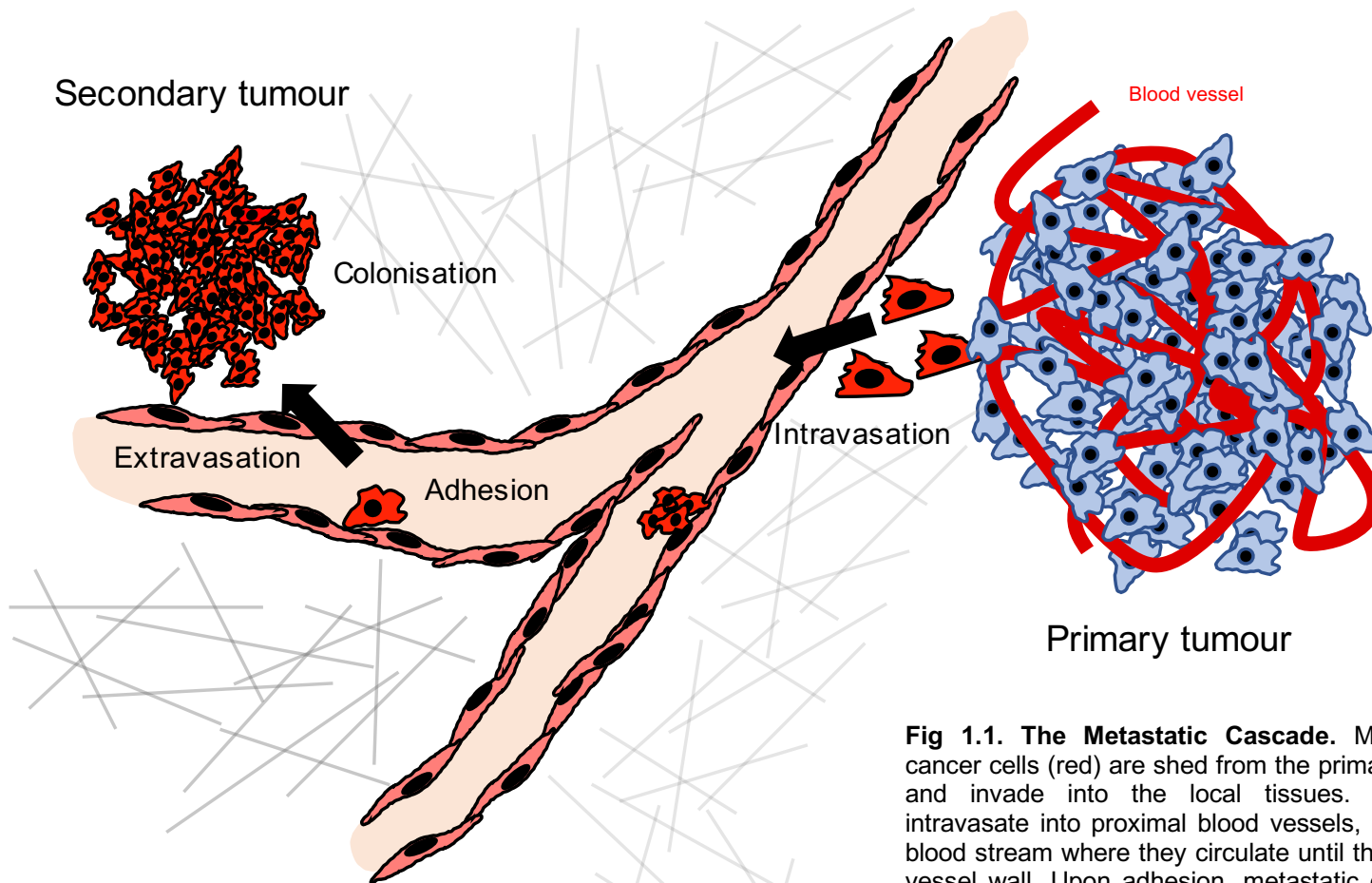


**Fig 1.1. The Metastatic Cascade.** Metastatic cancer cells (red) are shed from the primary tumour (blue) and invade into the local tissues. Metastatic cells intravasate into proximal blood vessels, crossing into the blood stream where they circulate until they adhere to the vessel wall. Upon adhesion, metastatic cells extravasate out of the circulation and colonise organ tissues forming secondary tumours.

## **1.2.1 Initiation of metastasis**

### *1.2.1a Epithelial to mesenchymal transition*

As tumours grow numerous cellular and tissue changes occur, resulting in the progression from benign growths to malignant metastatic tumours. A number of factors such as genetic instability, stromal cell interactions and microenvironmental cues can influence these changes (Chiang and Massagué, 2008). The initiation of metastasis is described by initial loss of cell-cell complexes and polarity which are characteristic of epithelial cells (Yilmaz and Christofori, 2009). The adaptation from an epithelial to mesenchymal cell state, commonly referred to as the epithelial to mesenchymal transition (EMT), has been extensively characterised (Kalluri and Weinberg, 2009). Acquisition of the mesenchymal phenotype requires extensive remodelling of the actin cytoskeleton and results in increased migratory potential (Mani et al., 2008). The EMT is part of the normal embryonic development programme. However, when this occurs unchecked in adults it can lead to the progression of cancers (Thiery, 2002). The junctional proteins, epithelial-cadherin (E-cadherin) and neural-cadherin (N-cadherin), are common markers of epithelial or mesenchymal cells. Their expression is often used as markers of EMT in cancer, where low expression of E-cadherin and high expression of N-cadherin is indicative of a mesenchymal phenotype (Thiery et al., 2009).

Additionally, several transcriptional regulators of EMT, including Twist, Slug, Snail, ZEB1 and ZEB2 have been found to downregulate the expression of E-cadherin, upregulate N-cadherin expression and drive the metastatic progression of tumours (Thiery et al., 2009). For example, overexpression of Twist was found to potentiate the metastatic spread of cancers through negative regulation of E-cadherin (Yang et al., 2004). However, the activation of EMT reprogramming is thought to occur on a spectrum rather than in definitive on/off states. It has been shown that reversal of EMT is important in the formation of metastatic sites in secondary organs (Ocaña et al., 2012; Tsai et al., 2012).

### *1.2.1b The microenvironment and metastasis*

The microenvironment plays a wide role in the establishment of metastatic disease. As tumour size increases, without sufficient blood supply, the ability for oxygen and other molecules to reach cancer cells become limited to their diffusion penetrance (~200 µm) (Wilson and Hay, 2011). Therefore, areas of the tumour lacking adequate blood supply become hypoxic, further driving the metastatic and invasive phenotype

of cancer cells. Normal tissue oxygen saturation is usually in the region of 38 mm Hg, which is equivalent to 5% oxygen (Bristow and Hill, 2008). However, oxygen saturation may differ in certain organs due to their functional and metabolic requirement (Stroka et al, 2001). For example, in the medulla of the kidney, oxygen levels fall below 4% in the normal physiological range (Epstein et al, 1994). Parts of the liver also experience a degree of hypoxia as the hepatovenous oxygen saturation is below 4%, whereas systemic arteriole oxygen levels are closer to 13% (Wolfe et al, 1983). Hypoxia is a result of the normal oxygen tension of a given tissue falling below its normal physiological range and is a common hallmark of solid tumour growth (Bristow and Hill, 2008).

At the cellular level, hypoxia results in the stabilisation of hypoxia inducible factor (HIF), a potent transcription factor which elicits the expression of many genes by the binding of hypoxia response elements (HREs) within their promoter regions (Wang et al, 1995). Normally, HIF1 $\alpha$  has a high rate of degradation, meaning HIF1 $\alpha$ /HIF1 $\beta$  dimers cannot form (Harris et al, 2002). Under hypoxic conditions, HIF1 $\alpha$  is stabilised, allowing the dimerisation of the HIF1 $\alpha$  and HIF1 $\beta$  subunits (Harris et al, 2002). The transcription factor Snail, which regulates EMT was shown to be upregulated by hypoxia as well as positively regulating matrix metalloproteinases (MMPs) in breast cancer (Lundgren et al, 2009; Ota et al, 2009). MMPs themselves can be upregulated by HIF and potentiate tissue invasion, blood vessel remodelling and metastasis (Harris, 2002).

MMPs are heavily implicated in cancer metastasis as they mediate several processes that promote the disease, such as angiogenesis, metastasis and invasion, inflammation, and turn-over of growth factors (Kessenbrock et al. 2010; Hanahan and Weinberg 2011). Degradation of the surrounding extracellular matrix through the expression of membrane bound MMPs, or release of tumour derived MMPs, aids in the proteolysis of extracellular matrix (ECM) during local invasion. For example, membrane type 1-MMP (MT1-MMP or MMP14) functions at the cell surface, near the leading edge of migrating cancer cells (Itoh 2006). This allows the cancer cells to degrade the surrounding ECM and carve out so-called 'microtracks', tubular excavations in the ECM, which provide a path of least resistance for the cell to migrate along (Friedl and Wolf 2008). Furthermore, the expression of MT1-MMP in breast cancer patients has also been shown to be associated with poor prognosis and higher rates of cancer invasion and metastasis (Shiomi and Okada, 2003).

Hypoxia and elevated tissue hydrostatic pressure within developing tumours results in the vasculature adopting an often immature, heterogenous, disorganised and tortuous phenotype (Carmeliet and Jain 2000). The leaky and incompetent state of the tumour vasculature is in part due to the irregular spatial and temporal expression of angiogenic cues during its formation, unlike the controlled environment of neovascularisation during embryogenesis (Jain, 2003). The state of tumour vasculature is important in the establishment of metastatic disease as migrating cancer cells are able to more easily traverse the loosely formed and poorly supported vasculature (often lacking pericytes) to gain entry to the circulation (Chang et al., 2000). It has also been suggested that the unorganised blood vessels and the turbulent shear flow associated with such a structure can contribute to cancer cells shearing off into the blood stream, highlighting a further mechanism of cancer cell dissemination (Chang et al., 2000).

### **1.2.2 Intravasation**

Once cancer cells have reached local blood vessels, they must penetrate the endothelium and its supporting cells in order to reach the lumen; a process known as intravasation. Intravasation remains an understudied aspect of the metastatic cascade, due to difficulties in modelling this aspect of local invasion. In patients, this process occurs early on, often before detection of the primary tumour has occurred, making intravasation a very difficult aspect of tumour progression to both target and study *in vitro* and *in vivo*. However recent developments using intravital microscopy have begun to shed light on the mechanisms of intravasation (Harper et al., 2016).

Studies have indicated that intravasation and metastasis of cancer cells occur very early on in the establishment of primary disease. Hosseini et al. (2016) found that up to 80% of metastases arise from early disseminated cancer cells. It was shown that human epidermal growth receptor 2 positive (HER2+) breast cancer cells with high expression of Twist and low expression of E-cadherin, disseminated very early on, before primary tumours were even detectable masses (Hosseini et al., 2016). These disseminated cells underwent a period of dormancy (up to 12 weeks) and eventually led to metastatic growth (Harper et al., 2016). This study also showed that early disseminated cells were far more successful in generating metastatic outgrowths compared to their later disseminating counterparts (Harper et al., 2016)

At the initial stages of intravasation, cancer cells invade locally into the immediate microenvironment. Often termed metastatic initiating cells (MICs), these cells have undergone EMT, engaging the phenotypic switch from static epithelial-like cells to the migratory and invasive mesenchymal state. MICs will invade either as single (amoeboid) cells, or as a collective mass of cells (Madsen and Sahai, 2010). Many different factors are involved in this process of local invasion and eventual intravasation into the vasculature. Members of the Notch family of transmembrane proteins are critical regulators of this process, where endothelial Notch1 expression was recently found to be modulated by cancer cells (Sheldon et al., 2010; Wieland et al., 2017). Notch1 upregulation on endothelial cells is known to increase vascular cell adhesion molecule 1 (VCAM1) expression, a crucial regulator of endothelial cell-cell junctions during leukocyte transmigration (van Wetering et al., 2003). Similarly, during the intravasation step of metastasis, cancer cells co-opt Notch1 activity and VCAM1 expression to gain entry into the vasculature (Wieland et al., 2017).

### **1.2.3 Adhesion of circulating cancer cells**

Adhesion and subsequent extravasation require close interactions between the cancer cell and the endothelial cells, with active contribution from both cell types to facilitate transendothelial migration (TEM) (Reymond, d'Água and Ridley 2013). Extravasation and TEM refer to the movement of cells through an endothelial barrier to exit the blood stream and enter a tissue. Metastatic cells which intravasate into the circulation must adhere to the endothelium in order to extravasate and colonise secondary tissues. As with leukocytes, cancer cells have been observed undergoing rolling, tethering, firm adhesion and transmigration *in vitro* (Figure 1.2)(Ley et al., 2007). However, tethering and rolling of cancer cells have rarely been observed *in vivo* (Reymond, d'Água and Ridley 2013), although intraluminal crawling of cancer cells prior to extravasation from the vasculature has been shown in a zebrafish model of adhesion and extravasation (Follain et al., 2018).

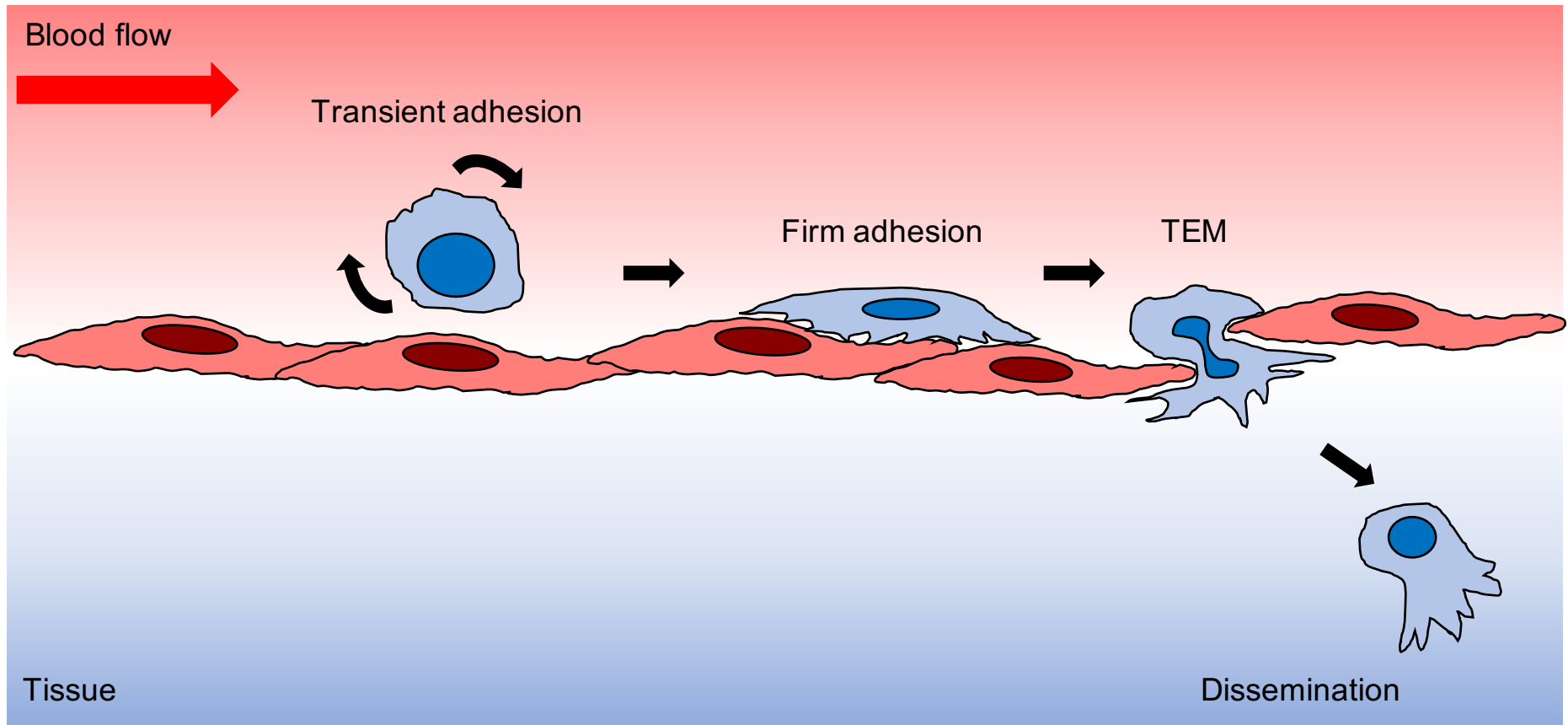


**Fig 1.2 Cancer cell adhesion and transendothelial migration.** Once in the vasculature, cancer cells circulate until they adhere to the vascular wall. Initial transient adhesion reduces the velocity of the circulating cancer cells and engagement of multiple adhesion molecules eventually leads to the firm adhesion of the cancer cell to the endothelial monolayer. Cancer cells extravasate out of the blood flow by transendothelial migration (TEM) and disseminate into the surrounding parenchyma.

Historically it was thought that the adhesion and extravasation of circulating cancer cells was determined by the diameter of the vasculature, particularly capillaries. Although the effect of vessel size cannot be completely disregarded, evidence suggests that other factors such as adhesion receptors and other cellular constituents such as platelets and monocytes are more important. The surgical redirection of ascitic fluid in patients with metastatic ovarian cancer (for reasons of palliative care), resulted in the introduction of large numbers of metastatic cells into the venous circulation (Tarin et al., 1984). However, in the majority of these patients, overt metastatic growth was not observed, despite this large influx of metastatic cells (Tarin et al., 1984). The metastatic cells in the study would have encountered numerous size-restricted capillaries and despite this, metastasis was not evident (i.e. in the lungs). Furthermore, recent studies by Follain et al. (2018) have shown that size restriction of blood vessels was not a key determinant in cancer cell adhesion.

#### *1.2.3a Receptors in cancer cell adhesion*

A broad repertoire of adhesion molecules has been shown to mediate the adhesion of cancer cells to the endothelium. Selectins play a pivotal role in tethering and rolling of leukocytes to the endothelium in the initial stages of adhesion (Ley et al., 2007). Endothelial-selectin (E-selectin) binds to ligands present on the leukocytes, and these interactions have been shown to slow the leukocyte, and prolong the exposure of other receptors to the endothelial cell surface, leading to the activation of further adhesion molecules which are required for firm adhesion (Ley et al., 2007). The action of E-selectin has been shown at lower velocities (Kunkel and Ley, 1996), whereas leukocyte-selectin (L-selectin) and platelet-selectin (P-selectin) are functional at higher velocities and require shear flow to facilitate leukocyte rolling on the endothelium (Finger et al., 1996; Lawrence et al., 1997). Cancer cells often overexpress modulated selectin ligands such as sLe<sup>a</sup> and sLe<sup>x</sup> which regulate adhesion to the endothelium (St Hill, 2011). These have been shown to bind to P-, E- and L- selectins, indicating that selectins play a key role in the establishment of metastasis through adhesion (Kim et al. 1998). Additionally, platelet-selectin (P-selectin) and E-selectin expression can also be upregulated by inflammatory cytokines such as TNF- $\alpha$  and IFN- $\gamma$  to facilitate the adhesion of circulating cancer cells (Zen et al., 2008).

*In vivo* knock out models of E- and P- selectin highlighted the dependency of cancer-endothelial interactions on host selectin expression as metastasis was greatly attenuated in these models (Köhler et al. 2010; Kim et al. 1998). L-selectin has been

implicated in the recruitment of leukocytes to metastatic micro-emboli which form within the lumen of vessels. The presence of monocytes in the embolus aids in extravasation of metastatic cells. Similarly, P-selectin potentiates metastatic dissemination through recruitment of platelets to micro-emboli, aiding adhesion of tumour cell clusters to the vascular wall, while attenuating immune cell detection and destruction of the cancer cells (Joyce and Pollard, 2009).

Another important regulator of cancer cell dissemination is the hyaluronan receptor, CD44. This transmembrane protein is highly expressed by cancer cells and mediates adhesion to endothelial cells through binding of E-selectin (Zen et al., 2008). CD44 binding to hyaluronan also facilitates interactions of metastatic cancer cells with the ECM of bone; a microenvironment enriched in hyaluronic acid (Draffin et al., 2004). This interaction enabled successful metastatic formation of breast cancer in the bone. Other receptors involved in cancer spread include MUC1, a highly glycosylated transmembrane mucin receptor, found to be overexpressed in cancer (Nath and Mukherjee, 2014). The MUC1 receptor is widely implicated in adhesion of cancer cells during the metastatic cascade (Horm and Schroeder, 2013) through binding of intracellular cell adhesion molecule 1 (ICAM1) (Regimbald et al., 1996) as well as E-selectin (Geng et al., 2012).

An important family of adhesion proteins modulated in tumour development are integrins. Integrins are comprised of two subunits; an  $\alpha$  subunit of which there are 18 subtypes, and a  $\beta$  subunit of which there are 8 known subtypes; combination of these subunits results in an array of 24 known unique integrin complexes. Integrins are particularly involved in the interaction between cells and the extracellular environment (Guo and Giancotti, 2004). The heterologous combination of integrin subunits confers a broad specificity to the ECM substrate in which they engage. For example,  $\alpha\beta1$  integrin has a high affinity in binding fibronectin (Soldi et al., 1999) whereas  $\alpha\beta3$  binds to denatured collagen type 1 (Davis, 1992).

In the context of cancer cell adhesion to the endothelium, integrins play a key role in the more advanced stage of adhesion, mediating the firm interaction required for cancer cells to initiate the uncoupling of endothelial cell junctions to allow transendothelial migration. In particular, the expression of  $\alpha4\beta1$  integrin (commonly referred to as VLA-4) binds to the endothelial molecule VCAM-1. In cancer metastasis, expression of VLA-4 in metastatic cells allows binding of VCAM-1 and

facilitates the adhesion of metastatic cells to the vascular wall, leading to eventual metastatic lesion formation (Schlesinger and Bendas, 2015).

Clustering of integrins bound to their cognate ligands initiates the process of outside-in signalling. This results in recruitment of other adhesion complexes, facilitating the development and maturation of focal adhesions, and modification of cell migration. Integrins also bind to the actin cytoskeleton, in association with a vast complex of supporting adaptor proteins including talin, paxillin, vinculin, tensin and  $\alpha$ -actinin (Avraamides, Garmy-Susini and Varner 2008). This places integrins at the interface of the cell membrane, whilst also conferring signal transduction through modulation of adaptor proteins and the actin cytoskeleton and vice versa. In addition to outside-in signalling, intracellular protein complexes can also initiate inside-out signalling to alter integrin-ECM interactions and further modify adhesion of cancer cells (Shen, Delaney and Du 2012).

#### **1.2.4 Endothelial cell-cell junctions**

The endothelium forms a dynamic interface between the lining of the vasculature and the cellular components of the blood. Acting primarily as a conduit for blood, the endothelium interacts with many cell types including but not limited to; immune cells, platelets, erythrocytes and in the context of metastatic cancer, disseminating cancer cells. Because of the large variety of cells that the endothelium encounters, its functions also vary widely. Tissue and blood homeostasis, fluid retention, neovascularisation, and the TEM of immune cells are controlled by endothelial cells. Endothelial function has been directly linked to a number of pathological conditions such as coronary heart disease, atherosclerosis, type 1 diabetes, hypertension and the metastasis of malignant cancer cells (Carmeliet 2003; Potente, Gerhardt and Carmeliet 2011).

The layer of cells which line the lumen of blood vessels is, depending on the tissue, a tightly regulated continuous monolayer of endothelial cells. This lumenised contiguous layer of cells is connected through a series of junctional complexes maintained at endothelial cell-cell contacts. Different categories of junctions found at endothelial cell-cell contacts have been described which involve a plethora of cell adhesion molecules (Dejana, 2004). These broadly fit into 3 groups: the Tight junctions (TJ), the adherens junctions (AJ) and several other molecules (such as

PECAM, CD99 and CD155 and CD146) which do not reside within either of these complexes (Figure 1.3)(Lampugnani, 2012).

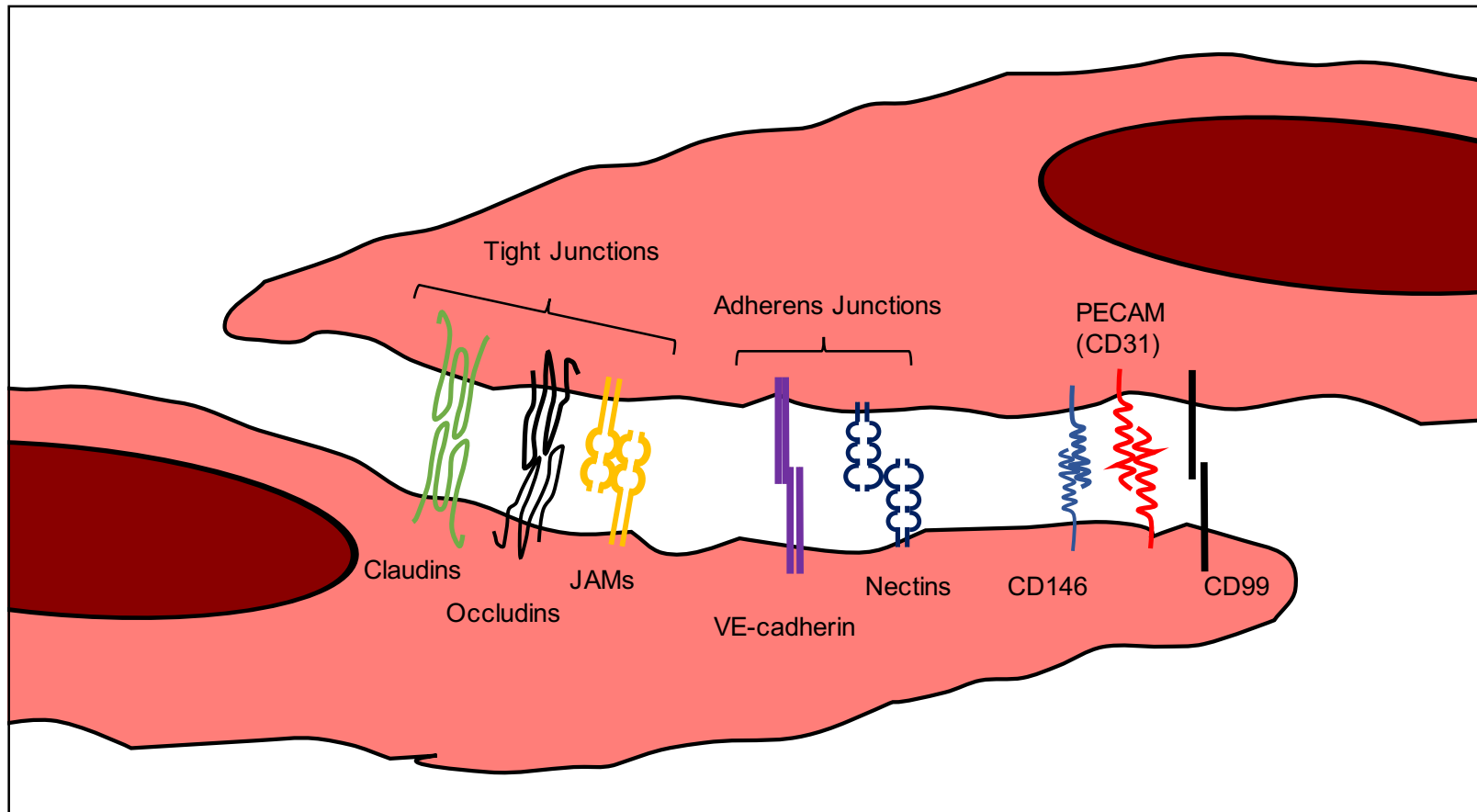


**Fig 1.3 Endothelial cell-cell junctions.** Endothelial cell-cell junctions are stabilised by a number of receptors. These receptors fall broadly into 3 different groups. The tight junctions (TJ) are formed of claudins, occludins and junctional adhesion molecules (JAMs). The adherens junctions (AJ) are comprised of VE-cadherin and nectins. Other adhesion molecules such as CD146, PECAM and CD99 are found at endothelial junctions and mediate cohesion but do reside within TJ or AJ.

One of the main components of the AJs is Vascular Endothelial-cadherin (VE-cadherin or CD144), a member of the cadherin family. VE-cadherin is essential in maintaining endothelial cell-cell contact through *trans* interactions in the extracellular domain (Lampugnani et al. 1992). The intracellular terminal motif of VE-cadherin complexes with a number of adapter proteins such as  $\alpha$ -catenin,  $\beta$ -catenin and plakoglobin which facilitate the anchoring to the actin cytoskeleton (Ben-Ze'ev and Geiger, 1998). P120 catenin also binds to the juxtamembrane region of VE-cadherin and stabilises it at the plasma membrane to maintain permeability (Iyer et al., 2004). Nectins, a family of adhesion molecules have also been found to regulate endothelial cell-cell contact through homophilic interactions within AJs (Takahashi et al., 1999). Nectins are found complexed with afadin and ponsin which associate nectin to the actin cytoskeleton (Takahashi et al., 1999).

The TJs are comprised of several different molecules which mediate the cell-cell contacts between endothelial cells and are largely responsible for regulating permeability of vessels. Junctional adhesion molecules (JAMs), claudins and occludins are all present within the tight junctional complexes (Bazzoni, Martínez-Estrada et al. 2000). Zonula Occludins (ZO-1, 2 and 3) molecules are localised on the intracellular leaflet of the membrane and link the cytoplasmic regions of claudins, occludins and JAMs transmembrane complexes to the cytoskeleton for stabilisation (González-Mariscal et al., 2003). Both claudins and occludins are four-pass transmembrane receptors with two extracellular domains and intracellular N and C termini (Krause et al., 2008). Occludin has one identified splice variant, whereas claudins are a much larger family of 20 proteins. Of this large family, the most studied is claudin 5, which is widely reported for regulating the permeability of blood vessels and is highly expressed in the vasculature of the blood brain barrier, where tight regulation of transport between the blood and the brain is required (Nitta et al., 2003). JAMs are another key molecule of TJs, of which there are 4 homologous subtypes, JAM-A, B and C and the coxsackie and adenovirus receptor (CAR) (Ebnet, 2017). The JAMs regulate endothelial permeability in a similar manner to claudins and occludins, and similarly bind to the intracellular adapter protein ZO-1 and cingulin to anchor with the actin cytoskeleton (Bazzoni, Martínez-Estrada, et al., 2000).

As already alluded to, numerous other adhesion molecules are responsible for regulating the cell-cell contacts between endothelial cells. These receptors do not fall into the category of AJs or TJs but have been found to regulate leukocyte TEM. A member of the immunoglobulin superfamily, CD146 (or melanoma cell adhesion

molecule – (MCAM)) is expressed at the endothelial cell-cell contacts in a homophilic manner and is also involved in regulating monocyte transendothelial migration (Bardin et al., 2001; Bardin et al., 2009). Similarly, CD99 and PECAM are also complexed at endothelial junctions in a homophilic conformation. PECAM undergoes both homophilic and heterophilic interactions, where binding to the  $\alpha\beta 3$  integrin has been reported between leukocytes and endothelial cells (Piali et al., 1995). The role of PECAM in maintaining permeability in the vasculature is apparent in genetic ablation of endothelial PECAM in mice, where increased permeability was observed as well as deregulated leukocyte migration (Graesser et al., 2002). Although the role of CD99 in endothelial monolayer integrity has not been previously described, its localisation to endothelial cell-cell contacts and importance in leukocyte transendothelial migration are well reported (Schenkel et al., 2002; Lou et al., 2007; Dufour et al., 2008). The role of CD99 in regulating cancer cell-EC interactions will be explored in more detail.

### **1.2.5 Extravasation and transendothelial migration**

Transendothelial migration or transmigration, refers to the step in the metastatic cascade where cancer cells penetrate through the endothelium lining blood vessels into surrounding tissue. As with adhesion, there is considerable overlap between the mechanisms of leukocyte adhesion and TEM with that of cancer cells (Madsen and Sahai, 2010). The success rate for cancer cells in transmigrating and forming metastases is very inefficient (< 0.01%) (Chambers, Groom and MacDonald 2002; Fidler 1970) which has been postulated to be due to a lack of multiple integrins required for adhesion and TEM (Madsen and Sahai, 2010). Once a circulating cancer cell has adhered to the endothelium, a series of events occur which allow the bound cells to traverse the endothelial monolayer. Most importantly the uncoupling of multiple endothelial cell-cell junctional complexes is required for migrating cancer cells to penetrate the endothelium and colonise the surrounding tissue. TEM may be split into two pathways; 1) paracellular TEM directs migrating cells to the cell-cell junctions where the uncoupling of adhesion molecules allows the migrating cell to pass through the endothelium, and 2) transcellular TEM which involves the migrating cells movement through the endothelial cells cytoplasm by the reorganisation of the actin cytoskeleton (Mamdouh, Mikhailov and Muller 2009; Reymond, d'Água and Ridley 2013).

As well as being implicated in adhesion, several integrin complexes facilitate the TEM of cancer cells. The integrin complex  $\alpha\beta3$  is required for the TEM of metastatic cancer cells and was shown to be highly expressed by cancer cells undergoing TEM (Bauer, Mierke and Behrens 2007). Depletion and blockade of  $\alpha\beta3$  utilising siRNA knockdown and specific antibodies, respectively, reduced TEM (but not adhesion) in a panel of metastatic cancer cell lines (Bauer, Mierke and Behrens 2007). Cancer cells expressing  $\alpha\beta3$  were also shown to bind endothelial platelet cell adhesion molecule 1 (PECAM1) facilitating cancer cell adherence and transmigration through the vasculature (Weber et al., 2016).

Of the adhesion receptors present at endothelial cell-cell contacts, a number have been implicated in the transmigration of metastatic cancer cells. Global and endothelial specific JAM-C knock out mice were utilised by Langer, et al. (2011) to show that JAM-C is implicated in cancer cells crossing the EC barrier in establishing metastatic dissemination. The CD146 molecule has been implicated in the adhesion and TEM of metastatic melanoma cells (Xie et al., 1997; Melnikova et al., 2009). Use of CD146 knock out mice indicated that host endothelial CD146 was required for VEGF-induced FAK activation (Jouve et al. 2015). These authors show that VEGF-induced FAK is required for melanoma cell transmigration during haematogenous dissemination. Melanoma CD146 expression was also shown to be critical for adhesion and transendothelial migration, as shRNA knockdown reduced both events *in vitro* and *in vivo* (Melnikova et al., 2009). Interestingly, CD146 knock out mouse ECs also had significantly lower VEGFR2 and VE-cadherin expression than control mice ECs, suggesting an additional role for CD146 in regulating EC phenotype (Jouve et al., 2015).

Cancer cells secrete several factors shown to aid the transmigration of metastatic cancer cells. The cytokine transforming growth factor  $\beta$  (TGF $\beta$ ), was shown to activate angiopoietin-like protein 4 (ANGPTL4) transcription in metastatic cancer cells (Padua et al., 2008). Metastatic cancer cell secreted ANGPTL4 induced the uncoupling of endothelial cell-cell junctions and aided the extravasation of cancer cells in the lungs through increased endothelial permeability (Padua et al., 2008). This disruption of endothelial monolayer integrity upon tumour cell extravasation was shown to be due to ANGPTL4 binding of VE-cadherin,  $\alpha\beta1$  and claudin 5 (Huang et al. 2011). Activation of the GTPase Rac1 was also found in this study, which facilitated the uncoupling of endothelial cells through modulation of the actin cytoskeleton (Huang et al. 2011).

Secretion of CCL2 by colon cancer cells and its binding to endothelial CCR2, led to downstream activation of JAK-STAT signalling and p38 MAPK. This resulted in E-selectin-dependent endothelial junctional disruption and subsequent extravasation of cancer cells (Wolf et al., 2012). Furthermore, E-selectin activation by monocytes coordinated with metastatic tumour cells and resulted in endothelial VE-cadherin phosphorylation and cell-cell disruption to facilitate cancer cell transmigration (Tremblay et al., 2006). Conditioned media from cancer cells was additionally found to activate the expression of endothelial E- and P- selectin in a STAT3-dependent manner, without which the transmigration and metastatic dissemination of Lewis Lung cancer cells was greatly diminished (Kim et al. 2017). Cancer cells also release metalloproteinases such as MMP1, MMP2 and MMP9, ADAM12 as well as other proteases which aid in the uncoupling of the adherens and junctional complexes between endothelial cells, allowing migration of the cancer cell in a paracellular fashion through the endothelial cell-cell contacts (Reymond, d'Água and Ridley 2013; Fröhlich et al. 2013).

Metastasising cancer cells employ a variety of other mechanisms during transendothelial migration, including the recruitment of different cellular constituents of the blood to aid their successful transmigration. Evani et al. (2013) showed that under flow conditions monocytes aggregate with breast cancer cells and potentiate the adherence to endothelial cells activated by the inflammatory cytokine TNF- $\alpha$ . Platelets also facilitate the binding and TEM of circulating cancer cells (Gasic, Gasic and Stewart 1968; Kim et al. 1998; Labelle, Begum and Hynes 2011). Interaction of cancer cells and platelets can potentiate the metastasis of cancer cells in the adhesion and TEM of these cells (Gasic, Gasic and Stewart 1968; Kim et al. 1998). This was highlighted by models where depletion of platelets from mice greatly reduced metastatic lesion formation (Gasic, Gasic and Stewart 1968). As well as facilitating metastasis, the recruitment of platelets by circulating cancer cells has been shown to reduce immune cell detection and destruction of metastatic tumour cells. In cancer cell platelet aggregates, platelets act a shield to natural killer cell mediated detection and elimination, allowing cancer cells to evade such destruction (Nieswandt et al., 1999).

A very different mechanism of transmigration was recently reported in which metastatic cancer cells induce endothelial cell necroptosis (a form of inducible apoptosis) in order to successfully transmigrate. Endothelial cell death was activated

by triggering of endothelial death receptor 6 (DR6) through the expression of amyloid precursor protein (APP) by cancer cells (Strilic et al., 2016). This represents a novel route of transmigration which does not follow other models of paracellular or transcellular mechanisms.

### **1.3 Ras and Rho family GTPases**

The actin cytoskeleton provides structure and support to cells whilst also retaining the capability to rapidly disassemble and assemble during cellular movement. This requires the cooperation of several molecular pathways which coordinate the dynamic restructuring of the cytoskeleton in a spatial and temporal manner. The GTPases represent a family of molecular switches that play a pivotal role in the regulation of the actin cytoskeleton. Ras-like GTPases, so named because of their homology to Ras, are low molecular weight proteins with a 5 looped G-box domain which confers a GTP binding sequence motif (Bourne, Sanders and McCormick 1991). With 167 family members, the Ras-like GTPases represent an array of versatile molecular switches that act in many aspects of cellular signalling. This superfamily of Ras-like GTPases is subdivided into five subfamilies; Ras, Ran, Arf, Rab and Rho (Rojas et al., 2012).

The family of Rho GTPases (or Ras homologous GTPases), of which there are over 20 members, are distinguished from the Ras family GTPases by the presence of a 12 amino acid insert domain between the 4<sup>th</sup> and 5<sup>th</sup> G-box motifs (Freeman, Abo and Lambeth 1996). The Rho GTPases were first identified as playing a central role in the coordination of the actin cytoskeleton (Hall, 1998), but have since been shown to function in many other aspects of cell signalling (Ridley 2001). The most studied members of this family include Rac1, Cdc42 and Rho which are highly conserved throughout the evolution of eukaryotes (Boureux et al., 2007).

Like many of the GTPases, Rho GTPases cycle between an active GTP bound form and an inactive GDP bound form. This cycling is regulated by guanine exchange factors (GEFs) and GTPase activating proteins (GAPs) which activate and inactivate Rho GTPases respectively, through hydrolysis of GTP (Vetter and Wittinghofer 2001). When in their active conformation, Rho GTPases recruit and activate downstream effectors to elicit cellular processes. For example, Cdc42 in its active confirmation, mobilises the regulators and effectors of actin polymerisation such as members of the Wiskott Aldrich Syndrome protein (WASP) (Rohatgi et al. 1999) and

the Actin Related Protein complex ARP2/3 (Ma, Rohatgi and Kirschner 1998) to facilitate nucleation of actin. In this example of Cdc42, active GTP-bound Cdc42 binds to the GTP binding domain (GBD) present in WASP (Miki, Miura and Takenawa 1996). WASP proteins remain in an autoinhibitory state until Cdc42 (or other Rho GTPases) bind and initiate a conformational change, releasing the C-terminal Verprolin-Cofilin-Acidic (VCA) domain (Kim et al., 2000). The VCA domain of WASP binds G-actin monomers and the ARP2/3 complex and so facilitates actin branching, nucleation and the formation of new barbed actin filaments (Machesky and Insall, 1998).

The Rho GTPases, Rac, Rho and Cdc42, all have specific functions in regulating and controlling the actin cytoskeleton to elicit specific phenotypes. Rac1 is well characterised in coordinating actin polymerisation in the ruffling membrane (Ridley et al. 1992). Whereas RhoA has been heavily implicated in stress fibre formation and actomyosin contraction (Paterson et al., 1990). The coordination of downstream Rho associated serine/threonine kinase (ROCK) has been shown to mediate stress fibre formation (Leung et al., 1996). The activity of Cdc42 has been shown to facilitate the formation of filopodia through N-WASP and ARP2/3 activation to drive migration (Miki et al. 1998).

However, as the understanding of Rho GTPases and their interactions has grown, the complexity of the network they operate within to control actin dynamics has also expanded. Thus, considerable overlap in Rho GTPase function in certain aspects of actin regulation is apparent. For example, in the formation of lamellipodia, found at the leading edge of migrating cells, rapid actin polymerisation occurs through the control of multiple Rho GTPases. As mentioned above, GTP bound Rac1 binds WAVE (a member of the WASP family) which activates ARP2/3 resulting in actin polymerisation localised to the lamellipodia (Ridley et al. 1992; Eden et al. 2002). Active RhoA has also been found localised to the lamellipodial region of migrating cells and is thought to contribute to actin dynamics through modulation of formins; proteins that associate with the barbed end of actin filaments to control actin polymerisation (Ridley, 2015). Both Cdc42 and Rac act in coordination to drive integrin and focal adhesion complexes in lamellipodia through the regulation of downstream p21 activated kinases (PAKs) (Kurokawa et al., 2004; Rane and Minden, 2014). This highlights the complexity of Rho GTPase signalling in enabling appropriate actin modulation from specific stimuli.

The Rho GTPases are implicated in many aspects of tumour and vascular biology including maintenance of the endothelial barrier (Kouklis et al. 2004; Ramchandran et al. 2008), development of angiogenesis (Barry et al. 2015), and the facilitation of cancer cell dissemination (Ellenbroek and Collard 2007). GTPases have also been shown to control actin dynamics during cancer metastasis, partially by regulating expression of receptors directly involved in facilitating cancer metastasis. This includes actin remodelling pertinent to invadopodia formation, which as previously discussed are required for cancer cells to traverse endothelial barriers (Olson and Sahai, 2009). Cdc42 is one of the Rho GTPases known to play a role in both vascular development and cancer metastasis (Reymond et al. 2012). Reymond et al. (2012) showed the requirement of Cdc42 signalling for  $\beta$ 1 integrin expression and activity which facilitated cancer TEM and dissemination. The role of Rho GTPases in regulating TEM will be explored in more detail.

### **1.3.1 GTPases in TEM**

The role of endothelial Rho-GTPases in the transendothelial migration of leukocytes is well documented, with implications for Cdc42, RhoA and Rac1 all reported (Heemskerk, van Rijssel and van Buul 2014). However, the role of endothelial Rho-GTPases in cancer cell transendothelial migration are much less well described in comparison to leukocyte TEM. Transendothelial migration of metastatic lung carcinoma cells was found to rely on the activity of the endothelial RhoA GTPase and ROCK. These were required for actin contractility of endothelial cells upon cancer transmigration. The rearrangement of actin through modulation to myosin light chain (MLC) and cofilin were found to be downstream effectors of the activation of RhoA and ROCK. Without which, the success of cancer cell transmigration was abrogated as the uncoupling of endothelial TJs, and in particular the redistribution of ZO-1, was limited (Li et al., 2006). Another example of endothelial cytoskeletal remodelling during cancer metastasis was highlighted in the transcellular intravasation of breast cancer. Engagement of endothelial MLC kinase through activation of the regulatory light chain lead to myosin II contraction. This facilitated endothelial cytoskeletal remodelling required for mediating transcellular cancer cell intravasation (Khuon et al., 2010).

Uncoupling of the major endothelial adherens protein, VE-cadherin, has been shown to occur upon monocyte cell transmigration through phosphorylation of the cytosolic domain by the PI3K subunit p110 $\alpha$  (Cain, Vanhaesebroeck and Ridley 2010). p110 $\alpha$

was shown to facilitate Rac1 activity in uncoupling VE-cadherin and disrupting the endothelial barrier to allow monocyte transmigration (Cain, Vanhaesebroeck and Ridley 2010). This study was important as it implicated GTPase activity in the disassembly of VE-Cadherin during transmigration. Other lines of evidence have shown that cancer cells induce the destabilisation of endothelial junctions. It was recently shown that melanoma secreted osteonectin and this molecule induced the retraction of endothelial cells via actin reorganisation (Tichet et al., 2015). This occurred through activation of endothelial VCAM-1 and downstream p38 MAPK signalling which mobilised MLC and subsequent actomyosin contraction, which facilitated the melanoma cell extravasation (Tichet et al., 2015). Although no direct evidence implicated Rac1 GTPase activity in this study, it has previously been shown that ligation of VCAM-1 facilitated leukocyte migration in a Rac1-dependent manner (van Wetering et al., 2003). Finally, cancer derived C-terminal fibrinogen-like domain of angiopoietin-like 4 (cANGPTL4) was found to induce the activation of endothelial Rac1 to mediate barrier disruption by dissociation of VE-cadherin and claudin 5 to facilitate cancer metastasis (Huang et al. 2011).

#### **1.4 Colonisation**

Following extravasation of cancer cells into the metastatic niche, cancer cells can occupy secondary sites in a different form. They may remain in a senescent 'dormant state' as either dormant micrometastases or singular dormant cells (Holmgren, O'Reilly and Folkman 1995). They may reside in close contact with blood vessels, adopting a pericyte-like morphology, and surrounding the blood vessel in a cuff-like manner (Er et al., 2018). Factors governing the progression of metastatic growth at secondary sites is still the subject of great debate. However, the influence of immune cells and the surrounding stroma are thought to play an important role in determining the outcome of metastatic colonisation (Quail and Joyce, 2013).

##### **1.4.1 Organ-specific metastasis**

Dissemination of metastatic cancer cells results in widespread distribution of cancer cells throughout the body. However, secondary tumours will only develop in particular organs. Organ-specific metastasis or 'tissue tropism' of metastatic cancers was first denoted by Steven Paget's 'Seed and soil' hypothesis in 1889 (Paget, 1889). This suggested that for secondary tumours to arise, the microenvironment of the organ (the 'soil') had to be permissive to growth of metastatic cells (the 'seed'). Over 100

years later, experiments by Fidler and Kripke showed that within a heterogeneous tumour cell population, subpopulations exist that have the ability to preferentially metastasise to specific organs (Fidler and Kripke, 1977). Recent studies have started to unveil the fundamental molecular mechanisms which govern this process.

It was previously thought that the preference for metastatic tumours for specific tissues was due to mechanical restraints (such as tissue architecture), and the ability of extravasated cells to proliferate within specific tissues, suggesting organ-specific growth governed the secondary site of metastasis rather than preferential 'homing' to particular organs (Chambers, Groom and MacDonald 2002). Several cancers are known to exhibit tissue tropism in metastasis and one of the most prominent examples of metastatic tissue tropism is in gastrointestinal cancers where cancer cells are shed to the liver resulting in the propensity of liver metastases (Gupta and Massagué, 2006). This is thought to occur due to the livers anatomical positioning downstream of the mesenteric vasculature. Endothelial cells of hepatic sinusoids are also highly fenestrated which potentiates the extravasation of metastatic cells (Chambers, Groom and MacDonald 2002).

The specificity of metastasis for organs based on favourable metastatic sites downstream of the primary tumour is insufficient to explain how metastatic breast cancers can give rise to secondary tumours of the bone, liver, brain and lung – where clearly other mechanisms must govern organ-specific metastasis (Gupta and Massagué, 2006). Another well reported examples are of uveal melanoma of the eye, where metastases of the lung arises in over 90% of patients (Carvajal et al., 2017) and the specificity of prostate and breast cancers to metastasise to the bone. Yoneda et al. (2001) showed that breast cancer preferentially metastasises to the bone *in vivo*. This was shown to be attributable to upregulated CD44 expression (Draffin et al., 2004). Work from McFarlane et al. (2015) indicated CD44 directed this preference for metastasis to the bone microenvironment through interactions between the cancer cells and the bone microvasculature.

#### **1.4.2 Breast cancer brain metastasis**

Breast cancer is the most common cancer in the UK, accounting for 15% (55,122 cases) of all new cases in 2015 and is the 4<sup>th</sup> most common cause of cancer death. At diagnosis, between 6-7% of breast cancers cases are found to be late stage metastatic tumours (Cancer Research UK 2016b). Metastasis to the brain occurs in

a high percentage of breast cancer cases. Studies have reported incidence of breast cancer brain metastasis (BCBM) ranging between 13-30% (Nayak, Lee and Wen 2012). Autopsy data of breast cancer metastasis indicates similar rates to the above study, with 16-30% of breast cancer cases developing brain metastasis (Tsukada et al., 1983). Triple negative breast cancer (TNBC) and HER2 overexpressing breast cancers are the two subtypes with the greatest likelihood of developing brain metastasis (Dawood et al., 2009; Anders et al., 2011). Cancer cells that establish as brain metastases can be in a dormant state and are often clinically undetectable for decades before symptoms develop, making diagnosis challenging (Valastyan and Weinberg, 2011; Tabouret et al., 2012).

Despite this, the last decade has seen considerable progress in determining the mechanisms of breast cancer specificity for the brain. This in part, is due to better *in vivo* models of brain metastasis which have emerged. Data from these models have elucidated specific genes in mediating BCBM. Bos et al. (2009) showed that breast cancer cells selected *in vivo* by their ability to preferentially home to the brain were enriched in a specific subset of genes. One of these enriched genes *ST6GALNAC5*, which encodes sialyltransferase 7E, is paramount in facilitating cancer cell adhesion and transmigration across the blood brain barrier (Bos et al. 2009). Other *in vivo* studies have shown the importance of HER2 in the outgrowth of brain metastatic lesions in breast cancer (Palmieri et al., 2007).

Cyclooxygenase-2 (COX2), MMP1 and 2 and epiregulin were shown to be upregulated in metastatic breast cancers which specifically metastasise to the lungs (Minn et al., 2005). Upregulation of these specific genes and their subsequent protein expression was found to aid extravasation of cancer cells through disruption of endothelial cell-cell junctions in the lungs specifically which could be potently inhibited using either interfering RNA or specific inhibitors (Gupta et al., 2007). COX2 and MMP1 were also found to be important in the homing of breast cancer to the brain, where MMP1 mediated the degradation of claudin 5 and occludin of the endothelial cell-cell contacts of the blood brain barrier (Bos et al. 2009; Wu et al. 2015).

Recently, Follain et al. (2018) showed that shear flow is a major determinant in the adhesion and extravasation of circulating cancer cells. This work highlighted that circulating cancer cells are prone to extravasate at sites of low shear flow (less than 400-600  $\mu\text{m/s}$ ) (Follain et al., 2018). This concept was extended to clinical data,

where MRI scans indicated areas of low perfusion in the brain were more likely to harbour metastatic lesions (Follain et al., 2018). Additionally, the premetastatic priming of endothelial cells of the BBB by cancer released exosomes plays a significant role in the preferential homing of metastatic cells to the brain (Hoshino et al., 2015). Similarly it was shown that cancer cell derived exosomes modulated endothelial Notch1 expression (Sheldon et al., 2010) which was recently shown to be important in cancer cell extravasation (Wieland et al. 2017).

### **1.5 The blood brain barrier**

The blood brain barrier (BBB) was first described by Paul Ehrlich in 1885 where it was found that dyes introduced intravenously diffused into tissues of all organs except the brain (Ehrlich, 1885). The BBB is primarily a barrier between the brain parenchyma and circulation of the body, ensuring that the transport of molecules from the circulation to the brain is tightly regulated. This prevents substances which may inflict damage to the brain from entering the cerebral tissues.

As the interface between the brain and the blood, the BBB regulates the transport of ions, proteins and essential molecules whilst also restricting the movement of harmful substances into the brain. The size of molecules greater than 400-500 Da (approximately a 4 or 5 amino-acid peptide) are prohibited from crossing the BBB into the brain (Pardridge, 2005). The presence of tight junctional formation in the BBB forces the transport of certain molecules directly through the endothelial cells via a transcellular route (Begley and Brightman, 2003). The passive diffusion of gaseous molecules such as O<sub>2</sub>, CO<sub>2</sub> and lipophilic molecules occurs without perturbation to the BBB. Transporter complexes present in the membranes of the BBB endothelial cells are responsible for the active transport of molecules such as glucose by GLUT1 and amino acids by excitatory amino acid transporters (EAAT)1–3. Another amino acid transporter in the BBB, LAT1 (L-system for large neutral amino acids) is an example of a bidirectional transporter, operating down a concentration gradient (Abbott, Rönnbäck and Hansson 2006).

The regulated movement of molecules across this barrier is attributable to complex TJs between endothelial cells of the BBB. The TJs at endothelial cell borders form focal points where opposing membranes come into very close contact, often dubbed 'kissing points' where the intermembrane space between two adjacent membranes is completely absent (Tsukita, Furuse and Itoh 2001). These focal points of TJs are

the site of intertwined 'TJ strands' which consist of aggregated integral membrane proteins which present from adjacent endothelial cells and anastomose forming a paired TJ strand (Staehelein, 1974).

As already discussed (Section 1.2.4) the TJs consist of several transmembrane adhesion molecules and juxtamembrane adapter molecules stabilising the transmembrane molecules by anchoring to the actin cytoskeleton. Occludin was the first molecule to be identified within TJs and is a core transmembrane receptor of these structures (Furuse et al., 1993). Although expressed within TJs, the expression of occludin appears to be dispensable in TJ formation during development, as knockout studies in mice have shown that TJ morphology is unchanged by the lack of occludin (Saitou et al., 2000). However, clinical studies have shown that recessive mutations in occludin results in neurological disorders and calcification of the brain (O'Driscoll et al., 2010). Occludin is also the subject of phosphorylation by multiple kinases and has been suggested to regulate TJ maintenance rather than formation (Bauer et al. 2014).

Expression of JAM-A, JAM-B and JAM-C have also been shown to be highly expressed in TJs and regulate paracellular permeability and leukocyte transmigration (Bazzoni, Martinez-Estrada et al. 2000). The importance of JAM expression in the BBB was indicated by a study of a JAM-C homozygous mutation which caused perturbed lens development, neurological calcification and cerebral haemorrhage in humans (Mochida et al., 2010). Members of the claudin family also contribute to the TJs of the BBB, where claudin 3, claudin 5 and claudin 12 have all been implicated (Wolburg and Lippoldt, 2002). Of these, claudin 5 is most highly expressed in the TJs of the blood brain endothelial cells (Morita et al., 1999) and plays a wide role in selective transport across the BBB (Nitta et al., 2003). This was highlighted in claudin 5 null mice which displayed greatly reduced capacity in size selectivity at the BBB, where molecules <800 Da were able to cross into the brain parenchyma, indicating increased permeability (Nitta et al., 2003).

Many of the transmembrane receptors within TJs bind intracellular adaptor proteins through their cytoplasmic regions. These membrane-associated guanylate kinase (MAGUK) proteins include the adaptors ZO-1, 2, and 3 which bridge transmembrane molecules of TJs to other regulatory proteins and the actin cytoskeleton, forming the so called 'TJ cytoplasmic plaque' (Bauer et al. 2014). The expression of ZO proteins allows signal transduction has been suggested to regulate many processes due to

conserved nuclear localisation and export motifs within ZO proteins (Bauer et al. 2014). Other cytoplasmic proteins which link the TJs to the actin cytoskeleton include cingulin, AF-6 and 7H6 (Hawkins and Davis, 2005).

As in other endothelial cell-cell junctions, adherens junctions (AJs) are also present within the BBB and contribute to its restrictive phenotype. These consist of adhesion molecules such as VE-cadherin and PECAM-1 and cadherin (Rubin and Staddon, 1999). It has been shown that the expression of claudin 5 is under the control of VE-cadherin, which sequesters  $\beta$  catenin and Foxo1 which represses the promoter of the claudin 5 gene (Taddei et al., 2008). Whether this impacts on the role of these molecules in maintaining the BBB remains unclear. The molecules listed above are highly expressed within the TJ of the BBB compared to capillaries of other organs to confer greater barrier function. The tightly regulated BBB is highlighted by transendothelial electrical resistance (TEER), a measure of endothelial monolayer integrity. TEER of the BBB is significantly greater ( $>1000 \text{ ohm.cm}^2$ ) than that of other endothelial barriers (2-20  $\text{ohm.cm}^2$ ) (Abbott, Rönnbäck and Hansson 2006).

Endothelial cells of the BBB are in close association with astrocytes, pericytes, microglia and neuronal processes; often referred to as the 'neurovascular unit' (Figure 1.4)(Hawkins and Davis, 2005). The retentive nature of the BBB is in part due to these cells which surround endothelial cells of the BBB and are within close proximity (Abbott, Rönnbäck and Hansson 2006). *In vitro* studies show that supporting cells of the neurovascular unit can influence the expression of junctional molecules and the integrity of the endothelial component of the BBB (Huang et al. 2012). The release of TGF $\beta$ , basic fibroblastic growth factor (bFGF) and angiopoietin 1 (ANG1) by astrocytes can induce a BBB phenotype in endothelial cells *in vitro* (Lee et al., 2003). It is also known that fibroblasts contribute to the stabilisation and maintenance of adherens junctions in the BBB through the production of fibroblastic growth factor (FGF). It has been shown that FGFs inhibit RhoA through FGF receptor-induced activation of the PI3K-Akt-Rac1 pathway, leading to the stabilisation of adherens junctions in the BBB and thereby stabilising cell to cell contacts (Huang et al. 2012).

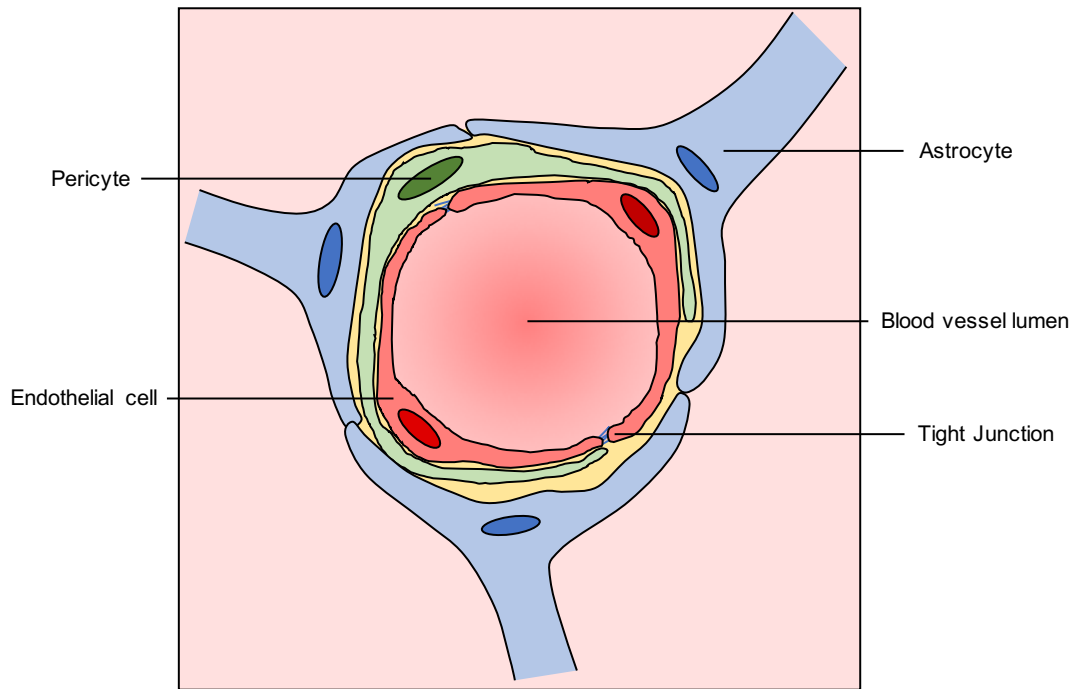


**Fig 1.4 The blood brain barrier (BBB).** The 'neurovascular unit' is comprised of endothelial cells, which are supported by pericytes and astrocytes. Tight junctions present at endothelial cell contacts maintain low permeability of the BBB. Image adapted from (Cheng and Hung, 2007)

### **1.5.1 The organotypic nature of endothelial cells in the BBB**

The organotypic nature of endothelial cells has been known for some time; endothelial cells of the liver sinusoids form fenestrated capillaries whereas vasculature of the BBB is tightly regulated and impermeable. Specific genetic profiles govern the organotypic nature of endothelial cells. For example, *Prox1* is largely responsible for driving the development of the lymphatic vasculature (Hong et al., 2002). However, the underlying gene expression and associated molecular mechanisms which are concordant with the organ specific phenotype of microvasculature have only recently been appreciated. It was recently shown that the endothelial cells of the BBB phenotype are governed by a specific genetic profile. The enrichment of a distinct subset of transcription factors such as *Foxq1*, *Zic3* and in particular *Foxf2* were shown to be key in determining BBB endothelial cell phenotype (Hupe et al., 2017).

In the BBB, further work has shown that specific genes are expressed across the venule-arterial axis across which capillary beds span. The specific genes were expressed in a gradient across this axis and represent the specialisation of endothelial cells within either the venule or arterial compartment. This has been shown in two studies which conducted single cell sequencing on cells of the brain and were able to delineate specific clusters of genes with the smooth transition of expression across the venule-arterial axis (Vanlandewijck et al., 2018; Saunders et al., 2018).

## **1.6 VEGF signalling in endothelial cells**

### *1.6.1 Vascular development*

Early on during development, vasculature is formed through differentiation of mesodermal progenitor cells in both the yolk sac and the embryo. This is termed vasculogenesis, as the *de novo* formation of the vascular network stems from mesodermal precursors which differentiate into endothelial cells (Flamme, Frölich and Risau 1997). The formation of blood islands from mesodermal progenitors occurs in the yolk sac whereas angioblast formation through aggregation of these precursor endothelial cells occurs in the embryo at embryonic day (E) 7.0 in mice (Potente, Gerhardt and Carmeliet 2011). The formation of the vascular plexus, a primitive form of the vascular network, arises from fusion of blood islands in the yolk sac. In the embryo, angioblasts differentiate into endothelial cells forming the dorsal and ventral aorta (De Val and Black, 2009). Further to this, the development into a

mature functional vascular network relies on the growth, anastomosis and intussusception of existing blood vessels which is widely directed by angiogenesis. Angiogenesis refers to the sprouting and remodelling of pre-existing endothelial cells in the development of new blood vessels. Sprouting angiogenesis is initiated by two distinct populations of endothelial cells; tip cells and stalk cells. Tip cells adopt a migratory and polarised phenotype and are guided by chemotactic cues whilst adjacent stalk cells proliferate and initialise lumen formation (Geudens and Gerhardt, 2011). Thus, sprouting, proliferation and migration are all important aspects of endothelial biology which contribute to angiogenic maturation of the vasculature during development (Adams and Alitalo 2007; Carmeliet 2003). It was recently shown that the recruitment of erythro-myeloid precursors (which give rise to haematopoietic stem cells in the yolk sac) also contribute to the development of organ vasculature showing an alternative lineage of endothelial expansion in the embryo (Plein et al., 2018).

#### *1.6.2 VEGF family*

The development of the vascular network during embryogenesis is orchestrated by the key regulator of angiogenesis, vascular endothelial growth factor (VEGF) (Hoeben et al., 2004). VEGF was initially identified as a potent mitogen of endothelial cells and described for its induction of vascular permeability (Senger et al. 1983). The mammalian VEGF family consists of 5 members; VEGFA, VEGFB, VEGFC, VEGFD and placental derived growth factor (PlGF) (Ferrara, Gerber and LeCouter 2003). *VEGFA*, the most studied of the VEGF family genes, consists of 8 exons separated by 7 introns (Tischer et al., 1991; Houck et al., 1991). Alternative splicing of these exons generates two distinct families of isoforms, the proangiogenic VEGFA<sub>xxx</sub> (or VEGFA<sub>xxx</sub>a) and anti-angiogenic VEGFA<sub>xxx</sub>b isoforms (where xxx denotes the amino acid number of the protein)(Dehghanian, Hojati and Kay 2014). Within VEGFA<sub>xxx</sub> isoform family, the structure and function of the different isoforms differs. For example, VEGF<sub>165</sub> contains a heparin binding domain (HBD) encoded by exon 6 and 7 of *VEGFA* which confers plasma membrane and neuropilin binding capabilities. In contrast the VEGF<sub>121</sub> isoform lacks a HBD and associated function due to splice variation and is regarded as a more-readily diffusible form (Dehghanian, Hojati and Kay 2014; Ferrara, Gerber and LeCouter 2003). VEGFA<sub>165</sub> is the predominant proangiogenic isoform of VEGFA and in this thesis reference to VEGF or VEGFA refers to the VEGFA<sub>165</sub> isoform, unless otherwise specified.

### 1.6.3 VEGF receptors

The VEGF family of proteins elicit cellular responses by binding various transmembrane proteins located at the plasma membrane. The family of VEGF receptors (VEGFRs) which include VEGFR1, VEGFR2 and VEGFR3, are all receptor tyrosine kinases (RTKs) and predominantly elicit downstream kinase signalling following ligand binding. The VEGFRs are structured as an extracellular domain which contains 7 Ig-like domains, a single transmembrane region and a tyrosine kinase domain (Shibuya et al., 1990). Ligand binding induces receptor dimerisation and autoactivation of intracellular tyrosine kinase domains to initiate signal transduction cascades.

The VEGFA binding of endothelial VEGFR2 elicits many of the key aspects required of angiogenesis including migration, proliferation and survival through synchronous activation of multiple downstream pathways (Olsson et al., 2006; Abhinand et al., 2016). This is reflected by the high expression of VEGFR2 during embryonic vessel development and angiogenesis (Millauer et al., 1993). The importance of VEGFR2 in vascular formation is apparent in knock out mice where embryonic lethality is observed (Shalaby et al. 1995). VEGFA binds to VEGFR2 with a 10-fold lower affinity than to VEGFR1 (Shinkai et al., 1998). Ligand binding of VEGFR2 is facilitated by Ig-like domains 2 and 3 of the extracellular portion (Fuh et al., 1998). VEGFR2 has also been shown to bind plasmin cleaved VEGFC and VEGFD which also mediate signalling in angiogenesis and lymphangiogenesis (McColl et al., 2003).

Binding of VEGFA to VEGFR2 causes dimerisation of VEGFR2, upon which weak homotypic interactions occur to stabilise the receptors. This facilitates the trans/autophosphorylation of several tyrosine residues in the cytoplasmic domain of the receptor. Phosphorylation of one of the key VEGFR2 tyrosine autophosphorylation sites, Y1175 (Y1173 in mice), mediates the activation of phospholipase C  $\gamma$  (PLC $\gamma$ ), and subsequent signal transduction required for angiogenesis (Cunningham et al., 1997). PLC $\gamma$  activates protein kinase C (PKC) which leads to mobilisation of RAS-dependent ERK activity and subsequent proliferation of endothelial cells (Meadows, Bryant and Pumiglia 2001). Y1175 phosphorylation also results in activation of PI3K pathway and downstream AKT phosphorylation to mediate changes in proliferation (Fujio and Walsh, 1999; Dayanir et al., 2001; Holmqvist et al., 2004). The importance of Y1173 phosphorylation in angiogenesis was shown in knockout mice lacking this tyrosine residue, where the phenotype recapitulated that of a VEGFR2 knockout (Sakurai et al. 2005). It was also

shown that VEGFA induced phosphorylation of VEGFR2 at Y1214, regulated the recruitment and activation of the non-catalytic tyrosine kinase Nck. The activation of Nck and subsequent complex with Fyn, activated PAK1 and led to the activation of Cdc42 and p38 MAPK, thereby coordinating actin reorganisation and migration (Lamallice, Houle and Huot 2006). There are many other tyrosine residues in the cytoplasmic tail of VEGFR2 which are activated upon VEGFA binding, potentiating the ligand induced signal transduction required for successful angiogenic response.

Although VEGFR1 has a higher affinity for VEGFA binding than VEGFR2, the kinase activity of VEGFR1 upon activation and homodimerisation is markedly reduced compared to that of VEGFR2-VEGFA complexes. This is thought to occur due to a lack of positive regulatory phosphorylation sites (Ito et al., 1998) and repressor motifs positioned in the juxtamembrane region which inhibits PI3K activity (Gille et al., 2000). The splice variant of VEGFR1 which produces soluble VEGFR1 (sVEGFR1) also has the ability to strongly bind VEGFA and negatively regulate angiogenesis (Kendall and Thomas, 1993). The high affinity of VEGFR1 and sVEGFR1 for VEGFA and poor kinase activity upon activation have led to the view that VEGFR1 acts a decoy receptor or VEGF trap, limiting the angiogenic response. Findings also show that VEGFR1 expression is predominantly found in the stalk cells of developing branching vessels, and that VEGFR1 expression in tip cells is limited (Jakobsson et al., 2010). The role of VEGFR1 in dampening angiogenesis is exemplified by VEGFR1 knockout mice which are embryonically lethal and exhibit overt overgrowth of vasculature (Fong et al., 1995). Additionally, VEGFR1 is also known to bind VEGFB and PlGF to modulate cellular responses.

The final VEGFR, VEGFR3, is widely implicated in mediating lymphangiogenesis through ligand induced activation driven predominately by VEGFC, but also by VEGFD (Kukk et al., 1996). The affinity of VEGFR3 for VEGFC is greater than that of VEGFR2 (Makinen et al., 2001). The activation of VEGFR3 has been shown to lead to both homodimerisation and heterodimerisation with VEGFR2 (Dixelius et al., 2003). Like the other two VEGF receptors, tyrosine phosphorylation drives the signal transduction downstream of VEGFR3 required for lymphangiogenesis with activation of PI3K and PKC mediated ERK1/2 pathways (Makinen et al., 2001). VEGFR3 is also required for angiogenesis, as high VEGFR3 expression is observed during development in the vascular plexus (Kukk et al., 1996). High VEGFR3 expression has also been observed during tumour angiogenesis and in tip cells during sprouting

(Carmeliet et al. 2009). It is therefore clear that the angiogenic response is a concerted effort from all members of the VEGF and VEGFR family.

#### 1.6.4 Coreceptors of VEGFR

Several coreceptors are known to modify signal transduction following VEGFA-induced activation of VEGFR2. One of the major coreceptors of VEGFR2 are the neuropilins (NRP). Two neuropilins are present in mammalian cells, NRP1 and NRP2, which show 44% homology with each other (Nakamura and Goshima, 2013). While NRP1 is implicated in signalling pertaining to vascular development and angiogenesis, NRP2 appears to play a greater role in regulating lymphatic development (Koch et al., 2011). NRP1 enhances the binding of VEGFA to VEGFR2 whilst also enhancing the downstream signalling of VEGFR2 in angiogenesis (Soker et al., 1998). It does so by stabilising the VEGFA-VEGFR2 ligand-receptor interaction, potentiating VEGFR2 signal transduction (Whitaker, Limberg and Rosenbaum 2001). It was also shown that the cytoplasmic PDZ domain of NRP1 is critical in the formation of the NRP1-VEGFR2 complex (Prahst et al., 2008).

The endothelial cell adhesion molecule CD146 has been implicated as a coreceptor of VEGFR2 (Jiang et al., 2012). The extracellular domain of CD146 was found to be crucial in VEGF induced VEGFR2 phosphorylation (at Y1214) and subsequent downstream signalling through p38 and AKT signalling (Jiang et al., 2012). It was also shown that the intracellular domain of CD146, which complexed with ezrin-radixin-moesin (ERM), was involved in VEGFR2 signalling during angiogenesis (Jiang et al., 2012). The importance of these CD146-VEGR2 interactions were shown *in vivo* where reduced angiogenesis was observed upon conditional knockout of CD146 in ECs as well as using antibodies which masks regions of CD146 important in binding VEGFR2 (Jiang et al., 2012). An isoform of CD44 containing exon 6 termed CD44v6 is another receptor which has been found in a complex with VEGFR2. Similarly to CD146, CD44v6 was found to complex with ERM and elicit downstream signalling in MAPK from VEGF induced activation of VEGFR2 (Tremmel et al., 2009). VE-cadherin also binds VEGFR2 to mediate downstream PI3K signalling (Carmeliet et al. 1999). The depletion or truncation of VE-cadherin lacking the intracellular domain produced a similar reduction in AKT activation and altered endothelial function (Carmeliet et al. 1999). Furthermore, VE-cadherin knock out mice are embryonically lethal due to severe vascular defects (Carmeliet et al. 1999).

Although many integrins have been shown to function in angiogenesis (Avraamides, Garmy-Susini and Varner 2008) the importance of integrin  $\alpha\beta 3$  was initially indicated by high expression in blood vessels and importantly, that antibody blockade inhibited angiogenesis (Brooks, Clark and Cheresch 1994). Integrin  $\alpha\beta 3$  has since been shown to act as a coreceptor for VEGFR2, binding to both VEGFA and VEGFR2 through a critical extracellular domain of the  $\beta 3$  subunit which is indispensable in VEGFR2 phosphorylation and downstream signalling (Soldi et al. 1999; Borges, Jan and Ruoslahti 2000). The association of VEGFR2 and  $\alpha\beta 3$  in VEGFA induced angiogenesis is also important in stimulating migration of endothelial cells in angiogenesis through regulation of MAPK and FAK (Masson-Gadais et al., 2003).

#### *1.6.5 Angiogenesis in cancer*

Levels of VEGF and angiogenesis are high within development during the establishment of the vascular network. However, beyond these developmental stages, VEGF levels decrease and angiogenesis is limited to pathological conditions such as in tumours, psoriasis, age-related macular degeneration and wound healing. Angiogenesis during tumour progression is one of the hallmarks of cancer (Hanahan and Weinberg 2011). During tumour formation, the so called 'angiogenic switch' results in the mobilisation of proximal blood vessels to facilitate the vascularisation of tumours (Hanahan and Folkman 1996). Without the establishment of blood supply, the proliferation rate match that of apoptosis, hence limiting tumour growth and making them dormant. Upon vascularisation of the tumour, the rate of proliferation greatly outweighs that of apoptosis, leading to tumour expansion (Holmgren, O'Reilly and Folkman 1995).

One of the key drivers of tumour vasculogenesis and angiogenesis is hypoxia. As described (section 1.2.1b), hypoxia brings about the stabilisation of the transcription factor HIF which binds to HREs in the promoter of numerous genes to elicit changes in angiogenesis. One of the notable HRE containing promoters is that of *VEGFA*, where the rapid 30-fold upregulation of *VEGFA* mRNA upon HIF1 $\alpha$  stabilisation has been observed compared to normoxic conditions (Carmeliet 2003; Shweiki et al. 1992). Endothelial VEGFR2 protein expression is also upregulated by hypoxia, in a posttranslational manner, which also confers increased tyrosine activity of the receptor (Waltenberger et al., 1996).

### **1.7 p53 tumour suppressor**

p53, often referred to as the guardian of the genome (Lane, 1992), plays a pivotal role in regulating cellular homeostasis in response to stress with wide reaching influence over many facets of cellular function including but not limited to; metabolism, cell fate, cell cycle and DNA damage response (Junttila and Evan 2009; Kruiswijk, Labuschagne and Vousden 2015; Kasthuber and Lowe 2017). These functions endow p53 with potent tumour suppressor capabilities, allowing adaptation and repair to cellular stress whilst also retaining the ability to trigger cell death where reparation is not possible. Post-translational modifications of p53 are induced by a number of stimuli which cause genotoxic stress (UV light, ROS, hypoxia etc) (Kruiswijk, Labuschagne and Vousden 2015). These post-translational modifications alter p53 localisation, stability and conformation to facilitate p53 functionality as a transcription factor (Vousden, 2002). An example of this is ATM/ATR-dependent phosphorylation of p53 by Chk1/2 following DNA damage (Kastan et al., 1992; Shieh et al., 2000). This phosphorylation inhibits MDM2 suppression of p53 which under normal cellular homeostasis, rapidly turns over p53 via ubiquitination and proteasomal degradation (Kubbutat, Jones and Vousden 1997; Haupt et al. 1997; Honda, Tanaka and Yasuda 1997; Bálint, Bates and Vousden 1999). Stabilised p53 is then able to elicit the appropriate transcriptional regulation required to maintain fidelity or trigger cell death (Vousden 2002). Autonomous regulation of active p53 is maintained through a negative feedback loop whereby active p53 drives expression of MDM2 expression (Wu et al. 1993; Barak et al. 1993).

Discovery of p53 was made through its association with simian virus 40 large T antigen (SV40 Tag), a cancer-causing virus in rodents. Binding of SV40 Tag to p53, inactivates p53 function as a tumour suppressor whilst also increasing the concentration of p53 (Linzer and Levine 1979; Lane and Crawford 1979). Subsequent isolation and characterisation of p53 at first led to miss identification of p53 as a proto-oncogene due to the use of mutated p53 cDNA clones utilised in studying the function of p53 (Finlay et al., 1988; Hinds et al., 1989). The apparent elevated expression of p53 in transformed cells and low levels in non-transformed cells also contributed to this misidentification as it seemingly corroborated cloning studies (Dippold et al., 1981; Benchimol et al., 1982). However further work went on to indicate p53s profound role as a tumour suppressor (Finlay et al., 1989). The statistic that over 50% of tumours harbour mutant p53 indicates its importance as a tumour suppressor (Olivier et al., 2002). It is now widely regarded that p53 orchestrates a wide network of responses as a tumour suppressor (Kruiswijk, Labuschagne, and Vousden 2015; Kasthuber and Lowe 2017).

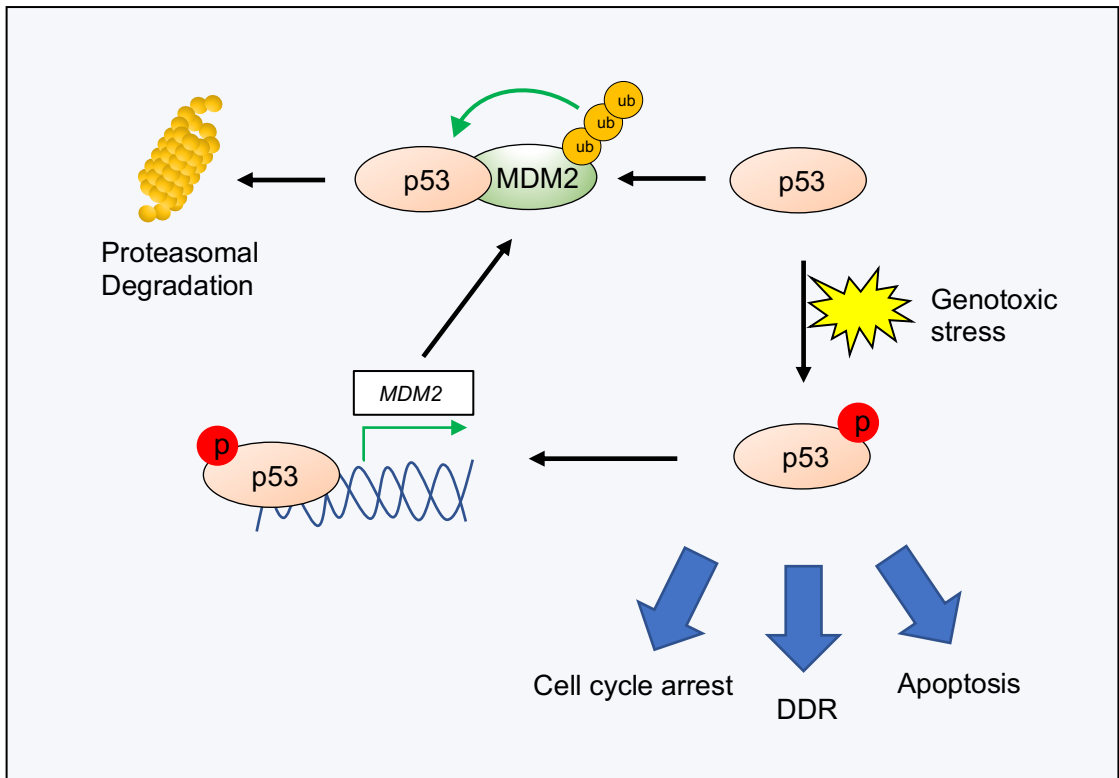


**Figure 1.5. p53 signaling.** Under normal homeostasis, p53 is ubiquitinated by MDM2 resulting in the proteasomal degradation of p53. When cells undergo genotoxic stress, p53 is phosphorylated inhibiting the MDM2 dependent degradation and activating downstream pathways such as cell cycle arrest, DNA damage response (DDR) or apoptosis. Active phospho-p53 also induces the expression of MDM2 resulting in a negative feedback loop which regulates p53 levels.

### 1.7.1 Endothelial p53

Several studies have highlighted the role of p53 in the endothelial cell phenotype in a number of pathological scenarios. The role of p53 in the onset of atherosclerosis has been widely reported (Guevara et al., 1999; Mercer and Bennett, 2006; Minamino and Komuro, 2007). The SUMOylation of p53 under conditions of disturbed flow (often encountered in atherosclerosis) was found to be proatherogenic, potentiating EC apoptosis and inflammation (Takabe, Alberts-Grill and Jo 2011; Heo et al. 2013). Furthermore, the loss of endothelial specific markers and cell-cell junctional molecules is observed during the *trans*-differentiation of endothelial cells to mesenchymal cells (EndoMT) which has been observed in the pathogenesis of atherosclerotic plaque formation (Piera-Velazquez, Li and Jimenez 2011). Interestingly, p53 is also required in the neovascularisation of damaged cardiac tissue where a similar transition of mesenchymal cell-endothelial cell occurs. Increased expression of p53 within damaged tissue was shown to be required for the *trans*-differentiation of supporting mesenchymal cells into endothelial cells which facilitated repair (Ubil et al., 2014). Senescence of endothelial progenitor cells is also mediated by p53 signalling (Miyachi et al., 2004; Rosso et al., 2006). In diabetes, endothelial senescence occurs in a p53/p21 dependent manner and results in diminished neovascularisation (Rosso et al., 2006). This was shown to be due to AKT activity downstream of p53/p21 signalling resulting in activation of senescence in endothelial cells (Miyachi et al., 2004).

The implication of p53 in angiogenesis has previously been shown where inhibition of MDM2 mediated degradation of p53 by treatment of endothelial cells with nutlin-3 resulted in reduced endothelial migration and subsequently attenuated angiogenesis (Secchiero et al., 2007). Furthermore, p53 also plays a role in tumour angiogenesis. It has been shown that p53 regulates the expression of HIF1 $\alpha$  through MDM2 mediated degradation (Ravi et al., 2000). In p53<sup>-/-</sup> tumours, this suppression of HIF1 $\alpha$  is lifted, resulting in increased expression of HIF1 $\alpha$  and concomitant expression of HIF1 target genes such as VEGFA. Furthermore, this study showed that p53<sup>-/-</sup> tumours bear higher vascular formation due to the deregulation of HIF1 $\alpha$  and subsequent upregulation of VEGF (Ravi et al., 2000). Additionally, in the angiogenesis of cardiac hypertrophy it was shown that heat shock transcription factor 1 (HSF1) suppresses p53 expression resulting in increased HIF1 endothelial expression and subsequent angiogenic stimulation through VEGF induction (Sano et al., 2007; Zou et al., 2011). Finally, p53 has also been shown to upregulate

semaphorin 3E (sema3E) in response to hypoxia (Moriya et al., 2010). Sema3E is also involved in vascular patterning during development and has been shown to inhibit angiogenesis in postnatal models (Sakurai et al. 2012). Here Sema3E was shown to inhibit angiogenesis by blocking activation of VEGFR2 in a p53 dependent manner (Moriya et al., 2010).

## 1.8 Aims

This project set out to investigate cancer-endothelial cell interactions during metastasis. The main objectives of this thesis were to investigate the role of receptors which had not previously been implicated in facilitating the metastatic spread of cancer through adhesion and transmigration. Particular focus was given to receptors with a known function in leukocyte-endothelial cell interactions, which have not been implicated in cancer-endothelial interactions. Endothelial phenotype and angiogenesis were also investigated, as these aspects of endothelial biology are pertinent to tumour progression.

**Chapter 3:** Described studies on the tissue specificity of metastasis in breast cancer brain metastasis. It was hypothesised that the tissue specificity of breast cancer for the brain was in part due to the ability of breast cancer cells to interact with the endothelium of the BBB. Brain metastatic variants of the breast cancer cell line MDA-MB-231 were employed to investigate the adhesion and TEM of this metastatic variant to BBB endothelial cells. Using clinical data and *in vitro* assays, a role for the adhesion molecule CD146 was assessed in the interactions of breast cancers and the BBB.

**Chapter 4:** The aims of this chapter were to investigate the phenotype of *in vitro* models of the BBB and in particular the cell line hCMEC. The hCMEC cell line were compared to primary endothelial cells in order to elucidate their suitability as BBB models. An assessment of VEGF signalling and concurrent angiogenic potential were the main criteria in determining endothelial phenotype and explored the role of p53 in VEGFR2 signalling. It was hypothesised that p53 expression is involved in the regulation of endothelial phenotype through the modulation of VEGFR2 expression. siRNA and stable knockdown of p53 using shRNA was used to investigate the relationship between p53 and VEGFR2, along with downstream angiogenic assays to assess endothelial cell function.

**Chapter 5:** Metastatic cancer cells hijack leukocyte migration machinery of the endothelium to achieve metastatic dissemination. In this chapter the role of CD99 (a prominent receptor in leukocyte TEM), was elucidated in cancer adhesion and TEM. The objective of this study was to explore CD99 function of both cancer and endothelial cells and determine its role in downstream processes regulating metastasis by *in vitro* and *in vivo* methodologies. It was hypothesised that CD99 regulates the TEM of metastatic cancer cells in a manner analogous to that of leukocyte

transmigration. siRNA knockdown of CD99 in both HUVEC and MDA-MB-231 were performed to assess the role of CD99 in TEM using *in vitro* adhesion and TEM assays. Additionally, luciferase expressing MDA-MB-231 cells were employed for the evaluation of CD99 expression in metastasis *in vivo*.

## Chapter 2 Materials and Methods

### 2.1 Cell lines

Human umbilical vein endothelial cells (HUVEC) (Promocell) are derived from human umbilical cords and pooled from multiple donors. Human cerebral microvascular endothelial cells (hCMEC/D3) referred to as hCMEC (VH Bio Ltd) are an immortalised cell line isolated from human temporal lobe microvessels from tissue removed to treat epilepsy (Weksler et al., 2005). The breast cancer cell line MDA-MB-231 (MDA-231) was isolated from the pleural effusion of a patient with metastatic breast cancer (Cailleau, Olivé and Cruciger 1978), and was purchased from the European Collection of Cell Cultures (ECACC). Brain metastatic derived MDA-MB-231 cells (BrM) were generated by serial *in vivo* passage of MDA-MB-231 cells in mice and subsequent isolation of cancer cells from metastatic lesions of the brain (Yoneda et al., 2001) and were a kind gift from Dr. Mihaela Lorgier (University of Leeds). Firefly luciferase expressing MDA-MB-231 cells were also obtained from Dr. Mihaela Lorgier (University of Leeds) and were generated by the lentiviral transduction of MDA-MB-231 (performed by Mihaela Lorgier) as previously described (Rippaus et al., 2016). Human brain microvascular endothelial cells are primary endothelial cells derived from human brain (HBMEC)(ScienCell). Human Dermal Fibroblasts (HDF)(Promocell) are isolated from the dermis of juvenile foreskin from a single donor. MCF7 breast cancer cell line was isolated from the pleural effusion of a patient with metastatic breast cancer (Soule et al., 1973), and was purchased from the ECACC. SKBR3 breast cancer cell line was isolated by (Fogh, Fogh and Orfeo 1977) from the pleural effusion of a patient with metastatic breast cancer and were a kind gift from Dr. Laura Matthews (University of Leeds). PC3 cell line are a metastatic prostate cancer cell line isolated from the bone metastases of a 62-year-old male Caucasian (Kaighn et al., 1979) and were purchased from the ECACC. HEK293T cells were generated by stable transfection of HEK293 cells with SV40 Large T antigen (DuBridge et al., 1987) and were obtained from Dr. Adam Odell (University of Leeds).

#### 2.1.1 Cell culture

All endothelial cell lines were cultured in Endothelial cell basal medium (ECBM)(Promocell) supplemented with 2% FCS (v/v), 0.4% endothelial cell growth supplement, 0.1ng/ml epidermal growth factor (recombinant human), 1ng/ml basic fibroblast growth factor (recombinant human), 90µg/ml heparin, 1µg/ml

hydrocortisone. Cells were grown on 0.2% gelatin (Sigma) (w/v in PBS) coated plates. Endothelial cells were allowed to grow to confluency before passaging every 2-3 days. hCMEC/D3 cell lines were grown to passage 35 before discarding as cells begin to lose endothelial characteristics (Weksler et al., 2005). Similarly, HUVEC cells were grown to passage 8 or 9. MDA-231 and BrM breast cancer cell lines were cultured in 10% (v/v) foetal calf serum (FCS) (Biosera)(Sigma) supplemented RPMI-1640 (Sigma) and required passaging every 3-5 days. HDF, MCF7, SKBR3, PC3 and HEK293T cells were cultured in 10% FCS supplemented Dulbecco's modified essential media (DMEM)(Sigma). All cell lines were incubated at 37°C under 5.0% CO<sub>2</sub>.

Cells were harvested using 10x trypsin (Sigma) diluted 1:10 in phosphate buffered saline (PBS; 137 mM NaCl, 2.7 mM KCl, 1.8 mM KH<sub>2</sub>PO<sub>4</sub>, 10 mM Na<sub>2</sub>HPO<sub>4</sub> pH 7.4). Culture medium was removed, cells were washed with 1x PBS, and incubated with 1 ml of 1x trypsin at 37°C until cells began to detach. Growth medium was added to dilute and inactivate the trypsin and cells were pelleted by centrifugation at 300 x g for 5 minutes at room temperature (RT) before passaging (1:5 for all cancer cell lines and 1:4 for all endothelial cells) or using in subsequent assays.

### **2.1.2 Freezing and thawing cells**

Cells were frozen down and stored in batches for future use. Cells were cultured until 70-80% confluent before harvesting as described as above. Following pelleting of cells by centrifugation at 300 x g for 5 minutes at RT, cells were resuspended at 1x10<sup>6</sup>/ml in 100 % FCS solution containing 8.5% DMSO (Sigma). Cells were then transferred in 1ml aliquots to 1ml cryovials (Thermo Scientific) and placed at -80°C for 24-48 hours in Mr Frosty freezing container (Thermo Scientific) containing isopropanol for cooling at approximately -1°C/min. Cryotubes of cells were transferred to liquid nitrogen for long term storage. For thawing of cells, cryovials were removed from storage and transported on dry ice. Cells were thawed by placing cryovials in 37 °C waterbath for 3-4 minutes, until cells are 70% thawed. Cells were then gently resuspended in 1-2ml warm medium, gently pipetting up and down in cryovial and then transferring to 15ml falcon tubes (Corning). Resuspended cells were then pelleted by centrifugation at 300 x g for 5 minutes at RT. Medium was aspirated and cells resuspended in 5ml of growth medium and transferred to T25 flasks (Corning) and incubated at 37°C under 5.0% CO<sub>2</sub>. Medium was replaced following 24 hours and cells were passaged (as described above) at least once before use in experiments.

### **2.1.3 Cell counting**

Cells were harvested as described (section 2.2.1). 10µl of resuspended cells were aliquoted to a 50µl Eppendorf tube. Aliquoted cells were diluted 1:2 in Trypan blue (Thermo Scientific) and either loaded onto disposable or reusable slides and counted automatically in cells/ml or loaded onto a 1/400mm<sup>2</sup> Neubauer haemocytometer (Hawksley) and counted using an inverted microscope (Olympus). An average was calculated for cells/ml by counting from 4 squares, accounting for dilution factor of the trypan blue (1:2) and the haemocytometer dimensions of (1x10<sup>4</sup>) to calculate cells per ml. Otherwise, cells were counted using a Countess II FL Automated Cell Counter (Thermo Scientific).

### **2.1.4 Cell tracker green (CTG) labelling of cells**

MDA-231, BrM and PC3 cells were detached using trypsin (as described above) and resuspended in growth medium. Cells were counted as described above and 1x10<sup>5</sup> cells were pelleted by centrifugation at 300 x g for 5 minutes. Supernatant was removed and cell pellets were resuspended in 1ml of serum free RPMI media containing 0.4 µM cell tracker green-CMFD (Invitrogen) and incubated for 30 min at 37 °C. Cells were then pelleted by centrifugation at 300 x g for 5 minutes and supernatant discarded. Cells were washed by resuspending in 1ml 10% FCS supplemented RPMI media and pelleting cells once more. Cells were then resuspended at 2x10<sup>5</sup>/ml of 10% FCS supplemented RPMI media for subsequent assays.

### **2.1.5 Adhesion assay**

Endothelial cells were seeded at a density of 1x10<sup>4</sup> per well of a 96 well plate (Corning) and incubated for 24-48 h or until confluent monolayers were present in each well. MDA-231 or BrM cells were labelled with Cell Tracker Green for 30 min in serum free RPMI (SFM-RPMI) media at 37°C. MDA-231 cells were washed in SFM RPMI once before being seeded at 1x10<sup>4</sup> per confluent EC monolayer. Adhesion assay was incubated at 37°C and MDA-231 and BrM cells were allowed to adhere to the EC monolayers for 15, 30, 60 and 120 minutes, after which each plate was washed 1x in PBS, and fixed in 4% (w/v) paraformaldehyde (PFA)(Sigma) for 10 minutes, and washed twice in PBS before storing at 4°C and analysed using Live Cell Imager - Incucyte Zoom (Essen bioscience).

### **2.1.6 Transendothelial migration assay**

24 well Thincert 3.0µm or 5.0µm pore diameter, transparent transwell filters (Greiner Bio-One Ltd) were coated with 0.2% (w/v) gelatin and HUVEC or hCMEC/D3 were seeded at a density of  $2 \times 10^4$  cells per insert. Cells were seeded in 300µl ECBM media, with 500µl in the lower chamber of the transwell insert. Endothelial cells were grown 24-48 hours to allow formation of confluent monolayers before  $2 \times 10^4$  breast cancer cells were seeded to the upper chamber. MDA-231 and BrM cells ( $2 \times 10^5$ /ml) were CTG labelled as described in (section 2.1.4), before seeding to confluent EC monolayers in 1:1 ECMB:RPMI media. MDA-231 and BrM cell migration was halted at 18 h by fixing in 4% PFA for 10 min followed by washing twice in 1x PBS (250µl for upper chamber and 500µl for lower chamber). Upper chambers of transwells were then scraped using cotton wool buds to remove cells on the upper layer of the transwell insert, leaving cells that had migrated to the underside of the membrane intact. Transwells were then washed twice in PBS. Migrated cells were then imaged using the EVOS microscope (Thermo Scientific).

### **2.1.7 Live cell imaging of intercalation**

The spreading of cancer cells on endothelial monolayers is indicative of cancer transmigration. This has previously been described as 'intercalating' as cancer cells displace the endothelium and embed within the EC monolayer (Reymond et al. 2012; Onken, Li and Cooper 2014) Cancer cell intercalation was determined by live cell imaging. Endothelial cells were seeded to 96 well plates at a density of  $1 \times 10^4$ /well in 100µl to achieve confluent monolayers in 24-48 h. Once confluent endothelial monolayers were established, CTG labelled cancer cells were seeded onto endothelial monolayers at a density of  $1 \times 10^4$  per well in 50µl of media (total media volume 150µl including endothelial culture medium). Plates were then imaged immediately using Live Cell Imager - Incucyte Zoom. Images were taken every 5 min for 4 h using 20x objective.

### **2.1.8 Flow cytometry**

Cultured cells were washed in PBS and trypsinised with 1x Acutase (Gibco). Cells were washed in ice cold PBS followed by centrifugation at  $300 \times g$  for 5 min. Supernatant was removed followed by repeat washing in PBS. Cells were resuspended in 100µl FACs buffer (PBS, 2% FCS, 0.09% NaN<sub>3</sub>). Cells were stained

with fluorophore conjugated antibodies and relevant isotype control antibodies (see Table 1) at  $1 \times 10^6$  cells per 100 $\mu$ l staining buffer in 5ml FACs tubes (Corning), for 30 min at RT. Stained cells were washed 2x in ice cold PBS, followed by centrifugation and discarding supernatant between each wash. Stained cells were then fixed in 100 $\mu$ l Cytotfix Fixation buffer (BD biosciences) at RT for 10 minutes before washing twice in 500 $\mu$ l PBS/FACs tube. Cells were resuspended in 300 $\mu$ l of FACs buffer and stored at 4°C until analysis on LSRII flow cytometer (BD Biosciences).

**Table 1. Flow cytometry antibodies**

Target	Conjugate	Manufacturer	Clone	Host	Volume antibody/ 1x10 <sup>6</sup> cells
CD273	PE	BD Biosciences	MIH18	Mouse	5 $\mu$ l
CD274	PE	BD Biosciences	MIH1	Mouse	5 $\mu$ l
CD54	APC	BD Biosciences	HA58	Mouse	10 $\mu$ l
CD56	FITC	Miltenyi Biotec	REA196	Mouse	10 $\mu$ l
CD34	PE	BD Biosciences	8G12	Mouse	10 $\mu$ l
CD155	PE	Biologend	SKII.4	Mouse	5 $\mu$ l
CD99	APC	Biologend	HCD99, 12E7	Mouse	5 $\mu$ l
CD99	FITC	Biologend	HCD99, 12E7	Mouse	5 $\mu$ l
EGFR	AF647	BD Biosciences	EGFR.1	Mouse	5 $\mu$ l
CD44	FITC	Miltenyi Biotec	DB105	Mouse	5 $\mu$ l
CD146	APC	Biologend	SHM-57 or P1H12	Mouse	5 $\mu$ l
EPCAM	FITC	Abcam	B29.1, VU-ID9	Mouse	5 $\mu$ l
CD62E	APC	BD Biosciences	685H11	Mouse	10 $\mu$ l
CD46	FITC	BD Biosciences	E4.3	Mouse	10 $\mu$ l
VEGFR2	AF488	Biologend	7D4-6	Mouse	10 $\mu$ l
CD31	AF488	Biologend	WM-59	Mouse	5 $\mu$ l
CD144	Biotin	BD Biosciences	clone 75	Mouse	5 $\mu$ l

## **2.2 Cell lysate preparation for SDS-PAGE**

Cells were washed in PBS before being lysed in lysis buffer (2% SDS (Sigma) in PBS). Cell lysates were boiled at 100°C for 5 minutes, and sonicated using Sonicator (Soniprep 150 – MSE) for 1-2 seconds. Protein concentration of samples was then determined using Pierce™ bicinchoninic acid assay BCA Protein Assay Kit (Thermo Scientific). Cell lysates were then mixed with 2x sample buffer (100 mM Tris-HCl, 4% SDS, 20% glycerol, 0.2% bromophenol blue, 10% β-mercaptoethanol) and stored at -20°C.

### **2.2.1 SDS-PAGE and Western Blotting**

Cell lysate samples were loaded into 8, 10, 12 or 15% SDS page gels (8,10, 12 or 15% acrylamide, 380mM Tris pH8.8, 0.1% SDS, 0.1% APS, 0.1% TEMED) set with 4% stacking gel (4% acrylamide, 120mM Tris pH6.8, 0.1% SDS, 0.1% APS, 0.1% TEMED) for electrophoresis. Samples were loaded along with 5µl of SeeBlue Plus 2 prestained protein standard (Invitrogen) and were electrophoresed for 1h 20min at 120V (12V/cm) in 1x running buffer (25mM Tris, 192mM glycine, 0.1% SDS) in an electrophoresis tank (Bio-Rad).

Nitrocellulose membranes (GE Lifesciences) were activated by soaking in Transfer buffer (25mM Tris, 192mM glycine, 20% methanol) for 1 minute. Filters (Bio-Rad) and blotting paper (Whatman) were also soaked in Transfer buffer. Gels were transferred to nitrocellulose by layering membrane over SDS-PAGE gel and placing on filters and blotting paper submerged in transfer buffer. Transfer was completed for 1 hour at 15V using semi dry transfer machine (Bio-Rad).

Following transfer, nitrocellulose membranes were blocked for 1 hour at RT shaking in 1x TBST (25 mM Tris base, 134 mM sodium chloride, pH 7.5, 0.1 % v/v Tween-20) with 1% bovine serum albumin (BSA) (Thermo Scientific). Following blocking, membranes were probed with primary antibody (see Table 2) in 1% BSA TBST overnight at 4°C. Membranes were washed 3x in TBST over 30 min, before probing with horse radish peroxidase (HRP) conjugated secondary antibody (see Table 2) in 1% BSA TBST for 1 hour at RT with constant agitation. Membranes were then washed again 3x in TBST over 30 minutes before developing in 1ml per blot of enhanced chemiluminescence solution (ECL) for 1 minute: Solution 1 (0.4mM p-coumaric acid, 2.5mM Luminol, 0.1M Tris pH8.5), Solution 2 (0.02% H<sub>2</sub>O<sub>2</sub>, 0.1M Tris pH 8.5) mixed in a 1:1 ratio or ready-made super enhanced chemiluminescence

(ECL) (BioRad). Membranes were then placed in a light proof case and exposed to ECL Hyperfilm (GE Healthcare) for between 1 second and approximately 10 minutes depending on the strength of signal. Chemiluminescence of membranes was also detected using ChemiDoc imager (BioRad) in some instances.

**Table 2. Western blotting antibodies**

<b>Target</b>	<b>Manufacturer</b>	<b>Product number, reference</b>	<b>Dilution</b>	<b>Origin</b>	<b>Size (KDa)</b>	<b>Clonality</b>
$\beta$ actin	Sigma	AC-74	1:10000	Mouse	42	Monoclonal
GAPDH	Origene	2D9	1:10000	Mouse	36	Monoclonal
CD146	Cell Signalling Technologies	P1H12	1:500	Mouse	120	Monoclonal
CD99	Biolegend	HCD99, 12E7	1:1000	Mouse	36	Monoclonal
Phospho-VEGFR2	Cell Signalling Technologies	19A10	1:1000	Rabbit	230	Monoclonal
VEGFR2	Cell Signalling Technologies	D5B1	1:1000	Rabbit	210, 230	Monoclonal
VEGFR2	R&D Technologies	AF357	1:1000	Goat	210, 230	Polyclonal
Phospho-AKT	Cell Signalling Technologies	D9e	1:1000	Rabbit	60	Monoclonal
AKT	Cell Signalling Technologies	9272	1:1000	Rabbit	60	Polyclonal
Phospho-ERK1/2	Cell Signalling Technologies	9101	1:1000	Rabbit	42, 44	Polyclonal
ERK2	Santa Cruz Biotechnology	(C-14) sc-154	1:2000	Rabbit	42, 44	Polyclonal
p53	Santa Cruz Biotechnology	FL393	1:1000	Rabbit	53	Polyclonal
CD31	Thermo Scientific	JC/70A	1:1000	Mouse	130	Monoclonal
VE-cadherin	Santa Cruz Biotechnology	BV9	1:1000	Mouse	130	Monoclonal
Cdc42	Cell Signalling Technologies	11A11	1:1000	Rabbit	21	Monoclonal
Rac1	Millipore	23A8	1:1000	Mouse	21	Monoclonal
ARP3	Cell Signalling Technologies	4738	1:1000	Rabbit	47	Polyclonal

Claudin 5	Santa Cruz Biotechnology	A-12, sc-374221	1:1000	Mouse	23-35	Monoclonal
Anti-Rabbit HRP	Cell Signalling Technologies	7074	1:5000	Goat		
Anti-Mouse HRP	Cell Signalling Technologies	7076	1:5000	Horse		

### **2.2.2 Immunofluorescent confocal microscopy**

18 x 18 mm, 0.25 mm Coverslips (VWR) were sterilised in 70% ethanol and left to dry for 10 minutes. For endothelial cells, coverslips were coated in 0.2% gelatin for 1 hour, followed by 1 hour drying after removal of excess gelatin. Cells were seeded to coverslips and grown to confluence. Cells were gently washed 2x in PBS before being fixed in 4% PFA for 10 minutes. Cells were then gently washed twice in PBS. Cells were permeabilised using 0.2% Triton X-100 (Sigma) for 5 minutes. Cells were blocked in 3% BSA in 1x PBS for 1 hour prior to staining. Coverslips were then stained in 30-40µl staining buffer (1% Horse serum, 0.1% BSA, 0.02% NaN<sub>3</sub>) with appropriate antibodies (see Table 3) overnight in a humidifier. Coverslips were washed 3x with PBS before addition of secondary fluorophore conjugated antibodies (1:1000) in the same manner as described for primary antibodies and incubated for 1 hour at RT. Coverslips were washed twice in PBS. Final incubation with Hoechst (Sigma) stain at 1:10,000 (from stock solution) for 10 minutes at RT as with other antibodies, followed by 2x wash in PBS. Coverslips were mounted to frosted glass microscope slides (Thermo Scientific) with Fluoromount-G (SouthernBiotech) (for 24 hours at RT away from light). Cells were analysed using a Confocal Laser Scanning A1R Microscope (Nikon) or Widefield TiE fluorescent microscope (Nikon).

**Table 3. Immunofluorescent antibodies**

<b>Target</b>	<b>Manufacturer</b>	<b>Clone</b>	<b>dilution</b>	<b>Origin</b>	<b>Clonality</b>
p53	Santa Cruz Biotechnology	FL393	1:100	Rabbit	Polyclonal
SV40	Abcam	PAb416	1:100	Mouse	Monoclonal
VEGFR3	R&D Technologies	AF394	1:100	Goat	Polyclonal
VEGFR2	R&D Technologies	AF357	1:100	Goat	Polyclonal
VEGFR1	R&D Technologies	AF321	1:100	Goat	Polyclonal
ZO-1	Santa Cruz Biotechnology	H-300, sc-10804	1:100	Rabbit	Polyclonal
VE-cadherin	Santa Cruz Biotechnology	BV9	1:100	Mouse	Monoclonal
CD31	Abcam	Ab124432	1:100	Rabbit	Polyclonal
CD99	Biolegend	HCD99, 12E7	1:100	Mouse	Monoclonal
Claudin 5	Santa Cruz Biotechnology	A-12, sc-374221	1:100	Mouse	Monoclonal
CD146	Cell Signalling Technologies	P1H12	1:50	Mouse	Monoclonal
Phalloidin	Invitrogen		1:250		
Hoechst	Sigma		1:10000		

### **2.2.3 siRNA transfection**

HUVEC, MDA-231 and BrM were transfected with SMARTpool siRNA (GE lifesciences) targeting CD99 and CD146. hCMEC cells were transfected with SMARTpool siRNA (GE lifesciences) targeting VEGFR2 and individual siRNA duplexes targeting p53 (Ambion) (see Table 4). Scrambled siRNA was used as a control along with untransfected or mock cells. Transfections were performed using Lipofectamine 200 RNAiMax (Invitrogen) transfection agent and Opti-MEM I Reduced Serum Medium, GlutaMAX Supplement (Gibco). Cells were transfected with 10 pmol of siRNA per well of a 12 well plate ( $1-2 \times 10^5$  cells/well) and 30pmol siRNA in a 6 well plate ( $2-4 \times 10^5$  cells/well). Cells were washed and detached using 1x trypsin and counted. Cells were then resuspended in Opti-MEM media at  $2-4 \times 10^5$ /ml. For a single well of a 6 well plate, 30pmol siRNA duplexes were made in 250 $\mu$ l of OptiMEM media and incubated at RT for 5 min. At the same time 5 $\mu$ l Lipofectamine was made up in 250 $\mu$ l of OptiMEM and incubated at RT for 5 min. siRNA and Lipofectamine mix were combined within the 6 well plate and gently mixed before incubating at RT for 20 minutes. Following this OptiMEM suspended cells were added to siRNA Lipofectamine complexes at  $2-4 \times 10^5$  cells in 1ml of OptiMEM. Cells were incubated in this mixture for 4-6 hours, before transfection medium was aspirated and replaced with supplemented normal culture medium. siRNA treated cells were incubated for 24-72 hours before further assaying. Reactions were scaled up to T75 flasks (Corning) for siRNA transfections for *in vivo* experiments and GTP-Cdc42 pulldown assays.

### **2.2.4 Kaplan-Meier survival curves**

For survival and distant metastatic free disease curves, an online database of gene expression and relapse free and overall survival data sourced from GEO, EGA and TCGA data was analysed ([www.kmplot.com](http://www.kmplot.com)). Gene expression data and clinical data are integrated to allow analyses of the prognostic value of particular genes. Patient samples are divided into two groups (high and low expressing) based on quantile expression of the gene of interest. Hazard ratios with 95% confidence intervals and logrank P values are calculated and both groups are then compared by Kaplan-Meier survival curves.

**Table 4. siRNA sequences and product details**

<b>Gene Symbol</b>	<b>Pool Catalog Number</b>	<b>Duplex Catalog Number</b>	<b>GENE ID</b>	<b>Gene Accession</b>	<b>GI Number</b>	<b>Sequence (5' » 3')</b>
MCAM	L-003686-00	J-003686-05	4162	NM_006500	71274106	UAGUUGAAGUUAAGUCAGA
MCAM	L-003686-00	J-003686-06	4162	NM_006500	71274106	CAAGUCAUCUGGUACAAGA
MCAM	L-003686-00	J-003686-07	4162	NM_006500	71274106	GAAGAACCGGGUCCACAUU
MCAM	L-003686-00	J-003686-08	4162	NM_006500	71274106	GGAAGUCACCGUCCCUGUU
CD99	L-016245-00	J-016245-05	4267	NM_002414	34147599	GGAUGGUGGUUUCGAUUUA
CD99	L-016245-00	J-016245-06	4267	NM_002414	34147599	CUUCAUUGCUUACCAGAAA
CD99	L-016245-00	J-016245-07	4267	NM_002414	34147599	GAACCCACCCAAACCGAUG
CD99	L-016245-00	J-016245-08	4267	NM_002414	34147599	CGUUUCAGGUGGAGAAGGA
VEGFR2	L-003148-00	J-003148-09	3791	NM_002253	223403530	
VEGFR2	L-003148-00	J-003148-10	3791	NM_002253	223403530	
VEGFR2	L-003148-00	J-003148-11	3791	NM_002253	223403530	
VEGFR2	L-003148-00	J-003148-12	3791	NM_002253	223403530	
Scrambled control siRNA (ON-TARGETplus Non-targeting control pool, Dharmacon; D-001810)						
TP53 siRNA; p53 (Ambion; s605) Cat. No. 4390824						
<i>Silencer</i> <sup>™</sup> Negative Control No. 2 siRNA (Ambion) Cat. No. AM4637						

### **2.2.5 Tubulogenesis assay**

HDF cells were seeded at density of  $2 \times 10^4$  cells per 0.2% gelatin coated 48 well plate in supplemented ECBM:RPMI media at a ratio of 1:1. Following incubation overnight at 37°C under 5.0% CO<sub>2</sub>, hCMEC or HUVEC cells were seeded at a density of  $5-6 \times 10^3$  cells per well of HDFs. Cocultures were cultured for 24 hours before media was replaced with ECMB for controls wells, ECBM + VEGFA (10ng/ml or 25ng/ml)(PeproTech).

VEGF supplemented media was changed every 2 days for a period of 9 days before cocultures were washed 2x in PBS and then fixed in 4% PFA for 10 minutes. Wells were washed twice in PBS before staining with a fluorophore conjugated antibody mouse anti-CD31 (Biolegend) (1:400 dilution) in PBLEC staining solution (0.1% BSA, 1% Tween, 0.05% NaN<sub>3</sub>, 1mM CaCl<sub>2</sub>, 1mM MgCl<sub>2</sub>, 0.1mM MaCl<sub>2</sub>) for 1-2 hours at RT with constant agitation, after which cocultures were washed 2x in PBS before imaging using EVOS microscope and Live Cell Imager - IncuCyte.

### **2.2.6 Lentiviral transduction**

Lentiviral supernatants were produced in HEK293T cells following transfection using Lipofectamine 200 RNAiMax (Invitrogen) transfection agent with 3<sup>rd</sup> generation packaging plasmids and either pLKOshp53 (Addgene #19119), pLKOshScr (Addgene #1864). Early passage (p28) hCMEC cells were transfected with pLKOshScr or pLKOshp53 lentiviral supernatants diluted (1:1) with ECMB supplemented media with polybrene (8µg/ml)(Sigma) overnight. The following day viral supernatants were removed and replaced with fresh supplemented media. Following 24 hours, transfected cells were selected using puromycin (Sigma) supplemented ECBM media (2µg/ml). Selected cells were pooled as a population and bulked up before being frozen down (section 2.1.2) and stored at -80°C or in liquid nitrogen.

### **2.2.7 Matrigel cord formation assay**

Matrigel (Corning) was thawed on ice for 4 hours. Matrigel and ECBM (Promocell) were mixed (1:1) in Eppendorf tubes and kept on ice. 100µl of the ECBM matrigel mix were placed in a chilled 96 well plate well (pipetting carefully so as not to introduce bubbles) and then incubated at 37°C for an hour until the matrigel/ECBM had solidified into a gel which was tested by gently tilting the plate.  $5 \times 10^3$  ECs per well were seeded in 100µl of ECBM to the solidified ECBM matrigel coated plates and incubated at 37°C

overnight to allow cord formation. Cords were subsequently imaged using the Incucyte imaging system at 4x magnification and quantified using ImageJ 'angiogenesis analyser' plugin.

### **2.2.8 Electrical cell substrate impedance sensing (ECIS) barrier integrity measurement**

The disruption or impedance of ion current flow from an can be utilised for the determination of endothelial barrier integrity. ECIS makes use of these principles to allow real-time analysis of endothelial barrier function through the constant measurement of AC frequency through endothelial monolayers. ECIS plates (Applied BioPhysics) were coated with 0.1% Gelatin (in PBS) for 1-2 hours at 37°C. Excess gelatin was carefully aspirated without touching electrical nodes in the base of wells. Plates were left to dry in laminar flow hood for 10 minutes (without lids firmly on) before endothelial cells were seeded. Endothelial cells were detached and resuspended in appropriate media before counting. Cells were seeded at a density of  $4 \times 10^4$  per well of the ECIS plate in 300µl of appropriate media. Cells were incubated in plates for 24 hours before loading onto ECIS Z0 16W Array station (Applied BioPhysics) and measuring barrier function.

### **2.2.9 RT-PCR**

Total RNA was isolated from HUVEC, hCMEC and HBMEC, using RNeasy Plus Kit according to manufacturer's instructions (Qiagen). Approximately  $1 \times 10^6$  cells were harvested from 6 well plate by washing of cells in 1x PBS, and addition of Buffer RLT Plus (Qiagen) according to the manufacturer's protocol. Cells were disrupted using a cell scraper and transferred to a 1.5ml Eppendorf tube. Lysates were then homogenised by vortexing for 1 minute. Cells were filtered in a step- wise manner through high and low stringency solutions (Qiagen) along with centrifugation according to manufacturer's instructions. Harvested mRNA was eluted from RNeasy spin columns in RNase free water and stored at -80°C. mRNA samples were quantified and purity checked using the NanoDrop Lite Spectrophotometer (Thermo Scientific) according to the manufacturer's protocol.

Using High-Capacity RNA-to-cDNA Kit (Thermo Scientific) cDNA was synthesized according to the manufacturer's instructions using 200-500 ng RNA. A master mix containing 44% 5x Reaction Buffer, 11% RNase Inhibitor, 22% dNTP Mix, 11% Reverse Transcriptase, 11% Oligo d(T) was combined with diethylpyrocarbonate

(DEPC)-treated water and mRNA (master mix and mRNA were combined in 9:11 respectively). Samples were placed into C1000 Thermal Cycler (Biorad) to incubate at 42°C for 60 min followed by 70°C for 5 min.

Gene expression of *Foxf2* and *Slc7a1* (Table 5) was analysed by Taqman-based qPCR analysis using Applied Biosystems QuantStudio 5 Real-Time PCR Systems (Thermo Scientific), following the standard PCR cycling sequence (Table 6) using ribosomal subunit *18s* (Table 6) as an internal control. Results for qPCR target genes were normalised to internal *18s* controls. Statistical analysis of qPCR data was carried out using  $\Delta\Delta C_t$  method (Livak and Schmittgen, 2001). Changes in gene expression of HMBEC and hCMEC were compared by fold change relative to HUVEC.

**Table 5. Taqman qPCR gene expression probes**

Gene	Supplier	Assay ID	Dye	Amplicon length
<i>18s</i>	Thermo Scientific	Hs03003631_g1	FAM-MGB	69
<i>FOXF2</i>	Thermo Scientific	Hs00230963_m1	FAM-MGB	77
<i>Zic3</i>	Thermo Scientific	Hs00185665_m1	FAM-MGB	90

**Table 6. Cycling protocol used for Taqman gene expression qPCR**

Initial denaturation	Denaturation	Annealing
95°C	95°C	60°C
5 min	10 sec	3 sec
1x	35x	35x

### 2.3 Cell viability assay

Cell viability was determined using Zombie™ live/dead cell discriminator (Biolegend). siRNA treated MDA-231 cells were detached 72 post transfection and suspended in RPMI supplemented media. Cells were counted and resuspended at  $1 \times 10^6$ /ml. Cells from each condition of siRNA treatment (mock, scrambled control and CD99 siRNA see section 2.2.3) were transferred to 5ml FACs tubes. Cells were pelleted by

centrifugation at 300 x *g* and washed twice in PBS and the supernatant discarded. A separate tube of cells was kept aside and incubated in 0.1% Tween PBS solution for 10 min to permeabilise the cells as a positive control. Cells were then stained with Zombie™ live/dead cell discriminator (Biolegend) at (1:1000) in 100 µl PBS per tube for 30 mins RT. Cells were pelleted by centrifugation at 300 x *g* for 5 minutes and supernatants discarded before washing 1x in PBS. Cells were then pelleted once again by centrifugation and resuspended in 300µl of PBS and analysed on the LSRII flow cytometer.

### **2.3.1 Real Time Cell Analyser (RTCA) XCELLigence**

Real-time monitoring of cellular proliferation, spreading and migration were measured using an electrical impedance-based assay using the xCELLigence RTCA DP instrument (ACEA Biosciences, Inc.). Cells were seeded into specialised plates in which an array of sensors are imbedded within the base of each well, allowing measurement of multiple parameters through disruption (or impedance) of electrical flow between sensor nodes. E-plate RTCA assays proliferation, migration and morphology of cells in 2D and an arbitrary unit (cell index) is applied to the quantified measurements. For assesement of spreading and migration,  $5 \times 10^3$  MDA-231 cells siRNA reverse transfected (48h post transfection) were seeded to E-plates (ACEA Biosciences, Inc.) and analysed using xCELLigence RTCA DP instrument. Impedance was measured every 15 minutes for 24 h.

For real-time monitoring of cellular migration, MDA-231 were plated in serum-free media to the upper chamber of specialised Transwell-style plates (cell invasion and migration (CIM) plates) (ACEA Biosciences Inc.), in which sensors embedded within the underside of the porous Transwell membrane allow real-time analysis of migration and invasion. The lower chambers were loaded with 10% FCS-containing complete growth media to act as a chemoattractant. Impedance was measured every 15 minutes for 24 h. Data from each time point were exported and compiled in Excel from a minimum of 3 biological replicates for comparison of siRNA treated cells.

For monitoring of endothelial barrier disruption by cancer cells, E-plates were coated prior to plating endothelial cells, with human fibronectin (Sigma) 10 µg/ml for 2h at RT under a laminar flow hood. Wells were then rinsed twice in PBS and air dried before seeding of endothelial cells. ECs were seeded at  $1 \times 10^4$  in 100µl per well of an E-plate and plates were loaded into the xCELLigence RTCA DP instrument. ECs were grown to confluency for 24-48 hours before addition of cancer cells.  $1 \times 10^4$  MDA-231 cells in

50µl were loaded to wells containing EC monolayers and impedance was measured every 15 minutes for 24 h. Data were analysed using fold change in barrier integrity upon seeding of cancer cells to EC monolayers compared to HUVEC monolayers alone.

### **2.3.2 Scratch/Wound migration assay**

MDA-231 cells were seeded at a density of  $2 \times 10^4$ /well of a 96 well plate in 100µl of 10% FCS supplemented RPMI media and grown to confluency over 24-48 hours. Once confluent, cells were serum starved for 2 hours prior to 'wounding'. Culture medium was removed using an aspirator and replaced with serum free RPMI media (supplemented with 1% BSA). Following serum starvation, scratch wounds were made using 'Incucyte wound maker implement' (a device with a pin for each well of a 96 well plate, which is lowered and moves laterally to score a scratch in confluent cell monolayers). Once scratched, medium was gently removed by aspirator and monolayers gently washed with PBS before replacing with supplemented RPMI media. The assay was imaged following 18-24 hours to assess closure of the wound. Images were analysed using ImageJ 'MRI\_Wound\_Healing\_Tool-1' plugin.

### **2.3.3 Proliferation assay – crystal violet**

Cell proliferation was determined using crystal violet staining assay which is described in detail by (Feoktistova, Geserick and Leverkus 2016). Cells were washed twice in 1x PBS and detached using trypsin. Cells were counted and seeded to 24 well plates in triplicate at a density of  $1 \times 10^4$  for 24, 48, 72 and 96 hours under normal culture conditions. Following culture for indicated time periods cells were washed twice in 1x PBS before fixation in 4% PFA for 10 minutes at RT. PFA was then aspirated and fixed cells were washed twice in 1x PBS before storing at RT until plates from all time points had been processed as described.

PBS was aspirated and cells stained in 1ml of crystal violet staining solution (0.5% crystal violet powder (Sigma-Aldrich), 20% Methanol) for 20 min at RT with gentle agitation. An empty well (without cells) from each plate was also stained with crystal violet for background readings during quantification. Following staining plates were thoroughly rinsed with water four times. Following washing, plates were inverted and placed on filter or tissue paper and air dried overnight without plate lids. Stained cells were solubilised in 1ml 100% Methanol/well and incubated with gentle agitation for 20 min at RT with lids on the plate. 200µl of solution/well was taken from each stained

well, transferred to a 96 well plate and the optical density of each well was measured at 570 nm (OD<sub>570</sub>) using a plate reader. Average OD<sub>570</sub> of control empty wells was subtracted from OD<sub>570</sub> of wells containing cells.

### **2.3.4 ECM adhesion assay and immunofluorescence**

ViewPlate 96 well black plates (PerkinElmer) were coated with either 0.2% w/v gelatin, fibronectin (10µg/ml in PBS)(ProSpec-Tany TechnoGene, Ltd) and collagen type 1 (10µg/ml in 0.1M acetic acid)(Merck Millipore). Plates were incubated at 37 °C for 2 hours before aspirating excess ECM coating and rinsing 2x with PBS and air drying for 30 min at RT. 1x10<sup>4</sup> cells/well of siRNA treated MDA-231 cells were seeded to coated ViewPlate 96 well plate and allowed to adhere for 30 min. Unbound cells were then washed away in PBS and fixed in 4% PFA for 10 min at RT. Cells were then permeabilised in 0.2% Triton X-100 and blocked for 1 hour in 3% BSA PBS before staining using TexasRed phalloidin (Thermo Scientific (1:200) and Hoechst (1:10,000) in PBLEC staining buffer (0.1% BSA, 1% Tween, 0.05% NaN<sub>3</sub>, 1mM CaCl<sub>2</sub>, 1mM MgCl<sub>2</sub>, 0.1mM NaCl) at RT for 2-4 hours. Following this, cells were rinsed 2x in PBS before subsequent imaging was carried out using an Operetta HTS imager (Perkin Elmer). Image analysis was performed using Columbus software. 3D actin distribution plots were generated using ImageJ '3D surface plot' analysis.

### **2.3.5 *In vivo* experimental metastasis**

Female CB17-SCID mice (aged 6-8 weeks) were purchased from Charles River Laboratories. All *in vivo* procedures were performed by Dr Alison Taylor and in accordance with the Animals (Scientific Procedures) Act 1986 Amendment Regulations 2012 following ethical review by the University of Leeds Animal Welfare and Ethical Review Committee (AWERC) Home Office UK PPL No. 70/7544. 72 h following siRNA knockdown, luciferase expressing MDA-231 cells were detached using trypsin and resuspended in RPMI supplemented media. Cells were strained using 70µm cells strainers (Thermo Scientific) to remove aggregates of cells and were pelleted before resuspending at 5x10<sup>6</sup>/ml in PBS. 5x10<sup>5</sup> cells/mouse were injected into the main tail vein of mice (injections were performed by Dr Alison Taylor under the approved UK Home Office project license (No. 70/7544)). For imaging, D-luciferin substrate (Sigma) was injected intraperitoneally into mice (2µg/mouse) and mice were anaesthetised with isoflurane and scanned using an IVIS Spectrum imaging unit (PerkinElmer)(performed by Dr Alison Taylor under the approved UK Home Office

project license (No. 70/7544)). Bioluminescent imaging of mice was carried out at 6h, 24h, 48h and 72h post injection and then weekly for 4 weeks.

### **2.3.6 GTP-Cdc42 immunoprecipitation**

GTP-bound Cdc42 was assessed using Cdc42 Activation Assay Biochem Kit™ (Cytoskeleton, Inc.). Cells were grown to confluency in T75 flasks, then detached, washed in appropriate media and counted. Cell density was adjusted so equal numbers of cells were used per condition.  $3-5 \times 10^6$  cells were reseeded to 0.2% gelatin coated T75 flask at equal densities (per condition of siRNA treatment), and left to adhere for 30 minutes for HUVEC and 4 hours for MDA-231 cells. Following this, cells were placed on ice and media removed. Cells were gently washed in ice cold PBS which was quickly aspirated. Cells were then lysed in 500µl ice cold lysis buffer (provided in kit) and lysates collected using a cell scraper and placed in 1.5ml Eppendorf tubes on ice. Lysates were immediately cleared by centrifugation at 10,000 x g at 4°C for 1 min. Supernatant was then transferred to a new Eppendorf tube on ice. An aliquot of 20-30 µl of this supernatant was used for protein quantification determined using Pierce™ bicinchoninic acid assay BCA Protein Assay Kit. Remaining lysate was then either rapidly cooled and stored at -80°C for use at a later date or immediately processed for immunoprecipitation. Lysates were rapidly frozen in a slurry of dry ice and 100% Methanol until completely frozen and transferring to -80°C for storage.

If using frozen stored lysates, these were incubated in a water bath at RT until thawed and placed on ice. 300-800 µg of protein were used (as per the Cdc42 Activation Assay Biochem Kit™ protocol) and added to 20 µl (20 µg) of p21 activated kinase 1 protein (PAK1) – p21 binding domain (PBD) coated beads which were incubated on a rotator at 4°C for 1 h. PAK1-PBD beads and lysate were then pelleted by centrifugation at 3-5,000 x g at 4°C for 1 min. 90% of supernatant was carefully removed, taking care not to disturb the pellet. Pelleted beads were washed by adding 500µl Wash Buffer to Eppendorf in a manner which resuspends beads without the need for inverting or pipetting up and down. Beads were then centrifuged at 3-5000 x g at 4°C for 3 min before carefully removing supernatant. Pelleted beads were then mixed with 20 µl 2x Laemmli sample buffer (section 2.2) and thoroughly resuspended. Samples were boiled at 100°C for 2 minutes before analysis by SDS-PAGE using 15% gels (see SDS-PAGE section 2.2.1). Input control lysates, which had not been subject to immunoprecipitation with PAK1-PDB beads were electrophoresed alongside pulldown samples to determine total Cdc42 protein expression.

### **2.3.7 Statistical analysis**

P-values were calculated using two-tailed students T-test, one-way ANOVA or two-way ANOVA using Prism7 software (GraphPad). Results were deemed significant if  $p < 0.05$  and were denoted: \* $p < 0.05$ , \*\* $p < 0.005$ , \*\*\* $p < 0.0005$ , \*\*\*\* $p < 0.00005$ . Statistical analysis was performed on mean values generated from  $n \geq 3$  biological replicates. Error bars represent standard error (unless stated otherwise in the figure legends) and were calculated using the standard deviation in Prism7.

For clinical survival data, statistical analysis was calculated using the online tool (Lánczky et al., 2016), where patient cohorts are compared by a Kaplan-Meier survival plot, and hazard ratio with 95% confidence intervals and logrank p-value are calculated.

## Chapter 3 Investigating cancer-endothelial cell interactions using a breast cancer metastasis model

### 3.1 Introduction

Dissemination of cancer cells in the circulation results in their widespread distribution throughout the body. However, metastatic lesions often develop in only select organs. Although we have started to appreciate the fundamentals of why this occurs, further analysis to identify key biomarkers which allow prediction of metastatic sites remains a challenge. The specificity in colonisation of metastatic sites has long been proposed, the first prominent example of this was described Steven Paget's 'Seed and soil' hypothesis in 1889 (Paget, 1889). Fidler and Kripke's seminal work (1977), made significant inroads regarding this phenomenon, showing that within a heterogeneous tumour cell population, subpopulations exist that have a propensity to metastasise to specific organs.

Metastasis to the brain occurs in a high percentage of breast cancer cases. Studies have reported incidence of breast cancer brain metastasis (BCBM) ranging between 13-30% (Nayak et al., 2012). Autopsy data of breast cancer patients with metastasis indicate similar rates, with 16-30% of these cases developing brain metastases (Tsukada et al., 1983). Triple negative breast cancers (TNBC; those that lack receptors for oestrogen, progesterone and the human epidermal growth factor receptor (HER) 2) as well as HER2 overexpressing breast cancers represent two molecular subtypes with the greatest likelihood of developing brain metastases (Dawood et al., 2009; Anders et al., 2011). The TNBC cell line MDA-MB-231 is widely used in the study of breast cancer and metastatic disease. The isolation of clones of MDA-MB-231 based on their preference to metastasise to specific tissues has been previously utilised to uncover drivers of tissue specificity in breast cancer metastasis. Isolated metastatic clone cell lines were generated by the serial *in vivo* passage of MDA-MB-231 cells and subsequent isolation of cells from metastatic lesions of the lung (Minn et al., 2005), bone (Yoneda et al., 2001; Kang et al., 2003) or brain (Yoneda et al., 2001; Bos et al., 2009). Isolated cells can then be reintroduced *in vivo* and show homing to the tissues from which they were isolated. This technique has proved very powerful in delineating the preference of sites of metastatic breast cancers. Bos et al. (2009) showed that breast cancer cells selected *in vivo* by their ability to preferentially home to the brain were enriched in a specific subset of genes. One of the enriched genes, *ST6GALNAC5* (which encodes the sialyltransferase 7E), was shown to be critical for breast cancer cells to cross the BBB and colonise the brain parenchyma. Other examples using this

*in vivo* selection of subclones with brain homing properties have indicated the importance of HER2 in the outgrowth of brain metastatic lesions (Palmieri et al., 2007).

Brain metastases can be asymptomatic and remain clinically undetectable for decades due to dormancy of micrometastatic lesions (Valastyan and Weinberg, 2011; Tabouret et al., 2012). A number of factors limit the ability of metastatic cells to breach the BBB and recent work has begun to elucidate the mechanisms of this process. Follain et al. (2018) showed that shear flow is a major determinant in the adhesion to the endothelium and extravasation of circulating cancer cells. This work highlighted that circulating cancer cells are prone to extravasate at sites of low shear flow (less than 400-600 m/s). This concept was applied to clinical data, where use of MRI indicated that areas of low perfusion in the brain were more likely to harbour metastatic lesions (Follain et al., 2018). The interaction between the cancer cells and cells of the local brain microenvironment are critical in the establishment of metastatic lesions. Studies have shown that the successful outgrowth of extravasated cancer cells relies on their capacity to co-opt blood vessels (as a mechanism of resistance to anti-VEGF therapy) (Donnem et al., 2013). Pericyte coverage of endothelial cells is an important aspect of the BBB physiology. In brain metastasis, the cell adhesion molecule L1CAM has been shown to be vital in the perivascular positioning of metastasising breast cancer cells post extravasation in the brain (Er et al., 2018). This presumably supplies these metastatic cells in close proximity to blood vessels allowing uptake of transported molecules (Kienast et al., 2010). Distal factors such as exosomes, platelets and immune cells can also influence metastatic formation in specific organs. Premetastatic priming of endothelial cells of the BBB by cancer shed exosomes plays a significant role in the preferential homing of metastatic cells to the brain. Hoshino et al. (2015) showed that the uptake of cancer-derived exosomes (containing certain integrin molecules) by BBB ECs primed the tropism of disseminating metastatic cells specifically to the brain.

These examples indicate that the crosstalk between metastatic cells and the cerebral vasculature are critical in the establishment of metastatic disease. Here I set out to investigate the interactions of MDA-MB-231, brain metastatic derived MDA-MB-231 subclones (referred to as BrM) and BBB ECs, to investigate whether metastatic organ tropism is directed by cancer-endothelial cell interactions.

### **3.2 Cancer cells preferentially adhere to HUVEC cells over hCMEC**

As the endothelial component is the initial point of contact between disseminating metastatic cells and the BBB, this thesis investigates the interactions of breast cancer cells and the endothelium rather than those of the supporting cells of cerebral vasculature. The working hypothesis was that the BrM line would show preferential binding and transmigration across a BBB-derived EC compared to a non-brain EC.

An initial comparison between MDA-231 and BrM for their ability to adhere to endothelial monolayers of human umbilical vein endothelial cells (HUVEC) or a cell line representing human cerebral microvascular endothelial cells (hCMEC/D3 referred to as hCMEC) cell line was performed (Figure 3.1). Cell Tracker Green (CTG) labelled MDA-231 and BrM cells were seeded onto confluent endothelial monolayers for up to 2 hours before washing, fixation, and imaging. Results indicated that both cancer cell lines adhered to HUVEC monolayers in greater numbers than to the hCMEC cell line endothelial monolayers (Figure 3.1A-B). This raised interesting questions regarding the repertoire of adhesion molecules expressed by hCMEC and whether this differs to HUVEC expression. These questions regarding the phenotype of the hCMEC cell line are the focus of Chapter 4 and are not discussed in further detail here.

Comparison of MDA-231 and BrM indicated a slight reduction in the ability of BrM to bind to HUVEC monolayers. However, this enhanced binding of MDA-231 was only significant at the 60-minute time point (Figure 3.1A). The opposite was true for BrM cells adhering to the hCMEC monolayers. Results showed that the BrM line had a small but consistent ability to preferentially adhere to the hCMEC cell line monolayers compared to MDA-231. Again, this difference was only significant at a singular time point of 60 minutes (Figure 3.1B). Although differences were small, results from the adhesion assays supported the original hypothesis that the specificity of the BrM line to metastasise to the brain may be conferred through their ability to preferentially bind to cerebral vasculature compared to MDA-231.

These results suggest that there is a difference in the ability of MDA-231 and BrM cells to bind to endothelium derived from brain vasculature compared to non-brain ECs. However, the difference in between MDA-231 and BrM is small, suggesting that other non-cancer cell intrinsic factors contribute to the ability of BrM cells to migrate to the brain.

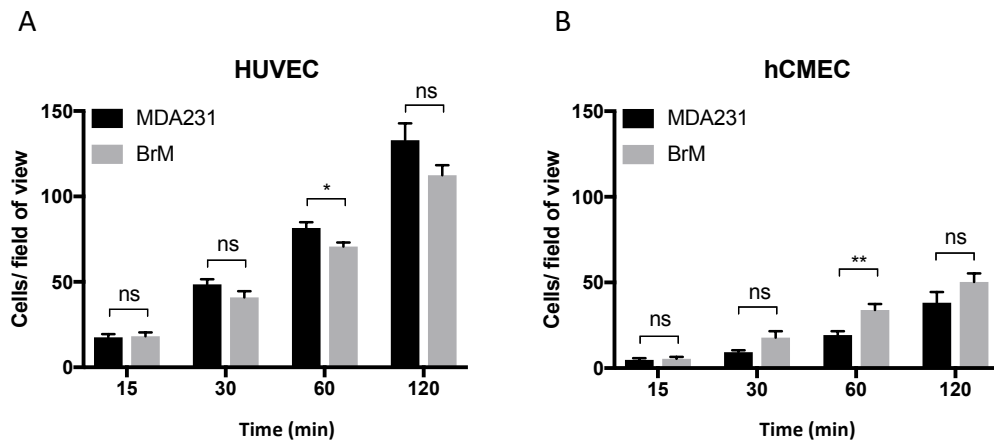


**Fig. 3.1. MDA-BrM show similar adhesion profile to MDA-MB-231.** **A**, Cell tracker green labelled MDA-231 and BrM cells were seeded at  $1 \times 10^4$  to confluent HUVEC monolayers for indicated time points. Unbound cells were washed away with PBS before fixation in 4% PFA. Adherent cells were then imaged using the Incucyte scanning microscope and quantified using imageJ software. **B**, Adhesion assay was carried out as in panel A, with hCMEC/D3 endothelial monolayers. Data are representative of  $n=3$  independent replicates. Bars show mean. Error bars indicate standard error. Statistical analysis was performed using students t-test. \* $p < 0.05$ , \*\* $p < 0.005$ .

### **3.3 BrM shows reduced capacity to traverse endothelial barriers compared to MDA-231 cells**

The adhesion assays indicated that BrM exhibited a slight preference in adhering to BBB derived ECs. I therefore investigated whether this impacted on the ability of BrM to cross EC monolayers. Using a transwell assay, transendothelial migration (TEM) of both MDA-231 and BrM cells across HUVEC and hCMEC cell line endothelial monolayers was investigated. ECs were grown to confluency on the upper side of transwell chambers before seeding cell tracker green (CTG) labelled MDA-231 or BrM cells onto the upper chambers in serum free medium. Lower chambers of the transwell assay contained 10% foetal calf serum containing medium, providing a stimulus for tumour cells to migrate through EC monolayers. Counting and quantification of CTG labelled cancer cells which had undergone TEM through the transwell membrane were performed to assess TEM efficiency. Results showed that the BrM line showed significantly decreased rates of transendothelial migration compared to the parental cell line (Figure 3.2). Interestingly, the source of the EC monolayers (the hCMEC cell line or HUVEC) did not affect cancer cell TEM. In transwell assays with no EC monolayer, similar rates of chemotaxis were observed between MDA-231 and BrM suggesting that endothelial TEM was specifically altered in the BrM population. Furthermore, it was observed that an increased number of cancer cells were present on the underside of transwell filters with an EC monolayer than without. It is possible that this due to an increased number of cells dropping from filter into the media of the lower chamber of the transwell assay in the absence of EC monolayer and thus fewer cells were quantified when imaging the underside of filters.

To further analyse the transendothelial migration of both MDA-231 and BrM, live cell microscopy was employed to visualise the spreading of cancer cells on endothelial monolayers. This behaviour has been described as 'intercalating' as cancer cells displace the endothelium and embed within the EC monolayer (Reymond et al. 2012; Onken, Li and Cooper 2014). Labelled MDA-231 and BrM were seeded at equal densities to confluent HUVEC monolayers and imaged for 4 hours to capture intercalation of CTG labelled cancer cells as they adhered to the endothelial monolayer (Figure 3.3A). Quantification of the percentage of cancer cells that underwent intercalation indicated that BrM cells were significantly impaired in their ability to intercalate compared to MDA-231 (Figure 3.3B). Intercalation quantification was calculated by a change in cell circularity past a threshold defined in the Incucyte analysis software. An example of the imaging mask applied to intercalation live cell imaging is shown (Figure 3.3C). Results from live cell imaging therefore corroborate

results from the transwell migration assays, suggesting that *in vitro*, BrM cells exhibit a greatly reduced capacity to traverse EC barriers compared to their parental MDA-231 counterparts.

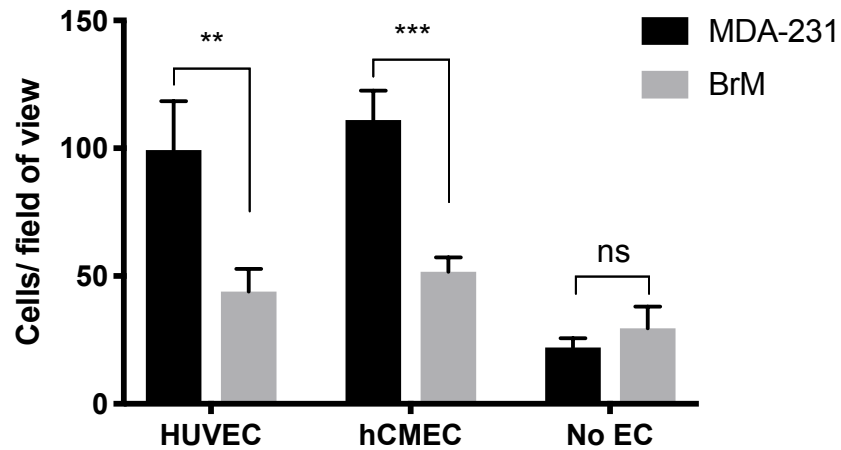


**Fig. 3.2. BrM line show reduced capacity to transmigrate across HUVEC and hCMEC monolayers compared to MDA-231.** For transendothelial migration assays, upper transwell chambers were seeded with HUVEC or hCMEC and left for 48hr to allow formation of confluent monolayers before the addition of MDA-231 or BrM cells. For simple chemotactic migration assays, MDA-231 or BrM cells were seeded to upper chambers of transwell in the absence of an endothelial monolayer. Cell tracker green labelled MDA-231 or BrM cells were seeded to upper chambers of transwell for 18hr before washing and fixing of membrane. Cells in the upper chamber were then removed and cells on the underside of the membrane were imaged and counted using ImageJ software. Data are representative of n=3 independent replicates. Error bars indicate standard error. Statistical analysis was performed using two-way ANOVA test. \*\*p<0.005, \*\*\*p<0.0005.

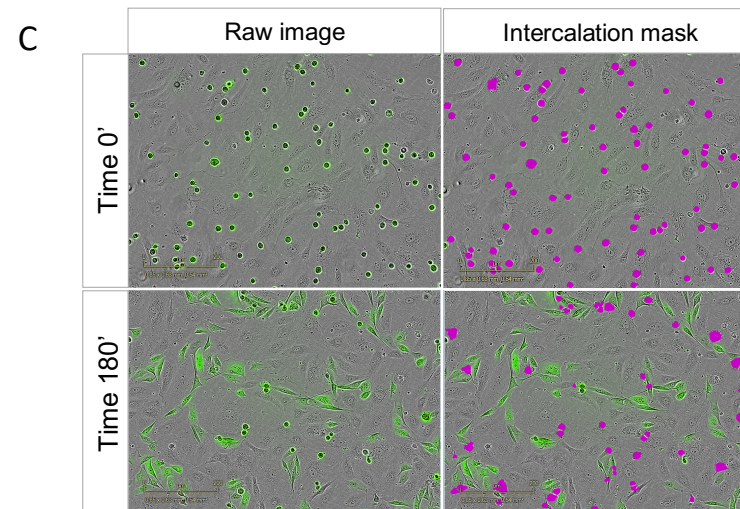
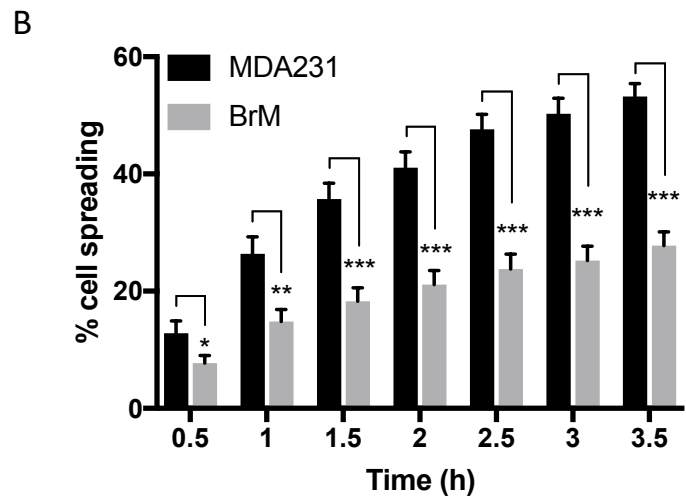
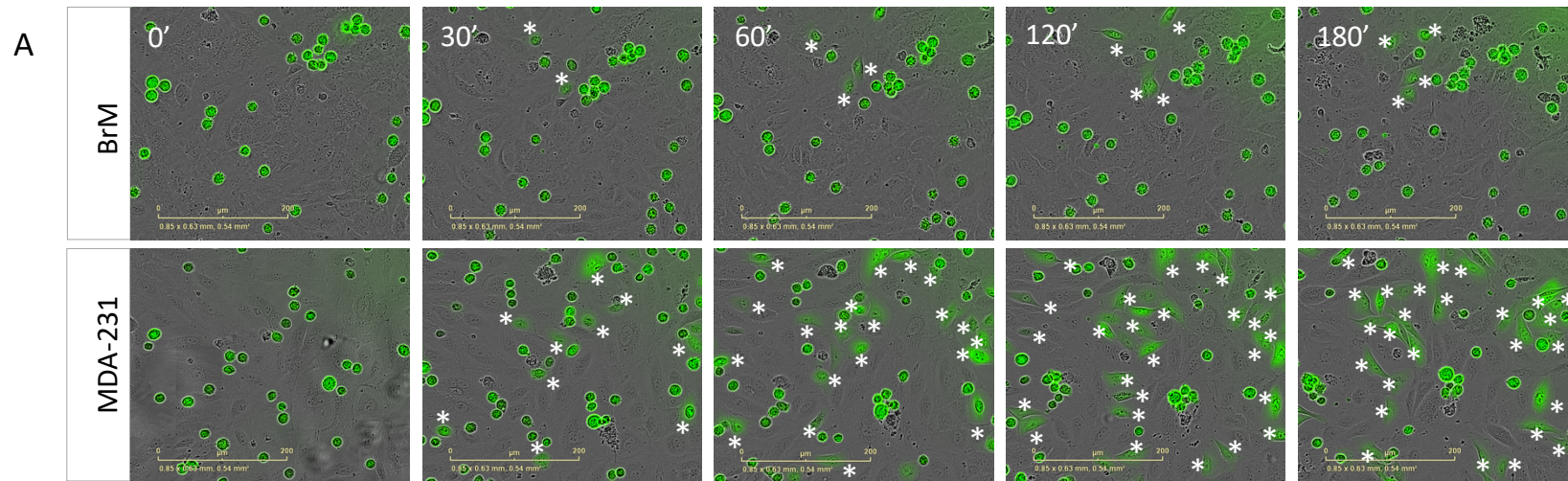


**Fig. 3.3. BrM show reduced capacity to intercalate into HUVEC monolayers compared to MDA-231. A,** MDA-231 and BrM cells were labelled and seeded on top of confluent HUVEC monolayers and imaged for 4h using Incucyte live cell imaging microscopy to capture intercalation of cancer cells. Asterisks indicate an intercalating cells. Scale bar: 200  $\mu\text{m}$ . **B,** Quantification of data in panel a, showing intercalation of cells as a percentage of total cells. **C,** Example of analysis mask used in quantifying intercalating cancer cells using Incucyte software. Cells masked in pink are detected as above a set threshold of circularity, indicating they have not undergone intercalation. Data are representative of n=3 independent replicates. Error bars indicate standard error. Statistical analysis was performed using students t-test. \* $p < 0.05$ , \*\* $p < 0.005$ , \*\*\* $p < 0.0005$ .

### **3.4 BrM express high levels of CD146**

To further investigate the phenotype of BrM cells, a small panel of cell surface receptors (CD44, CD99, CD155, CD146 and EPCAM) were tested for expression by flow cytometry, comparing BrM with MDA-231. As the focus of this study was to investigate the interactions of cancer cells and the endothelium, the receptors explored by flow cytometry were selected based on their reported function as adhesion molecules. This would highlight any pronounced differences between the two lines which may be contributing to the difference in TEM phenotype observed in Figures 3.2 and 3.3. CD44 has previously been implicated in the adhesion of cancer cell to the endothelium through binding of hyaluronan (Draffin et al., 2004). CD99 has not previously been investigated in terms of cancer cell adhesion, but is widely documented as mediating leukocyte endothelial interactions (Schenkel et al., 2002; Lou et al., 2007). CD146 (MCAM, MelCAM, MUC18), originally described as an adhesion molecule in metastatic melanoma, also has a reported function in the adhesion and transendothelial migration of monocytes (Xie et al., 1997; Bardin et al., 2009; Melnikova et al., 2009). Overexpression of EPCAM in breast cancer has been shown to correlate with poor prognosis (Gastl et al., 2000; Osta et al., 2004). Although no direct role has been reported for EPCAM in the adhesion of cancer cells to the endothelium, its expression is a useful indicator of metastatic phenotype of breast cancer cells and was hence incorporated into our panel of markers (van der Gun et al., 2010). Finally, CD155 has been implicated in the adhesion of leukocytes to endothelial cells and facilitates the TEM of leukocytes through vascular barriers (Sullivan, Seidman and Muller 2013; Reymond et al. 2004).

Results of cell surface phenotyping indicated high expression of surface CD146 on BrM compared to relatively low CD146 expression on MDA-231 cells (Figure 3.4A). Little difference was observed in the expression of the other receptors tested (CD44, CD99, CD155 and EPCAM) (Figure 3.4A). CD146 was found to be significantly increased when quantifying the median fluorescent intensity (MFI) of both MDA-231 and BrM from 3 independent experiments (Figure 3.4 B).

Analysis of CD146 expression of BrM and MDA-231 by western blotting also indicated higher protein expression of CD146 in BrM but and no differences in CD99 expression (Figure 3.4C). Immunofluorescent microscopy of CD146 was carried out to substantiate flow cytometry and again indicated high expression of CD146 in the BrM cells (Figure 3.5) with evidence of intense, punctate CD146 expression in BrM

cells viewed at higher magnification. Of interest, immunofluorescent microscopy of the actin cytoskeleton also indicated differences between the two lines. High expression of actin was localised in the protrusions of MDA-231 cells whereas this pattern of staining appeared to be absent in BrM (Figure 3.5). These data show that CD146 expression is significantly upregulated in the BrM cells compared to the MDA-231 cell line.

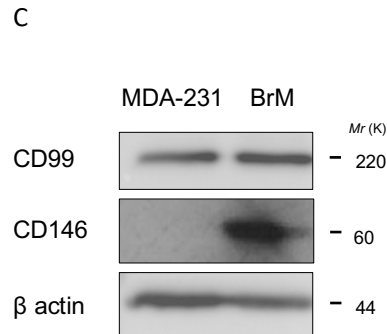
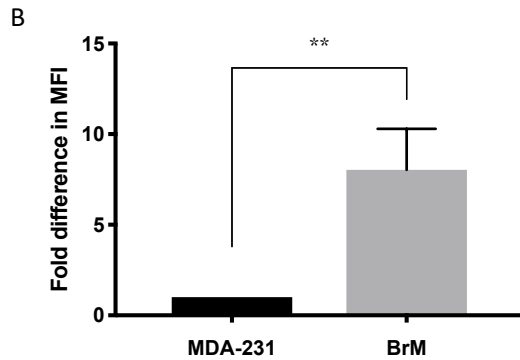
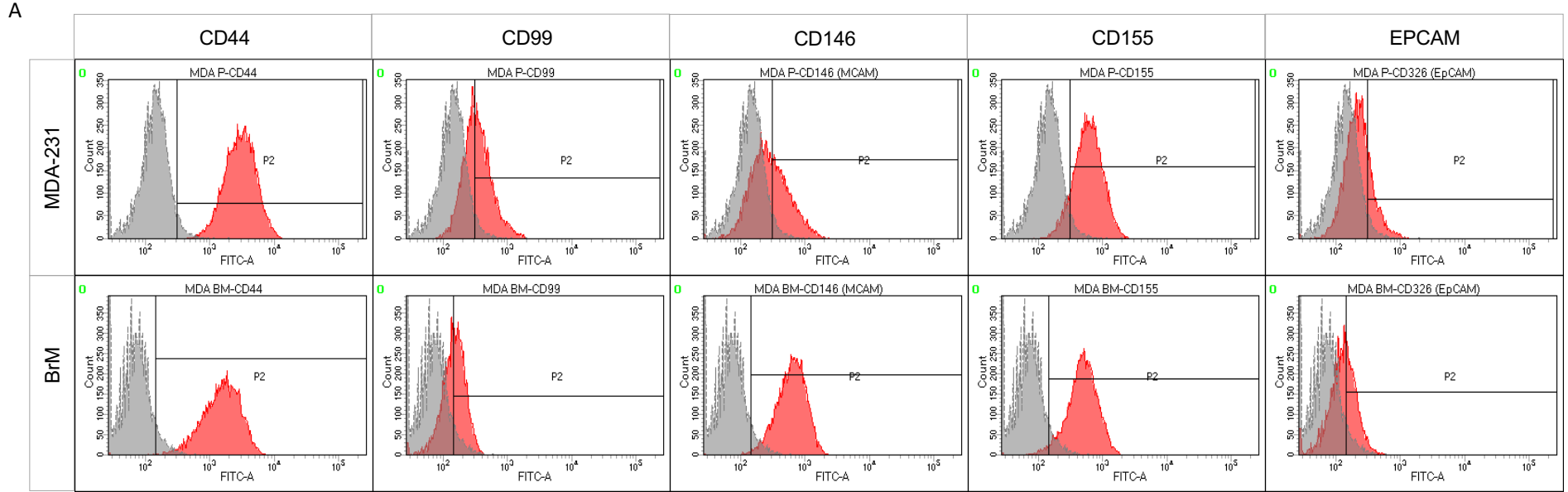


**Fig. 3.4. BrM express high levels of surface CD146 compared to MDA-231.** BrM and MDA-231 cells were fixed in 4% PFA and stained with indicated antibodies before analysis by flow cytometry. **A**, Histograms show grey isotype and indicated antibody staining of CD44, CD99, CD146, CD155 and EpCAM. **B**, Quantification of median fluorescent intensity of CD146 expression of MDA-231 and BrM cells. Data are representative of n=3 independent replicates. Error bars indicate standard error. Statistical analysis was performed using students t-test. \*\*p<0.005. **C**, Western blot indicating CD146 expression in MDA-231 and BrM cells.

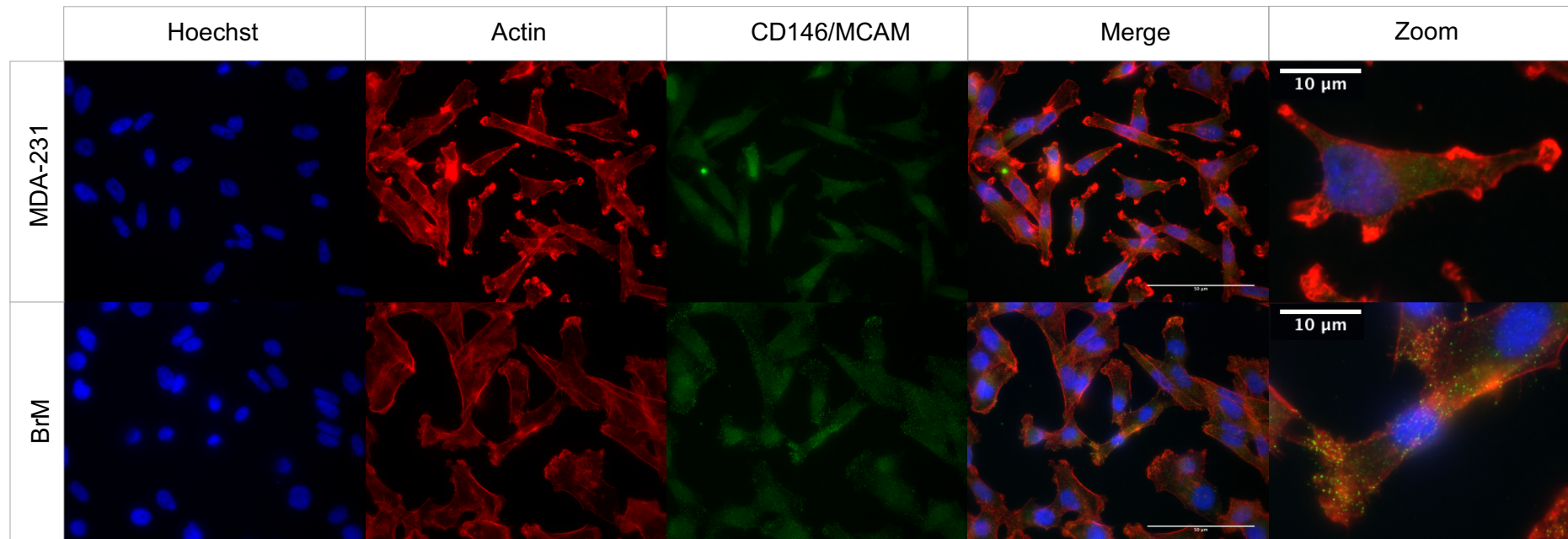


**Fig. 3.5. BrM express high levels of CD146 compared to MDA-231.** Immunofluorescent microscopy of BrM and MDA-231. Cells were grown on coverslips to subconfluency before fixation in 4% PFA and stained as indicated. Images were taken in 3 random fields of view using Nikon TiE widefield microscope. Images were assembled using ImageJ. Scale bar: 50 $\mu$ m (10 $\mu$ m in zoom image).

### **3.5 CD146 depletion increases adhesion and TEM of BrM**

As large differences in TEM (Figure 3.2) and CD146 expression (Figure 3.4 and 3.5) had been observed in BrM cells compared to MDA-231, it was hypothesised that there was a relationship between CD146 expression and the capability of BrM cells to transmigrate. As previously mentioned, CD146 has been implicated in the TEM of melanoma cells and monocytes (Xie et al., 1997; Bardin et al., 2009; Melnikova et al., 2009). Therefore, siRNA was used to target CD146 in BrM and MDA-231 cells to investigate the effects of knocking down CD146 on adhesion and TEM.

siRNA depletion of CD146 was achieved using standard transfection methodologies (see section 2.2.3) and resultant expression assessed by flow cytometry; high efficiency of knockdown was evident in BrM with a 75% reduction in expression (Figure 3.6A-B). Although the expression of CD146 on MDA-231 is significantly lower than that of BrM cells, a consistent and significant reduction of CD146 expression could still be achieved using CD146 siRNA on the MDA-231 cells (Figure 3.6C-D).

Adhesion assays were carried out to investigate whether the depletion of CD146 impacted on the ability of BrM or MDA-231 cells to adhere to endothelial monolayers. Unexpectedly, CD146 depletion significantly increased the number of both MDA-231 and BrM cells bound to the HUVEC endothelial monolayer at the 60 and 120-minute timepoints (Figure 3.7A-B). Conversely, (Melnikova et al., 2009) showed that knockdown of CD146 by shRNA in melanoma cells significantly reduced adhesion to human dermal microvascular endothelial cells. Coupled with the results above, this suggests that the role of CD146 in adhesion to endothelial cells is dependent upon the identity of the interacting cell types used and this itself is a likely reflection of cell type specific differences in the array of receptors that regulate cell adhesion events.

Next, the ability of CD146 depleted BrM and MDA-231 cells to intercalate into endothelial monolayers was assessed by live cell microscopy. Quantification of cell intercalation of CTG labelled cells indicated that CD146 knockdown had little impact on spreading and intercalation of either MDA-231 and BrM CD146 depleted cells and the endothelium (Figure 3.7D).

To assess TEM using another method, transwell migration assays were used to investigate TEM of CD146 depleted MDA-231 and BrM cells. Results showed that CD146 depleted BrM cells significantly increased the number of transmigrating cells,

suggesting an increased migratory and invasive phenotype (Figure 3.8A-B). These results suggest that CD146 does not play a role in intercalation of EC monolayers but that CD146 does suppress BrM TEM.

The depletion of CD146 in MDA-231 has previously been shown to inhibit migration and TEM (Zabouo et al., 2009). In agreement with this, knockdown of CD146 in MDA-231 reduced the number of cells undergoing TEM after 18 hours (Figure 3.8C). However, in transwells (with the absence of EC), an increase in migrating MDA-231 cells was observed (similar to the phenotype of BrM).

Taken together, these results suggest that the depletion of CD146 in BrM increases their ability to adhere and traverse EC monolayers, whilst depletion of CD146 in MDA-231 cells decreases their capacity to undergo TEM, but increases adhesion. This suggests that CD146 is acting to reduce the metastatic phenotype of BrM cells. To investigate whether these results observed are representative of breast cancer patients, survival curves using publicly available clinical data were utilised.

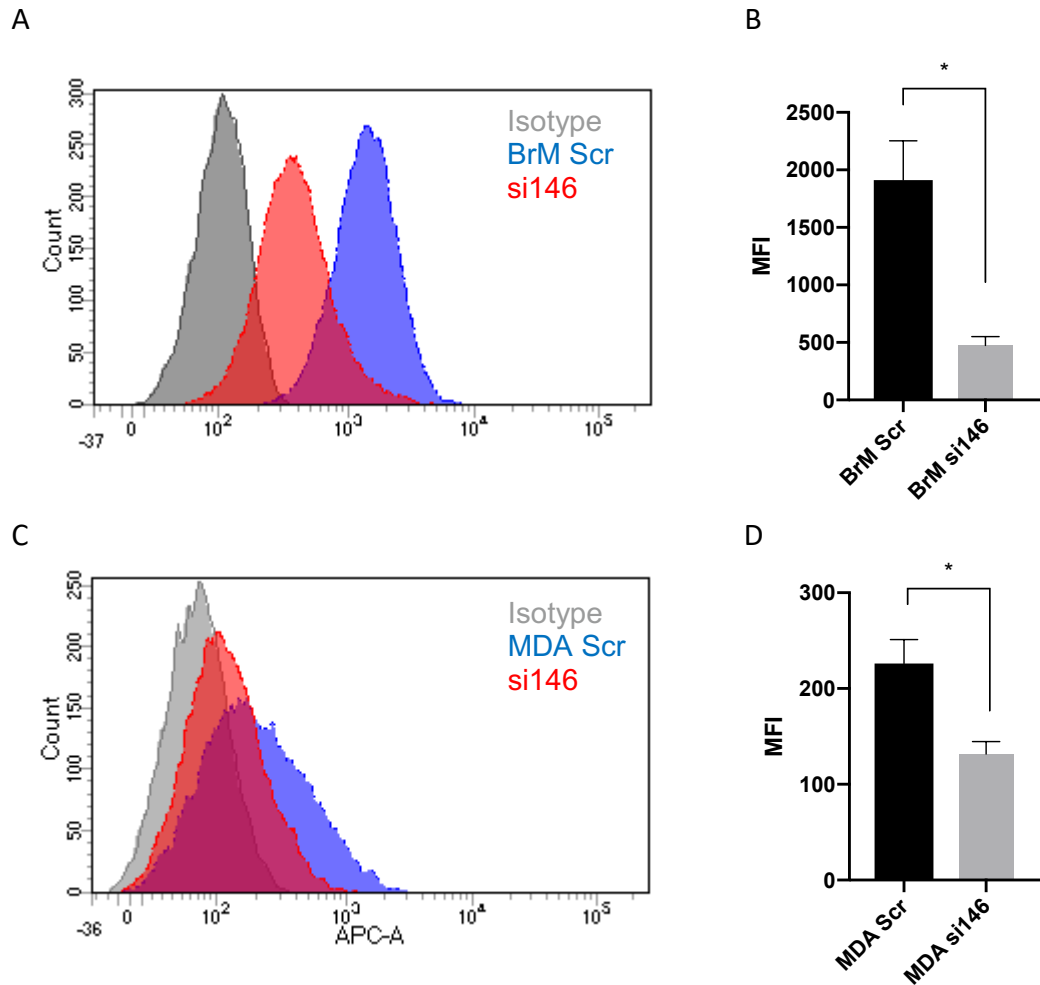


**Fig. 3.6. CD146 siRNA depletion in MDA-231 and BrM.** MDA-231 and BrM CD146 expression was knocked down using siRNA using standard transfection methods. CD146 knockdown was assessed by comparison to scrambled control by flow cytometry. Knockdown of CD146 was quantified by median fluorescent intensity as shown. **A**, BrM cells were transfected CD146 or scrambled control siRNA for 72h before analysis of cell surface CD146 by flow cytometry. **B**, Quantification of median fluorescent intensity of Scr and si146 treated BrM cells. **C**, MDA-231 cells were transfected CD146 or scrambled control siRNA for 72h before analysis of cell surface CD146 by flow cytometry. **D**, Quantification of median fluorescent intensity of Scr and si146 treated MDA-231 cells. Data are representative of n=3 independent replicates. Statistical analysis was performed using paired students t-test. \*p<0.05.

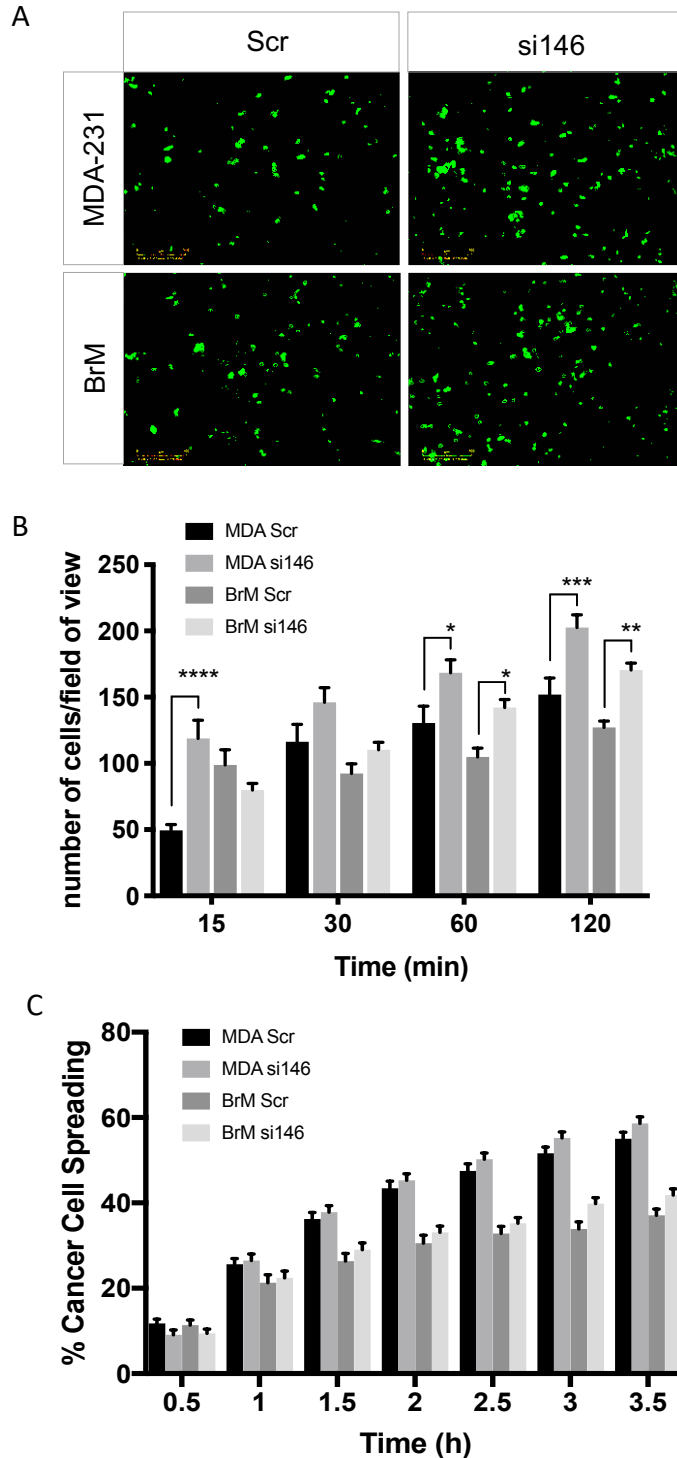


**Fig. 3.7. CD146 depletion increases MDA-231 and BrM adhesion but not intercalation.** **A**, MDA-231 and BrM cells were transfected CD146 or scrambled control siRNA for 72h before being CTG-labelled and left to adhere to confluent HUVEC monolayers for indicated time points. Unbound cells were washed away with PBS before fixation in 4% PFA and subsequent imaging. **B**, quantification of bound cells in adhesion assay. **C**, MDA-231 and BrM cells treated with CD146 siRNA were seeded on top of confluent HUVEC monolayers and imaged for 4h. Intercalating cells were quantified using Incucyte analysis software as a percentage of total cells. No significance in p values ( $<0.05$ ) was found when comparing Scr and si146 of MDA or BrM at any time point. Data are representative of  $n=3$  independent replicates. Error bars indicate standard error. Scale bars: 300  $\mu\text{m}$ . Statistical analysis was performed using two-way ANOVA test. \* $p < 0.05$ , \*\* $p < 0.005$ , \*\*\* $p < 0.0005$ , \*\*\*\* $p < 0.00005$ .

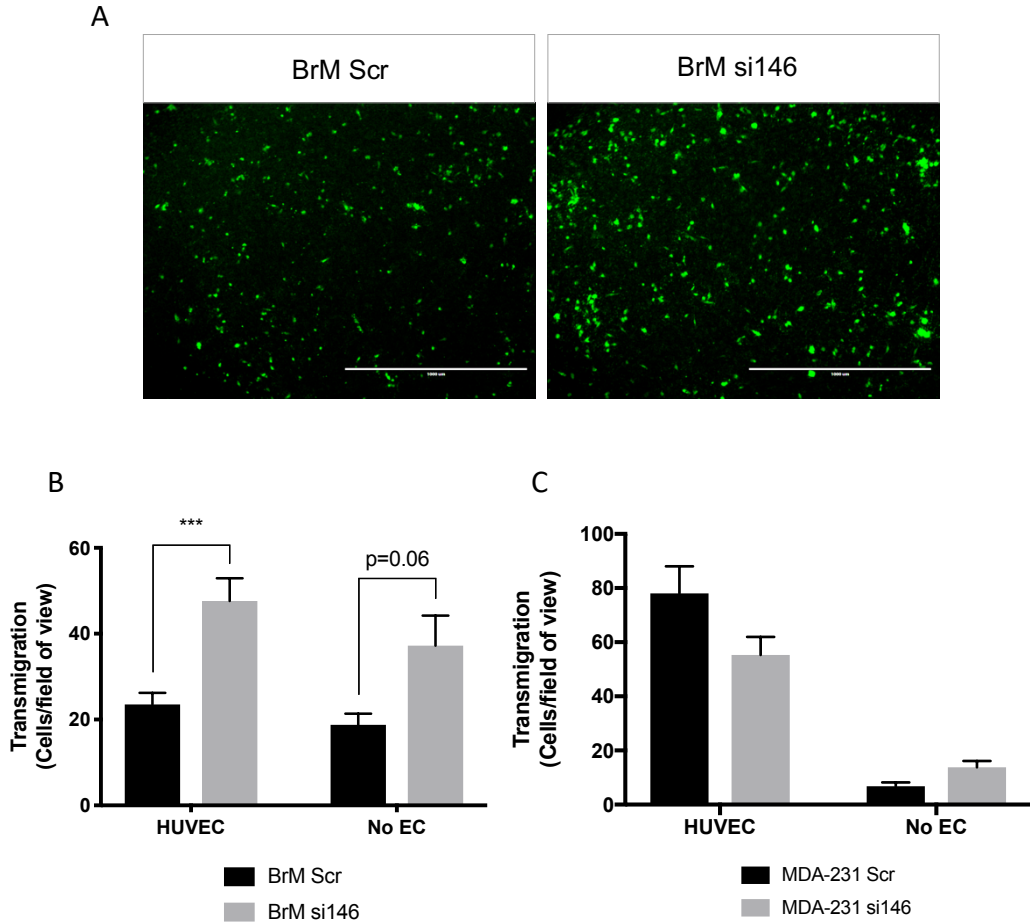


**Fig. 3.8. CD146 depletion increases BrM migration and transendothelial migration.** For transendothelial migration assays, upper transwell chambers were seeded with HUVEC and left for 48hr to allow formation of confluent monolayers before the addition of BrM treated with indicated siRNA. For simple chemotactic migration assays, BrM cells were seeded to upper chambers of transwell in serum free media in the absence of an endothelial monolayer. 10% FCS containing media was placed in the lower chamber to establish a chemotactic stimulus for migration. CTG labelled siRNA treated BrM or MDA-231 cells were seeded to upper chambers of transwell (+/- EC) for 18hr before washing and fixing of membrane. Cells in the upper chamber were then removed and cells on the underside of the membrane were imaged and counted using ImageJ software. **A**, Representative images of siRNA treated CTG BrM that have transmigrated through an EC monolayer. **B**, Quantification of BrM TEM shown in panel A. **C**, Quantification of siRNA treated MDA-231 transmigration (+/- EC). Data are representative of n=3 independent replicates for BrM data and n=2 independent replicates for MDA-231 data. Error bars indicate standard error. Scale bar: 1mm. Statistical analysis was performed using two-way ANOVA test. \*\*\*p<0.0005.

### 3.6 High CD146 expression negatively correlates with recurrence and metastasis free survival of ER and PR negative breast cancers

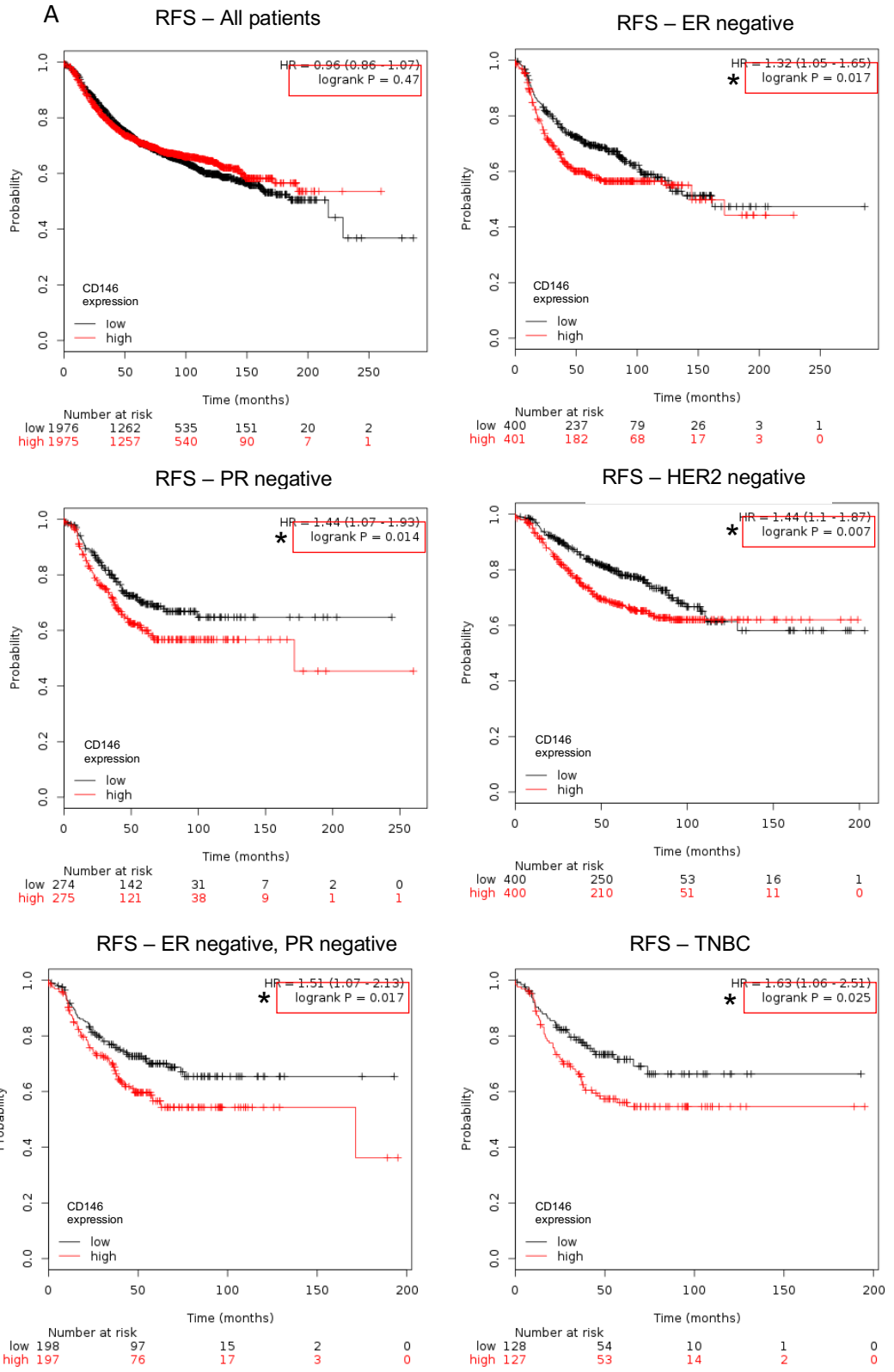
High expression of CD146 has been associated with poor prognosis using large patient data sets in a variety of solid tumours. Zeng et al. (2012) showed a strong correlation between TNBC and CD146 expression. Kruijff et al. (2018) show that CD146 is a prognostic factor of metastasis free survival and overall survival and that CD146 expression was most prevalent in TNBC cases. Garcia et al. (2007) showed that CD146 expression in tissue microarrays was indicative of poor prognosis and breast cancer metastasis. A recent meta-analysis also highlighted the prognostic importance of CD146 expression in assessing solid tumour progression in a number of different cancers (Zeng et al. 2017). In lung adenocarcinoma, IHC expression of CD146 was used to correlate expression with poor survival (Oka et al., 2012). However, no work to date has shown any association between CD146 expression and metastasis to the brain specifically.

The online tool (<http://kmplot.com/analysis/>) allows the generation of Kaplan–Meier survival curves to predict correlations between survival metrics and high or low mRNA expression (Lánczky et al., 2016). Microarray data have been acquired from 5143 different patient breast cancer samples. This tool was used to investigate whether CD146 expression is associated with increased or decreased recurrence free survival (RFS) or distance metastatic free survival (DMFS) in a cohort of breast cancer patients. Experimental data shown in this chapter indicates that CD146 regulates TEM of MDA-231, but suppresses BrM TEM. It was therefore predicted that *in silico* results would show that high CD146 expression confers reduced metastatic free survival, as the literature suggests. Results show that across all breast tumour samples, CD146 alone could not predict outcome of patient prognosis using RFS (Figure 3.9A). However, further stratification of these results by molecular subgrouping of tumours indicate that patients with ER<sup>neg</sup>, PR<sup>neg</sup>, ER<sup>neg</sup>+PR<sup>neg</sup> tumours and high CD146 expression had significantly worse prognosis than those with low CD146 expression (Figure 3.9A). Furthermore, patients harbouring HER2+ tumours and high CD146 also exhibited significantly decreased RFS as did patients with TNBC (Figure 3.9A). Next, the online tool was used to investigate whether CD146 expression could be used to predict DMFS of patients. As with RFS data, across all subtypes of breast cancer, CD146 expression alone could not predict outcome of metastasis (Figure 3.9B). Again, stratification of patients into PR<sup>neg</sup> or ER<sup>neg</sup>+PR<sup>neg</sup> clustering indicated that high CD146 expression in these groups

conferred an increased probability of metastasis (Figure 3.9B). Interestingly, ER<sup>neg</sup> stratification along with grouping of high and low CD146 expressing tumours did not result in any significant change in DMFS, suggesting a correlation between PR expression and CD146 expression in predicting DFMS. There was an insufficient number of samples to plot meaningful predictions of DMFS for TNBC cases; however, Kaplan–Meier curves suggest that high CD146 expression in these samples results in reduced DMFS.

These data show that, in agreement with previously reported studies, CD146 can be used as a determinant of patient outcome as those with high CD146 expressing breast cancers have a significantly poorer prognosis. In particular this was found in breast cancers which are hormone receptor negative and my results suggest that this might result from the role played by CD146 in adhesion and TEM. As the survival data does not indicate the origin of metastasis, it is hard to reconcile experimental results from the BrM line with that of the *in silico* data. Future work should focus on delineating whether high CD146 expression in primary tumours results in increased propensity in developing brain metastasis.

Data presented in this chapter has uncovered a potentially important role for CD146 in the progression of BCBM. Using an *in vitro* model of BCBM, CD146 was identified as being highly expressed on the brain metastasis derivative of the MDA-231 cell line. siRNA knockdown studies indicated that upregulation of CD146 modulated the adhesion and transmigration of both parental and BrM cells. Finally, mining of publicly available patient mRNA data revealed that increased CD146 expression was associated with decreased overall survival and increased rates of metastatic dissemination.



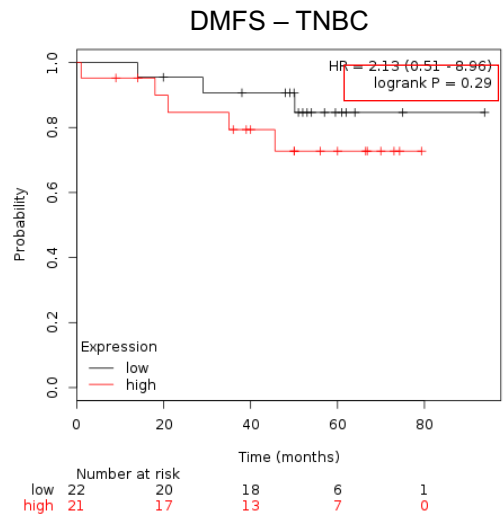
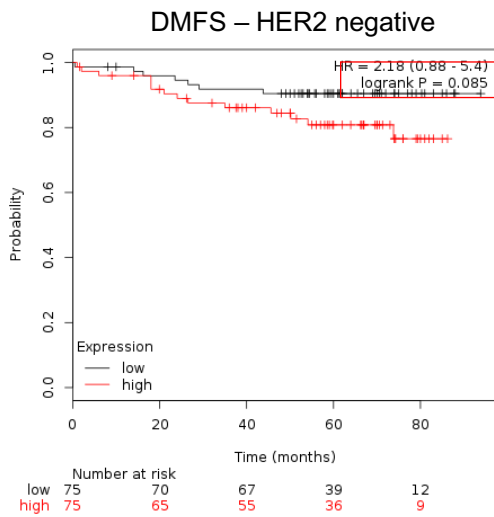
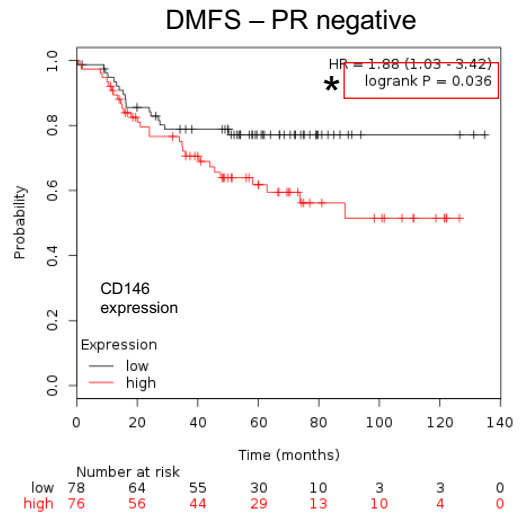
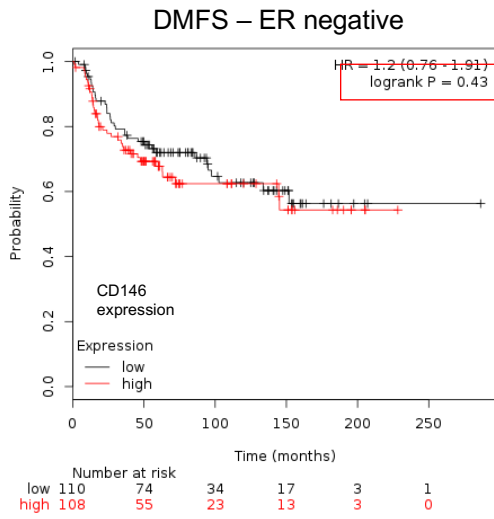
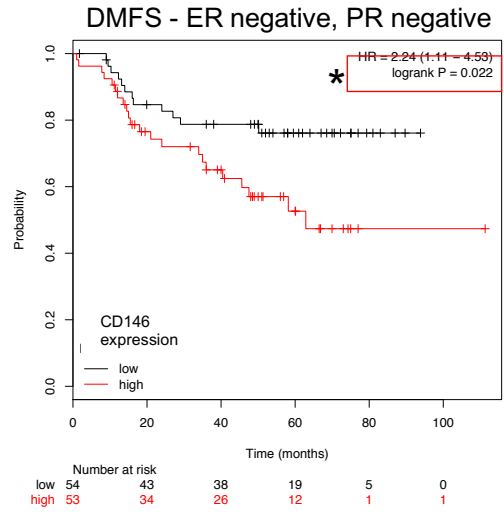
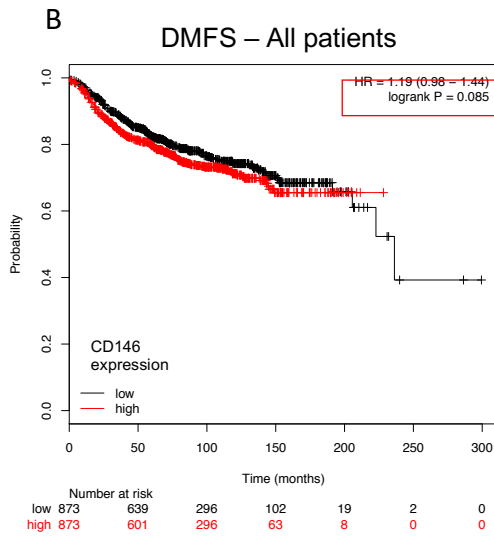


**Fig. 3.9. High CD146 expression in patient breast cancer correlates with poor survival and probability of metastasis.** Kaplan-Meier survival curves were generated for high and low CD146 mRNA expression in breast cancer patients using an online tool ([www.kmplot.com](http://www.kmplot.com)) (Lánczky et al., 2016). **A**, Probability of relapse-free survival (RFS) was generated across all patient samples with high and low CD146 expression. Further stratification was performed according to molecular subtypes of breast cancer as indicated in panels. **B**, Probability of Distant Metastatic Free Survival (DMFS) was generated across all patient samples with high and low CD146 expression. Further stratification was performed according to molecular subtypes of breast cancer as indicated in panels. Statistics were performed by software within the online tool used. \* $p < 0.05$

### 3.7 Discussion

This chapter describes how the brain metastatic variant (BrM) of the TNBC cell line MDA-231 was used to investigate the tropism of breast cancer cells to the blood brain barrier. The hypothesis was that the brain tropism of BrM cells is in part due to their ability to specifically bind to endothelial cells of the BBB to enable access to the brain parenchyma. The hCMEC cell line has been widely used as a model of the endothelial cell component of the BBB (Dauchy et al., 2008; Coureuil et al., 2010; Haqqani et al., 2013; Infanger et al., 2013). Here, hCMEC and BrM cell lines were utilised to investigate the adhesion and TEM of breast cancer brain metastasis (BCBM) *in vitro*. CD146 was found to be highly expressed by BrM cells compared to MDA-231 cells. Knockdown with siRNA was used to determine whether CD146 was implicated in the regulating interactions between BrM and endothelial cells to facilitate adhesion and TEM. Finally, microarray data from an online cohort of patient data, was used to see whether CD146 correlated with decreased survival and metastatic dissemination of breast cancers.

Using the well characterised model of *in vivo* passaged metastatic cells with specificity for the brain, BrM cell adhesion and migration across BBB ECs was investigated. Adhesion at time points of 60 minutes differed significantly (Figure 3.1) and showed MDA-231 bind preferentially to HUVEC over BrM cells (Figure 3.1A), and BrM preferentially adhere to hCMEC over MDA-231 (Figure 3.1B). At first this appears to agree with the hypothesis that BrM cells show preference in adhering to BBB-derived hCMEC cells compared to non-homing MDA-231. However, this was not consistently found at other time points, and comparing adhesion of both cancer lines to either HUVEC or hCMEC indicated that both MDA-231 and BrM bound very poorly to hCMEC, an issue which is addressed further in subsequent chapters. A previous comparison of hCMEC and primary brain rat endothelial cells indicated that melanoma cells bound in far greater numbers to hCMEC (Fazakas et al., 2011). However, in this study the authors suggest that the difference in host species of the ECs probably accounts for this difference. It is broadly cited that adhesion of cells to the BBB is increased in inflammatory scenarios, and that otherwise, adhesion molecules show low expression in BBB ECs, in order to limit the influx of immune cells into the brain (Engelhardt and Ransohoff 2012). This is highlighted by studies which show that E- and P-selectin expression is not induced in the BBB in cerebral autoinflammatory models and does not facilitate the adhesion or transmigration of leukocytes (Engelhardt et al. 1997; Barkalow et al. 1996). Additionally, T cells were

shown to arrest in CNS microvasculature without rolling (presumably due to the lack of functional selectins), relying instead on  $\alpha 4$  integrin-VCAM1 interactions for adhesion (Vajkoczy, Laschinger and Engelhardt 2001). This could explain the relatively low adhesion of cancer cells to hCMEC monolayers compared to HUVEC monolayers.

As no consistent differences in the adhesion of MDA-231 or BrM to ECs was observed, the ability of BCs to cross BBB vasculature was investigated. BrM cells appeared to show a defect in TEM compared to MDA-231 *in vitro*. This was apparent across both HUVEC and hCMEC monolayers where little difference in cancer cell TEM was noted, although Transwell migration in the absence of ECs was enhanced in BrM compared to MDA-231 cells. The success of metastasis relies heavily on the extravasation of cancer cells to target organs (Gupta et al., 2007). It has previously been shown that extravasation of metastatic cells in the brain is a prolonged process in comparison to extravasation of other organs (Paku et al., 2000; JuanYin et al., 2009; Loriger and Felding-Habermann, 2010). The difference in organ specific rates of transmigration are presumably due to differences in vascular barrier function. Metastatic cells have been found to reside intraluminally in brain capillaries for up to 7 days before extravasation is complete (Loriger and Felding-Habermann, 2010). Whereas extravasation in other organs can be completed within 6 hours (Paku et al., 2000). This may offer an explanation as to the difference in TEM observed between MDA-231 and BrM. Additionally, *in vivo* brain metastasis studies have indicated that a small percentage of BrM cells will remain intraluminal and not undergo TEM (Loriger and Felding-Habermann, 2010). It is possible that this effect is exacerbated *in vitro* and may contribute to the reduced TEM of BrM compared to MDA-231.

The greatly reduced ability of BrM cells to undergo TEM suggests that these cells may have lost their migratory capacity. It has been shown that during the metastatic cascade, disseminating cells from the primary tumour undergo EMT to acquire invasive and migratory traits that are required for successful dissemination (Thiery et al., 2009). Reversal of this EMT state has also been shown to be crucial in the formation of metastatic sites post extravasation (Ocaña et al., 2012; Tsai et al., 2012). As MDA-231 and BrM cells represent aspects of the metastatic process, it is possible that BrM cells have undergone MET reprogramming, resulting in reduced invasive and migratory potential, compared to MDA-231 which are arguably still in a mesenchymal state. This reversal may explain the reduced migration of BrM cells in

comparison to MDA-231, although alterations in expression of plasma membrane proteins may also contribute.

In agreement, flow cytometry of cell surface markers showed that CD146 expression was markedly increased in BrM cells compared to MDA-231. Increased CD146 expression has been described for breast cancer cell lines and patients' samples in many studies (Zeng et al. 2012; de Kruijff et al. 2018; Garcia et al. 2007; Zeng et al. 2017; Imbert et al. 2012), however the precise role that CD146 plays in the aetiology of breast cancer is contradictory. Originally described as a cell adhesion molecule of melanoma cells (Lehmann, Riethmüller and Johnson 1989), CD146 has since been shown have a multifaceted role in a number of cell types, from endothelial cell-cell contacts, to neuronal development (Bardin et al., 2001; Tu et al., 2013). In breast cancer, it has been shown that CD146 controls the EMT, with overexpression of CD146 found to drive cells towards a more mesenchymal state with greater invasive capacity *in vitro* and *in vivo* (Zeng et al. 2012). Furthermore, knockdown of CD146 expression in MDA-231 decreased invasive potential and reversed EMT (Zeng et al. 2012). Work from Zabouo et al. (2009) shows similar results, where shRNA knockdown of CD146 in MDA-231 reduced vimentin expression and motility/invasion. Another study implicated CD146 expression in invasion and motility, similarly showing that forced expression in MCF7 increased these attributes, whereas blocking endogenous CD146 expression in MDA-231 reduced invasion and motility (Zeng, Cai and Wu 2011). This body of work suggests a pro-invasive role for CD146 in breast cancer.

Conversely, a number of studies suggest a tumour suppressive role for CD146. CD146 was proposed as a tumour suppressor by Shih et al. (1997) who showed by IHC that CD146 expression was present in a number of normal breast epithelia samples, but was present in very few breast cancer cases. Additionally, this study showed that forced expression of CD146 also produced smaller tumours *in vivo*, indicative of a suppressive role for CD146 (Shih et al., 1997). Mishra et al. (2015) suggest that sema3a attenuates breast cancer growth and vascularization through the PTEN-dependent, FOXO3-driven expression of CD146. This was shown in MDA-231 cells, both *in vitro* and *in vivo*, to suppress BC invasion (Mishra et al. 2015). Furthermore, work from Chakraborty et al. (2006) showed in the ER positive breast cancer cell line MCF7, activation of the non-receptor protein-tyrosine kinase Syk, following exposure to hypoxia, upregulated CD146 expression and subsequently attenuated *in vivo* xenograft breast cancer progression. Thus, CD146 expression

may be suppressive to cancer development under some circumstances. It has also been suggested that there is an inverse relationship between CD146 and CD44, where forced doxycycline-induced CD44 expression in MCF7 cells decreased CD146 expression (Ouhtit et al., 2017). Upon siRNA suppression of this increase in CD146, greater invasive potential was conferred to cells in Transwell migration assays (Ouhtit et al., 2017). Overall, these studies outline a tumour repressive role of CD146 in breast cancer progression. These opposing depictions of CD146 were therefore considered when investigating CD146 expression in the BrM model.

Previously, MDA-231 preference to metastasise to the bone *in vivo* was shown to be attributable to CD44 expression which was upregulated in bone seeking MDA-231 cells (Yoneda et al., 2001). CD44 is known to bind to hyaluronic acid with great affinity, which is highly expressed in the bone microenvironment (Draffin et al., 2004). The bone seeking subclone was also shown to preferentially adhere to human bone microvascular endothelial cells (HBMECs), indicating that the preference for bone metastasis may be directed by their increased capacity to bind bone microvasculature through upregulated CD44 expression (McFarlane et al., 2015). It was hypothesised that the same logic may apply to the BrM subclone and that high CD146 expression, which was found exclusively in the BrM cells, may be influencing the capacity of BrM cells to adhere to EC monolayers. As already mentioned, CD146 has a reported function in the adhesion and transendothelial migration of monocytes (Xie et al., 1997; Bardin et al., 2009; Melnikova et al., 2009). CD146 knockdown appeared to significantly increase the adhesion of both MDA-231 and BrM cells at multiple time points (Figure 3.6D). This was unexpected given the role of CD146 in adhesion of monocytes and cancer cells. However, evidence of CD146 as a negative regulator of  $\alpha 3\beta 1$ ,  $\alpha 5\beta 1$  and  $\alpha 7\beta 1$  integrins which mediate adhesion of fibroblasts to laminin1 has previously been reported (Alais et al., 2001). Alterations in integrin expression upon CD146 loss could explain the increased adhesion observed upon CD146 depletion. The interaction between CD146 and integrins has previously been considered in endothelial cells, where a biochemical association between CD146 and integrins was absent (Bardin et al., 2001). This suggests that CD146 integrin regulation in adhesion may be cell type specific. It was reported by Xie et al. (1997) that forced expression of CD146 in melanoma cells increased adhesion to HUVEC and increased metastatic potential, but conversely reduced adhesion to laminin. Interestingly, T cells that express CD146, bind to laminin411 in the CNS vasculature and undergo TEM, mediating the recruitment of TH17 cells and promoting the development of MS (Flanagan et al., 2012). These lines of evidence suggest a role for CD146 in the regulation of adhesion to laminins, however they fail to

comprehensively explain the altered adhesion to endothelial cells, as laminins are a key component of the basement membrane (Yurchenco, Cheng and Colognato 1992).

The depletion of CD146 in MDA-231 caused a decrease in TEM compared to scrambled control, in line with reports which suggest that CD146 is required for MDA-231 TEM (Figure 3.7C)(Zabouo et al., 2009). Intriguingly, CD146 depletion in BrM cells had the opposite effect, reducing TEM and suggesting a differential role for CD146 in MDA-231 and BrM TEM. A number of studies have implicated CD146 in the regulation of MMP activity and expression (Imbert et al., 2012; Ouhtit et al., 2017). Therefore, the depletion of CD146 and consequent increase in TEM of BrM cells may be due to enhanced activity or expression of MMPs which facilitate increased TEM through degradation of endothelial cell-cell contacts (Reymond, d'Água and Ridley 2013). Other studies using patient derived brain metastasis alongside MDA-231 have been shown to upregulate MMPs (Bos et al., 2009). It would be of great interest to investigate whether other breast cancer brain metastasis models such as those used by Bos et al. (2009) also exhibit upregulation of CD146.

The apparent opposite role of CD146 in MDA-231 and BrM cells may relate to the different points in metastasis that these two lines represent, suggesting that the function of CD146 differs depending on the stage of metastasis in question. As MDA-231 represent a heterogenous population of metastatic cells which are able to form metastases at a number of sites around the body, CD146 function may facilitate extravasation allowing metastatic cells to survive and form secondary colonies. Without CD146 they are less capable of this (Figure 3.7C) (Zabouo et al., 2009). It is also possible that high CD146 expressing BrM may be a consequence of microenvironmental cues within the brain which induce CD146 expression. For example, CD146 has been shown to be important in the pericyte coverage of the blood brain barrier, as pericyte specific knockout mice resulted in decreased pericyte coverage of cerebral vasculature (Chen et al., 2017). Furthermore, metastatic cells have been shown to co-opt blood vessels in a pericyte-like manner during brain metastasis formation (Ghajar et al., 2013). However, the role of CD146 in pericyte-like coverage of vessels during metastasis is unknown.

The role of CSCs are important in the establishment of metastatic disease as they are endowed with tumour initiating capabilities which are required in the colonisation of secondary tissues (Lambert, Pattabiraman and Weinberg 2017). Therefore, EMT

is considered an important aspect of generating CSC traits (Mani et al., 2008). CD146 was shown to drive EMT and increase CSC-like properties in breast cancer (Zeng et al. 2012). It has been shown that CD146-expressing CSCs cells were also CD44-positive and CD24-negative, indicative of altered CSC properties (Zeng et al. 2012; Imbert et al. 2012). Investigation using IHC in breast cancer samples revealed CD146 expression has also been shown to strongly correlate with nestin, another well-established marker of stem like cells (Tampaki et al., 2017). In this study, nestin and CD146 expression was also found to correlate with TNBC status of breast cancer. The role of CD146 in establishing CSC populations in breast cancer brain metastasis has never been explicitly researched. Flow cytometry results indicated similar levels of CD44 expression in MDA-231 and BrM cells, however CD24 expression was not investigated (Figure 3.4A). Additionally, Zeng et al. (2012) found that CD146 expression dramatically altered cytoskeletal reorganisation through modulation of the GTPase RhoA. The activity of GTPases is known to be widely implicated in the activation of EMT (Yilmaz and Christofori, 2009). Immunofluorescence microscopy results indicated that MDA-231 exhibited dramatically altered actin cytoskeletal structure compared to BrM cells, with reduced actin rich protrusions present in the latter (Figure 3.5). As CD146 has been shown to regulate RhoA activity by Zeng et al. (2012), it is tempting to speculate that the altered actin arrangement of BrM is due to CD146-mediated GTPase activity.

The use of cell lines can be useful in gaining insight into mechanisms of metastasis, however cell lines such as MDA-231 and BrM are only representative of single cases of metastatic breast cancer, and so the validation of results using clinical data can be more informative. To reconcile experimental data with *in silico* data, CD146 expression was explored using online microarray datasets of breast cancer patient samples. Previous work has shown that CD146 expression correlated with metastatic disease and reduced survival (Zeng et al. 2012; de Kruijff et al. 2018; Garcia et al. 2007; Zeng et al. 2017). A strong correlation with high CD146 expression and recurrence was found in TNBC (Figure 3.9A), similar to results shown by (Zeng et al. 2012). These results, coupled with *in vitro* data showing that CD146 depletion reduced MDA-231 TEM, suggest a pro-invasive role for CD146, through regulation of invasive phenotype and TEM.

However, depletion in BrM cells increased TEM and migration, in opposition to results of MDA-231. One of the limitations of the *in silico* dataset are that the specific sites of metastasis in metastatic-free-survival data are not known. It would be of great

interest to know if high CD146 expression has a greater probability of resulting in metastasis to the brain, to validate *in vitro* results using the BrM cell line. Furthermore, exploration of protein levels of CD146 in clinical samples, using tissue microarrays for example, would also be of great interest as Kaplan-Meier plots were generated using mRNA expression data. Results presented in this chapter indicate a potential role for CD146 in the establishment of BCBM, through modulation of interactions between BBB endothelial cells and metastatic breast cancer cells. The next chapter describes the further characterisation of the BBB cell line hCMEC, as a model of the endothelial component of the BBB.

## Chapter 4 Regulation of the endothelial cell phenotype by p53

### 4.1 Introduction

The blood brain barrier (BBB) tightly regulates the transport of molecules (>400-500 Da) between the haematogenous circulation and the brain parenchyma (Banks, 2009). However, the BBB can be crossed by haematopoietic cells during infection and inflammation and by tumour cells during metastasis. In some scenarios, the dysfunction of the cerebral vasculature is secondary to the disease, but can greatly exacerbate symptoms and progression of the condition (Carvey, Hendey and Monahan 2009; Daneman 2012). For example, in some neurodegenerative disorders such as Alzheimer's disease, breakdown of the BBB is observed at early stages of the disease, but the exact role in the pathogenesis is yet to be fully elucidated (Montagne, Zhao and Zlokovic 2017). Thus, regulation of the BBB remains an area of research warranting further investigation.

A key obstacle in the development of targeted therapeutics for brain disease is the selective nature of the BBB, which limits the size and nature of compounds and ultimately their efficacy. At the apical-most layer of the BBB lies a contiguous layer of specialised endothelial cells, the subject of experiments described in this chapter. However, limited availability of brain tissue combined with the difficulty in purifying and culturing primary brain endothelial cells has restricted research in this area. This highlights the need for representative models of the BBB for the in-depth study of transport across the BBB in health and disease. Immortalised brain-derived endothelial cells represent such models.

The immortalised cell line hCMEC cell line has previously been used to study the endothelial component of the BBB (as described in section 3.7), where the cells were employed to study the interactions between breast cancer cells and the endothelium of the cerebral vasculature during brain metastases. This followed on from previous studies utilising this cell line to recapitulate the endothelial component of the BBB both *in vitro* and *in vivo* (Coureuil et al., 2009; Khaitan et al., 2009; Cristante et al., 2013; Infanger et al., 2013). The hCMEC cell line was isolated from a brain tissue sample acquired during elective surgery of an epilepsy patient. The selected endothelial cells were transduced with SV40 Large T antigen (Tag) and the telomerase component, hTERT, to achieve immortalisation (Weksler et al. 2005). SV40 Tag binds p53, inactivating its canonical functions whilst retaining high levels of p53 protein (Linzer and Levine 1979; Lane and Crawford 1979). SV40 Tag also

binds retinoblastoma protein (Rb), causing release of the Rb-bound transcription factor, E2F (DeCaprio et al., 1988). The inhibition of normal functions of p53 and Rb upon binding by SV40 Tag, induces high rates of proliferation and unchecked entry into the cell cycle. Following derivation of the hCMEC cell line, it was reported that the immortalised cells expressed several endothelial specific cell markers including CD31 and VE-cadherin, whilst also retaining tubule formation on particular matrices (Weksler et al. 2005). Other studies have sought to define the suitability of hCMEC cells as a model of the human BBB, by examining the expression of specific transporters, however results appear to be mixed (Ohtsuki et al., 2013a). Surprisingly though, the angiogenic response of hCMEC cells had not been studied in-depth.

Given that this cell line has been highly cited as a model of the endothelial component of the blood brain barrier (Dauchy et al., 2008; Coureuil et al., 2010; Haqqani et al., 2013; Infanger et al., 2013), work in this chapter sought to define whether hCMEC cells are an appropriate tool for studying the BBB. In doing so, results shown here provide a rationale for a greatly improved model of the BBB phenotype, derived from a simple modification of the parental hCMEC cell line. To my knowledge there are no published studies comparing the angiogenic function of hCMEC cells to other established endothelial cell lines. This work paves the way for much needed, improved models of endothelial BBB, necessary to allow further development in the study of the cerebral vasculature.

## **4.2 The expression of EC surface markers by the hCMEC cell line**

An initial comparison of endothelial cell markers was performed, comparing the phenotype of the immortalised hCMEC to the commonly used source of primary endothelial cells, HUVEC (Figure 4.1). Flow cytometry identified a number of endothelial specific markers, such as CD146/MCAM expressed by the hCMEC EC line. Other markers known to be expressed by endothelial cells such as CD99 and CD155, appeared to be expressed at similar levels between the two cell lines. Furthermore, the hyaluronan receptor CD44 exhibited slightly elevated expression in hCMEC cells, as did the epidermal growth factor receptor (EGFR) (Figure 4.1). The greatest differences noted were that of the expression of the haematopoietic/endothelial progenitor marker CD34, which was more highly expressed on hCMEC cells, along with the adhesion molecule ICAM-1 (CD54) compared to HUVECs (Figure 4.1). The CD34 molecule is expressed by endothelial progenitor cells and notably by tip cells of developing vasculature during angiogenesis (Fina et al., 1990; Siemerink et al., 2012). Conversely, the expression of CD34 is lost in endothelial cells of established arteries and veins (Fina et al., 1990). This initial comparison highlighted several differences in expression of cell surface markers between the immortalised hCMEC and primary non-brain HUVEC cell lines.

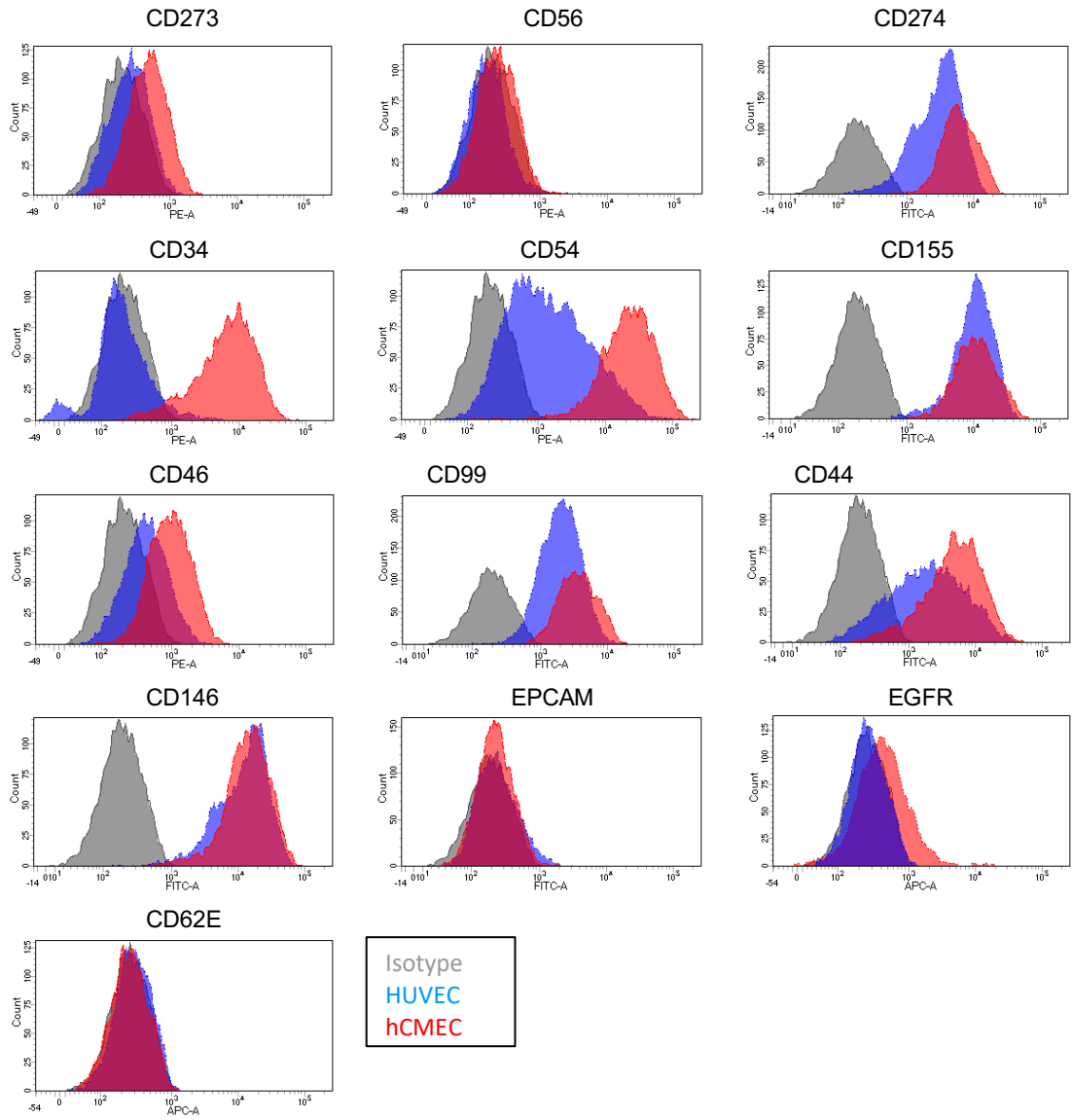


**Fig. 4.1. hCMEC express a number of endothelial cell surface markers.** Flow cytometry was used to examine expression of a small panel of cell surface markers (CD273, CD56, CD274, CD34, CD54, CD155, CD46, CD99, CD44, CD146, EPCAM, CD31, CD62E, CD144 and EGFR) including a number of endothelial specific markers (CD31, CD144 and CD146). HUVEC and hCMEC cells were grown to confluency before gentle trypsination and subsequent staining. Histogram overlays were assembled using FACS DIVA software. Isotype control (grey histograms), HUVEC (blue histograms), hCMEC (red histograms).

### **4.3 hCMEC express reduced VEGFR2 and exhibit greatly reduced angiogenic potential**

Arguably the most important function of the vascular system is the ability to form a network of tubules allowing dissemination of oxygen (via red blood cells) and nutrients. Development of this vascular network is primarily mediated through the VEGF signal transduction pathway (Hoeben et al., 2004). Binding of VEGFA to the receptor VEGFR2, results in synchronous activation of multiple signalling pathways mediating the migration, proliferation, and cell survival required for successful angiogenesis (Abhinand et al., 2016). The MAPK and PI3K pathway form two major branches of signal transduction induced by tyrosine phosphorylation of VEGFR2 (Koch et al., 2011) (Figure 4.2A).

A direct comparison of VEGFR2 expression and function between hCMEC and other endothelial cell lines has not been previously reported. Thus, I compared VEGFR2 expression in hCMEC cells to the commonly used non-brain endothelial cell line, HUVECs. Examination of VEGFR2 expression by immunofluorescence microscopy revealed a deficit of VEGFR2 in hCMEC when compared to HUVECs (Figure 4.2B). As previously discussed (section 1.6.3), VEGFR2, together with VEGFR1, is the main receptor of VEGFA. Ligand binding results in rapid tyrosine autophosphorylation in the C-terminal kinase domain of the receptor, leading to activation of a number of signal transduction pathways (Ferrara, Gerber and LeCouter 2003). Hence, VEGFR2 expression is critical to the function and phenotype of endothelial cells and reduced expression is likely to have profound phenotypic/functional consequences/effects.

Thus, the responsiveness of ECs (HUVECs, hCMECs, and primary brain endothelial cells (HBMECs)) to VEGF stimulation were compared by monitoring VEGFR2 phosphorylation. Western blotting revealed that treating HUVEC and HBMEC cells with 10 and 25 ng/ml recombinant VEGFA for 5 minutes resulted in rapid autophosphorylation of VEGFR2 at Y1175. However, neither total nor phosphorylated VEGFR2 was detected in VEGFA treated hCMEC cells (Figure 4.2C), corroborating the IF results (see Figure 4.2B). However, detection of VEGFR2 expression by VEGFR2 specific antibodies produced variable results which may explain difficulties in detecting VEGFR2 expression in hCMEC cells. To further examine the downstream signalling induced by VEGF stimulation, critical components of MAPK and PI3K pathways were examined in stimulated HUVEC and hCMEC cells by western blotting. Indeed, as expected VEGFA stimulation of

HUVECs resulted in concomitant increases in phosphorylated AKT (pAKT) and ERK (pERK). Interestingly, although there is a deficit of VEGFR2 expression in hCMEC, the downstream signalling cascade appears to remain intact, with comparable levels of pAKT and pERK evident in response VEGF stimulation, when compared to HUVECs (Figure 4.2D). This suggested that either functional VEGFR2 is present at very low levels in hCMEC capable of eliciting a robust signalling response, or that alternate activation of AKT and ERK is occurring by alternate VEGFR2-independent means.

A key functional outcome of VEGF signalling is the angiogenic response of endothelial cells, allowing the formation of new vasculature. Results indicating reduced VEGFR2 in hCMEC prompted the testing of angiogenic potential using an *in vitro* assay. The angiogenic potential of endothelial cells can be assayed by co-culturing them with fibroblasts in the presence of VEGFA (Bishop et al., 1999). This results in the formation of tubular networks through the elongation and branching of ECs to produce structures reminiscent of a primitive vascular network (Geudens and Gerhardt, 2011). Previous work has shown that tubules from these assays form lumens, and patent vessels which can be perfused to study endothelial permeability or trafficking of immune/cancer cells (Jeon et al., 2015). As expected, the HUVEC-fibroblast co-cultures developed multibranching vascular patterned networks at 10 ng/ml and 25 ng/ml VEGFA stimulation (Figure 4.3A-B). However, hCMEC-fibroblast co-cultures displayed greatly reduced tubular network formation under these conditions (Figure 4.3A-B). Truncated, isolated tubules of approximately 250  $\mu$ m length were routinely observed in hCMEC co-cultures, however the presence of these was not consistent across biological replicates. To ensure that hCMEC were indeed displaying reduced capacity to form tubules in the coculture assay, a number of optimisation experiments were employed. Even under conditions of varying hCMEC cell density, increased length of coculture duration and increasing concentrations of VEGF stimulation to 100ng/ml did not yield further tubule formation (data not shown).

To address whether this deficit was due to the brain origin of hCMEC cells, co-culture assays were also performed using primary brain endothelial cells (HMBEC). This showed that HMBEC were also very poor at producing tubules in response to increasing concentrations of VEGF (Appendix Figure 1). Furthermore, HMBEC cells also exhibited extremely slow proliferation rates compared to either hCMEC or HUVECs (data not shown). This may suggest the reduced ability of these cells to

undergo angiogenesis in co-culture assays, is due to their poor responsiveness to cell culture conditions, rather than a defect in VEGFR2 expression or activation, which was evidenced by functional expression via immunoblotting (Figure 4.2C).

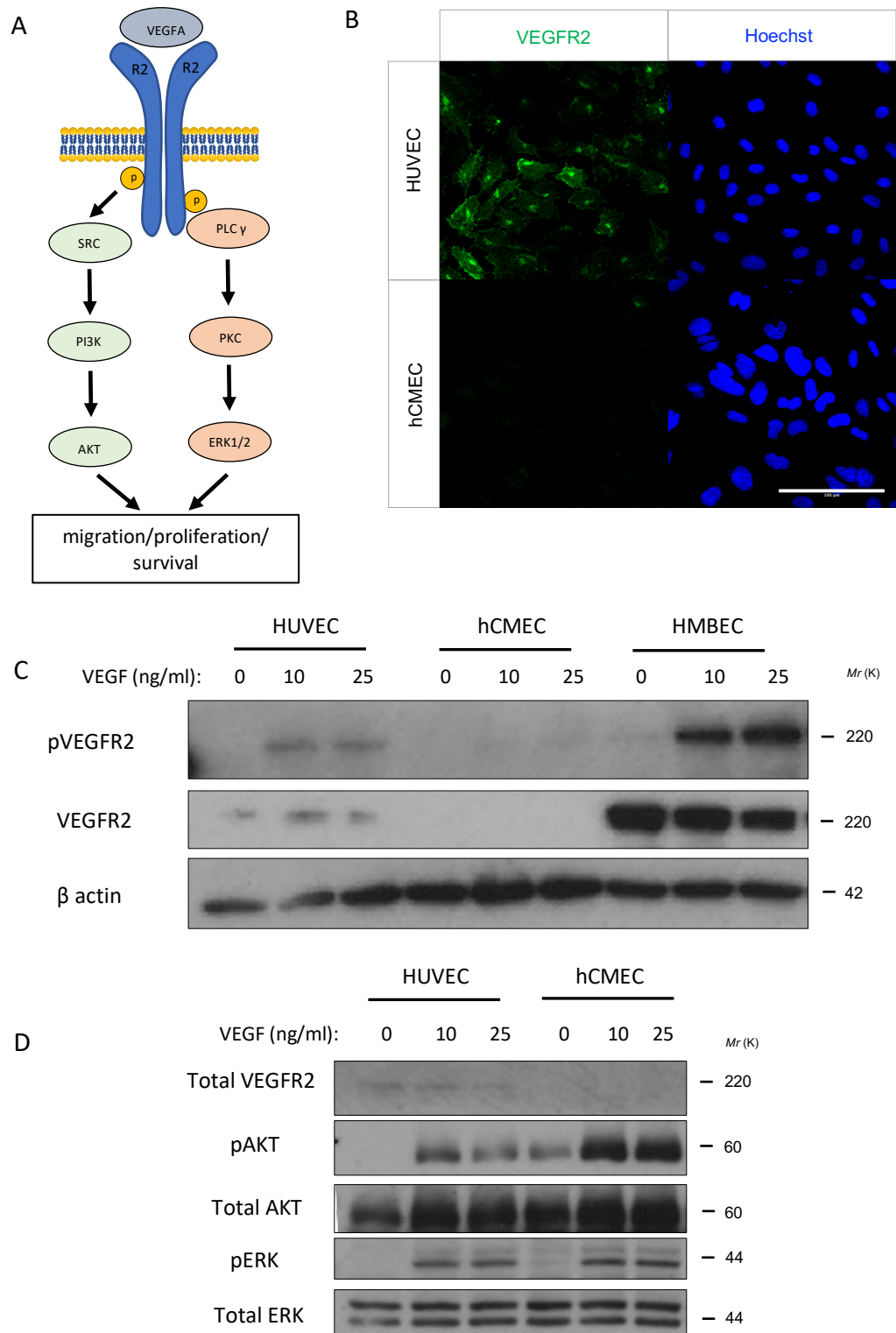


**Fig. 4.2. hCMEC express reduced VEGFR2 expression.** **A**, VEGFR signal transduction pathway. VEGFA ligand binds to VEGFR2 causing the dimerization and consequent phosphorylation of tyrosine residues in the cytoplasmic region of the VEGF receptor 2. Activation of downstream signaling of the PI3K pathway and the MAPK pathway results in a multitude of responses to VEGF stimulation. **B**, Immunofluorescence of VEGFR2 expression in HUVEC and hCMEC monolayers. Endothelial cells were grown to confluency on 0.2% gelatin coated coverslips before fixation in 4% PFA and subsequent staining for VEGFR2 and nuclear staining with Hoechst. Scale bar: 100µm. **C**, HUVEC, hCMEC and HMVEC cells were grown to confluency and serum starved for 2h. ECs were then treated VEGFA as indicated for 5 minutes before lysis and analysis of VEGFR2 Y1774 phosphorylation by western blotting. **D**, As in C, HUVEC and hCMEC immunoblotting for VEGFR2, pAKT, pERK1/2 and total AKT and ERK1/2. Data are representative of n=3 independent replicates

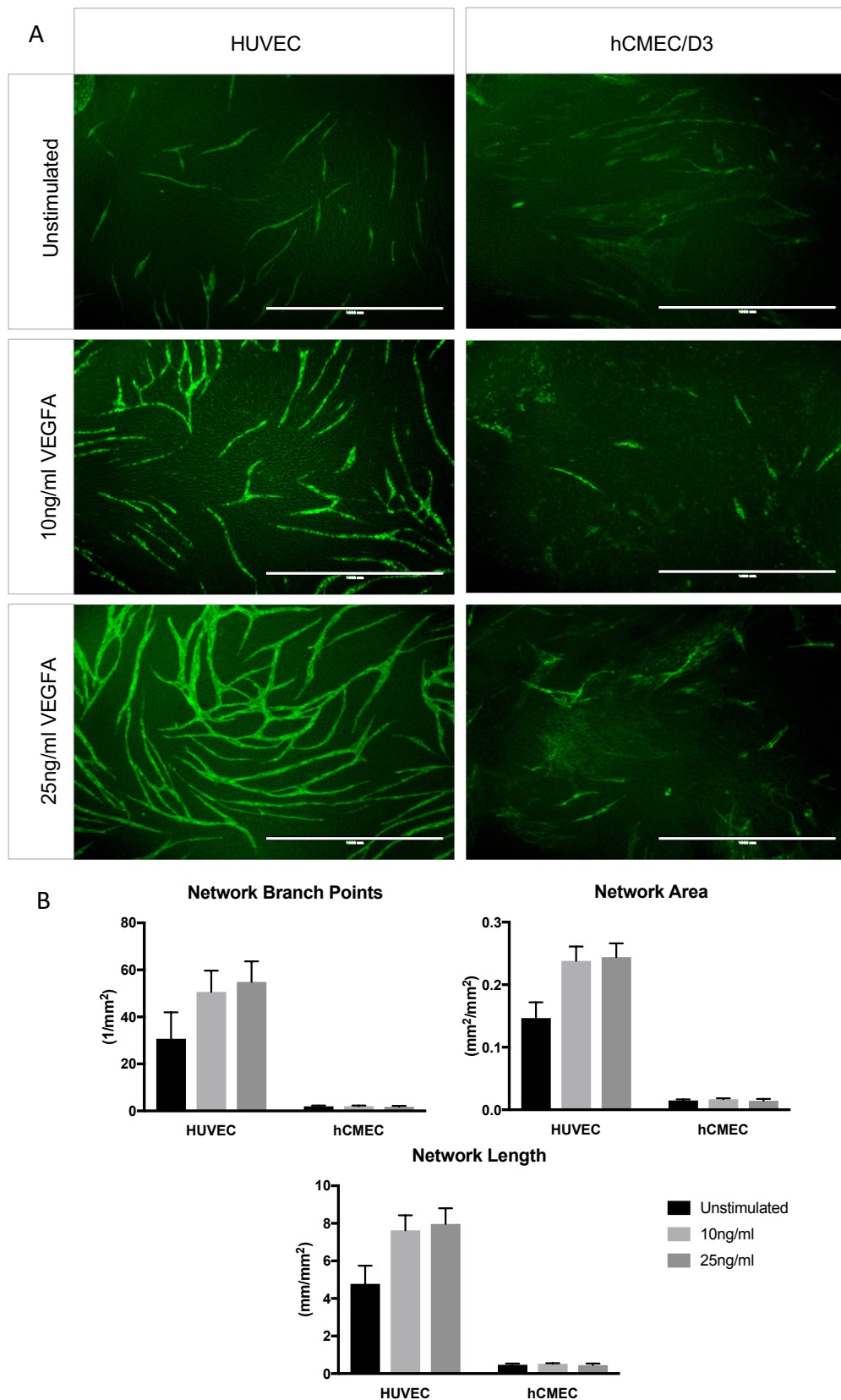


**Fig. 4.3. hCMEC exhibit poor angiogenic function.** **A**, HUVEC and hCMEC cells were grown upon a feeder layer of immortalised human dermal fibroblasts (HDF) for 9 days. Cocultures were supplemented with either control media, or media supplemented with 10 or 25ng/ml VEGFA. Cocultures were subsequently fixed in 4% PFA and stained with anti-CD31 and imaged on EVOS or Incucyte microscopy platforms. Scale bar: 1mm. **B**, Quantification of Network Branch points, Network Area and Network length was carried out using Incucyte angiogenesis software. Data are representative of n=3 independent replicates. Error bars indicate mean +/- standard error.

#### **4.4 hCMEC express high levels of inactive p53 which suppresses CD31 expression**

The cell line hCMEC/D3 was immortalised using SV40 Tag and hTERT in order to achieve prolonged proliferation and survival of cells (Weksler et al, 2005). The SV40 Tag binds p53 and inactivates its canonical functions, resulting in uncontrolled cell cycle progression, reduced apoptosis and, in rodents, tumourigenesis (Levine, 2009). Nuclear SV40 Tag expression in hCMEC was reported in the paper describing the derivation of the cell line (Weksler et al. 2005). To verify this, immunofluorescence microscopy was performed. Positive nuclear staining of SV40 Tag was apparent in hCMEC cells (Weksler et al, 2005) along with strong nuclear p53 expression (Figure 4.4A). The expression of p53 was further investigated in both hCMEC and HUVEC using immunofluorescence microscopy, where p53 was found to exhibit strong positive nuclear localisation in hCMEC compared to primary HUVEC endothelial cells (Figure 4.4B). Importantly, SV40 Tag is known to bind and inhibit p53 activity without compromising p53 expression levels (Linzer and Levine 1979; Lane and Crawford 1979).

Pfister et al. (2015) showed that mutated or inactive p53 alters chromatin remodelling around the promoter region of the VEGFR2 gene and alters its expression in breast cancer cells. However, very little work has been done exploring p53 activity in relation to endothelial VEGFR2 expression and function. It was therefore hypothesised that high levels of SV40 Tag present in hCMEC would neutralise p53 and potentially alter the endothelial phenotype of these cells via repression of VEGFR2 expression. RNA interference was used to reduce p53 expression, with the hypothesis that this would normalise the expression of VEGFR2 to levels observed in other endothelial cell lines (by de-repressing VEGFR2 promoter activity). Initial experiments using p53 siRNA depletion in hCMEC cells demonstrated a significant reduction in p53 expression (Figure 4.5A), and this was accompanied by an increase in CD31 expression when analysed by western blotting (Figure 4.5B). However, depletion of p53 did not increase the expression of VEGFR2 to levels that were detectable by western blotting (data not shown). Although changes in VEGFR2 upon p53 depletion with siRNA were not observed, the increased CD31 expression observed, supports the suggestion that suppression of the endothelial phenotype of hCMEC may be due to high concentrations of inactive p53.

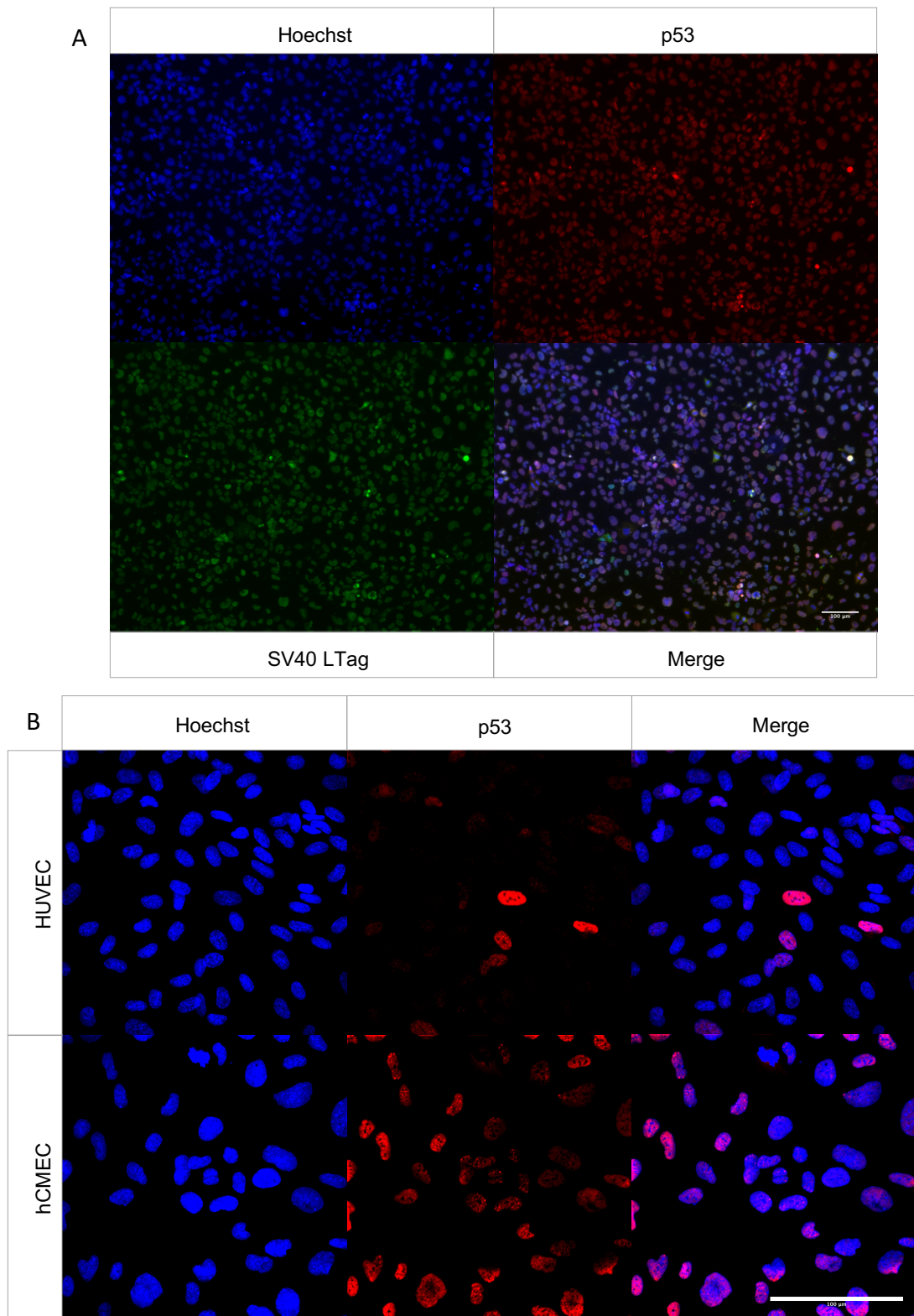


**Fig. 4.4. hCMEC express high levels of inactive p53 and SV40 LTag.** **A**, Immunofluorescence of SV40 Ltag, p53 and nuclear Hoechst expression in hCMEC monolayers. Endothelial cells were grown to confluency on 0.2% gelatin coated coverslips before fixation in 4% PFA and subsequent staining for p53, sv40 LTag and nuclear staining with Hoechst and imaging using EVOS microscopy system. Scale bar: 100 $\mu$ m. **B**, Immunofluorescence of p53 expression in HUVEC and hCMEC monolayers. Endothelial cells were grown to confluency on 0.2% gelatin coated coverslips before fixation in 4% PFA and subsequent staining for p53 and nuclear staining with Hoechst and imaging by widefield microscopy. Scale bar: 100 $\mu$ m.

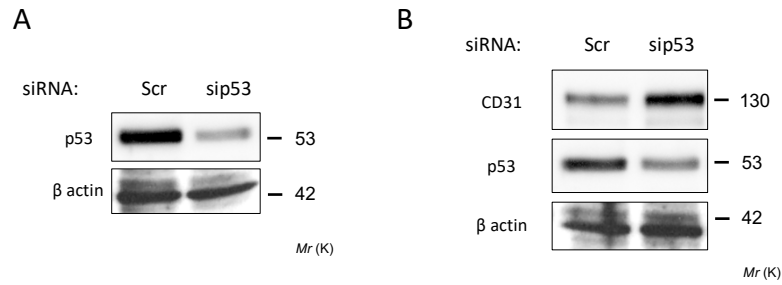


**Fig. 4.5. siRNA knockdown of p53 in hCMEC induces CD31 expression.** **A**, hCMEC cells were treated with p53 siRNA for 72 hrs before lysis and total cell lysate analysis of knockdown by western blotting using p53 specific antibodies. **B**, Immunoblotting of CD31 protein expression was analysed using specific antibodies and  $\beta$ -actin was used as a loading control. The data shown are representative of n=3 independent experiments.

#### 4.5 VEGFR2 suppression in hCMEC cells is p53-dependent

To further investigate whether SV40 Tag inactivated p53 and this was suppressing VEGFR2 expression, hCMEC cells were transduced with short hairpin (sh) RNA targeting p53 (termed shp53; performed by Dr. Adam Odell). Immunofluorescence microscopy revealed that substantial knockdown of p53 was achieved (Figure 4.6A). Observations by light-phase microscopy suggested a dramatic change in cell morphology of hCMEC shp53 compared to the shScr control line (Figure 4.6B). hCMEC shp53 cells appeared larger and, when grown to a confluent monolayer, exhibited a classical EC 'cobblestone' like morphology compared to shScr hCMEC which appear more compact and elongated.

The transient siRNA depletion of p53 in hCMEC cells resulted in increased expression of CD31 (Figure 4.5); it was therefore anticipated that a more pronounced expression of CD31 would be observed in stably transfected shp53 cells. Immunofluorescence microscopy and flow cytometry revealed that shRNA targeting p53 did indeed induce a significant upregulation in CD31 expression (Figure 4.7A) Importantly, VEGFR2 expression was also increased in shp53-targeted cells (Figure 4.7B). Expression of VE-cadherin (CD144), which plays a critical role in the formation of endothelial cell-cell complexes, was also upregulated when examined by flow cytometry and immunofluorescence microscopy (Figure 4.7A-B). This suggests that

inactivated p53 within hCMEC cells is repressing the expression of these endothelial markers in either a direct or indirect manner.

Vascular development, angiogenesis and endothelial phenotype is orchestrated by the convergence of multiple co-receptors and other VEGFRs alongside VEGFR2 (Koch et al., 2011). VEGFR1 has greater binding affinity for VEGFA than VEGFR2 and as such sequesters VEGFA from VEGFR2 (Shinkai et al., 1998). The requirement for this action becomes obvious in VEGFR1 knockout mice, where over-productive angiogenesis results in embryonic lethality (Fong et al., 1995). VEGFR3 expression plays an important role in lymphatic endothelial development (Kukk et al., 1996). The expression of VEGFR1 and VEGFR3 were examined by immunofluorescent microscopy in the shp53 hCMEC line; interestingly their expression was also upregulated upon p53 depletion (Figure 4.8A-B). Remodelling of the actin cytoskeleton was also observed, with redistribution of actin from linear actin fibres in shScr hCMEC to radial actin distribution upon p53 depletion (Figure 4.8B). Increased expression of ZO-1, indicative of the presence of tight junctional formation between cell-cell contacts (Bazzoni et al. 2000), was also apparent (Figure 4.8A). Interestingly, a re-distribution of CD99 expression was also noted (Figure 4.8A), with p53 depletion re-localising CD99 to the cell borders, where it has previously been described to reside within LBR complexes (Schenkel et al., 2002). However, no change in the total level of expression of CD99 was observed when examined by flow cytometry (Figure 4.7A-B).

The increase in VEGFR2 expression in shp53 hCMEC cells suggests normalisation of endothelial phenotype upon p53 knockdown. To test whether the change in VEGFR2 expression preserved receptor function, the shp53-treated hCMEC cells were stimulated with VEGF and autophosphorylation of VEGFR2 at Y1175, and downstream AKT and ERK phosphorylation examined by western blotting. The results indicated that in shp53-treated hCMECs, VEGFR2 becomes phosphorylated in response to 10 and 25 ng/ml VEGF stimulation (lanes 10, 11 and 12) compared to parental hCMECs and shScr control cells (lanes 4-6 and 7-9 respectively), which remain refractory to VEGF stimulation (Figure 4.9).

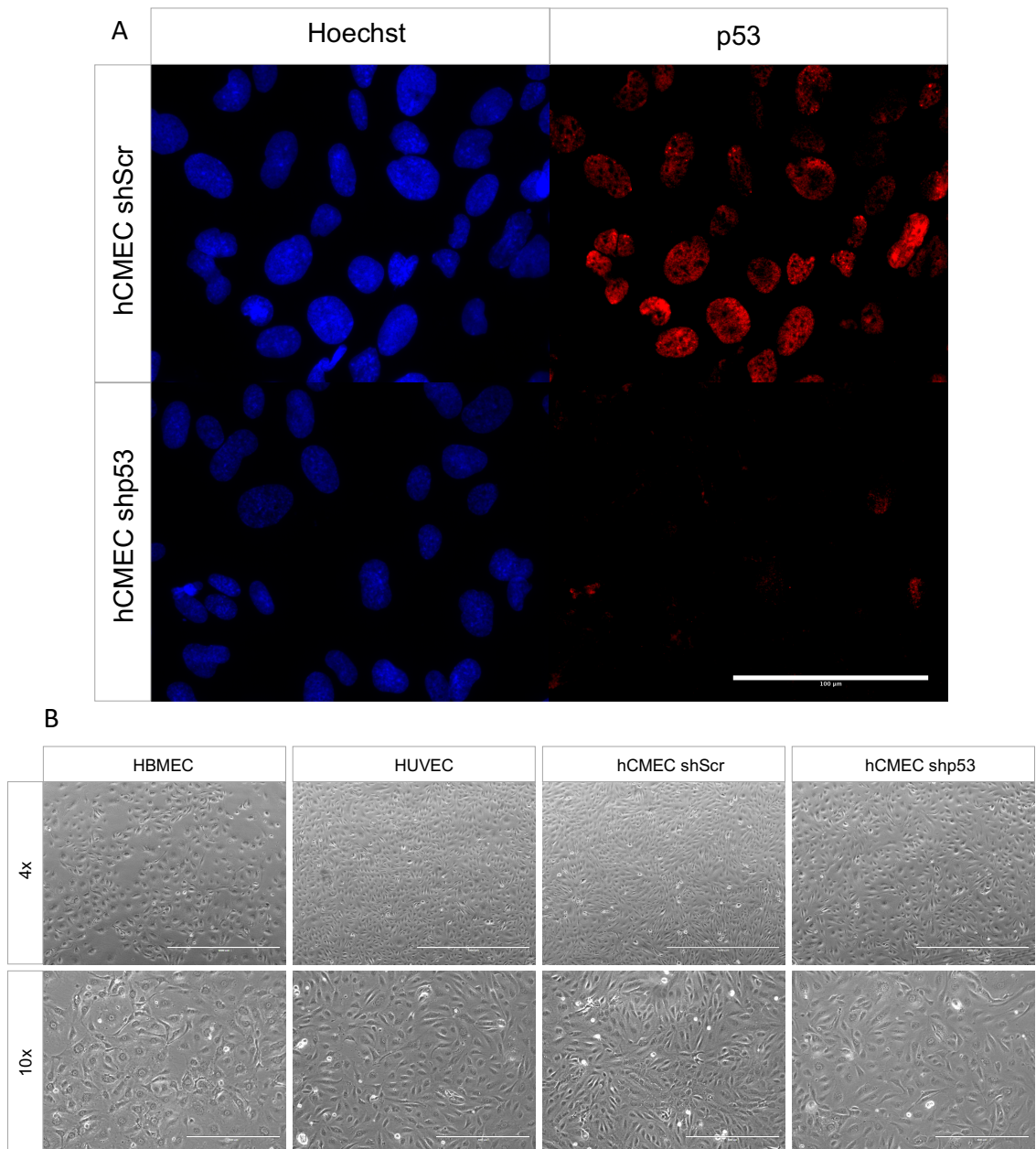


**Fig. 4.6. Generation of stable p53 shRNA knockdown hCMEC.** **A**, Immunofluorescence of p53 expression in shScr and shp53 hCMEC monolayers. hCMEC cells were infected with shp53 lentivirus for 24 hours before selection by culturing in 2ug/ml puromycin containing media. Subsequent populations of selected cells were grown to confluency on 0.2% gelatin coated coverslips before fixation in 4% PFA and subsequent staining for p53 and nuclear staining with Hoechst and imaging by widefield microscopy. Scale bar: 100 $\mu$ m. **B**, Brightfield microscopy of HBMEC, HUVEC, shScr and shp53 hCMEC monolayers. Endothelial cells were grown to confluency on 0.2% gelatin coated 12 well plates before imaging using EVOS microscope. 4x objective scale bar: 1000 $\mu$ m. 10x objective scale bar: 400 $\mu$ m.



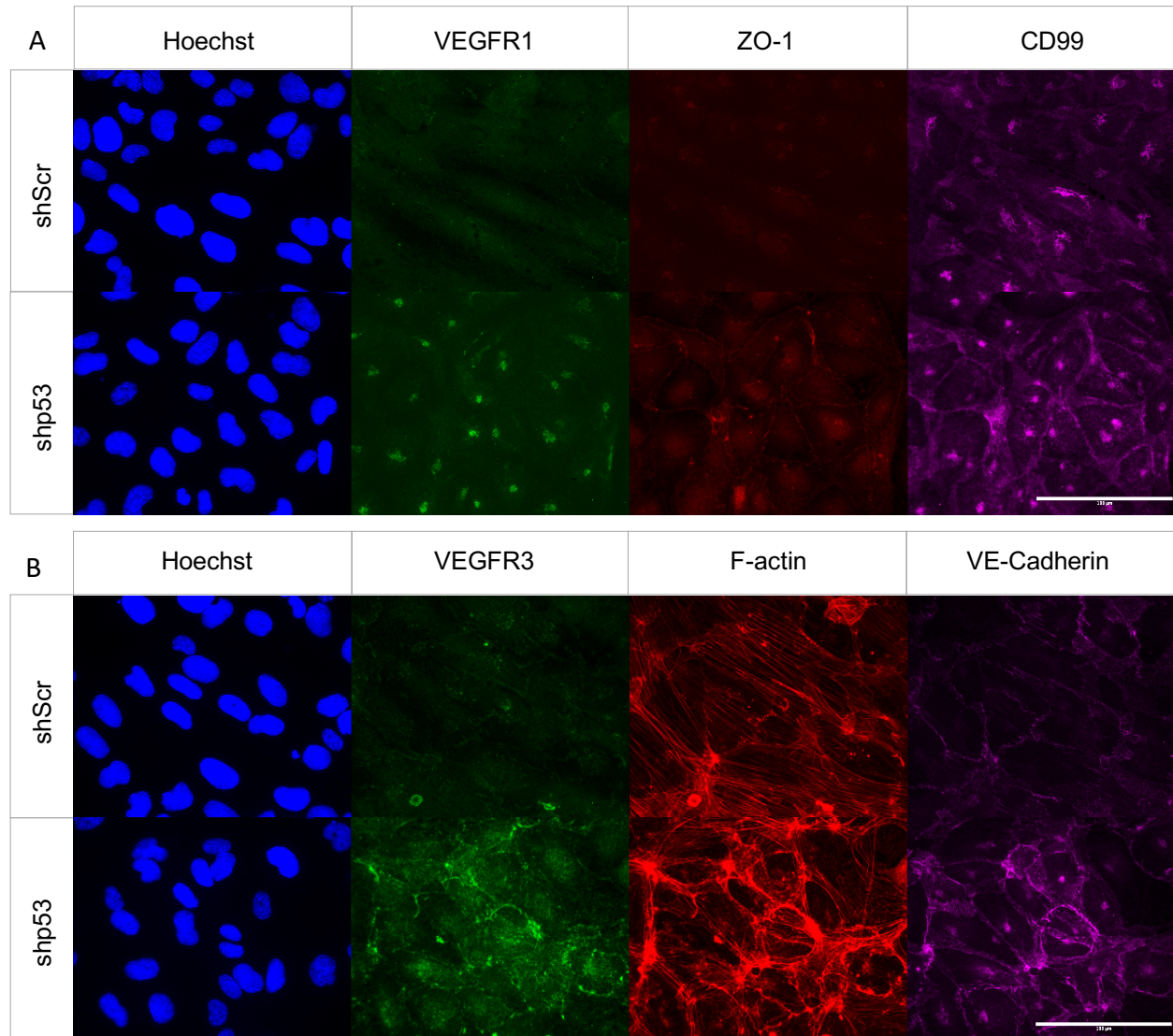


**Fig. 4.8. p53 knockdown induces expression of endothelial markers.** **A**, Immunofluorescence of VEGFR1, ZO-1 and CD99 expression in shScr and shp53 hCMEC monolayers. Cells were grown to confluency on 0.2% gelatin coated coverslips before fixation in 4% PFA and subsequent staining with indicated antibodies. **B**, Immunofluorescence of VEGFR3, actin and CD144 expression in shScr and shp53 hCMEC monolayers. Cells were grown to confluency on 0.2% gelatin coated coverslips before fixation in 4% PFA and subsequent staining with indicated antibodies. Scale bar: 100µm.

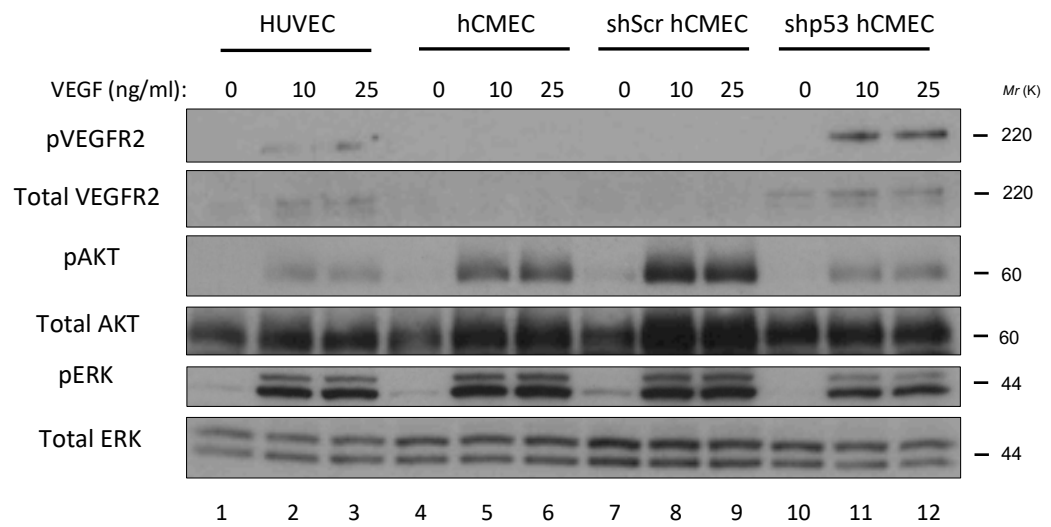


**Fig. 4.9. p53 knockdown restores VEGFR2 expression and function in hCMEC.** HUVEC, hCMEC, shscr hCMEC and shp53 hCMEC cells were grown to confluency and serum starved for 2h. Ecs were then treated with indicated concentration of VEGFA for 5 minutes before lysis and analysis of VEGFR2 Y1774 phosphorylation, pAKT, pERK1/2 and total VEGFR2, AKT and ERK1/2 by immunoblot. Data are representative of n=2 independent replicates.

#### **4.6 CD34 expression**

Results from EC surface screen by flow cytometry shown in Figure 4.1 indicated that CD34 expression, a marker of endothelial hematopoietic lineage, was highly expressed on hCMEC cells but was only very weakly expressed by HUVEC cells. Flow cytometric analysis of shp53 hCMEC cells indicated that CD34 expression was depleted to levels observed in HUVEC upon p53 depletion (Figure 4.10). These results suggest that expression of p53 in hCMEC may allow the dedifferentiation of hCMEC resulting in increased CD34 expression. In summary, p53 depletion in hCMEC induces expression of a number of endothelial molecules including VEGFR2, CD31 and VE-cadherin, to levels comparable with HUVECs. hCMECs endowed with upregulated and functional VEGFR2 following p53 knockdown, appear responsive to VEGF stimulation. Therefore, it was investigated whether this imparts a greater angiogenic response to VEGFA stimulation; which is the subject of the following experiments.

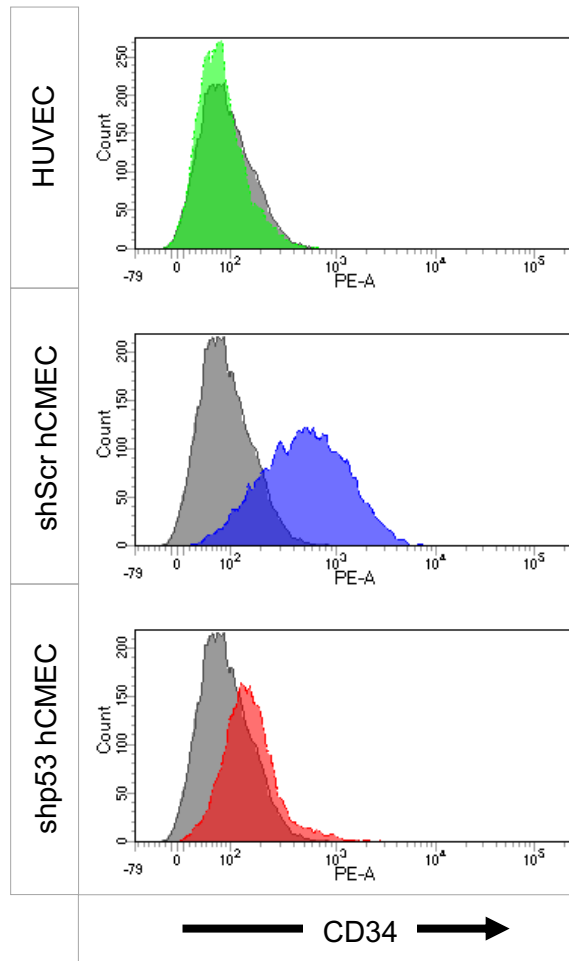


**Fig. 4.10. P53 depletion reduces CD34 expression in hCMEC.** HUVEC, shScr and shp53 hCMEC endothelial cells were grown to confluency before gentle trypsination and subsequent washing in PBS. Cells were stained with CD34 specific conjugated and relevant isotype control antibodies. Stained cells were then analysed by flow cytometry using BD LSRII FACS analysis. Data are representative of n=2 independent replicates.

#### **4.7 VEGFR2 upregulation increases hCMEC angiogenic potential**

An increase in VEGFR2 and other endothelial markers such as CD31 and CD144 would be expected to confer an increased capacity in angiogenic potential as many of these upregulated receptors have been shown to be critical in angiogenesis (DeLisser et al. 1997; Nelson and Nusse, 2004). Matrigel cord formation assays assess the ability of endothelial cells to form cord-like structures upon migration and cell-cell contact formation. To address whether p53 depletion was able to induce changes in cord formation, shp53 hCMEC cells were tested in this assay. Results indicated that shp53 hCMEC had a greater capacity to develop more complex networks, with significantly increased length of network branches and number of junctions compared to the scrambled control (Figure 4.11), indicative of a greater angiogenic potential. However, quantification of the number of branches in the networks formed indicated no significant difference between HUVEC, shScr hCMEC and shp53 hCMEC. Additional work within our laboratory has also demonstrated increased angiogenic potential of p53-depleted hCMEC cells within fibroblast EC co-culture assay (Dr. Adam Odell; unpublished observations). This assessed the prolonged angiogenic potential of hCMEC shScr and shp53 under VEGFA stimulation and indicated increased tubulogenesis upon p53 depletion, corroborating results shown in cord formation assay (Data not shown).

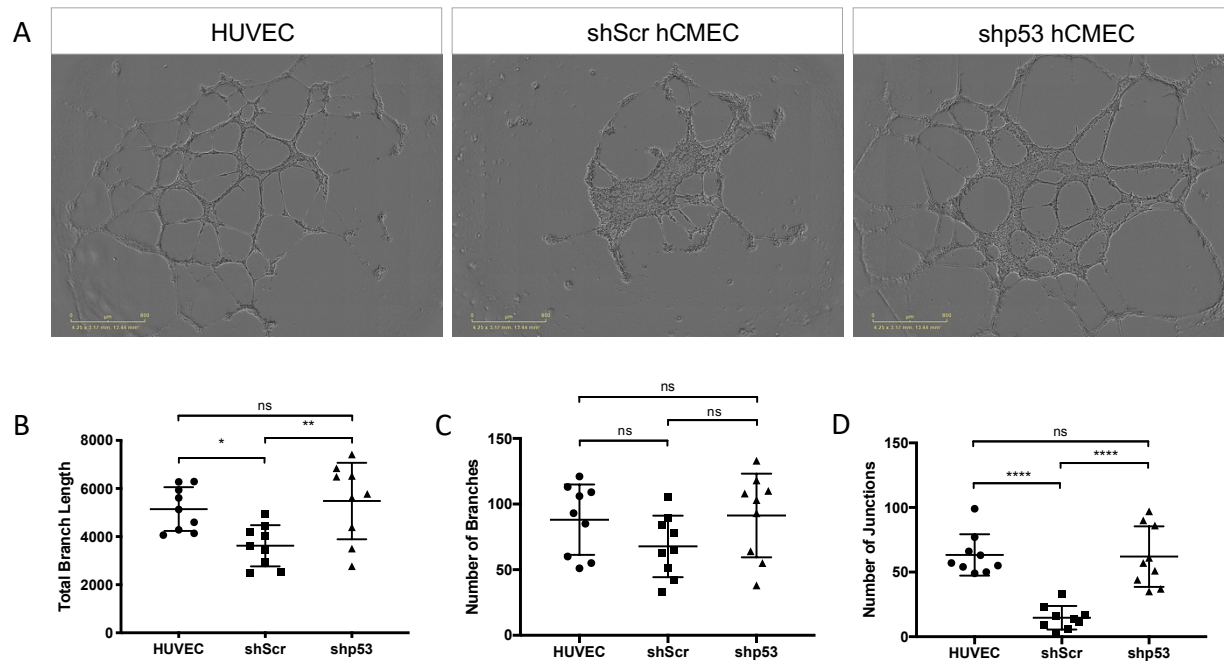


**Fig. 4.11. p53 knockdown normalises hCMEC angiogenic potential in cord formation assays.** **A**, Angiogenic potential was assessed using in vitro cord formation assays using ECBM matrigel (1:1) coated plates. Representative images of  $5 \times 10^4$  HUVEC, shScr and shp53 transduced hCMEC cells plated onto ECBM matrigel for 18h and imaged using live cell imaging. Scale bar: 800 $\mu$ m. Cord formation images were subject to ImageJ quantification indicating **B**, Total Branch Length **C**, Number of Branches **D**, Number of Junctions. Analysis was completed on n=3 independent replicates. Error bars indicate standard deviation. Statistical analysis was performed using one-way ANOVA with Tukey's multiple comparison.  $p^* < 0.05$ ,  $**p < 0.005$ ,  $****p < 0.00005$

#### **4.8 p53 depletion in hCMEC induces a more representative BBB phenotype**

The data in Figures 4.7, 4.9 and 4.11 show that p53 knockdown in hCMEC cells promotes an enhanced (or normalised) endothelial phenotype. Given the BBB origin of these cells, it was hypothesised that the expression of molecules associated with cerebral endothelial phenotype would be similarly modulated. Therefore, the expression of markers of BBB endothelial cells was explored in the normalised hCMEC.

Claudin 5 is localised in the tight junctions of endothelial cell-cell contacts and, in the BBB, plays a key role in maintaining the integrity of the endothelial barrier and controlling diffusion of small molecules into the brain (Morita et al., 1999; Nitta et al., 2003). Expression of claudin 5 in hCMEC endothelial cells has previously been found by proteomic analysis to exhibit 5-fold lower expression than that of primary isolated brain endothelial cells (Ohtsuki et al., 2013b). Expression of claudin 5 in shp53 and shScr hCMEC was tested using immunofluorescence microscopy and found to be significantly upregulated in the shp53 hCMEC, demonstrating that this endothelial BBB specific marker is upregulated upon the depletion of p53 (Figure 4.12A). Western blotting of HUVEC, hCMEC, shScr and shp53 lines indicated that claudin 5 is highly expressed by both HUVEC and shp53 lines, with a complete lack of expression in both hCMEC and shScr control lines (Figure 4.12B) validating results from immunofluorescence microscopy experiments.

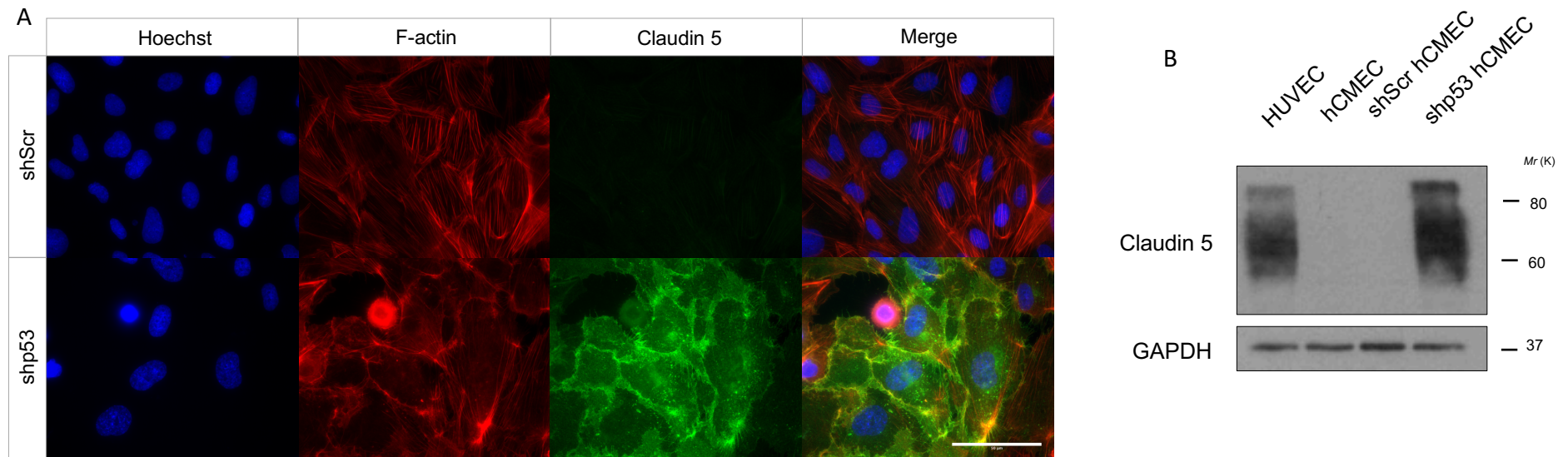


**Fig. 4.12. shp53 hCMEC exhibit increased expression of tight junctional marker claudin 5.** **A**, Immunofluorescence of claudin 5, actin and Hoechst nuclear staining in shScr and shp53 hCMEC monolayers. Endothelial cells were grown to confluency on 0.2% gelatin coated coverslips before fixation in 4% PFA and subsequent staining for claudin 5, actin and nuclear staining with Hoechst and imaging by widefield microscopy. Scale bar: 50 $\mu$ m. Images are representative of n=3 independent replicates. **B**, HUVEC, hCMEC, shScr hCMEC and shp53 hCMEC cells were grown to confluency before lysis and immunoblotting of claudin 5 and GAPDH as loading control. Data are representative of n=2 independent replicates.

#### **4.9 p53 depletion may not confer greater barrier properties to hCMEC**

The data above shows that the knockdown of p53 in hCMEC cells leads to an increase in the expression molecules associated with stabilisation of endothelial cell-cell contacts in the BBB (claudin 5, ZO-1, VE-Cadherin and CD31). The question remained whether this conferred increased barrier function. This was assessed using an impedance-based assay with cultured endothelial monolayers. This allows real-time, simultaneous comparison of barrier function between HUVEC, HMBEC, shScr and shp53 hCMEC. Measurement of electrical resistance indicated that, as expected, HUVEC (the only non-brain EC tested) displayed the lowest resistance and poorest barrier function. Interestingly, the primary brain endothelial line HMBEC, hCMEC shScr and shp53 all displayed greater resistance than HUVECs, with almost identical profiles (Figure 4.13). Previous comparisons of barrier function of hCMEC cells and HUVEC have highlighted the increased barrier function of hCMEC cells and formed part of the basis on which these cells were deemed a suitable model for cerebral vasculature (Weksler, Romero and Couraud 2013).

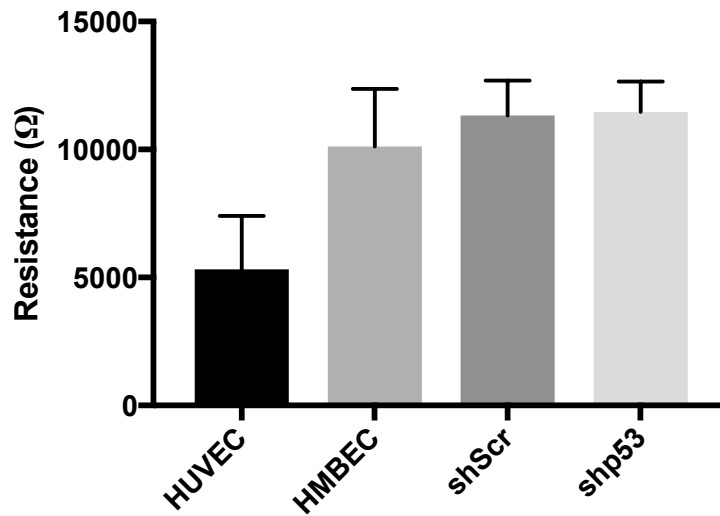


**Fig. 4.13. p53 knockdown may not alter hCMEC barrier function.** Endothelial cells were seeded to ECIS plates at a density of x cells to achieve a complete monolayer of cells. After 24 hours the ECIS plate was then loaded into the ECIS instrument and measurements were collected for 72 hours. Graph indicates resistance (in Ohms) at one 1 hour time point only. Data are representative of 4 technical replicates in n=1 independent experiment. Error bars indicate mean +/- standard error.

#### **4.10 p53 depletion does not alter key BBB endothelial transcription factors**

Recently the gene expression of brain endothelial cells has been comprehensively delineated using single cell sequencing (Hupe et al., 2017; Vanlandewijck et al., 2018). This analysis identified a subset of genes that regulate the specificity of the endothelial BBB phenotype and, as a result, the delineation of the genetic differentiation programmes of the arterio-venous landscape has become clearer (Hupe et al., 2017; Vanlandewijck et al., 2018). The analysis of genes encoding molecules previously highlighted as playing a role in shaping the brain EC phenotype was performed using qRT-PCR. Hupe et al. (2017) showed that the expression of the transcription factor FOXF2 is particularly important in driving the phenotype of cerebral endothelial cells. Therefore, a comparison of mRNA expression of FOXF2 in HUVEC, HBMEC, hCMEC, shScr and shp53 was carried out to determine whether p53 depletion induced changes in FOXF2 expression which might explain to phenotypic changes observed. In addition, qRT-PCR of the amino acid transporter SLC7A1 was performed, as it has recently been shown to be expressed highly in ECs of the BBB (Vanlandewijck et al., 2018). There was no significant difference in FOXF2 or SLC7A1 expression across the four brain endothelial cell lines tested (Figure 4.14). Importantly, shp53 hCMEC cells expressed levels similar to shp53 hCMECs, indicating that p53 was not regulating the expression of either FOXF2 or SLC7A1. These results show that phenotypic changes associated with p53 depletion may be due to changes in other transcription factors or may be a direct consequence of VEGFR2 upregulation.

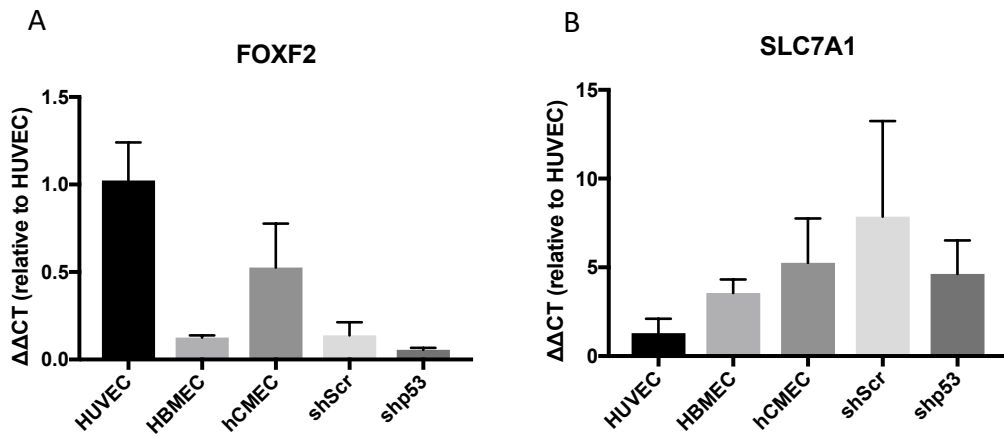


**Fig. 4.14. P53 depletion does not alter expression of key BBB transcription factors.** Indicated endothelial cell lines were cultured until confluent before PBS washing and lysis followed by RNA extraction. Gene expression of **A**, FOXF2 and **B**, SLC7A1 was determined by qRT-PCR using QuantStudio 5 Real-Time PCR System and Taqman probes. Expression is reported relative to HUVEC samples and standardised against GAPDH. Data are representative of n=3 independent replicates. Error bars indicate standard deviation.

#### **4.11 VEGFR2 depletion reverses the endothelial phenotype of hCMEC shp53**

The large increase in the expression of VEGFR2 observed upon p53 depletion suggested that the switch in endothelial phenotype of shp53 hCMEC might be driven by this change. As previously discussed, VEGFR2 is crucial to vascular development and angiogenesis. VEGFR2 forms a mechanosensory complex with CD31 and VE-Cadherin, allowing endothelial cells to sense and respond to shear flow (Tzima et al., 2005). The complex is dependent on the transmembrane domain of VE-cadherin which interacts with VEGFR2 (Coon et al., 2015). VE-Cadherin has been shown to be important in VEGFR2 receptor retention at the plasma membrane, forming a complex with  $\beta$ -catenin and p120 catenin, limiting its endocytosis (Lampugnani et al., 2006). Based on these interactions between VEGFR2, VE-Cadherin and CD31, it was hypothesised that depleting VEGFR2 using siRNA would decrease levels of VE-Cadherin and CD31 expression, thus reverting shp53 hCMEC cells back to their original phenotype of low-expressing CD31, VE-Cadherin ECs with poor angiogenic potential. Transfection of hCMEC shp53 with VEGFR2 siRNA successfully knocked down expression of VEGFR2 when analysed by western blot (Figure 4.15A). To determine whether expression of other endothelial markers was dependent on the absence of p53 and presence of VEGFR2, expression of CD31 and CD144 was analysed by Western blot. VEGFR2 knockdown in shp53 hCMEC reduced CD31 expression (Figure 4.15B) and VE-cadherin expression (Figure 4.15C). CD31 and VE-cadherin expression were determined on separate blots as indicated. Collectively this shows that VEGFR2 depletion resulted in a concomitant reduction in CD31 and VE-cadherin expression (Figure 4.15B-C). These data suggest that depleting p53 de-represses VEGFR2 resulting in a dramatic phenotypic change, and that this can be reversed by the knockdown of VEGFR2.

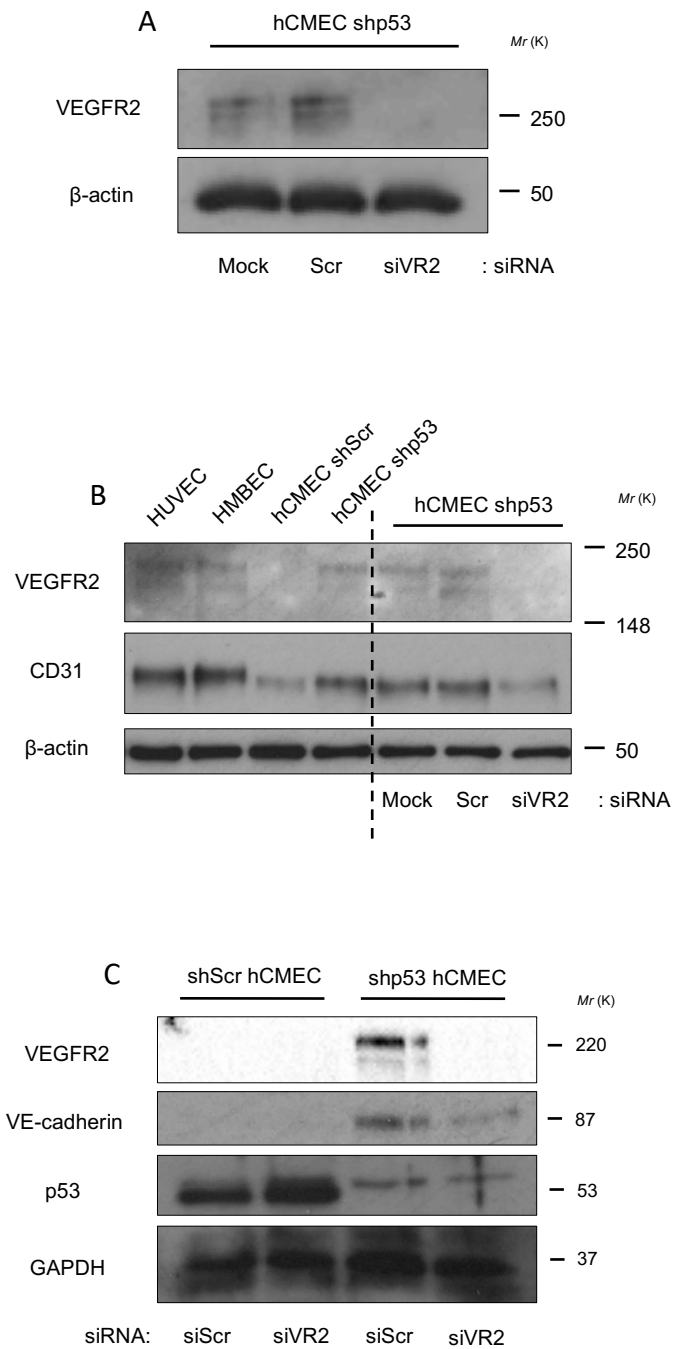


**Fig. 4.15. shp53 VEGFR2 depletion reduces expression of VE-Cadherin and PECAM1.** **A**, Western blotting was performed for VEGFR2 and β-actin loading control in indicated samples. Shp53 hCMEC were transfected with VEGFR2 siRNA for 72hr before lysing and analysis by western blot, alongside scramble control and mock untreated shp53 cells. **B**, As in A, with additional indicated samples and immunoblotting of CD31. **C**, Western blotting was performed for VEGFR2, VE-Cadherin, p53 and GAPDH loading control in indicated samples. ShScr and shp53 hCMEC were transfected with VEGFR2 siRNA for 72hr before lysing and analysis by western blot.

#### **4.12 Functional assessment of hCMEC shp53 line in cancer cell adhesion/TEM**

The original premise for the use of hCMEC was to recapitulate the endothelial component of the blood brain barrier in order to investigate the propensity of breast cancer to metastasise to the brain. Indeed, results from Chapter 3 suggested that the adhesion of the triple negative breast cancer to hCMEC monolayers resulted in comparatively low number of adhering cells, bringing into question the suitability of the hCMEC cell line.

As shown in this chapter, depletion of p53 in hCMEC induces a phenotypic switch to a more endothelial-like state, with upregulation of critical surface receptors. This therefore raises the question whether the phenotypic switch in hCMECs impacts on the adhesion and transendothelial migration of breast cancer cells. Thus, the contribution of the altered endothelial phenotype of the shp53 hCMEC line and its effect on the adhesion of TNBC cells, was tested. Unexpectedly, depletion of p53 in hCMEC cells resulted in a significant reduction in the number of MDA-MB-231 and BrM adhering at 15 and 30 minutes (Figure 4.16A-B). Live cell imaging was also employed to observe the intercalation/spreading of breast cancer cells across shp53 hCMEC monolayers compared to shScr hCMEC controls. Results indicated that there was no change in the ability of cancer cells to intercalate/transmigrate hCMEC monolayers with or without the presence of p53 (Figure 4.16C). This agrees with previous results which may suggest that barrier function of hCMEC was not altered upon p53 knockdown (Figure 4.13).

In this chapter, the regulation of hCMEC cell phenotype by p53 was explored. Collectively, these results show a role for SV40 Tag suppression of p53 activity which has direct consequences for hCMEC endothelial phenotype. This chapter has shown that inactive p53 expression reduced VEGFR2 expression, leading to defects in angiogenic response and expression of key endothelial receptors. Depletion of p53 rescued this phenotype, upregulating VEGFR2, CD31 and VE-cadherin expression and subsequently restoring angiogenic potential. This chapter therefore indicates that depletion of p53 in hCMEC may represent a novel approach in which this *in vitro* BBB cell line could be modulated to improve physiological relevance.

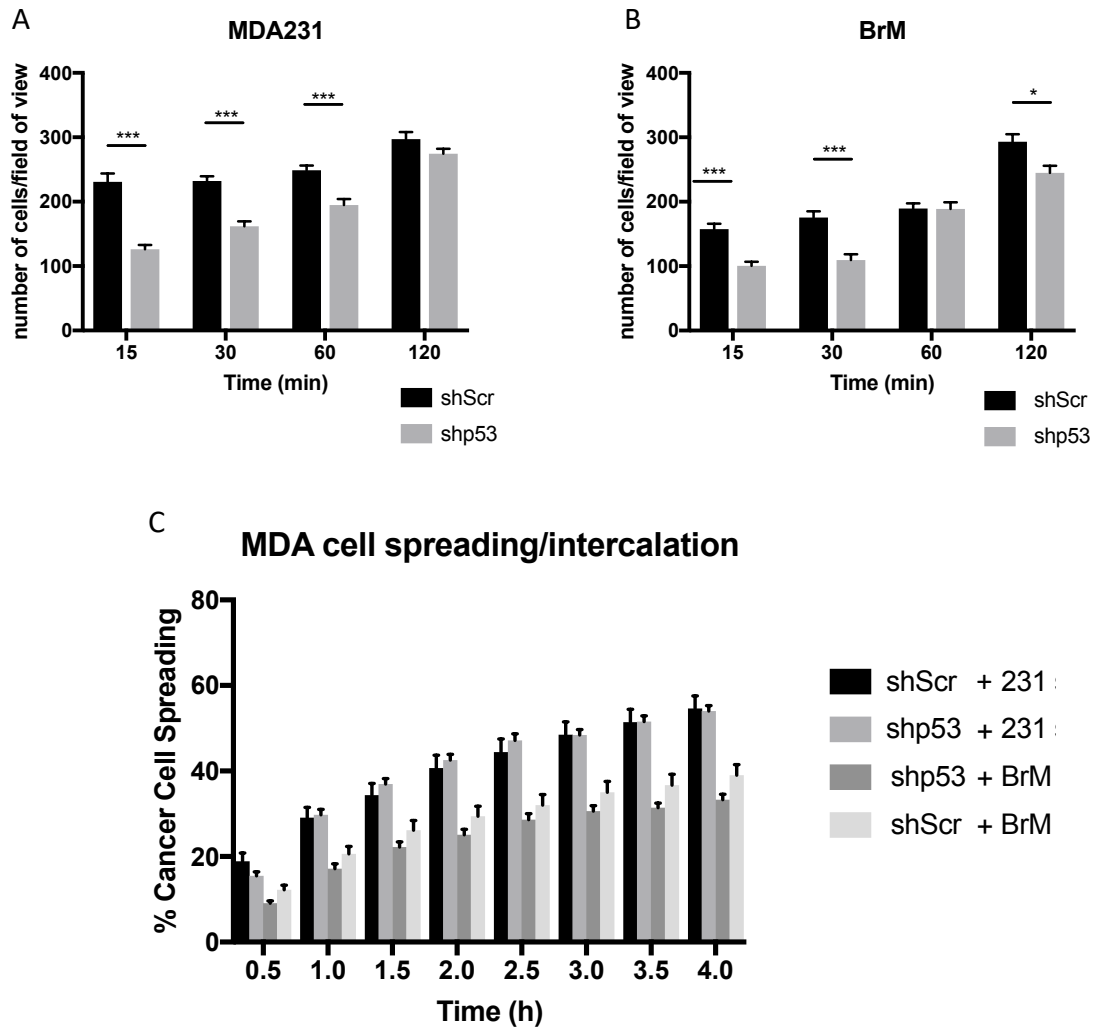


**Fig. 4.16. p53 depletion in hCMEC reduces cancer cell adhesion but does not affect intercalation.** **A**, MDA-MB-231 cells were CellTrackerGreen (CTG) labelled and left to adhere for indicated time points to either confluent shScr or shp53 hCMEC monolayers before subsequent washing, fixation and imaging using Incucyte microscope at 10x objective. **B**, BrM and MDA-231 cells were CTG labelled and left to adhere for indicated time points to either confluent shScr or shp53 hCMEC monolayers before subsequent washing, fixation and imaging using Incucyte microscope at 10x objective. Quantification of bound cells was performed using ImageJ. **C**, CTG labelled MDA-MB-231 cells were seeded on top of confluent shScr or shp53 hCMEC monolayers and imaged for 4h using an Incucyte live cell imaging platform at 20x objective. Statistics calculated for data in panel C indicated no significance between hCMEC shScr and shp53 in MDA-231 or BrM intercalation. Quantification of images is shown, indicating intercalation of cells as a percentage of total cells. Data are representative of n=3 independent replicates. Statistical analysis was performed using student t test. Bars indicate mean +/- standard error.  $p^* < 0.05$ ,  $p^{**} < 0.005$ ,  $p^{***} < 0.0005$ .

#### 4.13 Discussion

Cerebral endothelial cells undergo intimate interactions with cancer cells during metastasis. Therefore, as shown in chapter 3, these interactions were investigated *in vitro* to delineate specific mechanisms impinging on metastasis. Results from chapter 3 suggested that there was very little difference in the TEM of cancer cells across hCMEC in comparison to HUVEC. The rationale for investigating the phenotype of hCMEC cells was that, although this cell line has been widely used to recapitulate cerebral endothelial cells, most studies do not compare their results to a non-brain endothelial line, thus bringing into question whether the results obtained are genuinely specific to BBB endothelial cells or apply more widely to other endothelial cells. In using hCMEC as a model of the BBB, researchers may have unknowingly used an inadequate model for the reasons presented here. The hCMEC endothelial line has been extensively used to model the BBB endothelium (Dauchy et al., 2008; Coureuil et al., 2010; Haqqani et al., 2013; Infanger et al., 2013). However, the expression of VEGF receptors, putative endothelial receptors and a master regulator of angiogenesis, have not been previously characterised in the hCMEC cell line. A few studies report expression of VEGFR2 in hCMEC (Fischer et al., 2009; Krishnan et al., 2015), however, these studies do not compare the VEGFR2 expression (or activity) to that of other endothelial cell lines, whether they are derived from brain or not. The angiogenic nature of this cell line has not been previously evaluated in comparison to other established endothelial models.

VEGFR2 is a key receptor found in the endothelium and is critical to endothelial function and phenotype. VEGFR2 serves as one of the main receptors in transducing signals leading to survival, migration and proliferation which are necessary for angiogenesis (Ferrara, 2004). The importance of VEGFR2 in development is apparent in knock out animals where embryonic lethality occurs due to vascular defects (Shalaby et al., 1995). Comparison of hCMEC to HUVEC and primary brain ECs in VEGFR2 expression revealed a severe deficit of receptor expression and a greatly reduced capacity to form vasculature tubular networks *in vitro* (Figure 4.2-3). Krishnan et al. (2015) show hCMEC VEGFR2 expression in normoxic/hypoxic conditions, but no direct comparison is made to any other primary endothelial cells. These authors also show tube formation assays using Matrigel where in control/mock conditions, there is a severe lack of tube formation mirroring our results showing a lack of tube formation (Figure 4.10). The group originally derived the hCMEC cell line investigated how extracellular RNA can result in the activation of VEGFR2 through NRP-1 dependent co-receptor activity and phosphorylation shown in hCMEC in

response to treatment with extracellular RNA. Western blotting shows VEGFR2 expression again with no comparison to HUVEC or other ECs in this paper (Fischer et al., 2009). In both examples, the authors report that large amounts (40 µg) of protein were loaded for Western blotting, in comparison to 20-25 µg used in work presented in this thesis. In the context of these findings, the evidence from these studies suggests that VEGFR2 expression may be present in hCMEC but below the limit of detection when compared to ECs with 'normal' levels of VEGFR2.

In characterising this cell line, it was found that the hCMEC cells express high levels of p53 (Figure 4.4), which is most likely attributable to the transduction of hCMEC cells with SV40 Tag (Weksler et al., 2005). SV40 Tag binds p53, inactivating its function as a tumour suppressor whilst also increasing the concentration of p53 (Linzer and Levine 1979; Lane and Crawford 1979). Thus, hCMEC cells express high levels of inactive p53 which is evident by western blot and immunofluorescence (Figure 4.4-5). Alongside transduction of SV40 Tag, hCMEC were also transduced with the telomerase hTERT as part of the immortalisation process (Weksler et al., 2005). hTERT has been shown to regulate tumour angiogenesis (Falchetti et al., 2008). Furthermore, hTERT regulates VEGF expression through interaction with the transcription factor Sp1 (Liu et al. 2016). This suggests that the forced expression of hTERT in hCMEC may impact on the expression of VEGF or VEGFRs. Although the role of hTERT expression in hCMEC cells was not investigated, future work should consider the implications of hTERT activity on VEGFR2 expression in immortalised endothelial cells.

Depletion of p53 by shRNA resulted in the increased expression of VEGFR2 and other endothelial markers CD31 and VE-cadherin (Figure 4.7). The resulting increased VEGFR2 expression and switch in phenotype conferred an increased angiogenic potential of hCMEC cells (Figure 4.10). The p53 molecule has been previously implicated in angiogenesis; inhibition of MDM2-mediated degradation of p53 by treatment of endothelial cells with nutlin-3 resulted in reduced angiogenesis mediated by reduced EC migration *in vitro* and *in vivo* (Secchiero et al., 2007). A series of experiments (Ravi et al., 2000) revealed that wild type p53 promotes the MDM2-mediated degradation of the hypoxia inducible factor 1α subunit (HIF1α). In p53<sup>-/-</sup> tumours, the suppression of HIF1α is lost, resulting in increased expression of HIF1 and concomitant expression of HIF1 target genes (including the VEGFR2 ligand, VEGF). In particular, this study shows that p53<sup>-/-</sup> tumours bear higher microvessel density due to the deregulation of HIF1α and subsequent upregulation

of VEGF. It has also been shown that p53 also binds the Sp1 transcription factor which inhibits the transcription of VEGF (Pal et al., 2001). However, the direct influence of p53 control of VEGFR2 expression or regulation is less well characterized.

Pfister et al. (2015) showed that mutant p53 recruited the chromatin remodelling complex SWI/SNF to the VEGFR2 promoter, augmenting activity and subsequent transcription, showing mechanistically how mutant p53 gain-of-function of transcriptional control of VEGFR2 occurs in breast cancer. VEGFR2 expression in breast cancer is indicative of poor prognosis (Zeng, Cai and Wu 2011). Whether the inactivation of p53 by SV40 Tag mimics the mutant p53 in this study remains to be investigated. It has been shown that the binding of p53 by SV40 Tag results in disruption to DNA binding region of p53 (Lilyestrom et al., 2006). Screening of p53 mutants which induce loss of p53 canonical function have shown that SV40 Tag binding replicates the same loss of function elicited by mutation of DNA binding sites of p53 (Lilyestrom et al., 2006). Whether these p53 mutants result in suppression of VEGFR2 expression seems doubtful, as Pfister et al. (2015) showed that the same mutations result in increased VEGFR2 expression in breast cancer. Therefore, results imply an alternative role for p53, where inactive SV40 Tag bound p53 suppresses the expression of VEGFR2 through alterations to the DNA binding capacity of p53. However, this model has yet to be proven. As already mentioned, wild type p53 suppresses VEGF and HIF1 in an MDM2-dependent manner (Ravi et al., 2000). One could speculate that the depletion of p53 in hCMEC cells would de-repress VEGF and HIF1 regulation, which may influence VEGFR2 expression. Although the expression of VEGF or HIF1 in either hCMEC lines was not investigated, qPCR results have shown that p53 depletion in hCMEC has no effect on the levels of VEGFA mRNA (personal communication, Dr. Adam Odell). Altogether, the data suggest that p53 expressed in hCMEC is inhibiting VEGFR2 expression, although the mechanism by which this happens is not yet understood.

The transcription factor (TF) Kruppel-like factor 2 (KLF2) is a major TF in coordinating endothelial gene transcriptional control (Nayak, Lin and Jain 2011). KLF2 has a complex relationship regarding the regulation of VEGFR2, with conflicting evidence reported. Bhattacharya et al. (2005) reported that KLF2 suppressed VEGFR2 promoter activity by displacing Sp1, a positive regulator of VEGFR2 transcriptional activity. Others have shown an association of KLF2 with ETS in the activation of VEGFR2 in the embryonic vascular development (Meadows, Salanga and Krieg

2009). KLF2 expression is also repressed by p53 in a HDAC dependent manner (Kumar et al., 2011). This represents just one example of how p53 could coordinate with the KLF2 to elicit the effects on VEGFR2; however, several other relationships and conclusions could be drawn using other TFs as examples. FOXF2 which recently been shown to be fundamental in driving the specific phenotype of BBB ECs (Hupe et al., 2017). Therefore, I sought to address the general phenotypic changes observed, rather than focusing specifically on VEGFR2 upregulation. My hypothesis was that p53 depletion would increase the expression of transcription factors such as FOXF2, to mediate the changes in phenotype of hCMECs observed by p53 depletion; i.e. establish a more BBB-like phenotype. However, as shown (Figure 4.15), no change in FOXF2 expression across the panel of ECs mRNA that we tested was evident. As mentioned, many TFs converge on different pathways to elicit the organotypic nature of endothelial cells and a broader approach may be necessary to delineate the keys differences observed in shp53 hCMEC.

Depletion of VEGFR2 using siRNA resulted in concurrent downregulation of CD31 and VE-cadherin expression (Figure 4.16), implying that the phenotypic shift of shp53 hCMEC is reliant on VEGFR2 expression. The functions of VEGFR2 and VE-cadherin are indispensable in endothelial cells as their interaction at the cell membrane is vital for downstream signalling of VEGFR2 (Carmeliet et al., 1999). The VE-cadherin complex retains internalised VEGFR2 in proximity to the plasma membrane, limiting continual intracellular signalling (Lampugnani et al., 2006). Interaction between the two receptors also plays an important role in mechanosensory function of ECs. The transmembrane domain of VE-cadherin interacts with VEGFR2, acting as an adapter in the mechanosensory complex of VE-cadherin and VEGFR2 in sensing shear flow (Coon et al., 2015). As the functions and regulation of VEGFR2 and VE-cadherin are evidently interlinked, it is unsurprising that depletion of VEGFR2 in shp53 hCMEC conferred decreased VE-cadherin expression (Figure 4.16C). It is also possible that depletion of VE-cadherin in shp53 hCMEC would impact on VEGFR2 expression. CD31 is also known to associate with VEGFR2 and VE-cadherin in a mechanosensory complex which elicits downstream activation of signalling pathways such as NF- $\kappa$ B under shear flow (Tzima et al., 2005). However, CD31 does not appear to be implicated in VEGFR2 activity, expression or angiogenesis, but its role as a mechanosensor has been well documented in maintaining endothelial homeostasis (Osawa et al., 2002; Conway et al., 2013). Additionally, it would also be interesting to investigate whether CD31 impacts on VEGFR2 expression in the shp53 hCMEC in future work.

Dramatic changes in endothelial phenotype were observed upon p53 depletion in hCMEC. Therefore, it was also investigated whether p53 depletion resulted in the upregulation of markers associated with the BBB phenotype, which would suggest that shp53 hCMEC are more representative of the BBB. Claudin 5 is highly expressed in the tight junctions of the blood brain endothelial cells (Morita et al., 1999) and in part is responsible for the exquisite selective nature of the BBB (Nitta et al., 2003). Claudin 5 expression was found to significantly increased upon the depletion of p53 in hCMEC (Figure 4.13). Interestingly, VE-cadherin has been shown to regulate the expression of claudin 5 (Taddei et al., 2008). As a significant upregulation in VE-cadherin was found upon p53 depletion (Figure 4.7B and 4.8B), it is plausible that the increased expression in claudin 5 is driven by VE-cadherin expression. Claudin 5 has previously been investigated in detail in the hCMEC cell line. In the original derivation of hCMEC, the authors indicate that claudin 5 is expressed using immunofluorescent microscopy (Weksler et al., 2005). However, in the study by Weksler et al, no comparison to a primary BBB EC line or any other primary EC was made. Western blotting of claudin 5 in (see Figure 4.13B) indicated that the expression of shp53 hCMEC was similar to that of HUVEC. Luissint et al. (2012) investigated a novel binding partner of claudin 5 using hCMEC cells and show immunofluorescent microscopy and western blotting which indicate that the hCMEC express claudin 5. Again, no reference is made to other EC cells to enable comparison between levels of claudin 5. This makes it difficult to determine whether these levels are comparable to my results presented above. Interestingly, a membrane proteomic mass spectrometry comparison of hCMEC to a primary brain endothelial cell line indicated that claudin 5 was 5.27 fold higher in expression in the primary cells compared to hCMEC (Ohtsuki et al., 2013b), corroborating our results which suggest that hCMEC express low levels of claudin 5.

Many of the receptors found to be upregulated in shp53 hCMEC have known roles in adhesion and transmigration. CD31 has been extensively documented in the TEM of leukocytes (Muller et al., 1993; Muller, 1995; Liao et al., 1995) and is known to redistribute from EC cell-cell contacts upon cancer cells TEM, however CD31 is not required for melanoma TEM (Voura, Chen and Siu 2000). VE-cadherin aids the formation of cell-cell contacts of endothelial cells and the disruption and internalisation of VE-cadherin complexes in cancer cell TEM has been well documented (Weis et al., 2004; Rezaei et al., 2018). Therefore, it was hypothesised that the change in expression of these receptors influenced cancer cell adhesion and

TEM. Interestingly, live cell imaging showed no difference in the ability of either MDA-231 or BrM cells in spreading on shScr or shp53 hCMEC (Figure 4.16C). Furthermore, no difference between cancer cell TEM through HUVEC and hCMEC was evident in Chapter 3 (Figure 3.2), and so it is less surprising that no change in cancer TEM was noted between shScr and shp53 hCMEC lines. However, TEM using other methods such as Transwell migration assays was not investigated. Recently it was shown that metastatic cancer cells activate necroptosis (a form of programmed necrosis) in endothelial in order to allow escape of cancer cells out of the blood stream and into secondary tissues (Strilic et al., 2016). The role of mutant p53 in necroptosis of epithelial cells was recently shown by Watanabe et al. (2018). Although results indicated no change in the overall percentage of cancer cells undergoing transmigration upon hCMEC p53 knockdown, it would be interesting to investigate whether necroptosis-induced transmigration of cancer cells is altered by p53 expression.

Results from TEER experiments revealed little difference in endothelial monolayer resistance between shScr, shp53 hCMEC and primary HBMECs (Figure 4.14). However, each cerebral EC line exhibited higher TEER than HUVEC. As no difference in TEER between shScr and shp53 hCMEC was observed, it is expected that similar rates of cancer intercalation would be seen. Previous work has shown the relatively high permeability of hCMEC monolayers, citing this as a limitation of the use of hCMEC in modelling the BBB (Boyer-Di Ponio et al., 2014). However, results shown here suggest that TEER of hCMEC does not differ greatly from that of primary isolated BBB ECs (Figure 4.13). Together these results suggest that the upregulation of junctional molecules in hCMEC shp53 did not influence EC monolayer integrity, or cancer cell intercalation.

The loss of endothelial specific markers and a more fibroblastic like phenotype which is characterised by secretion of collagen type I and loss of cell-cell junctions are characteristics observed during the trans-differentiation of endothelial cells to mesenchymal cells (EndoMT) which has been observed in the pathogenesis of atherosclerotic plaque formation (Piera-Velazquez, Li and Jimenez 2011). Importantly, p53 has been widely implicated in the onset of atherosclerosis (Mercer and Bennett, 2006). The SUMOylation of p53 under conditions of disturbed flow conditions was found to be proatherogenic, potentiating EC apoptosis and inflammation (Takabe, Alberts-Grill and Jo 2011; Heo et al. 2013). Neovascularisation of damaged cardiac tissue also requires p53 activity. Increased expression of p53 upon damage was required for the trans-differentiation of

supporting mesenchymal cells into endothelial cells in the repair of damaged cardiac tissue (Ubil et al., 2014). One can speculate that as p53 appears to be involved in the process of mesenchymal-endothelial transition, then the same may be true of endothelial-mesenchymal transition, although proof of this remains to be seen. If this were true then it may be plausible to suggest that the inactivation of p53 in hCMEC cells has skewed their phenotype to a more mesenchymal cell type, with loss of endothelial-like markers and properties, resulting in decreased endothelial functions not dissimilar to the phenotype of hCMEC presented here. Results suggest that hCMEC exhibit high CD34 expression which is reduced upon p53 depletion (Figure 4.10). CD34 expression is a marker of endothelial hematopoietic lineage (Fina et al., 1990) and numerous studies have identified a role for p53 in the regulation of hematopoietic cells (Liu et al., 2009). This lends further support to the idea that hCMEC cells represent a skewed endothelial phenotype due to the inactivation of p53.

Although hCMEC did not undergo substantial tubule or cord formation *in vitro* (Figure 4.3 and 4.10) it is feasible that hCMEC may be permissive to activation by alternative receptors other than those of the VEGFR family to stimulate an angiogenic response. EGFR and FGFR result in the activation of pathways associated with survival, migration and proliferation necessary for angiogenesis (van Cruijssen, Giaccone and Hoekman 2005; Presta et al. 2005; Tabernero 2007). Activation of the FGF receptors mobilises survival, migration and proliferation of endothelial cells, much like VEGFR stimulation (Cross and Claesson-Welsh, 2001). Interestingly, p53 controls the expression of the EGFR receptor (Ludes-Meyers et al., 1996) which has been found expressed in tumour-associated endothelial cells (Amin et al., 2006). However, when EGFR expression was investigated in hCMEC cells, expression was only slightly increased compared to HUVEC (Figure 4.1). Hence, it may be possible that EGFR or FGFR compensate for the reduced VEGFR2 expression in hCMEC/D3 cells. One simple way to test this would be to repeat fibroblast co-culture assays and stimulate with EGF or FGF instead of VEGF and test the angiogenic response through tubule formation.

As hCMEC have been utilised to investigate BBB function in number of scenarios, the reduced expression of VEGFR represents a major drawback in utilising this cell line for further studies. Insufficient vascularisation of cerebral organoid models remains a critical impedance to the development of *in vitro* models of cerebrovascular research (Osaki, Sivathanu and Kamm 2018). Recently it was shown that *in vivo* implantation methods using iPSC derived cerebral organoids become vascularised

(Mansour et al., 2018). Previous work has shown that growing GBM cancer stem cells (CSCs) and hCMEC cells in supporting scaffolds *in vitro*, followed by subsequent engraftment *in vivo*, resulted in the potentiation of tumour growth and functional vascularisation of tumours (Infanger et al., 2013). The authors suggest that the hCMECs introduced alongside GBM CSCs, undergo anastomosis with the vasculature of the host, as well as forming vascular structures *in vitro* within scaffolds, to support tumour growth (Infanger et al., 2013). It is possible that the vascular structures are formed by the hCMEC cells themselves. However, it has previously been proposed that CSCs can transdifferentiate into CD31<sup>+</sup> cells which can form vascular-like structures without the presence of endothelial cells; a process termed vascular mimicry (Angara, Borin and Arbab 2017). This could account for the CD31 positive vascular structures presented in the study by Infanger et al. (2013). However, *in vitro* results presented here, utilising the robust fibroblast co-culture system (Bishop et al., 1999) did not result in the significant formation of tubules by hCMEC cells (Figure 4.3). This suggests either other factors may be able to initiate the tubulogenesis of hCMECs, or that the *in vitro* system used here does not adequately support the tubulogenesis of hCMEC. Current work (not presented here) is investigating whether shScr and shp53 hCMEC compared to HUVEC cells form vasculature in an *in vivo* Matrigel plug assay, which should definitively answer whether hCMEC are able to form vascular networks, and whether p53 knockdown influences the cells behaviour *in vivo* as well as *in vitro*. Furthermore, as we move closer to platforms which incorporate these organoids, the need for a representative BBB EC to vascularise these models will and already is apparent. It is possible that shp53 hCMECs can be utilised alongside future organoid models which incorporate aspects of the BBB, for more representative *in vitro* models.

Although this work highlights that depletion of p53 may result in a cell line which better represents the vascular unit of the BBB, there are still important questions that need to be answered regarding the role of p53 in VEGFR2/VEGF signalling/expression as this may have further implications in understanding the mechanisms of non-canonical p53 signalling. This work highlights the shortcomings of the immortalised hCMEC endothelial model and indicates that robust characterisation of proposed endothelial model cell lines should undoubtedly include angiogenic potential as this represents a key aspect of endothelial biology.

## Chapter 5 CD99 promotes adhesion and transendothelial migration of cancer cells through Cdc42

### 5.1 Introduction

Events in the metastatic cascade are similar to that those in leukocyte migration and parallels have previously been drawn between the mechanisms of adhesion and extravasation of cancer cells and leukocytes (Madsen and Sahai, 2010). In this chapter, the role of CD99 in the adhesion and transmigration of metastatic cancer cells was investigated. The highly glycosylated, type 1 single transmembrane receptor, CD99, participates in the transmigration of leukocytes across endothelial barriers (Schenkel et al., 2002; Lou et al., 2007). The CD99 molecule is a product of the pseudoautosomal gene *MIC2*, which is located in the pseudoautosomal regions of the X and Y chromosome (Goodfellow et al., 1986). The *MIC2* gene encodes 2 splice variants of CD99, a short and long isoform (Hahn et al., 1997). It was previously thought that conservation of CD99 was limited to primate homologues, with no recognisable homology to proteins with known structure (Smith, Goodfellow and Goodfellow 1993). However, CD99 was subsequently found to share substantial homology with two other proteins, CD99 antigen like 2 (CD99L2) (Suh et al., 2003) and the Xga blood group antigen, which shares 48% homology with CD99 (Ellis et al., 1994). In mice, an orthologue of human CD99 named D4 has been identified and encodes a protein which shares 46% homology with human CD99 (Park et al. 2005). This orthologue of human CD99D4 has been implicated in thymocyte apoptosis (Park et al. 2010) and the adhesion of neutrophils to the endothelium (Goswami et al., 2017).

In the context of the endothelium, CD99 localises to endothelial borders and resides in a complex with ezrin, soluble adenylyl cyclase (sAC), and PKA (Watson et al., 2015). Endothelial CD99 is also found within the lateral border recycling complex (LBRC); an intracellular compartment contiguous with the plasma membrane located proximally to endothelial cell-cell junctions (Mamdouh et al., 2009). During TEM, CD99 undergoes homophilic interactions between the leukocyte and endothelium, facilitating the movement of leukocytes in a paracellular fashion between endothelial cell junctions (Schenkel et al., 2002; Lou et al., 2007; Watson et al., 2015). During this process, activation of endothelial CD99 triggers signalling through sAC, which activates PKA and enables the rapid turnover of CD99 from LBRC to the endothelial cell junction, facilitating transmigration (Watson et al., 2015). Previous work has also

suggested endothelial CD99 is cleaved by matrix metalloproteases (MMPs) released from cancer cells; a process required to facilitate their transmigration (Bedau et al., 2017). Thus, manipulation of endothelial CD99 appears a common feature of transmigrating cells. Outside the context of the endothelium, CD99 plays a role in many aspects of cancer development (Manara et al., 2018).

Triple Negative Breast Cancer (TNBC) represents a molecular subgroup of breast cancer with the greatest likelihood of progressing to a metastatic stage (Rakha et al., 2007). The cell line MDA-231 is a well characterised model of TNBC and has been extensively used both *in vitro* and *in vivo* to model this disease type. To date, the role of CD99 in metastatic breast cancer has not been explored in detail, although overexpression of the short isoform of CD99 resulted in increased migratory behaviour and increased expression of MMPs (Byun et al., 2006). Here the role of CD99 in adhesion, TEM and the metastatic phenotype of MDA-231 is explored both *in vitro* and *in vivo*. However, CD99 has been implicated previously in the metastatic potential of other cancer types. In particular CD99 is overexpressed in the paediatric malignancy Ewing's sarcoma (ES), where CD99 is required for ES cells to metastasise. However, the role of cancer cell-endothelial cell interactions in this context has not been explored. In this chapter, the role of CD99 in the adhesion and transendothelial migration of metastatic cancer cells was examined, focusing particularly on breast cancer cells using both *in vitro* and *in vivo* approaches.

## 5.2 CD99 expression correlates with increased breast cancer metastasis and is broadly expressed by breast cancer cell lines

CD99 has previously been explored in patient samples of several different cancer types to establish a correlation between protein expression and survival metrics. It is well reported that Ewing sarcoma exhibits high expression of CD99 and is therefore used in the clinical diagnosis of the disease (Ambros et al., 1991; Lombart-Bosch et al., 2009). High expression of CD99 in glioblastoma has also been observed in patient samples (Urias et al., 2014), and forced overexpression of CD99 in glioblastoma cell lines potentiated migration and invasion *in vitro* and *in vivo* (Seol et al., 2012; Urias et al., 2014). It was also shown in a study of malignant melanoma, that 47 out of 78 cases were found to be CD99 positive using IHC staining of patient samples (Wilkerson, Glasgow and Hiatt 2006). Conversely, CD99 expression in the stroma of non-small cell lung cancer was found to correlate with better prognosis (Edlund et al., 2012).

A small study of 35 clinical samples indicated that CD99 expression was found in metaplastic or 'matrix producing' breast cancer samples (Milanezi et al., 2001). A more recent study using 80 breast cancer samples indicated that 78% of malignant breast tissue was highly expressing CD99 compared to 9% of adjacent healthy normal breast tissue (Baccar et al., 2013). To explore this in more detail, the Kaplan-Meier generator utilised in Chapter 3 were revisited to investigate CD99 expression in metastatic cases of breast cancer. The results shown in Figure 5.1A indicate that high expressing CD99 tumours are significantly more likely to progress to metastatic disease. Interestingly, stratification by molecular subtyping showed that ER-negative/PR-negative tumours with high CD99 expression had significantly poorer probability of metastatic free survival compared to CD99 low expressing tumours (Figure 5.1B). This was also the case for HER2-positive tumours (Figure 5.1C), but not for HER2-negative tumours (Figure 5.1D). These results indicate that CD99 may be an important prognostic factor in determining progression of both ER-negative/PR-negative and HER2-positive breast cancer to metastatic stages of the disease. Experiments in this chapter were therefore aimed at determining the role of CD99 in the metastatic process.

CD99 expression was therefore explored in a small panel of breast cancer cell lines. CD99 has been previously shown to be widely expressed throughout tissues of the body (Smith, Goodfellow and Goodfellow 1993). Previous reports have indicated that

the MCF7 breast cancer cell line expresses CD99 (Byun et al. 2006; Lee et al. 2017). It has also been reported that MDA-231 express very low levels of CD99 (Byun et al. 2006; Lee et al. 2002). Publicly accessible data presented in the Human Protein Atlas showed that two breast cancer cell lines, MCF7 and SKBR3, had similar levels of CD99 mRNA expression ([www.proteinatlas.org](http://www.proteinatlas.org)). The surface expression of CD99 was assessed by flow cytometry to validate the reported mRNA expression profiles. CD99 was expressed by the three TNBC cell lines examined (MDA-231, BrM, SKBR3), as well as the ER-positive breast cancer cell line MCF7 (Figure 5.1E). As previously reported, MDA-231 cells demonstrated the lowest maximal expression of CD99, whereas expression on MCF7 cells was the highest (Figure 5.1E). Interestingly, a transient double peak of CD99 expression was observed in BrM cells which was present during some experiments and suggests the presence of CD99 high and CD99 low expressing cancer cells within this population of BrM cells. The implication of CD99 in breast cancer brain metastasis has not been previously explored, however this expression pattern warrants future investigation into this biphasic expression in BrM cells. This is in comparison to the three other breast cancer cell lines which displayed normal distribution of CD99 expression (Figure 5.1E).

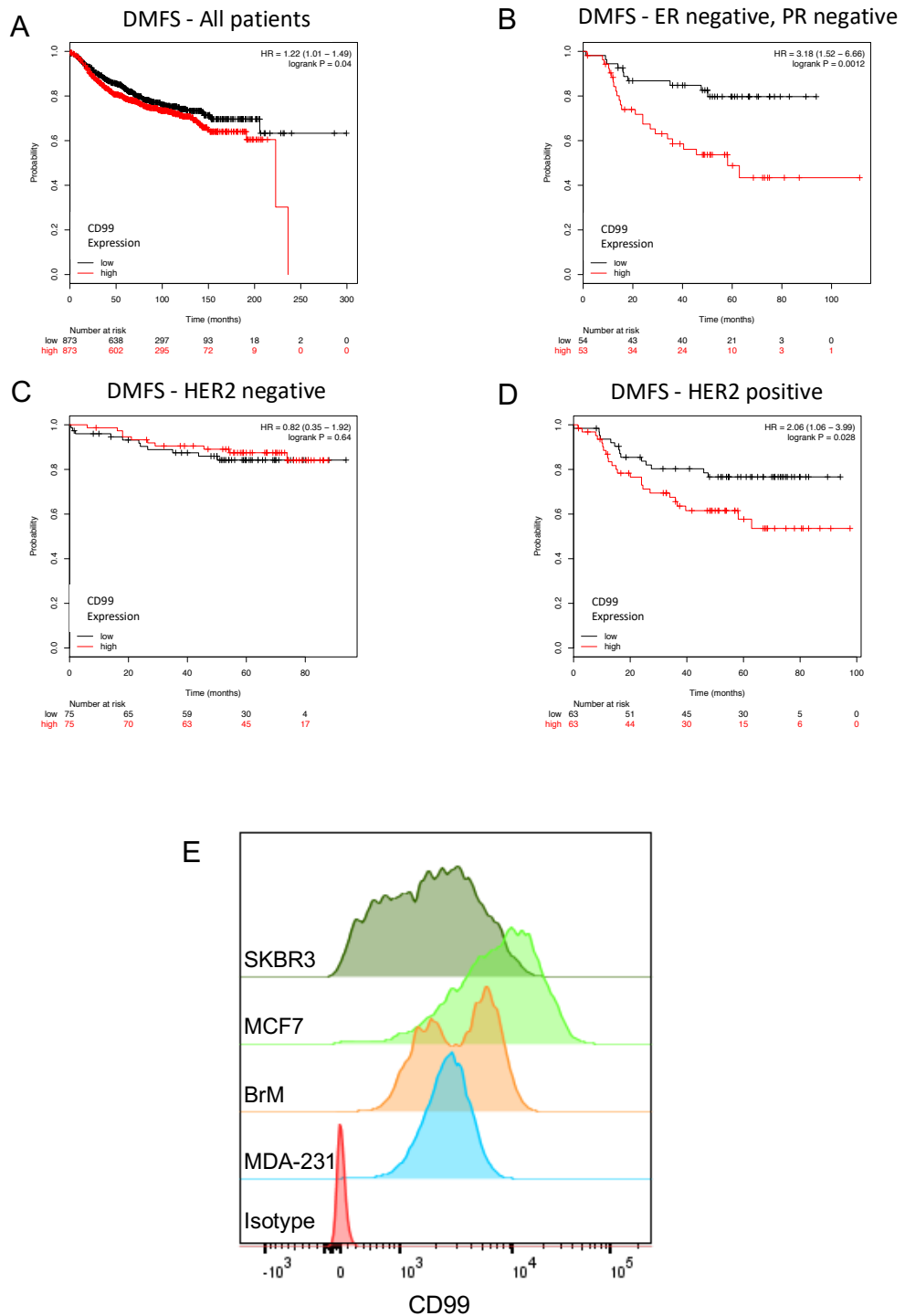


**Fig. 5.1. CD99 expression correlates with increased metastasis and is expressed broadly by breast cancer cell lines.** Kaplan-Meier survival curves were generated for high and low CD99 mRNA expression in 1747 breast cancer patients using an online tool ([www.kmplot.com](http://www.kmplot.com)) (Lánczky et al. 2016). **A**, High expression of CD99 in all breast cancer cases results in significant decrease in probability of Distant Metastatic Free Survival (DMFS). **B**, Patients with estrogen and progesterone negative tumours and high CD99 expression also showed decreased DMFS. **C**, HER2 negative, CD99 high expressing tumours show no significant difference in DMFS. **D**, HER2 positive, CD99 high expressing tumours show significantly reduced probability in DMFS. **E**, Range of breast cancer cell lines analysed by flow cytometry for CD99 expression. SKBR3, MCF7, BrM and MDA-MB-231 cells were trypsinised and fixed in 4% PFA before subsequent staining with CD99 conjugated antibodies and analysis by flow cytometry.

### 5.3 CD99 regulates breast cancer adhesion to endothelial cells

CD99 plays a role in the adhesion of cancer cells to ECM (Lee et al. 2017; Lee et al. 2015) and in neutrophil adhesion to endothelial cells (Goswami et al., 2017). A role for CD99 in the adhesion of cancer cells to endothelial cells has not been reported to date. Thus, the role of CD99 in breast cancer cell adhesion to EC monolayers was investigated. Cell tracker green (CTG)-labelled MDA-231 cells were assayed for adhesion to HUVEC monolayers over a two-hour period in the presence of an anti-CD99 blocking antibody (or control antibody). Use of the anti-CD99 antibody significantly reduced binding of CTG labelled MDA-231 to HUVEC endothelial monolayers at multiple time points, indicating a role for CD99 in adhesion of MDA-231 to the endothelium (Figure 5.2A-B)

CD99 is expressed by both the HUVEC and MDA-231 cells, therefore siRNA knockdown of CD99 in either MDA-231 or HUVEC CD99 was performed to identify a role for CD99 in the breast cancer cells and/or the endothelium. Pooled siRNA targeting CD99 (denoted si99) was effective at reducing CD99 expression in both HUVEC and MDA-231 cells when analysed by western blotting (Figure 5.3A). The efficiency of CD99 knockdown was assessed in MDA-231 cells using flow cytometry over a 7-day period; this indicated that >90% knockdown of CD99 was attained for up to 7 days compared to mock and scrambled siRNA controls (Figure 5.3B). Cell viability of mock and siRNA transfected MDA-231 cells at 72 hours of knockdown was investigated by vitality staining, which indicated that little cell death was occurring upon CD99 (or control) knockdown (Figure 5.3C).

Next, siRNA-treated cells were then used in adhesion assays to determine the role of CD99 in cancer cell adhesion to the endothelial monolayers. Results showed that CD99 depleted MDA-231 cells were significantly inhibited in their ability to adhere to endothelial cell monolayers at several time points, signifying that MDA-231 adhesion is at least partially reliant on the functional expression of CD99 (Figure 5.3D). Interestingly, knockdown of CD99 on endothelial cells did not alter the adhesion of MDA-231 cells at 15, 30 and 60 minutes but showed enhanced binding at 120 minutes (Figure 5.3E). Collectively, these data suggest that transient adhesion of breast cancer cells to endothelial cells is dependent on MDA-231 CD99 expression, whereas endothelial CD99 appears to be dispensable in this process, except at the time point of 120 minutes.

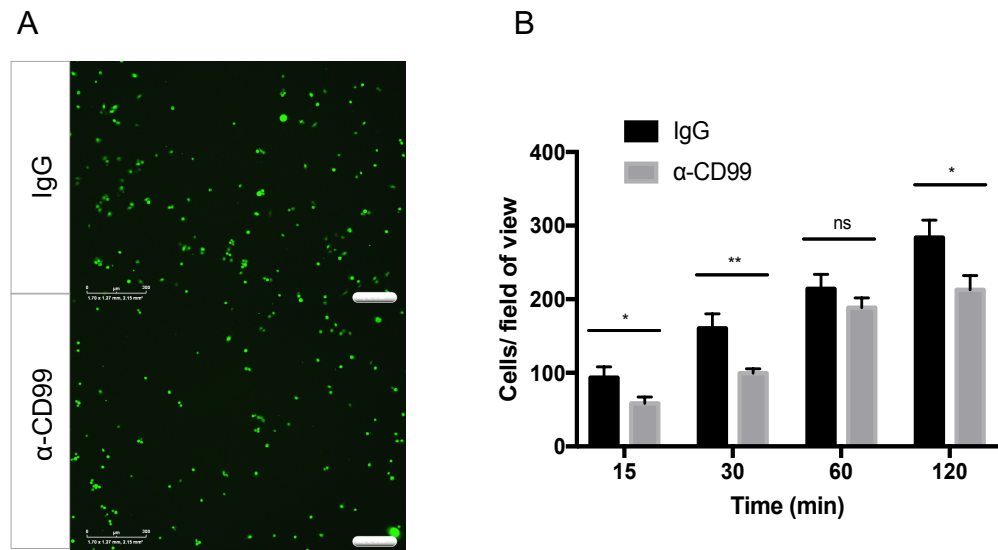


**Fig. 5.2. CD99 regulates breast cancer adhesion to endothelial cells.** **A**, MDA-231 cells were Cell Tracker Green-labelled and left to adhere for indicated time points to confluent HUVEC monolayers pretreated with either (1 $\mu$ g/ml) anti-CD99 functional blocking antibodies or IgG control. Unbound cells were washed away with PBS before fixation in 4% PFA before quantification of bound cells. Scale bar: 300  $\mu$ m. **B**, quantification of panel A. Data are representative of n=3 independent replicates. Error bars indicate Standard Error. Statistical analysis was performed using student's t-test. \* $p$ <0.05, \*\* $p$ <0.005.

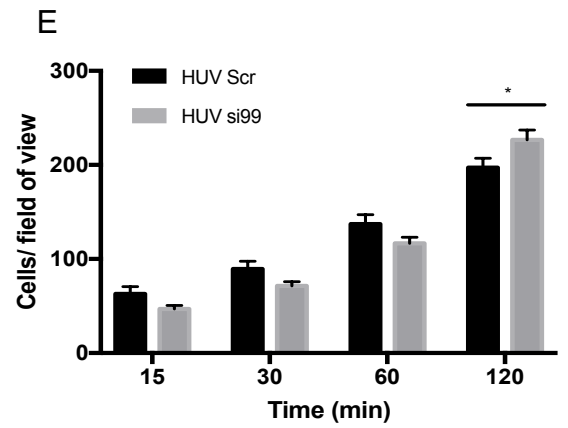
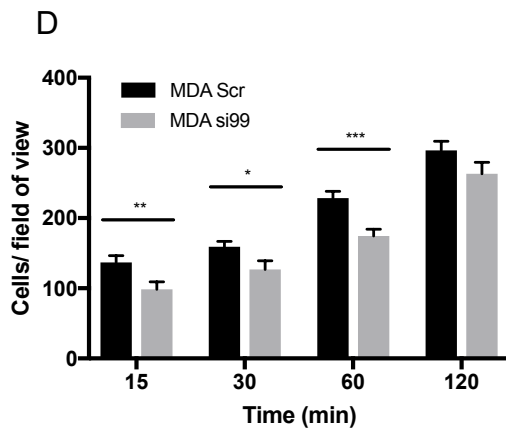
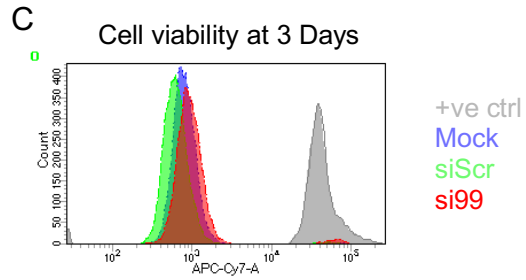
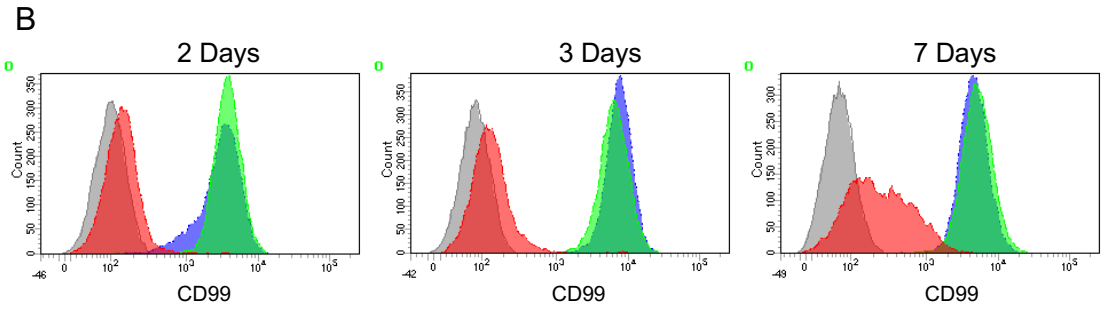
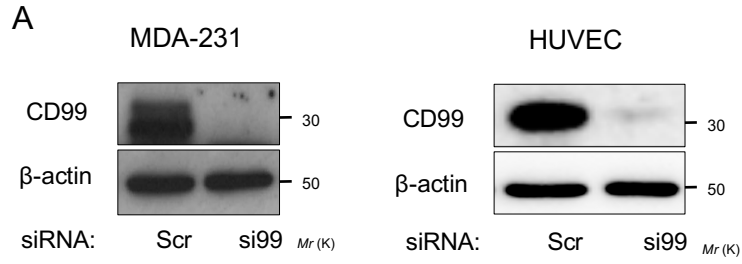


**Fig. 5.3. CD99 regulates breast cancer adhesion to endothelial cells.** **A**, MDA-231 and HUVECs transfected with siRNA against CD99 (or scramble control) for 72h before lysis and analysis of CD99 expression by western blotting in total cell lysates. Blots are representative images of n=3 replicates. **B**, MDA-231 cells were transfected CD99 siRNA and expression of CD99 monitored over a period of 7 days at indicated time points by flow cytometry. MDA-231 cells; mock, scramble or CD99 siRNA transfected were trypsinised and washed in PBS before staining with isotype control or CD99 conjugated antibodies before analysis by flow cytometry. **C**, Cell viability of mock, scrambled and CD99 siRNA treated MDA-231 cells was assessed using cell viability staining. Positive control including cells fixed in 4% PFA were additionally stained with Zombie. **D**, MDA-231 cells were transfected with Scrambled or CD99 siRNA for 72h before being CTG-labelled and left to adhere to confluent HUVEC monolayers for indicated time points. Unbound cells were washed away with PBS before fixation in 4% PFA and quantification of bound cells. **E**, HUVEC cells were transfected with Scrambled or CD99 siRNA for 72h and grown to confluent monolayers before seeding of CTG-labelled MDA-231 and left to adhere for indicated time points. Unbound cells were washed away with PBS before fixation in 4% PFA and quantification of bound cells. Data are representative of n=3 independent replicates. Error bars indicate standard Error. Statistical analysis was performed using student's t-test. \*p<0.05, \*\*p<0.005, \*\*\*p<0.0005

#### **5.4 CD99 suppresses transendothelial migration of metastatic cancer cells**

Adhesion precedes the extravasation of disseminated cells during the metastatic cascade (Reymond, d'Água and Ridley 2013). Therefore, the role of CD99 in the ability of MDA-231 cells to traverse endothelial monolayers was examined by live cell microscopy. MDA-231 cancer cells were treated with control or CD99 siRNA. Following 72 hours transfection, cancer cells were labelled with CTG and seeded to confluent HUVEC monolayers and imaged for 4 hours to capture cancer cell spreading and intercalation. Results showed that CD99 depletion in MDA-231 enhanced the rate of cancer cell spreading onto, and intercalation into the HUVEC monolayers (Figure 5.4A-B). For the MDA-231 live cell imaging results, at 4 hours, approximately 30% of CD99 siRNA treated MDA-231 had intercalated, compared to 20% of the scrambled control (Figure 5.4B). To address whether this effect was unique to this breast cancer cell line the experiment was repeated using the metastatic prostate cancer cell line PC3; results confirmed that CD99 knockdown in PC3 also enhanced spreading and intercalation on HUVEC monolayers (Figure 5.4C-D). Taken together, these results suggest that depletion of CD99 in MDA-231 and PC3 metastatic cells enhances intercalation into endothelial monolayers.

Cancer cells induce the dismantling of endothelial cell-cell contacts during extravasation (Stoletov et al., 2010), which can be measured by changes in electrical resistance of an endothelial monolayer. Further investigation of TEM was performed using Real Time Cell Analysis (RTCA) assays, as described in the materials and methods (Methods Section 2.3). The CD99 depleted MDA-231 exhibited an enhanced ability to disrupt endothelial barrier integrity at later time points of 24 hours (Figure 5.5A). However, this effect was not found at earlier time points of 60 minutes (Figure 5.5B), suggesting that CD99 depletion enhances the later stages of breast cancer cell extravasation, despite differences evident at the earlier time points of 4 hours seen during intercalation examined with live cell imaging (Figure 5.4B).

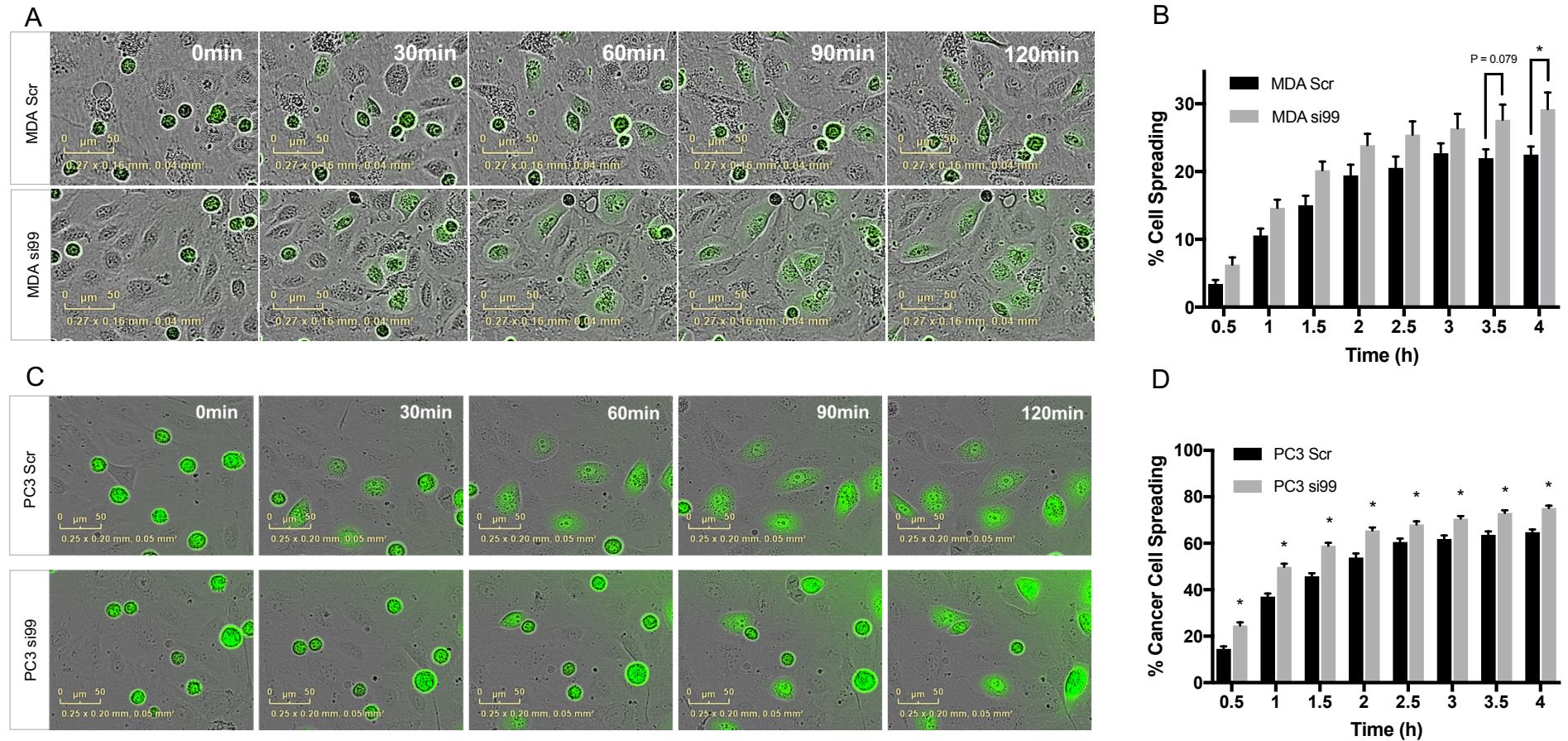


**Fig. 5.4. CD99 suppresses transendothelial migration of metastatic cancer cells.** **A**, MDA-231 cells were transfected with CD99 or scrambled control siRNA and were labelled with Cell Tracker Green before being seeded on top of confluent HUVEC monolayers and imaged for 4 hours using Incucyte live cell imaging to capture intercalating cells. Scale bar: 50  $\mu$ m. **B**, Quantification of data shown in panel A, showing intercalation of MDA-231 Scrambled and si99 cells as a percentage of total cells. **C**, PC3 cells were transfected with CD99 or scrambled control siRNA and were labelled with Cell Tracker Green before seeding on top of confluent HUVEC monolayers and imaging for 4 hours using an Incucyte live cell imager. Scale bar: 50  $\mu$ m. **D**, Quantification of data shown in panel A, showing intercalation of PC3 Scrambled and si99 treated cells as a percentage of total cells. Data is representative of n=3 independent replicates. Error bars indicate standard error. Statistical analysis was performed using student t-test. \*p<0.05.

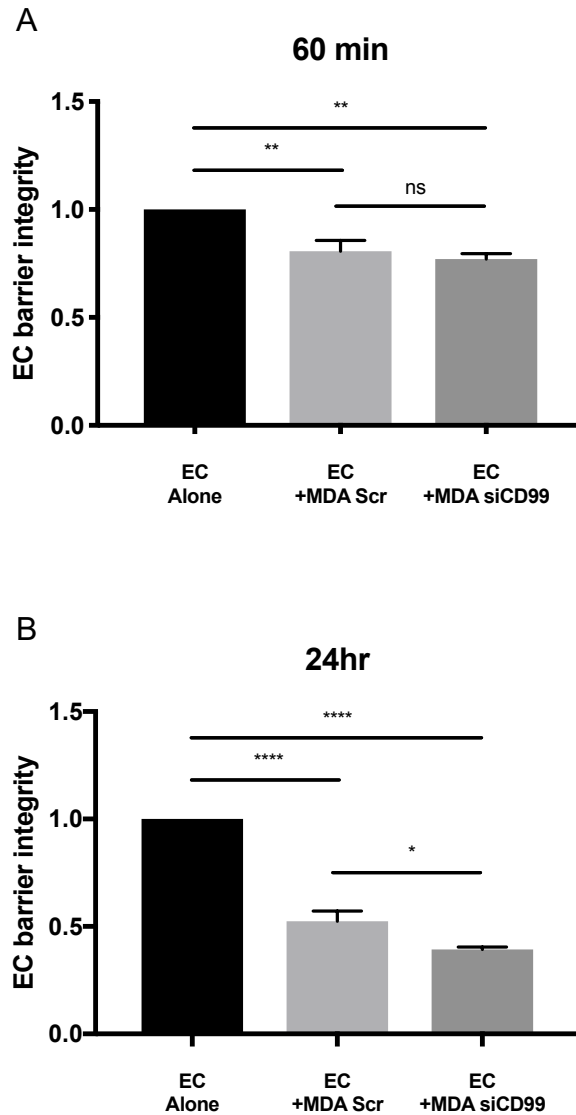


**Fig. 5.5. Depletion of MDA-231 CD99 enhances disruption of endothelial monolayers.** MDA-231 cells treated with scrambled control or CD99 siRNA were seeded to confluent HUVEC monolayers and changes in impedance were recorded continuously for 48h using E-plates in the XCELLigence Real Time Cell Analyser instrument. Data is presented as fold change in barrier integrity compared to HUVEC monolayers alone at indicated time points of **A**, 60 min and **B**, 24 hours from n=4 independent replicates. Error bars indicated standard error. Statistical analysis was performed using one-way ANOVA with Tukey's multiple comparison. \*p<0.05, \*\*p<0.005, \*\*\*\*p<0.00005

## **5.5 CD99 regulates chemotactic migration and spreading of breast cancer *in vitro***

The above results indicated that CD99 depletion potentiated the invasion of MDA-231 into HUVEC monolayers. This prompted further investigation into whether CD99 was impacted MDA-231 migration, invasion and motility in the absence of endothelial monolayers. Following 72 hours transfection of MDA-231 with control or CD99 siRNA, cells were seeded to RTCA plates for analysis of migration, invasion and motility. Cells were seeded into specialised plates in which an array of sensors are imbedded within the base of each well, allowing measurement of multiple parameters through disruption (or impedance) of electrical flow between sensor nodes. E-plate RTCA assays proliferation, migration and morphology of cells in 2D and an arbitrary unit (cell index) is applied to the quantified measurements. Results indicated that CD99 knockdown increased MDA-231 cell index significantly, suggesting an increase in proliferation, migration or morphology (Figure 5.6A). A scratch wound assay (a well characterised assay for 2D migration and motility) indicated that CD99 knockdown in MDA-231 had no significant impact on migration of MDA-231. However, four out of five assays performed showed a small increase in migration when CD99 was depleted (Figure 5.6B-C). Further analysis of the impact of CD99 depletion on migration was also performed using the RTCA instrument. Depleted or control MDA-231 cells were loaded into specialised Transwell-style plates (cell invasion and migration (CIM) plates), in which sensors were embedded on the underside of the porous Transwell membrane, allowing real-time analysis of migration and invasion. Migration and invasion of CD99 depleted MDA-231 cells (down a serum gradient) was measured for 24 hours and subsequent analysis showed a significant increase in migration compared to scrambled control (Figure 5.6D). This suggested that MDA-231 migratory and invasive potential was enhanced by CD99 depletion in the absence of an EC monolayer.

The E-plate RTCA assays are an amalgamation of proliferation, migration and morphology (culminating in changes in 'cell index'). To test the role of CD99 in cell proliferation, a simpler assay was performed. Control and CD99 depleted MDA-231 cells were cultured over 4 days before staining with crystal violet (Figure 5.7A) and the relative absorbance quantified using spectrophotometry. This approach indicated that there was no significant difference in proliferation between control or CD99 knockdown MDA-231 cells (Figure 5.7B). However, CD99 knockdown cells did exhibit a trend towards greater proliferative potential which failed to reach significance. When taken together, these results suggest that CD99 appears to

regulate both the migration and spreading of MDA-231 cells, conferring increased penetrability of endothelial monolayers evident in transmigration assays (Figure 5.4 and 5.5).

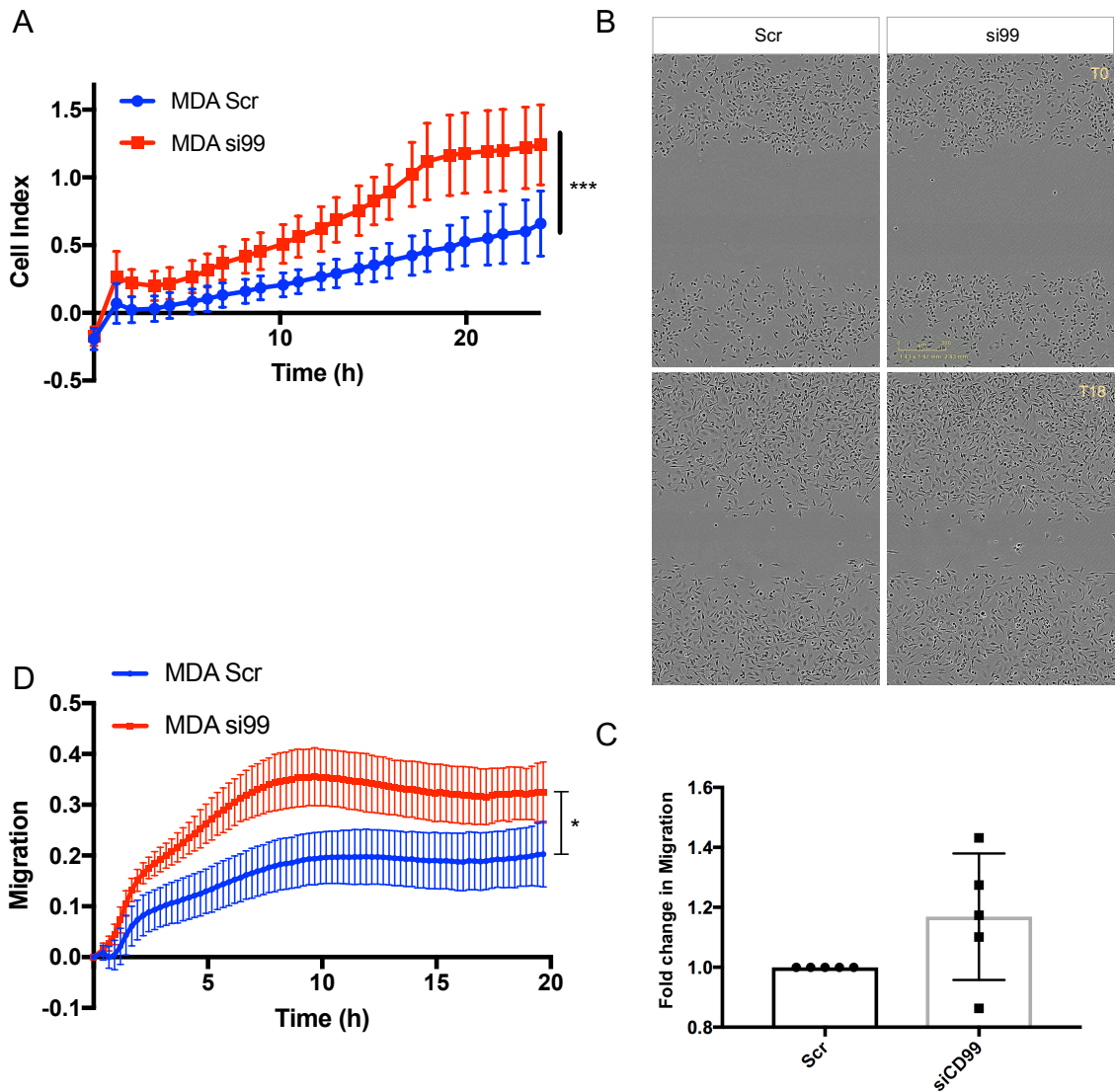


**Fig. 5.6. CD99 regulates chemotactic migration and spreading of breast cancer in vitro.** **A**, Proliferation, morphology, and adhesion of CD99 siRNA-transfected MDA-231 cells were examined using E-plates xCELLigence Real Time Cell Analyser (RTCA). Cells were seeded to E-plates and changes in impedance measured every hour for 24 hours. Error bars indicate standard error of  $n=3$  independent replicates. **B**, Representative images of scratch wound migration assay. CD99 and Scrambled control siRNA treated MDA-231 cells were seeded at equal density to 96 well plates until confluent. Cells were serum starved for 2-3 hours before 'wounding' using a Wound Maker tool (Essenbioscience). Migration of siRNA-treated MDA-MB-231 cells was subsequently monitored using Incucyte live cell imaging and quantified using Image J. Scale bar: 300  $\mu\text{m}$ . **C**, Quantification of B, from  $n=5$  independent replicates. Error bars indicate standard deviation. **D**, MDA-231 cells treated with control or CD99 siRNA were seeded to Cell Invasion/Migration (CIM) plates and changes in impedance monitored over 20 hours. Data are representative of  $n=3$  independent replicates. Error bars indicate standard error. Statistical analysis was performed using Analysis of Covariance (ANCOVA) and student t-test. \* $p<0.05$ , \*\*\* $p<0.0005$ .

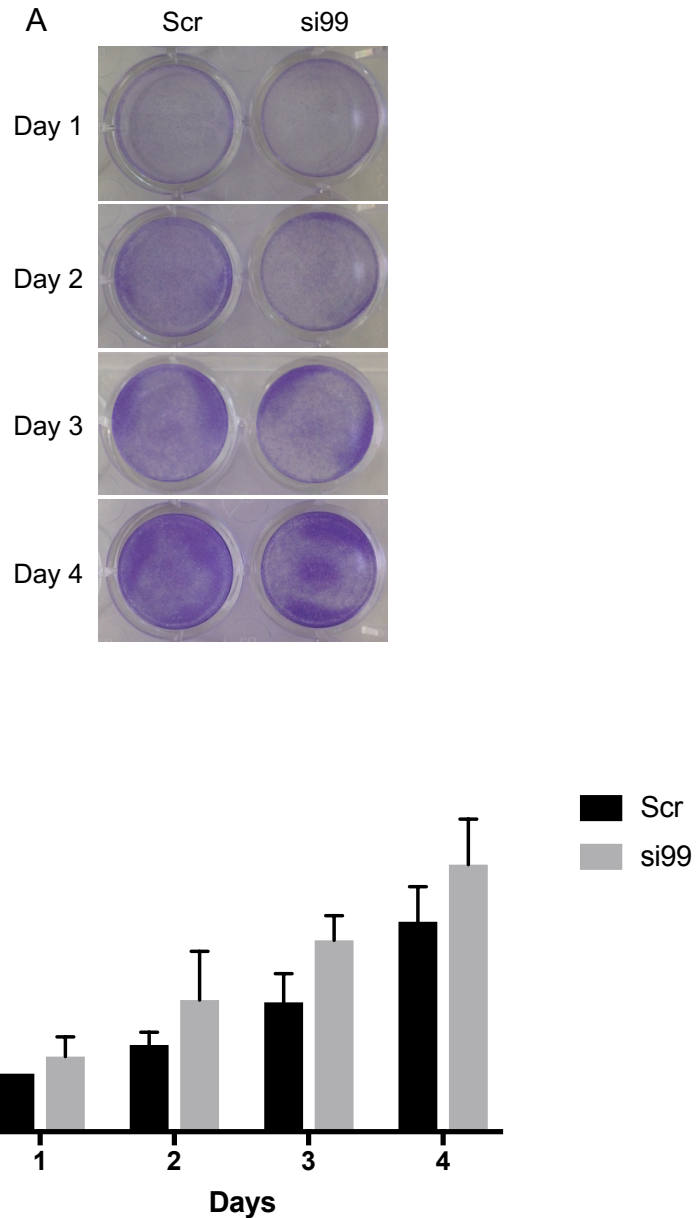


**Fig. 5.7. Proliferation of MDA-231 is not perturbed by CD99 depletion.** **A**, MDA-231 cells treated with control or CD99 siRNA were seeded to 24 well tissue culture dishes at the same density. Plates were left for 1,2,3 and 4 days before fixing in 4% PFA and subsequent staining with Crystal Violet. Images were taken prior to solubilising in Methanol. Images are representative of 3 independent replicates. **B**, Crystal violet stained cells were then solubilised in 100% methanol and spectrophotometry performed using a plate reader. Results were normalised to stained empty wells and background subtracted. Data presented here are normalised to Scrambled control at day 1 of proliferation assay. Data are representative of n=3 independent replicates. Error bars indicate standard deviation. Statistical analysis was performed using students t-test.

## 5.6 CD99 regulates actin dynamics upon adhesion to ECM substrates

The depletion of CD99 from MDA-231 and PC3 resulted in pronounced differences in the spreading phenotype of these cells upon intercalation into HUVEC monolayers and differences in Cell Index (representing changes in migration, invasion, and morphology) (Figures 5.4, 5.5 and 5.6). This suggested that CD99 may regulate the cytoskeleton and it was hypothesised that CD99 might regulate actin dynamics in these events. Cells which undergo adhesion and TEM are known to undergo substantial cytoskeletal remodelling (Olson and Sahai, 2009).

Therefore, the role of CD99 and MDA-231 cell spreading in the early adhesion to different ECM components was investigated (Appendix Figure 2). Staining of F-actin allowed observation of the actin rearrangement upon adhesion of control or CD99 siRNA transfected MDA-231 to different ECM substrates; gelatin, type 1 collagen, and fibronectin (Appendix Figure 2). The most prominent difference between control and CD99-siRNA treated cells was noted upon adhesion to type 1 collagen substrate (Figure 5.8A). At higher magnification (zoomed panels) the CD99 siRNA-treated MDA-231 cells (si99) showed strong cortical localisation of actin upon 30 minutes of adhesion to type 1 collagen (Figure 5.8A). This was most readily seen by actin profiles whereby actin staining was quantified and, using ImageJ software, represented in a 3D density plot of actin localisation (Figure 5.8A, end panel). These results suggest a role for CD99 in the regulation of cytoskeletal rearrangement. Furthermore, quantification of cell surface area indicated that CD99 depletion enhanced cell size, indicating greater cell spreading, on both gelatin and collagen substrates (Figure 5.8B). Cell roundness was also found to be significantly reduced in CD99-depleted MDA-231 when plated onto various ECM substrates when compared to control conditions (Figure 5.8C). Changes in cell roundness are also indicative of cell spreading upon adhesion, as the cell changes from a rounded-up morphology to a less-rounded, spread morphology. Interestingly, although a reduction in the number of MDA-231 cells adhering to HUVEC monolayers was noted initially (Figure 5.3C), a significant increase in MDA-231 cell adherence was noted to plastic and fibronectin, but not to gelatin or collagen (Figure 5.8D). An increase in PC3 cell spreading was also observed when CD99-depleted cells were plated on control (plastic only) conditions (Figure 5.9), suggesting the role of CD99 as a regulator of the cytoskeleton during adhesion, extends to metastatic cancer cells beyond MDA-231. Collectively, these results identify a role for CD99 in regulating the actin dynamics of adhering cells, and this in turn may influence additional features of tumour biology, such as metastatic dissemination.

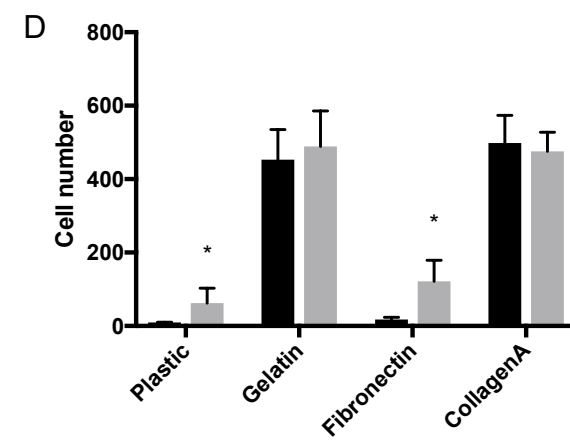
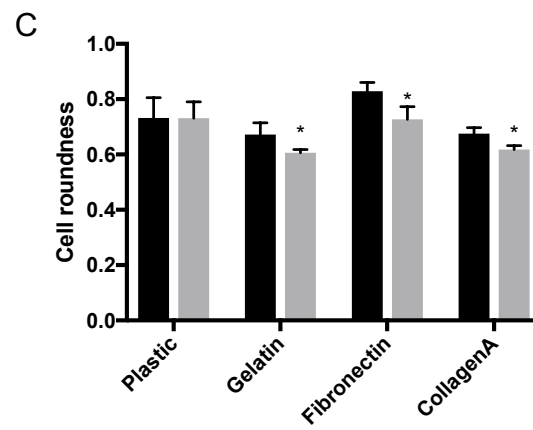
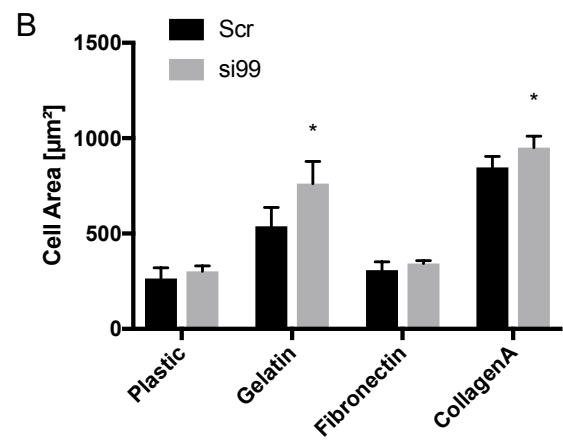
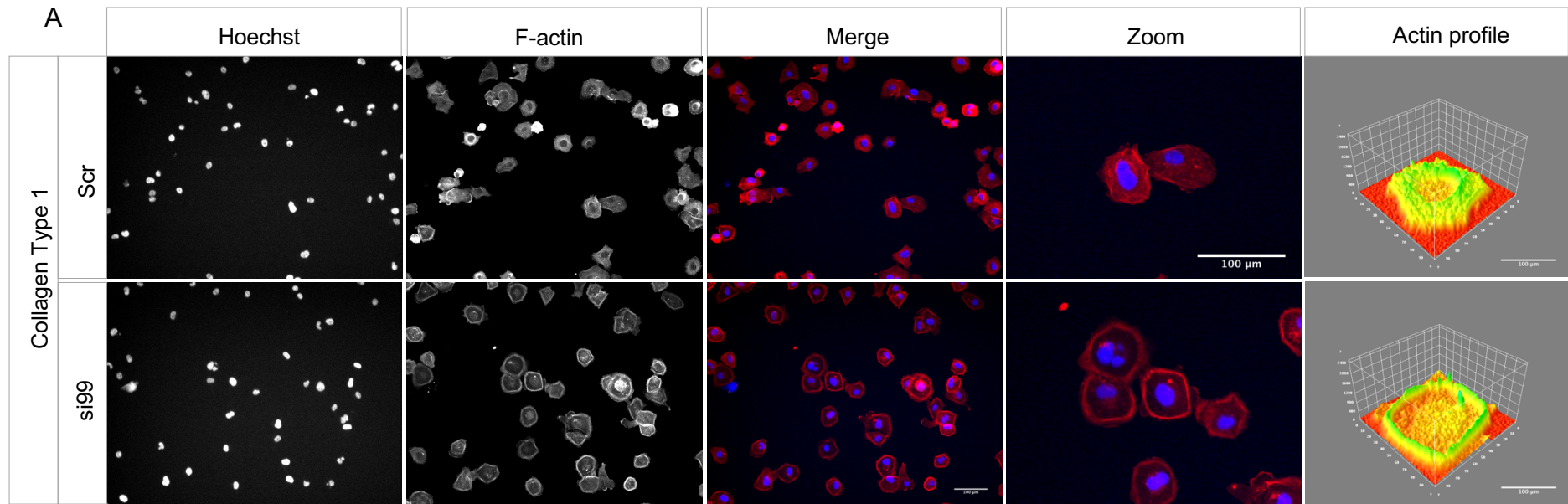


**Fig. 5.8. Actin reorganisation upon adhesion to ECM substrates is regulated by CD99.** **A**, 72 hours following transfection MDA-231 cells treated with control scrambled or CD99 siRNA were seeded to 96 well plates coated in Collagen type 1. After 30 minutes of adhesion, non-adherent cells were washed away with PBS and adherent cells were fixed in 4% PFA. Cells were then permeabilised and stained for F-actin and nuclear stain with Hoechst and imaged used high content Perkin Elmer Operetta microscope. 3D profile of F-actin stain was constructed using ImageJ. Scale bar: 100µm. **B**, Analysis of Cell Area (µm), Cell roundness and Cell number was carried out using Columbus Software. Data are representative of n=3 independent replicates. Error bars indicate standard deviation. Statistical analysis was carried out using students t-test. \*p<0.05.

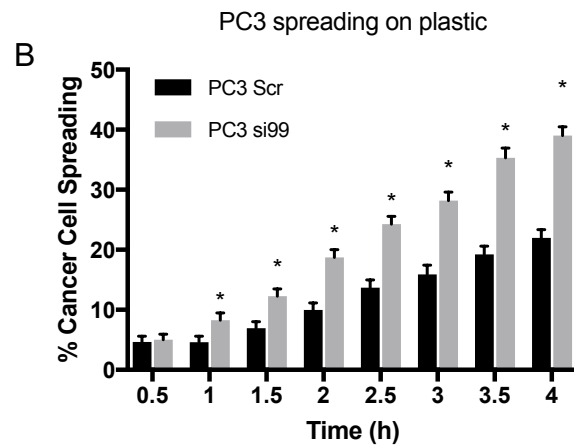
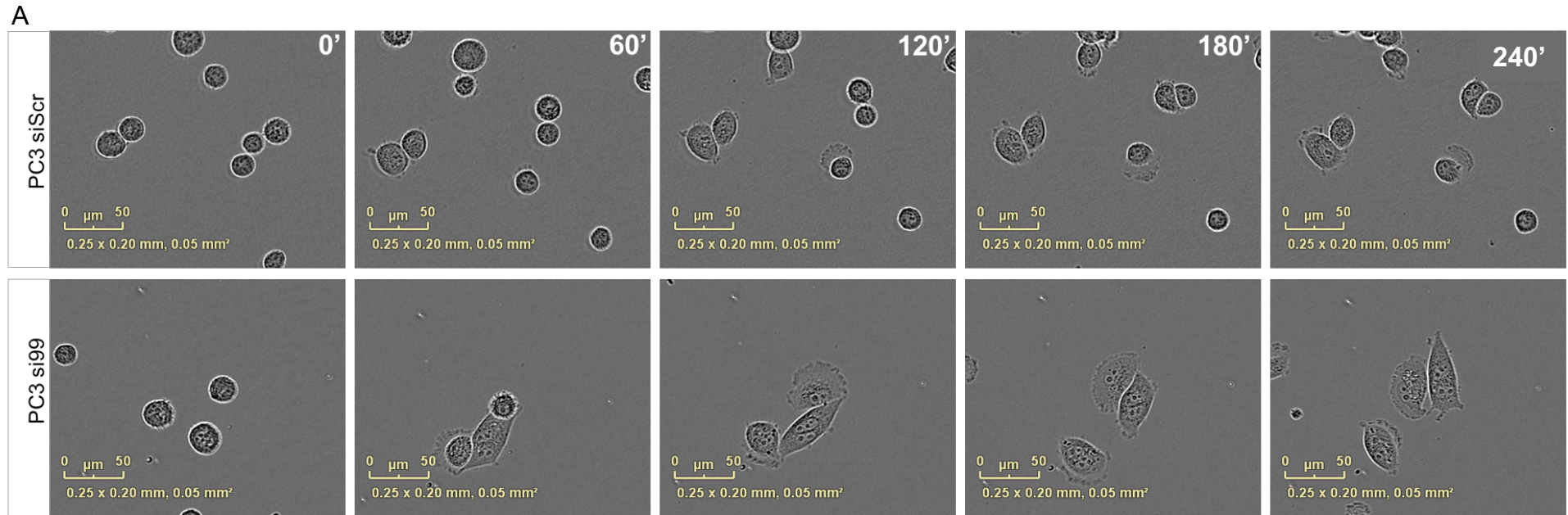


**Fig. 5.9. CD99 suppresses spreading of PC3 metastatic prostate cancer cells.** **A**, PC3 cells were transfected with CD99 or scrambled control siRNA for 72 hours before seeding to 96 well plates and subsequent live cell imaging for 4 hours using Incucyte microscope. Scale bar: 50  $\mu$ m. Images are representative of n=3 independent biological replicates **B**, Quantification of data in panel A, showing spreading of cells as a percentage of total cells. Data are representative of n=3 independent replicates. Error bars indicate standard error. Statistical analysis was performed using student t-test. \* $p < 0.05$ .

## 5.7 CD99 suppresses metastatic dissemination of breast cancer *in vivo*

Increased intercalation into endothelial monolayers, endothelial disruption and migration were observed *in vitro*, suggesting that CD99 depletion may potentiate metastatic dissemination *in vivo*. Therefore, CD99 knockdown was performed in luciferase-expressing MDA-231 cells (allowing them to be easily monitored upon *in vivo* injection). The luciferase expressing MDA-231 cells were transfected with mock, siCD99 or control siRNA, cultured for 72 hrs before injection into the tail vein of SCID mice (injections were performed by Dr Alison Taylor). Tail vein injection mimics haematogenous dissemination of cancer cells and is widely used as an experimental metastasis model *in vivo* (Kang et al., 2003; Minn et al., 2005; Bos et al., 2009). Cells injected into the tail vein often seed to the lung as this is one of the first major capillary networks that disseminated cells encounter upon introduction into the vasculature. Mock, scrambled control siRNA and siCD99 MDA-231 injected mice were imaged each week for 4 weeks (Appendix Figure 3). Bioluminescent imaging indicated that at weeks 3 and 4, mice injected with CD99-depleted MDA-231 cells showed significantly enhanced luciferase signal in the lungs (Figure 5.10A) compared to scrambled controls, suggestive of increased metastatic burden (Figure 5.10B). This is consistent with the *in vitro* data indicating a role for CD99 expression in constraining the migration and invasion of MDA-231 cells. Thus, CD99 expression appears to suppress the metastatic potential of MDA-231 cells *in vitro* and *in vivo*. Previous results presented in this chapter, suggest that this is regulated through modulation of transendothelial migration and alterations to actin plasticity.

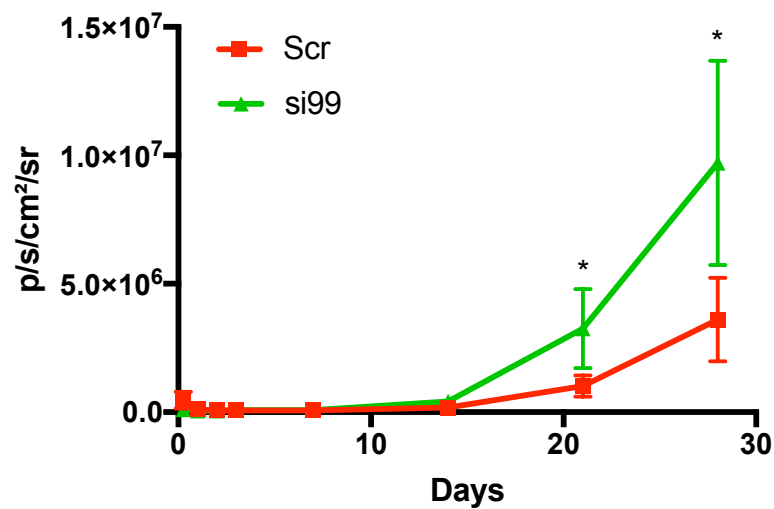
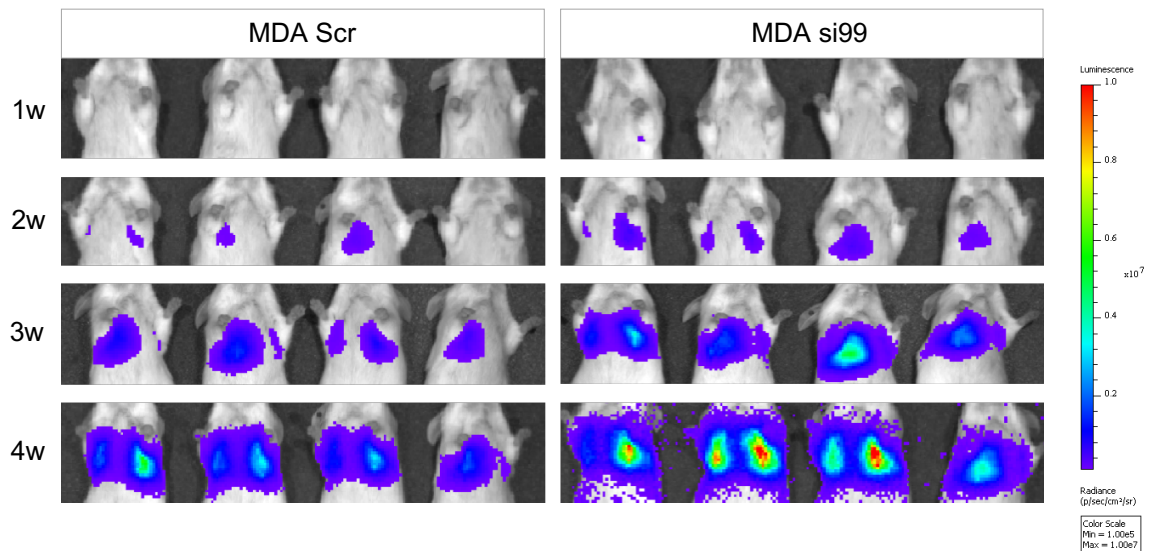


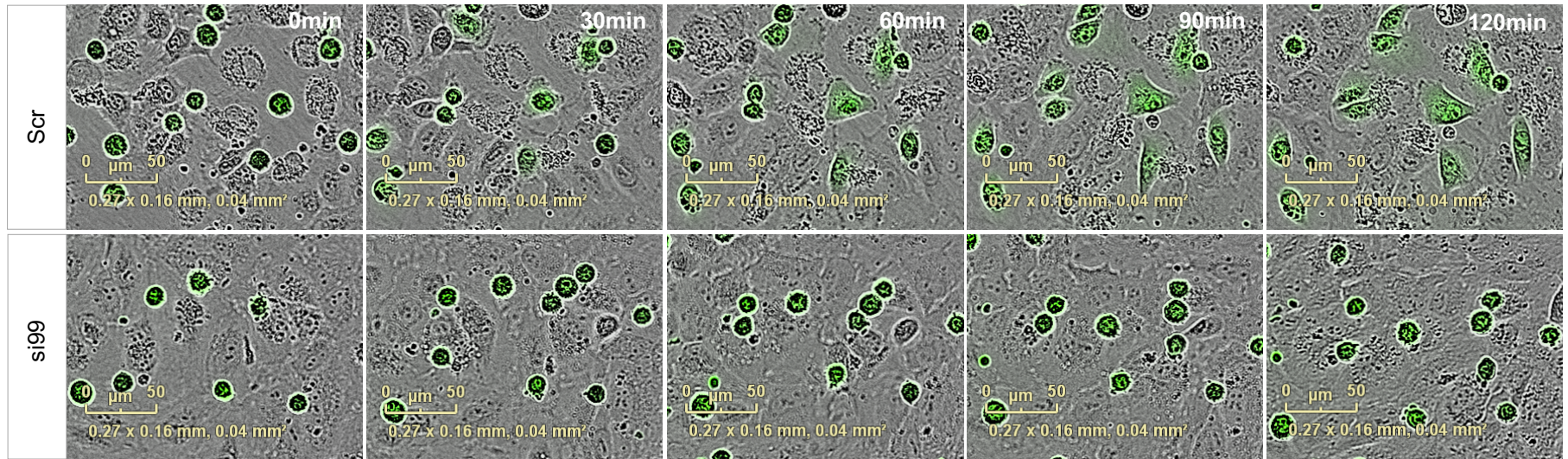
**Fig. 5.10. CD99 suppresses metastatic dissemination of breast cancer in vivo.** **A**, Luciferase expressing MDA-231 cells were transfected with scramble control or CD99 siRNA for 72h before tail-vein injection of  $5 \times 10^5$  cells into 5 mice per condition. BLI was performed weekly to monitor metastatic burden within the lungs of mice which successfully harboured lung metastases (4 mice per group) and mice were culled at week 4 before symptoms of metastatic burden began to show. **B**, Quantification of BLI. Error bars are indicative of standard deviation. Statistical analysis was performed using students t-test \* $p < 0.05$ .

## 5.8 Endothelial CD99 regulates cancer cell transendothelial migration

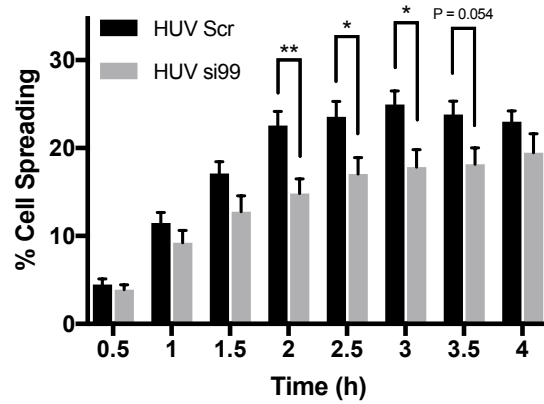
Metastasising cancer cells must undergo substantial structural changes to achieve successful transmigration. However, transmigration also requires reciprocal retraction of endothelial cell membranes facilitated by substantive cytoskeletal remodelling within the endothelial cell itself (Reymond, d'Água and Ridley 2013). This was recently highlighted by Follain, et al. who showed that the endothelium forms a cup-like structure around extravasating cancer cells, thereby minimising permeability as the extravasating cell transmigrates (Follain et al., 2018).

To explore this concept further, the role of endothelial CD99 in facilitating cancer cell TEM was investigated using live cell imaging. Previous reports have demonstrated that inhibition of CD99 using function-blocking antibodies inhibited the transmigration of leukocytes; arresting the migrating cells partway through the process of TEM (Schenkel et al., 2002). Furthermore, results presented in this thesis chapter have shown that application of anti-CD99 antibodies blocked MDA adhesion to HUVEC monolayers (see Figure 5.2). HUVECs treated with CD99 siRNA (or controls) underwent live cell imaging to analyse HUVEC-cancer cell interactions (Figure 5.11). The results showed that treatment of HUVEC monolayers with CD99 siRNA reduced the ability of MDA-231 cells to intercalate into the HUVEC monolayers (compared to scrambled control treated HUVEC monolayers) at multiple, early time points during the process (Figure 5.11A-B). However, this effect was greatest during the middle of the assay (Time = 2-3 hours). This was also evident in the intercalation of PC3 cells (Figure 5.11C), suggesting that CD99 regulates TEM of cancer cells in a manner analogous to leukocytes. TEM was further assessed using an RTCA assay, where treatment of HUVECs with CD99 siRNA was found to delay the barrier disruption induced by MDA-231 binding early during TEM (Time = 15 and 30 minutes; Figure 5.12A-B). Again, this effect was absent at later time points of 60 and 90 minutes, mirroring results from live cell imaging of intercalation (Figure 5.12C-D), and further strengthening the proposed role for CD99 in influencing the early events of cancer cell TEM.

A



B



C

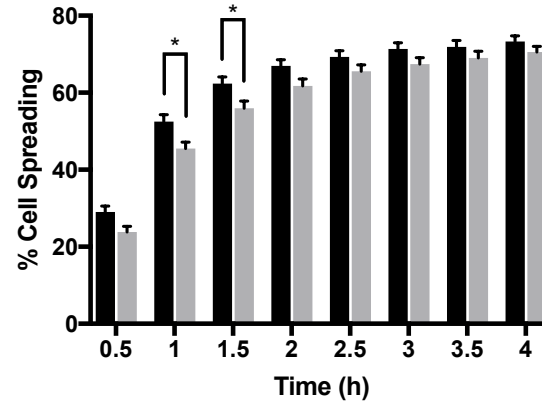


**Fig. 5.11. Endothelial CD99 regulates cancer cell transendothelial migration.** **A**, CTG labelled MDA-231 cells were seeded on top of confluent HUVEC monolayers that were transfected with CD99 or scrambled control siRNA and imaged for 4h using live cell imaging Incucyte microscope to capture intercalation. Scale bar: 50  $\mu$ m. **B**, Quantification of data in panel A, showing cancer cell spreading as a percentage of total cells. **C**, as in panel B except investigating PC3 intercalation into Scramble or si99 HUVEC monolayers. Data are representative of n=3 independent replicates. Error bars indicate standard error. \* $p < 0.05$ , \*\* $p < 0.005$ .

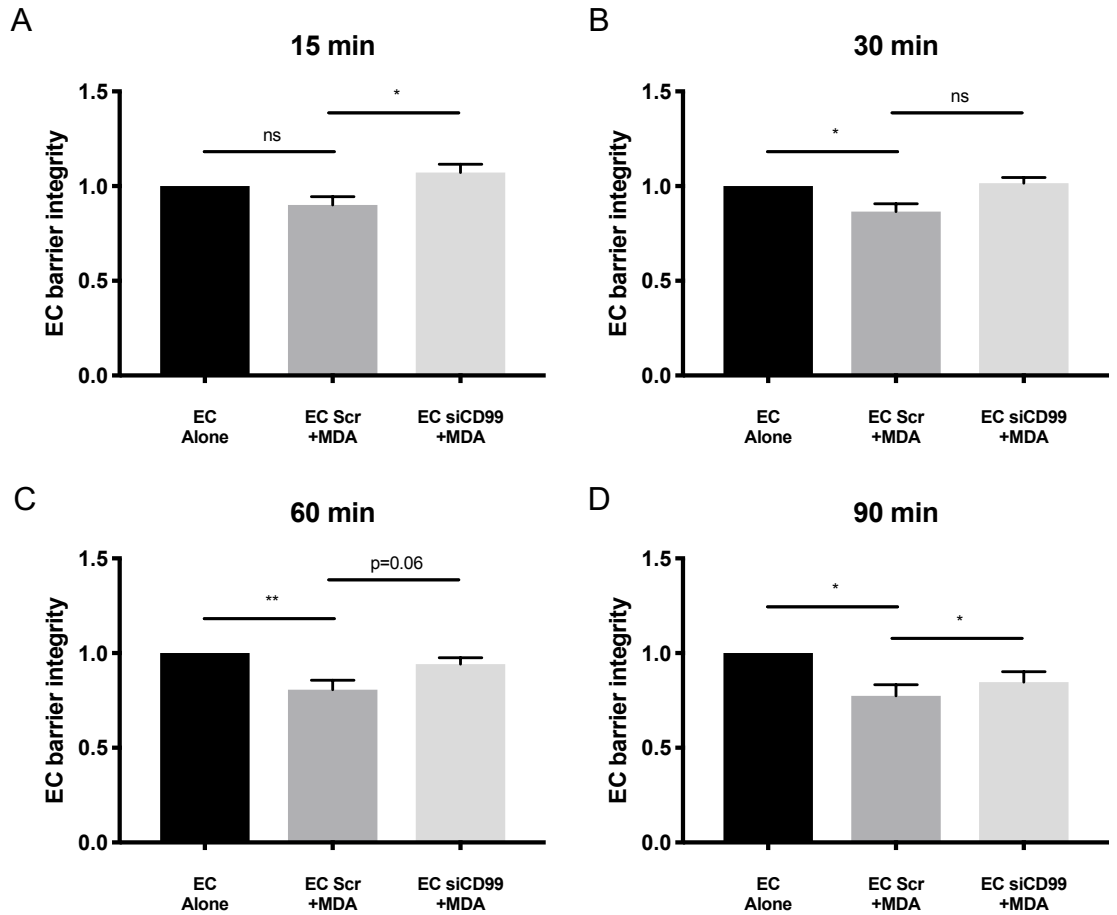


**Fig. 5.12. Depletion of HUVEC CD99 increases endothelial barrier integrity.** HUVEC were treated with scrambled control or CD99 siRNA and were seeded to XCELLigence E-plates and grown to confluency. MDA-231 cells were seeded to confluent HUVEC monolayers and changes in impedance were recorded continuously for 24h using Real Time Cell Analyser instrument. Data is presented as fold change in barrier integrity compared to HUVEC monolayers alone at indicated time points of **A**, 15 minutes **B**, 30 minutes **C**, 60 minutes and **D**, 90 minutes. Data is representative of n=4 independent replicates. Error bars indicated standard error. Statistical analysis was performed using one-way ANOVA with Tukey's multiple comparison. \*p<0.05, \*\*p<0.005.

## 5.9 CD99 modulates Cdc42 activity and expression

Results above implicate CD99 in the dramatic remodelling of the cytoskeleton upon adhesion of MDA-231 to ECM components. Furthermore, CD99 participates in distinct processes within HUVEC and MDA-231 cells, during the TEM of cancer cells. This prompted investigation into the potential link between CD99 and the Rho-GTPase family, a group of proteins implicated in TEM of cancer cells and regulation of cytoskeletal dynamics (Reymond et al., 2012).

Cdc42 regulates endothelial barrier stability via maintenance of adherens junctions at cell-cell contacts within endothelial cells (Kouklis et al., 2004; Ramchandran et al., 2008; Cerutti and Ridley, 2017). It was hypothesised that increased barrier stability of endothelial monolayers induced by CD99 loss (Figure 5.12) was facilitated by changes in Cdc42 activity, and that increased metastatic behaviour of MDA-231 may also be attributable to changes in Cdc42-dependent pathways. Initial investigation by western blotting showed that CD99 depletion increased the expression of Cdc42 in HUVECs (Figure 5.13A). However, raised levels of Cdc42 protein are difficult to equate with Cdc42 activity, as Cdc42 switches between an active GTP bound form and an inactive GDP bound form; it is the relative amount of the active form that is important in regulation of actin remodelling (Vetter and Wittinghofer, 2001). To determine whether increased Cdc42 expression conferred increased Cdc42 activity, GTP-bound Cdc42 was assessed by immunoprecipitation and subsequent western blotting. Active GTP-bound Cdc42 binds to p21 activated kinase 1 (PAK1) (Rane and Minden, 2014), thus PAK1-coated beads were used to immunoprecipitate GTP-bound Cdc42 from CD99 siRNA- (or control siRNA-) treated HUVECs. Initial results using CD99 knockdown HUVECs grown under normal culture conditions did not show any change in GTP-bound Cdc42 and also indicated variation in the upregulation of total Cdc42 expression upon CD99 knockdown (Figure 5.13B). This variation in Cdc42 expression may have been caused by differences in passage number of HUVEC cells between experiments or efficiency of CD99 knockdown. To further analyse the effects of CD99 depletion on GTP bound Cdc42, an adaptation in methodology was made, where control and CD99 siRNA-treated HUVECs were detached (from plastic) and allowed to adhere to gelatin-coated flasks for 30 mins prior to lysis, (to initiate adherence) and encourage activation of Cdc42. As expected, CD99 depletion not only increased Cdc42 expression but also increased active GTP bound Cdc42 when HUVECs were lysed early during adhesion (Figure 5.13C), supporting the proposal of CD99-dependent changes in Cdc42 activity occurring during adhesion. However, for MDA-231, 30 minutes of adhesion yielded no change

in GTP-Cdc42 (Figure 5.13D). Further adaptations to the protocol eventually yielded results where increased GTP-Cdc42 was observed when CD99 depleted MDA-231 cells lysates were taken after 4 hours adhesion to gelatin-coated plates (Figure 13E).

Previous reports linked active Cdc42 to mobilisation of additional regulators and effectors of actin polymerisation, including WASP and the ARP2/3 complex (Ma, Rohatgi and Kirschner 1998; Rohatgi et al. 1999). Indeed, depletion of CD99 using siRNA in HUVECs, also increased the expression of the downstream effector molecule of actin branching and polymerisation, ARP3, when assessed by western blotting (Figure 5.13F). This increase in ARP3 demonstrates that changes in Cdc42 expression and activation status upon CD99 depletion impacts on the signalling cascade regulating downstream actin dynamics.

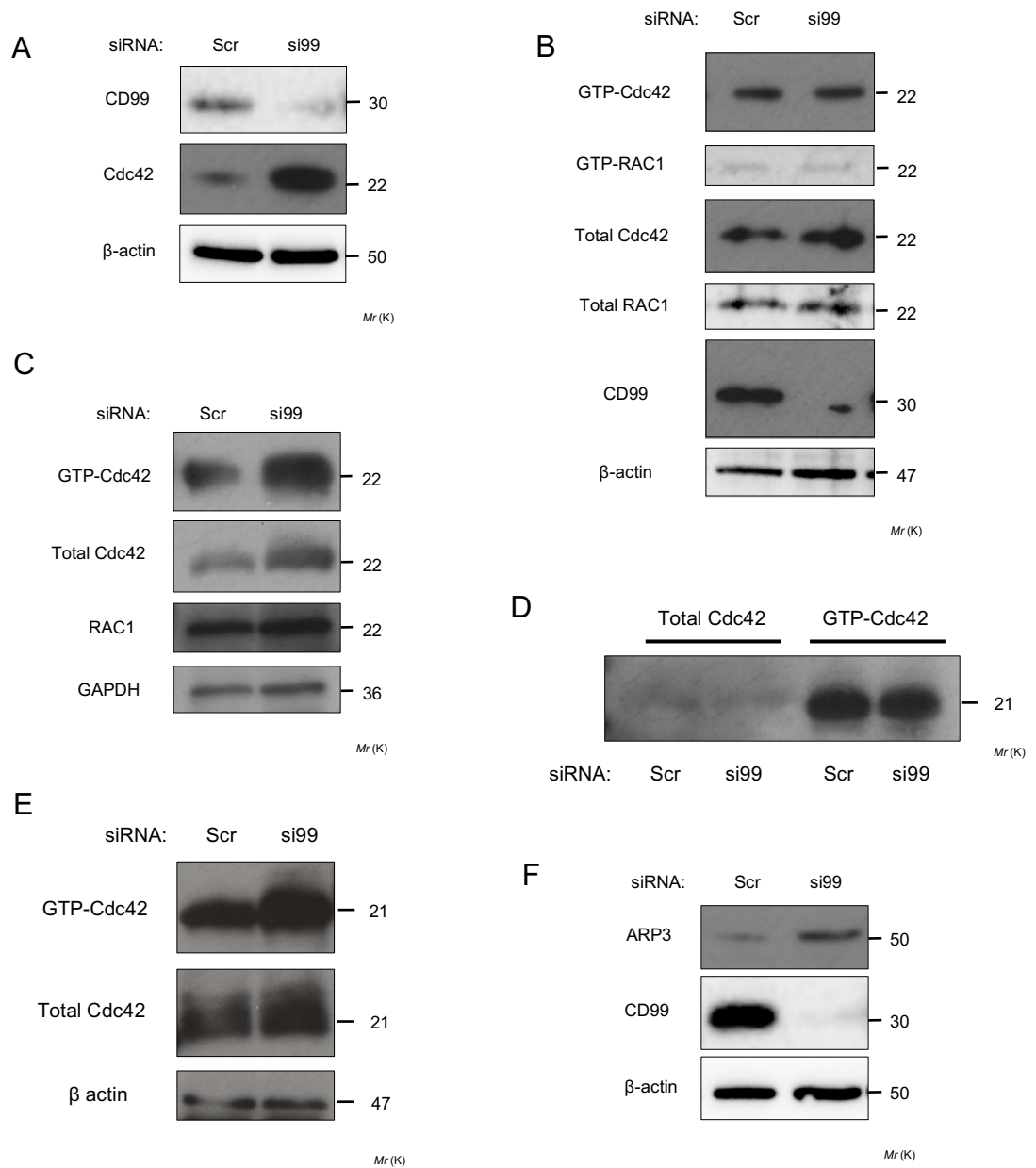


**Fig. 5.13. CD99 modulates Cdc42 activity and expression.** **A**, HUVEC were transfected with CD99 or Scrambled control siRNA and after 72h total cell lysates were analysed by western blot for CD99, Cdc42 and β-actin as loading control. **B**, HUVEC were transfected with scramble control and CD99 siRNA. 72h later, total cell lysates were incubated with PAK1-PBD agarose beads to immunoprecipitate GTP bound Cdc42. Beads and input controls were analysed by Western blot and immunoblotted for using Cdc42, RAC1 and CD99 specific antibodies. β-actin was used as loading control. **C**, As in panel B but following 72h transfection of HUVEC with siRNA, cells were detached and seeded to gelatin coated flasks for 45 min to adhere. Cells were then lysed and processed for PAK1-PBD pulldown and subsequent Western blotting for expression of the indicated proteins. **D**, MDA-231 were transfected with scramble control and CD99 siRNA. 72h later, total cell lysates were incubated with PAK1-PBD agarose beads to immunoprecipitate GTP bound Cdc42. Beads and input controls were analysed by Western blot and immunoblotted for using Cdc42. **E**, As in panel D but following 72h transfection of MDA-231 with siRNA, cells were detached and seeded to gelatin coated flasks for 4h to adhere. Cells were then lysed and processed for PAK1-PBD pulldown and subsequent Western blotting for expression of the indicated proteins. **F**, HUVEC were transfected with CD99 or Scrambled control siRNA and after 72h total cell lysates were analysed by western blot for ARP3, CD99 and β-actin as loading control.

### 5.10 Endothelial CD99 regulates *in vitro* angiogenesis

Angiogenesis requires dramatic changes in the migration and proliferation of endothelial cells (Herbert and Stainier, 2011). These changes are accompanied by cytoskeletal remodelling and increased activity by GTPases (Bryan and D'Amore, 2007). Cdc42 has also been heavily implicated in the angiogenic potential of endothelial cells (Bayless and Davis, 2002; Jin et al., 2013; Barry et al., 2015). To the best of my knowledge, a role for CD99 in angiogenesis has not been previously reported. As shown above, the depletion of CD99, increased both Cdc42 expression and activity in HUVECs (Figure 5.13C). It was hypothesised that CD99 may therefore impact of the angiogenic capacity of endothelial cells. Using a well characterised *in vitro* co-culture assay (Bishop et al., 1999), CD99 siRNA- treated HUVECs were analysed for their ability to form vascular networks and tubules (methods section 2.2.4). 7-day fibroblast-EC co-culture assays were performed and vascular networks analysed for CD31 expression, a marker of endothelial cells (Figure 5.14A). Results showed that reduced CD99 expression enhanced the network length, branch points and total network area during tubule formation (Figure 5.14B-D). These results suggest that CD99 expression negatively regulates the angiogenic potential of endothelial cells, however further work is required to delineate whether this also involves changes in Cdc42 activity.

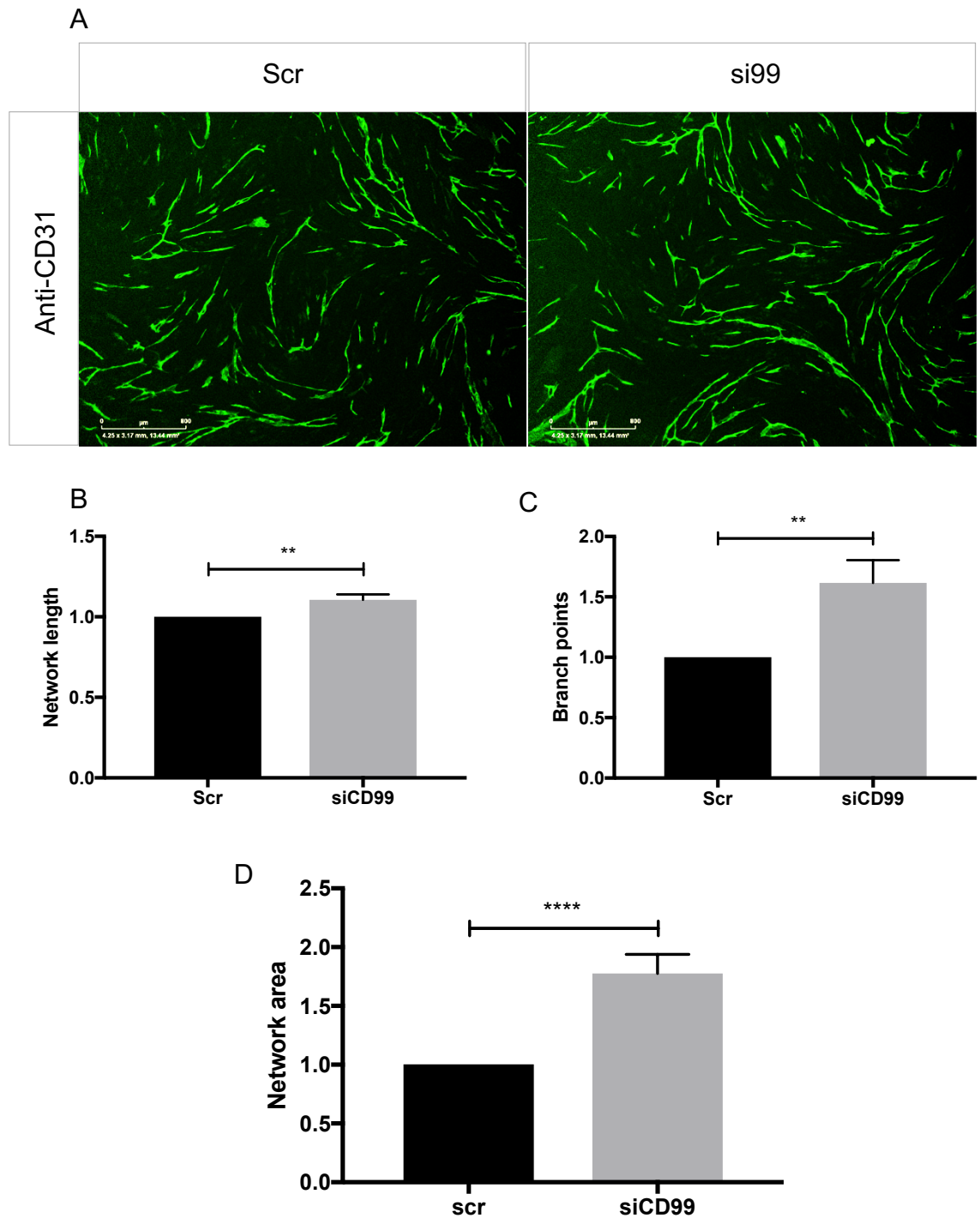


**Fig. 5.14. Endothelial CD99 regulates in vitro angiogenesis.** **A**, Representative images of angiogenesis assays of HUVEC treated with scrambled control or CD99 siRNA. siRNA treated HUVEC were cocultured with fibroblasts. After 7 days cocultures were washed with PBS and fixed with 4% PFA before staining endothelial cells with CD31 conjugated antibodies. Cocultures were then imaged using either EVOS microscope or Incucyte microscope. Scale bar: 800 $\mu$ m. Quantification of **B**, Network length **C**, Branch points and **D**, Network area were analysed using ImageJ. Data are presented as fold change compared to Scrambled control and are representative of n=3 independent replicates. Error bars are indicative of standard error. Statistical analysis was carried out using student t-test. \*\*p<0.005, \*\*\*\*p<0.00005.

In summary, this chapter has dissected the role of CD99 in the adhesion and transendothelial migration of metastatic cancer cells. It has been shown that CD99 regulates metastatic progression *in vivo* and cytoskeletal rearrangements determine cancer cell TEM *in vitro*. Furthermore, EC CD99 controls endothelial barrier function, thereby regulating tumour cell TEM. This chapter shows that CD99 mediates these effects by negatively regulating Cdc42 activity. These data identify CD99 as a regulator of cytoskeletal organisation, with impact on tumour migration and TEM, key components of the metastatic pathway.

## 5.11 Discussion

In this chapter it has been shown that CD99 suppresses the metastatic phenotype of cancer cells and reduces cancer cell transendothelial migration *in vitro* and *in vivo*. Additionally, CD99 was found to regulate the actin cytoskeleton through modulation of the activity and expression of the GTPase Cdc42. These alterations are proposed to be responsible for the phenotypic changes observed. Furthermore, results also demonstrate the involvement of endothelial CD99 in controlling barrier function and subsequently the TEM of cancer cells. Finally, CD99 was implicated in the angiogenic potential of endothelial cells, which may also be conferred through CD99-dependent regulation of Cdc42.

Using existing clinical data sets, the contribution of CD99 expression to patient outcomes following breast cancer diagnosis was examined (Figure 5.1). The patient data and Kaplan-Meier plots shown in Figure 5.1A-D indicated that high CD99 expression in breast cancer correlated with poor probability of metastatic free survival, suggesting a role for CD99 in breast cancer metastasis. Previous work has also indicated that CD99 expression is higher in malignant breast tissue compared to normal adjacent tissue, but no significance could be attributed to specific breast cancer stage and CD99 expression (Baccar et al., 2013). This study also showed a significant correlation between HLA class II negativity and CD99 positivity correlated with lymph node metastasis (Baccar et al., 2013). In addition, CD99 has previously been shown to associate with HLA class I in T and B cells, where CD99 was required for the transport of HLA class I from the Golgi apparatus to the plasma membrane through direct interactions with the transmembrane domain (Sohn et al., 2001; Brémond et al., 2009).

In other cancers, such as non-small cell lung cancer, high CD99 expression in the stromal compartment correlated with better prognosis for patients (Edlund et al., 2012). Interestingly, using the same online resource (Lánczky et al., 2016) for lung cancer patients, indicated that high CD99 expression correlated with significantly reduced overall survival (data not shown), suggesting that CD99 expression may be an indicator of poor prognosis across multiple cancer types. However, previous studies may have been hampered by small sample sizes in assessing CD99 as a reliable prognostic factor in breast cancer, and results presented here warrant further investigation into the contribution of CD99 to cancer survival. These results (which utilise gene expression data, not protein expression) indicated a possible role for

CD99 in breast cancer metastasis, hence *in vitro* and *in vivo* studies were performed to investigate this further.

The ability of metastatic cancer cells to adhere to and traverse vasculature has been directly linked to their capacity to form secondary metastatic lesions (Madsen and Sahai, 2010; Reymond et al., 2013a). Results suggest that endothelial CD99 expression may not play a major role in the adhesion of MDA-231 cells to endothelial monolayers (Figure 5.3E). This is consistent with previous studies using blocking antibodies which show that endothelial CD99 does not play a major role in the adhesion of monocytes or neutrophils to the endothelium (Schenkel et al., 2002; Lou et al., 2007). This suggests that it is unlikely CD99 participates in adhesion of cancer cells to EC through homophilic interactions. Recent work shows that endothelial CD99 binds to neutrophil Paired Immunoglobulin Like Receptor (PILR) to facilitate adhesion (Goswami et al., 2017) suggesting that other heterophilic interactions may mediate cancer cell adhesion through binding of CD99. Goswami et al. (2017) also showed that, under shear flow conditions, CD99 was required for ICAM-1 mediated adhesion of neutrophils to ECs. Results shown in Figure 5.3 were conducted under static conditions, and the influence of shear flow has been shown to significantly alter the adhesion of cancer cells (Follain et al., 2018). Further in-depth analysis of endothelial CD99 involvement in cancer cell adhesion should incorporate flow to better recapitulate the vascular microenvironment.

In contrast to endothelial knockdown, CD99 depletion in MDA-231 cells resulted in decreased adhesion to endothelial monolayers (Figure 5.3C). Conversely, it was shown that CD99 knockdown potentiated MDA-231 adhesion to fibronectin substrates and subsequent transendothelial migration across EC monolayers (Figure 5.8D). This suggests that interactions between MDA-231 cells and ECs involves a two-stage process. Initial transient adhesion of MDA-231 to ECs requires CD99 expression on MDA-231 cells and is disrupted by CD99 depletion. However, later-stage of firm adhesion and subsequent TEM is opposed by high CD99 expression, whereby enhanced adhesion and TEM is evident following CD99 loss, i.e. implying CD99 has opposite roles in the early and the later stages of TEM. Alterations in integrin expression or activity is one possible mediator of these time-dependent responses. Integrins, in particular the  $\beta 1$  integrin, have a pronounced role in cancer metastasis (Desgrosellier and Cheresh, 2010; Wang et al., 2012). One of the role of integrins is the firm adhesion of cells to the endothelium (Chen et al., 1999). The ligation of CD99 has previously been shown to activate the  $\alpha 4\beta 1$  integrin in T cells,

allowing the aggregation and adhesion to endothelial cells through interaction with its ligand VCAM-1 (Bernard et al., 2000). Whether  $\alpha 4\beta 1$  integrin is altered in MDA-231 cells depleted of CD99 and is involved in the observed reduction in adhesion to EC monolayers remains an area of active future research.

Other integrin-ECM interactions may also be involved in coordinating the cellular responses to CD99 depletion in both EC and MDA-231 cells. For example, in Ewing's sarcoma cells,  $\alpha 5\beta 1$  integrin was upregulated upon triggering of CD99 ligation using anti-CD99 antibodies (Cerisano et al., 2004). Interestingly,  $\alpha 5\beta 1$  integrin also functions as a fibronectin receptor and results from ECM adhesion assays presented here, indicated that knockdown of CD99 in MDA-231 cells increased the number of cells bound to fibronectin-coated surfaces. In contrast, previous work delineating the role of CD99 isoforms in MDA-231 cells indicated that forced expression of the short CD99 isoform also increased adhesion to fibronectin (Byun et al., 2006). As triggering of CD99 has been shown to increase integrins which mediate fibronectin engagement, it is possible that full-length CD99 knockdown may alter  $\alpha 5\beta 1$  expression, conformation, or signalling to facilitate adhesion. Furthermore, CD99 has also been implicated in regulating integrin signalling, whereby activation of CD99 by ligation with either CD99 antibodies or peptide fragments suppressed  $\beta 1$  integrin activity and downstream signalling (Lee et al. 2015; Lee et al. 2017). Interestingly, MCF7 breast cancer cell line adhesion to fibronectin was also significantly decreased by application of CD99-Fc peptide fragment; mediated by suppression of  $\beta 1$  integrin (Lee et al. 2017). This suggests that in the absence of CD99, regulation of integrin expression or activity is impeded, resulting in greater adhesion to ECM components and modification of migration and invasion. Given the known role for  $\beta 1$  integrins in metastasis, and the reported link between CD99 expression and their activity, it is possible that the activation of integrins could be responsible for the increased metastatic potential observed upon CD99 depletion. However, further work to identify whether  $\beta 1$  integrin expression is altered by CD99 depletion is required.

Platelets play an important role in metastasis where they have a known role in potentiating the adhesion and transmigration of cancer cells to vasculature (Gasic et al., 1968; Kim et al., 1998; Labelle et al., 2011). Interestingly, CD99 is expressed by platelets, but its role has not been previously explored in adhesion of leukocytes or cancer cells (Pliyev et al., 2013). Whether platelet CD99 binds to cancer cell CD99 and triggers activation of downstream signalling or is involved in binding of circulating cancer cells remains to be investigated.

CD99 is also suggested to participate in cell migration more generally. A significant enhancement in the TEM of CD99-knockdown MDA-231 cells was noted (Figure 5.4-5), along with increased migration towards a serum gradient (Figure 5.6D). However, no significant difference in 2D scratch migration assays was observed (Figure 5.6B-C). This suggested that motility was not affected by CD99 depletion, however more complex migration through 3D space, either through EC monolayers or Transwell pores, was specifically enhanced; an arguably more important step in the metastasis of tumour cells. As already alluded to, work by Byun et al. (2006) revealed that expression of the short isoform of CD99 in MDA-231 and MCF7 cells increased the migratory potential of cells in a scratch wound assay. This paper also indicates that MDA-231 express very low levels of CD99 in comparison to MDA-435 (a known misidentified melanoma cell line (Prasad and Gopalan, 2015)) and MCF7 cells. Work presented here, indicates that CD99 is expressed at levels only slightly lower than MCF7 cells (Figure 5.1E), and that CD99 expression does not influence MDA-231 migration in simple scratch wound assays. The use of siRNA specific to each isoform of CD99 would identify whether the effect on chemotaxis and transmigration observed are isoform-dependent in MDA-231.

Results shown in this chapter indicated that CD99 regulates the metastatic potential of cancer cells *in vivo* as well as *in vitro* (Figure 5.10). Although this depletion was transient (using only siRNA) it appeared to have a prominent effect on metastatic formation in the lungs - without evidence of significant changes in proliferation (Figure 5.7). As the expression of CD99 begins to recover 7 days post-siRNA transfection (Figure 5.3B), these results suggest that CD99 loss confers an advantage during the early initial extravasation steps of the metastatic cascade. It is anticipated that CD99-depleted MDA-231 cells would show enhanced TEM across lung vasculature *in vivo*, as was evident during live cell imaging of intercalation into HUVEC monolayers *in vitro* (Figure 5.4). This effect would enhance initial seeding of metastatic cells from the blood stream into the lung tissue, resulting in increased metastatic burden and altered disease outcomes, although this is not recapitulated in analysis of patient data-sets. Previous work in breast cancer has indicated that MMP and motility of breast cancer cells is regulated by CD99 (Byun et al., 2006). MMP function has previously been linked to Rho GTPase activity and data shown here may represent a potential link between CD99 expression and increased Rho GTPase activity (Cdc42). This may account for the change in expression in MMPs and contribute to the invasive capabilities of metastatic cancers cells (Bryan and D'Amore, 2007). The

involvement of CD99 in breast cancer research *in vivo*, to my knowledge, has not been previously explored, but is an area of future research focus. Results presented within this chapter support the rationale of increased GTPase activity, mediated through Cdc42, as responsible for the changes in invasive behaviour evident in CD99-depleted MDA-231 cells (Figure 5.13E).

Rho GTPases are well known to potentiate filapodial and lamellipodial formation and the invasive phenotype (Wang et al. 2005; Gertler and Condeelis 2011). Adhesion assays and staining for the actin cytoskeleton indicated that CD99-depleted MDA-231 cells displayed enriched actin within the lamellipodial region of the cell (Figure 5.8A). This was particularly obvious when the cells were adhering to collagen substrates. Members of the Rho GTPase family RAC1 and Cdc42 are required for actin polymerisation within the lamellipodia of cells, mediating downstream effectors to facilitate the assembly of actin monomers (Parsons, Horwitz and Schwartz 2010). These include members of the WASP family, and the ARP2/3 complex. Results consistently showed that CD99 depletion in MDA-231 increased spreading and intercalation, disrupting EC monolayers, and potentially increasing metastatic dissemination to the lungs *in vivo*. Furthermore, Reymond et al. (2012) showed that the knockdown of Cdc42 greatly reduced cancer cell intercalation and spreading on EC monolayers, supporting the proposed role for increased Cdc42 as responsible for the enhanced TEM evident following CD99 depletion.

Results indicate that MDA-231 CD99 depletion enhanced both Cdc42 activity and expression (Figure 5.13E). CD99 has previously been implicated in the regulation and activation of Rho-GTPases in cancer cells. Ligation of CD99 in Ewing's sarcoma by specific antibodies activates RAC1 dependent endosomal trafficking, leading to vacuole formation and subsequent apoptosis (Manara et al., 2016). In osteosarcoma, the forced expression of CD99 suppresses ROCK2 activity, reduces expression of ARP2 and the actin membrane anchoring protein ezrin, in turn attenuating metastasis (Zucchini et al., 2014). Previous work has also implicated CD99 in linking with the actin cytoskeleton in Ewing's sarcoma, where expression of the actin modulating protein, zyxin, was modulated by CD99 activation (Cerisano et al., 2004). Taken together, these findings suggest a novel role for CD99 in the regulation of actin cytoskeletal dynamics through modulation of CDC42 activity. However, the studies mentioned previously also suggest CD99 regulation of actin dynamics may be cell-type specific, participating in either the potentiation or arrest of a metastatic phenotype.

Collectively, experimental work in this chapter indicates that CD99 expression suppresses the metastatic phenotype of MDA-231 breast cancer cell line. This contrasts with *in silico* data which suggests that high CD99 expression correlates with greater probability of metastatic dissemination (Figure 5.1A-D). There is a clear disparity between these two observations, which needs addressing. As a cell line, MDA-231 is not representative of the landscape of molecular subtypes of breast cancers which present in the clinic. Although other breast cancer lines were not utilised, some experiments that were performed using the PC3 prostate cancer cell line in TEM live cell imaging assays, exhibited a similar trend to MDA-231 (Figure 5.4), suggesting that results observed are not limited to the MDA-231 cell line and breast cancer in general. It is also important to consider that *in silico* data presented here (Figure 5.1) indicates mRNA transcript expression rather than protein expression, and so further work utilising IHC analysis should be considered to validate these results.

The role of CD99 in the TEM of leukocytes has been extensively documented (Schenkel et al., 2002; Watson et al., 2015; Goswami et al., 2017). The blocking of CD99 using antibodies resulted in the arrest of leukocyte TEM part way through the endothelial junctions (Schenkel et al., 2002). Results presented here indicated a reduction in cancer cell intercalation and barrier disruption upon depletion of endothelial CD99 (Figure 5.11-12), indicating that EC CD99 functions in a similar manner during the control of cancer cell TEM, as it does for leukocyte TEM. Results in ECs also showed that CD99 depletion within HUVEC increased the expression and activity of CDC42 (Figure 5.13A-C). CD99 depletion also resulted in altered endothelial barrier function of HUVEC (Figure 5.12A-B). Active Cdc42 has previously been shown to modulate the barrier function of endothelial cells (Kouklis et al., 2004; Ramchandran et al., 2008). Although no direct evidence has been shown implicating Cdc42, the strong evidence for the role of Cdc42 in endothelial barrier function suggests that changes in Cdc42 activity upon CD99 knockdown are responsible for increased barrier function and reduced TEM. CD99 depletion also led to an increase in ARP3 (Figure 5.13F) a component of the ARP2/3 complex which plays an important role in actin nucleation and endothelial barrier function downstream of Cdc42 (Belvitch et al., 2017). This further supports the notion that CD99 controls barrier function and TEM through modulation of Cdc42 and actin polymerisation.

In endothelial cells it has been reported that CD99 is held in a signalling complex with ezrin, soluble adenylyl cyclase (sAC) and PKA, whose activation is stimulated by increased cAMP (Watson et al., 2015). Active PKA triggers the recycling of CD99 to the cell surface to facilitate the movement of the transmigrating leukocyte (Watson et al., 2015). It is possible that upon CD99 depletion, components of this complex are liberated, resulting in altered/increased PKA/cAMP signalling. PKA/cAMP signalling has been shown to promote direct, albeit weak, Cdc42 activation (Feoktistov et al., 2000). The activator of Cdc42, RAP1, is also elevated by increased cAMP PKA activity (Lerosey et al., 1991) and contributes to regulation of barrier function of ECs (Ando et al., 2013). Therefore, it is tempting to speculate that increased Cdc42 activity could be a direct or indirect consequence of uncontrolled PKA activation upon CD99 depletion. This may also be the case for CD99 regulation of Cdc42 in metastatic cells. Further work is required in delineating the mechanisms of CD99 induced Cdc42 activation, and whether CD99 ligation produces similar results.

Additional functions were also attributed to CD99 expression in ECs. It was observed that CD99 depletion impacted the angiogenic potential of endothelial cells, leading to increased tubule length and branch points of primitive *in vitro* vascular networks (Figure 5.14). Angiogenesis relies on the spatial and temporal coordination of endothelial migration and proliferation (Herbert and Stainier, 2011), and Cdc42 is critical in both the development of endothelial tubulogenesis and vascular development during vessel morphogenesis (Bayless and Davis, 2002; Jin et al., 2013; Barry et al., 2015); supporting the potential regulation of Cdc42 by CD99 and its role in controlling angiogenesis. As well as the direct role of CD99 in the regulation of integrins as previously discussed, Cdc42 is known to regulate expression and localisation of  $\beta 1$  integrins (Reymond et al., 2012). The action of  $\beta 1$  integrin has been shown to impact on angiogenic potential (Davis and Bayless, 2003). Furthermore,  $\beta 1$  integrin null mice exhibited perturbed endothelial apical-basal cell polarity, along with redistribution of junctional molecules VE-Cadherin, claudin 5 and CD99 (Zovein et al., 2010). As previously discussed, a number of reports have indicated that CD99 signalling impinges on  $\beta 1$  integrin expression (Bernard et al. 2000; Cerisano et al. 2004; Lee et al. 2015; Lee et al. 2017). Therefore, alterations in angiogenic potential may be due to CD99 signalling influencing Cdc42 activity and cytoskeletal integrity, contributing to changes in integrin expression angiogenic signalling programs. In summary, CD99 modulates the actin cytoskeletal dynamics through regulation of the GTPase Cdc42. This was found to impact on the capacity of endothelial cells to regulate angiogenic potential, barrier function and control of cancer cell

transmigration. In metastatic cancer cells, CD99 regulation of the cytoskeleton impacted on the migratory and invasive potential of cancer cells and consequently their ability to successfully metastasise.

## Summary and Discussion

This thesis explores the interactions between cancer cells and endothelial cells during the metastatic cascade. Unravelling the communication between these two cell types can provide important mechanistic insight which could form the basis of future therapies or provide rationale for biomarkers of metastatic disease. There is a lack of diagnostic tests to indicate that a cancer has undergone metastasis to secondary organs, which stems from a lack of understanding in the metastatic disease processes. The adhesion molecule CD146 has been shown to regulate adhesion and transmigration of different cancer types (Melnikova et al., 2009; Jouve et al., 2015) and additionally, regulates the vascularisation of tumours (Jiang et al., 2012). Further studies have indicated that levels of soluble CD146 in patient plasma correlate with progression and relapse following treatment in clear cell renal cell carcinoma (Dufies et al., 2018). This is an example of where the molecular mechanism of receptor action in metastasis has been delineated, culminating in its use in the clinic as a prognostic indicator of tumour progression.

Endothelial cells are an important aspect of the tumour microenvironment and contribute to the development of metastatic disease. As well as facilitating the transmigration of cells into secondary tissues, ECs are required for the neovascularization of tumours, providing new blood vessel growth and circulation to avascular sites. This thesis has focused on the steps of adhesion and transmigration by studying the endothelium as well as focusing on metastatic cancer cells themselves. In doing so, the role of several receptors has been assessed in facilitating adhesion and transendothelial migration of metastatic cancer cells whilst also investigating effects on angiogenesis.

Chapter 3 describes studies in the development of breast cancer brain metastasis, through cancer cell interactions with cerebral endothelial cells. This involved investigation into the adhesion and transmigration of brain metastatic cells through the endothelial BBB. The adhesion molecule CD146 was shown to be highly expressed by breast cancer brain metastatic cells and was shown in functional studies to suppress BrM adhesion and transmigration. *In silico* data indicated a significant correlation between high CD146 gene expression and metastasis in breast cancer. Clinical *in silico* data coupled with *in vitro* experimental data, suggest a complex model for CD146 in regulating metastasis. Depletion of CD146 was found to potentiate BrM adhesion and transmigration whilst having to the opposite effect on

MDA-231 cells. Whether this is due to EMT status of cell lines remains to be investigated.

Further work using patient samples to validate CD146 gene expression levels in metastasis free survival should also be the focus of future work. Utilising protein expression of CD146 in tissue microarrays of BCBM patient samples would further validate the involvement of CD146 in breast metastasis. Whether CD146 plays a substantial role in establishing BCBM remains to be determined through use of *in vivo* models as work shown here only utilised *in vitro* assays. Future work would investigate *in vivo* brain metastasis of CD146 depleted BrM cells. Furthermore, a model utilising the murine metastatic mammary cell line 4T1 with stable CD146 knockdown would eliminate limitations associated with using human cells in a mouse model. This would robustly indicate the role of CD146 in metastatic seeding of breast cancer cells to the brain.

The cerebral EC line hCMEC was described in chapter 3 to investigate tissue specificity in metastasis. Further work characterising the hCMEC cell line was therefore reported in chapter 4. This uncovered the role of p53 in dictating the endothelial phenotype. It was postulated that SV40 Tag inactivation of p53 during the immortalisation of the hCMEC cell line resulted in disruption of the normal endothelial phenotype. I found that that high expression of p53 in hCMEC suppressed the expression of VEGFR2, a key molecule in determining the endothelial phenotype. The disrupted endothelial phenotype was evident from the reduced angiogenic activity (in response to VEGF) and reduced expression of canonical endothelial receptors, CD31 and VE-cadherin. It was shown that reversal (or 'normalisation') of this poor endothelial phenotype could be achieved by depletion of p53 from hCMEC. This resulted in normalisation of VEGFR2 expression, conferring greater endothelial-like phenotype, with restored response to VEGF stimulation in angiogenesis assays. An increased expression of endothelial receptors CD31 and VE-cadherin was also shown in the absence of p53 expression. Importantly, it was shown that this normalised endothelial phenotype in p53 depleted hCMEC, could be reversed by the depletion of the VEGFR2 expression. This resulted in the reduced expression of CD31 and VE-cadherin, revealing novel functional interactions between p53, VEGFR2, CD31 and VE-cadherin. Future work will investigate whether the expression of VEGFR2 can be altered by depletion of other endothelial receptors such as CD31 and VE-cadherin. The expression of CD31 and VE-cadherin have been linked to VEGFR2 in previous studies, which showed that a mechanosensory

complex is formed between the three receptors to mediate alignment of endothelial cells to shear flow (Tzima et al., 2005). Future work would explore the basis of the regulatory loop between p53 and expression of key endothelial markers, which to my knowledge has not been previously described.

Results presented in this thesis indicated that VEGFR2 expression is suppressed by the presence of p53 in hCMEC cells. It would be of interest to investigate how p53 suppresses the expression of VEGFR2, as results presented in this thesis only indicated regulation of VEGFR2 protein expression and did not investigate gene expression changes. In hCMEC, p53 may be altered allowing it bind non-canonical p53 consensus sites to suppress VEGFR2 promoter activity. The use of chromatin immunoprecipitation (ChIP) analysis to investigate whether p53 associates with the VEGFR2 promoter could be employed to further investigate this. As already discussed (section 4.13), association of mutant p53 and the promoter region of VEGFR2 has been described in breast cancer (Pfister et al., 2015). However, the role of wild type p53 and regulation of VEGFR2 remains to be elucidated.

Furthermore, it was not investigated whether p53 depletion in hCMEC cells potentiated angiogenesis *in vivo* as only *in vitro* angiogenesis was investigated. Ongoing work with a collaborator has employed hCMEC shp53 cells in Matrigel plug assays to determine whether angiogenesis is also potentiated *in vivo*. This would strengthen the notion that p53 depletion enhances hCMEC angiogenic potential.

Recent studies highlighted differential gene expression in endothelial cells of particular tissues (Hupe et al., 2017; Vanlandewijck et al., 2018). Hupe et al. (2017) showed that the expression of FOXF2 was key in driving the BBB phenotype of ECs. Results shown in chapter 4 indicated that expression of FOXF2 decreased upon p53 depletion. However, greater expression of the BBB EC marker claudin 5 was found. This suggests that other transcriptional regulators of BBB phenotype may be inducing changes observed in normalised hCMEC cells. The use of gene expression profiling (using arrays or RNA-seq) would be very useful in investigating the widespread transcriptional changes induced by p53 depletion, and may indicate previously unknown p53 regulated genes in governing endothelial phenotype.

Interestingly, it was found that the normalisation of hCMEC by depletion of p53, did not alter the transmigration of cancer cells, but did increase cancer cell adhesion. Further work to delineate changes to hCMEC adhesion receptor expression upon p53 depletion is needed to investigate this further.

Interactions of cancer cells and endothelial cells has been known for some time, but there remains a dearth of studies on the specific mechanisms which facilitate these

interactions. In contrast, the molecular cues which govern the migration of leukocytes has been delineated in far greater detail and thus, many discoveries regarding cancer cell-endothelial interactions have been applied from these observations (Madsen and Sahai, 2010). The final chapter of this thesis describes work relating to CD99, a molecule which has been well defined for its role in facilitating leukocyte adhesion and transmigration.

The expression of CD99 was found to regulate the transmigration of cancer cells through an endothelial barrier. In cancer cells, CD99 expression appeared to suppress the metastatic phenotype, which was indicated by greater metastatic burden *in vivo* in CD99 depleted breast cancer cells. Actin cytoskeletal dynamics were also altered in the absence of CD99 expression. In endothelial cells, CD99 was required for the successful transmigration of cancer cells, as depletion of endothelial cell CD99 impaired cancer transmigration through greater EC barrier function. These alterations in cancer cells and ECs are suspected to be a consequence of altered GTPase activity. It was found in both ECs and breast cancer cells that CD99 depletion increased Cdc42 expression and activity. A known role for Cdc42 in the associated changes (invasion and metastasis in cancer and barrier function in ECs) has been previously shown by others (Cerutti and Ridley 2017; Reymond, d'Água and Ridley 2013); my work now links events at the cell surface mediated by CD99 to this regulation of Cdc42.

Results shown in chapter 5 indicated that CD99 may play a role in adhesion of cancer cells to the endothelium, as CD99 specific antibody blockade reduced cancer cell adhesion. Depletion of cancer cell CD99 reduced adhesion whereas depletion of endothelial CD99 had little effect until later time points where an increased number of cancer cells bound. These assays were performed under static conditions. Although a great deal of time was spent attempting to establish adhesion assays under shear flow conditions, little progress was made in investigating the role of CD99 in adhesion in these assays. Many adhesion receptors are known to be influenced by shear flow. Selectins rely on the flow induced mechanical perturbation of the receptor in order for it to function in the transient adhesion of leukocytes (Finger et al., 1996; Lawrence et al., 1997). Previous work does not indicate a flow dependent mechanism for CD99 in adhesion and transmigration of leukocytes, although additional research in this area should be considered as abnormalities in shear flow are known to contribute to vascular disease pathology (Davies, 2009).

Although CD99 was investigated in the interaction between vascular endothelial cells and cancer cells, further work in cancer dissemination via lymphatic vasculature should be considered. It has been previously shown that CD99 facilitates dendritic cell (DC) transmigration into the lymphatic vessels (Torzicky et al., 2012). Breast cancer metastasis to the local axillary lymph nodes is an important prognostic indicator in breast cancer progression (Jatoi et al., 1999). It would therefore be pertinent to investigate whether lymphatic CD99 expression propagates tumour metastasis to the lymph nodes.

The GTPase Cdc42 has been shown to be aberrantly expressed in many cancer types (Ellenbroek and Collard, 2007; Stengel and Zheng, 2011). By identifying a novel signaling pathway between CD99 and Cdc42, work shown in this thesis indicates that alternative methods of targeting Cdc42 signaling may be possible. Further studies are required to delineate whether the use of CD99 antibodies can alter Cdc42 activity through binding of surface CD99, as it is unclear if binding of CD99 mimics depletion with siRNA. Little is known about the mechanism by which CD99 antibodies interact with the CD99 receptor. Ligation of CD99 in Ewing's sarcoma has previously been shown to induce cell death through activation of Rac1 (Manara et al., 2016). Further work is required to delineate whether CD99 ligation results in receptor internalisation, cross-linkage of CD99 molecules, or inhibition of CD99 dimerisation. Interestingly, small molecular inhibitors which target CD99 and inhibit dimerisation and downstream signaling were recently shown to be effective at reducing *in vivo* tumour growth in Ewing's sarcoma in xenograft models (Çelik et al., 2018). My initial results indicated that these CD99 specific inhibitors reduced CD99 dimerization in endothelial cells (data not shown), however further work is required to investigate whether inhibition of CD99 dimerisation has any downstream effects on Cdc42 activity.

Results shown in chapter 4 indicated that CD99 expression was limited to an intracellular compartment which may be within the Golgi apparatus in hCMEC cells (Sohn et al., 2001). Interestingly, the depletion of p53 in hCMEC resulted in the redistribution of CD99 from intracellular localisation to concentrated expression at endothelial borders. This however, as shown in chapter 4, did not impact on the TEM of cancer cells, suggesting that the localisation of CD99 does not relate to its function in cancer cell TEM. Further work is required to elucidate whether downstream signaling still occurs when CD99 is retained intracellularly as seen in hCMEC. Knockdown of CD99 in normalised shp53 hCMEC indicated similar results to HUVEC, with reduced cancer cell transmigration (data not shown). This indicated the

similarities in CD99 function in shp53 hCMEC and HUVEC endothelial cells, validating both the normalisation of endothelial phenotype in hCMEC cells upon p53 depletion, and the role of CD99 in cancer cell transmigration.

In summary, my work has shown that cancer cells hijack receptors which facilitate leukocyte adhesion and transmigration for their own dissemination in metastasis, which may be facilitated through a novel signaling axis between CD99 and Cdc42. The role of molecules in the tissue specificity of breast cancer metastasis was also investigated, highlighting the potential role of CD146 in this aspect of tumour progression. Finally, this thesis highlights an important role for p53 in the modulation of endothelial phenotype in the BBB, through a previously undescribed mechanism of VEGFR2 regulation.

## References

- Abbott, N.J., Rönnbäck, L. and Hansson, E. 2006. Astrocyte–endothelial interactions at the blood–brain barrier. *Nature Reviews Neuroscience*. **7**(1), pp.41–53.
- Abhinand, C.S., Raju, R., Soumya, S.J., Arya, P.S. and Sudhakaran, P.R. 2016. VEGF-A/VEGFR2 signaling network in endothelial cells relevant to angiogenesis. *Journal of cell communication and signaling*. **10**(4), pp.347–354.
- Adams, R.H. and Alitalo, K. 2007. Molecular regulation of angiogenesis and lymphangiogenesis. *Nature Reviews Molecular Cell Biology*. **8**(6), pp.464–478.
- Alais, S., Allioli, N., Pujades, C., Duband, J.L., Vainio, O., Imhof, B.A. and Dunon, D. 2001. HEMCAM/CD146 downregulates cell surface expression of beta1 integrins. *Journal of cell science*. **114**(Pt 10), pp.1847–59.
- Ambros, I.M., Ambros, P.F., Strehl, S., Kovar, H., Gadner, H. and Salzer-Kuntschik, M. 1991. MIC2 is a specific marker for Ewing's sarcoma and peripheral primitive neuroectodermal tumors. Evidence for a common histogenesis of Ewing's sarcoma and peripheral primitive neuroectodermal tumors from MIC2 expression and specific chromosome aberration. *Cancer*. **67**(7), pp.1886–93.
- Amin, D.N., Hida, K., Bielenberg, D.R. and Klagsbrun, M. 2006. Tumor Endothelial Cells Express Epidermal Growth Factor Receptor (EGFR) but not ErbB3 and Are Responsive to EGF and to EGFR Kinase Inhibitors. *Cancer Research*. **66**(4), pp.2173–2180.
- Anders, C.K., Deal, A.M., Miller, C.R., Khorram, C., Meng, H., Burrows, E., Livasy, C., Fritchie, K., Ewend, M.G., Perou, C.M. and Carey, L.A. 2011. The prognostic contribution of clinical breast cancer subtype, age, and race among patients with breast cancer brain metastases. *Cancer*. **117**(8), pp.1602–1611.
- Ando, K., Fukuhara, S., Moriya, T., Obara, Y., Nakahata, N. and Mochizuki, N. 2013. Rap1 potentiates endothelial cell junctions by spatially controlling myosin II activity and actin organization. *The Journal of Cell Biology*. **202**(6), pp.901–916.
- Angara, K., Borin, T.F. and Arbab, A.S. 2017. Vascular Mimicry: A Novel Neovascularization Mechanism Driving Anti-Angiogenic Therapy (AAT) Resistance in Glioblastoma. *Translational oncology*. **10**(4), pp.650–660.
- Anon n.d. Cancer mortality statistics | Cancer Research UK. [Accessed 20 November 2018]. Available from: <https://www.cancerresearchuk.org/health-professional/cancer-statistics/mortality#heading-Zero>.
- Avraamides, C.J., Garmy-Susini, B. and Varner, J.A. 2008. Integrins in angiogenesis and lymphangiogenesis. *Nature reviews. Cancer*. **8**(8), pp.604–17.
- Baccar, A., Ferchichi, I., Troudi, W., Marrakchi, R., Ben Hmida, N., Jebini, S., Mrad, K., Ben Romdhane, K. and Benammar Elgaaied, A. 2013. CD99 and HLA-II immunostaining in breast cancer tissue and their correlation with lymph node metastasis. *Disease markers*. **34**(5), pp.363–71.
- Bálint, E., Bates, S. and Vousden, K.H. 1999. Mdm2 binds p73 $\alpha$  without targeting degradation. *Oncogene*. **18**(27), pp.3923–3929.
- Banks, W.A. 2009. Characteristics of compounds that cross the blood-brain barrier. *BMC neurology*. **9 Suppl 1**(Suppl 1), p.S3.
- Barak, Y., Juven, T., Haffner, R. and Oren, M. 1993. mdm2 expression is induced by wild type p53 activity. *The EMBO journal*. **12**(2), pp.461–8.
- Bardin, N., Anfosso, F., Massé, J.M., Cramer, E., Sabatier, F., Le Bivic, A., Sampol, J. and Dignat-George, F. 2001. Identification of CD146 as a component of the endothelial junction involved in the control of cell-cell cohesion. *Blood*. **98**(13), pp.3677–84.
- Bardin, N., Blot-Chaubaud, M., Despoix, N., Kebir, A., Harhour, K., Arsanto, J.-P., Espinosa, L., Perrin, P., Robert, S., Vely, F., Sabatier, F., Le Bivic, A.,

- Kaplanski, G., Sampol, J. and Dignat-George, F. 2009. CD146 and its Soluble Form Regulate Monocyte Transendothelial Migration. *Arteriosclerosis, Thrombosis, and Vascular Biology*. **29**(5), pp.746–753.
- Barkalow, F.J., Goodman, M.J., Gerritsen, M.E. and Mayadas, T.N. 1996. Brain endothelium lack one of two pathways of P-selectin-mediated neutrophil adhesion. *Blood*. **88**(12), pp.4585–93.
- Barry, D.M., Xu, K., Meadows, S.M., Zheng, Y., Norden, P.R., Davis, G.E. and Cleaver, O. 2015. Cdc42 is required for cytoskeletal support of endothelial cell adhesion during blood vessel formation in mice. *Development (Cambridge, England)*. **142**(17), pp.3058–70.
- Bauer, H.-C., Krizbai, I.A., Bauer, H. and Traweger, A. 2014. “You Shall Not Pass”-tight junctions of the blood brain barrier. *Frontiers in neuroscience*. **8**, p.392.
- Bauer, K., Mierke, C. and Behrens, J. 2007. Expression profiling reveals genes associated with transendothelial migration of tumor cells: A functional role for  $\alpha\beta 3$  integrin. *International Journal of Cancer*. **121**(9), pp.1910–1918.
- Bayless, K.J. and Davis, G.E. 2002. The Cdc42 and Rac1 GTPases are required for capillary lumen formation in three-dimensional extracellular matrices. *Journal of cell science*. **115**(Pt 6), pp.1123–36.
- Bazzoni, G., Martínez-Estrada, O.M., Mueller, F., Nelboeck, P., Schmid, G., Bartfai, T., Dejana, E. and Brockhaus, M. 2000. Homophilic Interaction of Junctional Adhesion Molecule. *Journal of Biological Chemistry*. **275**(40), pp.30970–30976.
- Bazzoni, G., Martínez-Estrada, O.M., Orsenigo, F., Cordenonsi, M., Citi, S. and Dejana, E. 2000. Interaction of Junctional Adhesion Molecule with the Tight Junction Components ZO-1, Cingulin, and Occludin. *Journal of Biological Chemistry*. **275**(27), pp.20520–20526.
- Bedau, T., Peters, F., Prox, J., Arnold, P., Schmidt, F., Finkernagel, M., Köllmann, S., Wichert, R., Otte, A., Ohler, A., Stirnberg, M., Lucius, R., Koudelka, T., Tholey, A., Biasin, V., Pietrzik, C.U., Kwapiszewska, G. and Becker-Pauly, C. 2017. Ectodomain shedding of CD99 within highly conserved regions is mediated by the metalloprotease meprin  $\beta$  and promotes transendothelial cell migration. *The FASEB Journal*. **31**(3), pp.1226–1237.
- Begley, D.J. and Brightman, M.W. 2003. Structural and functional aspects of the blood-brain barrier. *Progress in drug research. Fortschritte der Arzneimittelforschung. Progres des recherches pharmaceutiques*. **61**, pp.39–78.
- Belvitch, P., Brown, M.E., Brinley, B.N., Letsiou, E., Rizzo, A.N., Garcia, J.G.N. and Dudek, S.M. 2017. The ARP 2/3 complex mediates endothelial barrier function and recovery. *Pulmonary Circulation*. **7**(1), pp.200–210.
- Ben-Ze’ev, A. and Geiger, B. 1998. Differential molecular interactions of beta-catenin and plakoglobin in adhesion, signaling and cancer. *Current opinion in cell biology*. **10**(5), pp.629–39.
- Benchimol, S., Pim, D. and Crawford, L. 1982. Radioimmunoassay of the cellular protein p53 in mouse and human cell lines. *The EMBO journal*. **1**(9), pp.1055–62.
- Bernard, G., Raimondi, V., Alberti, I., Pourtein, M., Widjenes, J., Ticchioni, M. and Bernard, A. 2000. CD99 (E2) up-regulates  $\alpha 4\beta 1$ -dependent T cell adhesion to inflamed vascular endothelium under flow conditions. *European Journal of Immunology*. **30**(10), pp.3061–3065.
- Bhattacharya, R., SenBanerjee, S., Lin, Z., Mir, S., Hamik, A., Wang, P., Mukherjee, P., Mukhopadhyay, D. and Jain, M.K. 2005. Inhibition of Vascular Permeability Factor/Vascular Endothelial Growth Factor-mediated Angiogenesis by the Kruppel-like Factor KLF2. *Journal of Biological Chemistry*. **280**(32), pp.28848–28851.
- Bishop, E.T., Bell, G.T., Bloor, S., Broom, I.J., Hendry, N.F. and Wheatley, D.N.

1999. An in vitro model of angiogenesis: basic features. *Angiogenesis*. **3**(4), pp.335–44.
- Borges, E., Jan, Y. and Ruoslahti, E. 2000. Platelet-derived Growth Factor Receptor  $\beta$  and Vascular Endothelial Growth Factor Receptor 2 Bind to the  $\beta_3$  Integrin through Its Extracellular Domain. *Journal of Biological Chemistry*. **275**(51), pp.39867–39873.
- Bos, P.D., Zhang, X.H.-F., Nadal, C., Shu, W., Gomis, R.R., Nguyen, D.X., Minn, A.J., van de Vijver, M.J., Gerald, W.L., Foekens, J.A. and Massagué, J. 2009. Genes that mediate breast cancer metastasis to the brain. *Nature*. **459**(7249), pp.1005–1009.
- Boureaux, A., Vignal, E., Faure, S. and Fort, P. 2007. Evolution of the Rho Family of Ras-Like GTPases in Eukaryotes. *Molecular Biology and Evolution*. **24**(1), pp.203–216.
- Bourne, H.R., Sanders, D.A. and McCormick, F. 1991. The GTPase superfamily: conserved structure and molecular mechanism. *Nature*. **349**(6305), pp.117–127.
- Boyer-Di Ponio, J., El-Ayoubi, F., Glacial, F., Ganeshamoorthy, K., Driancourt, C., Godet, M., Perrière, N., Guillevic, O., Couraud, P.O. and Uzan, G. 2014. Instruction of circulating endothelial progenitors in vitro towards specialized blood-brain barrier and arterial phenotypes. *PLoS one*. **9**(1), p.e84179.
- Brémond, A., Meynet, O., Mahiddine, K., Coito, S., Tichet, M., Scotlandi, K., Breittmayer, J.-P., Gounon, P., Gleeson, P.A., Bernard, A. and Bernard, G. 2009. Regulation of HLA class I surface expression requires CD99 and p230/golgin-245 interaction. *Blood*. **113**(2), pp.347–57.
- Brooks, P.C., Clark, R.A. and Cheresh, D.A. 1994. Requirement of vascular integrin  $\alpha_v\beta_3$  for angiogenesis. *Science (New York, N.Y.)*. **264**(5158), pp.569–71.
- Bryan, B.A. and D'Amore, P.A. 2007. What tangled webs they weave: Rho-GTPase control of angiogenesis. *Cellular and Molecular Life Sciences*. **64**(16), pp.2053–2065.
- Byun, H.-J., Hong, I.-K., Kim, E., Jin, Y.-J., Jeoung, D.-I., Hahn, J.-H., Kim, Y.-M., Park, S.H. and Lee, H. 2006. A splice variant of CD99 increases motility and MMP-9 expression of human breast cancer cells through the AKT-, ERK-, and JNK-dependent AP-1 activation signaling pathways. *The Journal of biological chemistry*. **281**(46), pp.34833–47.
- Cailleau, R., Olivé, M. and Cruciger, Q. V 1978. Long-term human breast carcinoma cell lines of metastatic origin: preliminary characterization. *In vitro*. **14**(11), pp.911–5.
- Cain, R.J., Vanhaesebroeck, B. and Ridley, A.J. 2010. The PI3K p110 $\alpha$  isoform regulates endothelial adherens junctions via Pyk2 and Rac1. *The Journal of Cell Biology*. **188**(6), pp.863–876.
- Carmeliet, P. 2003. Angiogenesis in health and disease. *Nature Medicine*. **9**(6), pp.653–660.
- Carmeliet, P. and Jain, R.K. 2000. Angiogenesis in cancer and other diseases. *Nature*. **407**(6801), pp.249–257.
- Carmeliet, P., Lampugnani, M.G., Moons, L., Breviario, F., Compernelle, V., Bono, F., Balconi, G., Spagnuolo, R., Oosthuysse, B., Dewerchin, M., Zanetti, A., Angellilo, A., Mattot, V., Nuyens, D., Lutgens, E., Clotman, F., de Ruiter, M.C., Gittenberger-de Groot, A., Poelmann, R., Lupu, F., Herbert, J.M., Collen, D. and Dejana, E. 1999. Targeted deficiency or cytosolic truncation of the VE-cadherin gene in mice impairs VEGF-mediated endothelial survival and angiogenesis. *Cell*. **98**(2), pp.147–57.
- Carmeliet, P., De Smet, F., Loges, S. and Mazzone, M. 2009. Branching morphogenesis and antiangiogenesis candidates: tip cells lead the way. *Nature Reviews Clinical Oncology*. **6**(6), pp.315–326.
- Carvajal, R.D., Schwartz, G.K., Tezel, T., Marr, B., Francis, J.H. and Nathan, P.D.

2017. Metastatic disease from uveal melanoma: treatment options and future prospects. *The British journal of ophthalmology*. **101**(1), pp.38–44.
- Carvey, P.M., Hendey, B. and Monahan, A.J. 2009. The blood-brain barrier in neurodegenerative disease: a rhetorical perspective. *Journal of neurochemistry*. **111**(2), pp.291–314.
- Çelik, H., Sciandra, M., Flashner, B., Gelmez, E., Kayraklıoğlu, N., Allegakoen, D. V., Petro, J.R., Conn, E.J., Hour, S., Han, J., Oktay, L., Tiwari, P.B., Hayran, M., Harris, B.T., Manara, M.C., Toretzky, J.A., Scotlandi, K. and Üren, A. 2018. Clofarabine inhibits Ewing sarcoma growth through a novel molecular mechanism involving direct binding to CD99. *Oncogene*. **37**(16), pp.2181–2196.
- Cerisano, V., Aalto, Y., Perdichizzi, S., Bernard, G., Manara, M.C., Benini, S., Cenacchi, G., Preda, P., Lattanzi, G., Nagy, B., Knuutila, S., Colombo, M.P., Bernard, A., Picci, P. and Scotlandi, K. 2004. Molecular mechanisms of CD99-induced caspase-independent cell death and cell–cell adhesion in Ewing's sarcoma cells: actin and zyxin as key intracellular mediators. *Oncogene*. **23**(33), pp.5664–5674.
- Cerutti, C. and Ridley, A.J. 2017. Endothelial cell-cell adhesion and signaling. *Experimental Cell Research*. **358**(1), pp.31–38.
- Chakraborty, G., Rangaswami, H., Jain, S. and Kundu, G.C. 2006. Hypoxia regulates cross-talk between Syk and Lck leading to breast cancer progression and angiogenesis. *The Journal of biological chemistry*. **281**(16), pp.11322–31.
- Chambers, A.F., Groom, A.C. and MacDonald, I.C. 2002. Dissemination and growth of cancer cells in metastatic sites. *Nature Reviews Cancer*. **2**(8), pp.563–572.
- Chang, Y.S., di Tomaso, E., McDonald, D.M., Jones, R., Jain, R.K. and Munn, L.L. 2000. Mosaic blood vessels in tumors: Frequency of cancer cells in contact with flowing blood. *Proceedings of the National Academy of Sciences*. **97**(26), pp.14608–14613.
- Chen, C., Mobley, J.L., Dwir, O., Shimron, F., Grabovsky, V., Lobb, R.R., Shimizu, Y. and Alon, R. 1999. High affinity very late antigen-4 subsets expressed on T cells are mandatory for spontaneous adhesion strengthening but not for rolling on VCAM-1 in shear flow. *Journal of immunology (Baltimore, Md. : 1950)*. **162**(2), pp.1084–95.
- Chen, J., Luo, Y., Hui, H., Cai, T., Huang, H., Yang, F., Feng, J., Zhang, J. and Yan, X. 2017. CD146 coordinates brain endothelial cell-pericyte communication for blood-brain barrier development. *Proceedings of the National Academy of Sciences of the United States of America*. **114**(36), pp.E7622–E7631.
- Cheng, X. and Hung, M.-C. 2007. Breast cancer brain metastases. *Cancer and Metastasis Reviews*. **26**(3–4), pp.635–643.
- Chiang, A.C. and Massagué, J. 2008. Molecular basis of metastasis. *The New England journal of medicine*. **359**(26), pp.2814–23.
- Conway, D.E., Breckenridge, M.T., Hinde, E., Gratton, E., Chen, C.S. and Schwartz, M.A. 2013. Fluid Shear Stress on Endothelial Cells Modulates Mechanical Tension across VE-Cadherin and PECAM-1. *Current Biology*. **23**(11), pp.1024–1030.
- Coon, B.G., Baeyens, N., Han, J., Budatha, M., Ross, T.D., Fang, J.S., Yun, S., Thomas, J.-L. and Schwartz, M.A. 2015. Intramembrane binding of VE-cadherin to VEGFR2 and VEGFR3 assembles the endothelial mechanosensory complex. *The Journal of Cell Biology*. **208**(7), pp.975–986.
- Coureuil, M., Lécuyer, H., Scott, M.G.H., Boularan, C., Enslin, H., Soyer, M., Mikaty, G., Bourdoulous, S., Nassif, X. and Marullo, S. 2010. Meningococcus Hijacks a  $\beta$ 2-Adrenoceptor/ $\beta$ -Arrestin Pathway to Cross Brain Microvasculature Endothelium. *Cell*. **143**(7), pp.1149–1160.

- Coureuil, M., Mikaty, G., Miller, F., Lécuyer, H., Bernard, C., Bourdoulous, S., Duménil, G., Mège, R.-M., Weksler, B.B., Romero, I.A., Couraud, P.-O. and Nassif, X. 2009. Meningococcal type IV pili recruit the polarity complex to cross the brain endothelium. *Science (New York, N.Y.)*. **325**(5936), pp.83–7.
- Cristante, E., McArthur, S., Mauro, C., Maggioli, E., Romero, I.A., Wylezinska-Arridge, M., Couraud, P.O., Lopez-Tremoleda, J., Christian, H.C., Weksler, B.B., Malaspina, A. and Solito, E. 2013. Identification of an essential endogenous regulator of blood-brain barrier integrity, and its pathological and therapeutic implications. *Proceedings of the National Academy of Sciences of the United States of America*. **110**(3), pp.832–41.
- Cross, M.J. and Claesson-Welsh, L. 2001. FGF and VEGF function in angiogenesis: signalling pathways, biological responses and therapeutic inhibition. *Trends in pharmacological sciences*. **22**(4), pp.201–7.
- van Crujisen, H., Giaccone, G. and Hoekman, K. 2005. Epidermal growth factor receptor and angiogenesis: Opportunities for combined anticancer strategies. *International Journal of Cancer*. **117**(6), pp.883–888.
- Cunningham, S.A., Arrate, M.P., Brock, T.A. and Waxham, M.N. 1997. Interactions of FLT-1 and KDR with Phospholipase C  $\gamma$ : Identification of the Phosphotyrosine Binding Sites. *Biochemical and Biophysical Research Communications*. **240**(3), pp.635–639.
- Daneman, R. 2012. The blood-brain barrier in health and disease. *Annals of Neurology*. **72**(5), pp.648–672.
- Dauchy, S., Dutheil, F., Weaver, R.J., Chassoux, F., Daumas-Duport, C., Couraud, P.-O., Scherrmann, J.-M., De Waziers, I. and Declèves, X. 2008. ABC transporters, cytochromes P450 and their main transcription factors: expression at the human blood-brain barrier. *Journal of Neurochemistry*. **107**(6), pp.1518–1528.
- Davies, P.F. 2009. Hemodynamic shear stress and the endothelium in cardiovascular pathophysiology. *Nature clinical practice. Cardiovascular medicine*. **6**(1), pp.16–26.
- Davis, G.E. 1992. Affinity of integrins for damaged extracellular matrix: alpha v beta 3 binds to denatured collagen type I through RGD sites. *Biochemical and biophysical research communications*. **182**(3), pp.1025–31.
- Davis, G.E. and Bayless, K.J. 2003. An Integrin and Rho GTPase-Dependent Pinocytotic Vacuole Mechanism Controls Capillary Lumen Formation in Collagen and Fibrin Matrices. *Microcirculation*. **10**(1), pp.27–44.
- Dawood, S., Broglio, K., Esteva, F.J., Yang, W., Kau, S.-W., Islam, R., Albarracin, C., Yu, T.K., Green, M., Hortobagyi, G.N. and Gonzalez-Angulo, A.M. 2009. Survival among women with triple receptor-negative breast cancer and brain metastases. *Annals of Oncology*. **20**(4), pp.621–627.
- Dayanir, V., Meyer, R.D., Lashkari, K. and Rahimi, N. 2001. Identification of Tyrosine Residues in Vascular Endothelial Growth Factor Receptor-2/FLK-1 Involved in Activation of Phosphatidylinositol 3-Kinase and Cell Proliferation. *Journal of Biological Chemistry*. **276**(21), pp.17686–17692.
- DeCaprio, J.A., Ludlow, J.W., Figge, J., Shew, J.Y., Huang, C.M., Lee, W.H., Marsilio, E., Paucha, E. and Livingston, D.M. 1988. SV40 large tumor antigen forms a specific complex with the product of the retinoblastoma susceptibility gene. *Cell*. **54**(2), pp.275–83.
- Dehghanian, F., Hojati, Z. and Kay, M. 2014. New Insights into VEGF-A Alternative Splicing: Key Regulatory Switching in the Pathological Process. *Avicenna journal of medical biotechnology*. **6**(4), pp.192–9.
- Dejana, E. 2004. Endothelial cell–cell junctions: happy together. *Nature Reviews Molecular Cell Biology*. **5**(4), pp.261–270.
- DeLisser, H.M., Christofidou-Solomidou, M., Strieter, R.M., Burdick, M.D., Robinson, C.S., Wexler, R.S., Kerr, J.S., Garlanda, C., Merwin, J.R., Madri, J.A. and Albelda, S.M. 1997. Involvement of endothelial PECAM-1/CD31 in

- angiogenesis. *The American journal of pathology*. **151**(3), pp.671–7.
- Department of Health and Social Care n.d. 2010 to 2015 government policy: cancer research and treatment - GOV.UK. [Accessed 30 November 2018]. Available from: <https://www.gov.uk/government/publications/2010-to-2015-government-policy-cancer-research-and-treatment/2010-to-2015-government-policy-cancer-research-and-treatment>.
- Desgrosellier, J.S. and Cheresh, D.A. 2010. Integrins in cancer: biological implications and therapeutic opportunities. *Nature Reviews Cancer*. **10**(1), pp.9–22.
- Dippold, W.G., Jay, G., DeLeo, A.B., Khoury, G. and Old, L.J. 1981. p53 transformation-related protein: detection by monoclonal antibody in mouse and human cells. *Proceedings of the National Academy of Sciences of the United States of America*. **78**(3), pp.1695–9.
- Dixelius, J., Mäkinen, T., Wirzenius, M., Karkkainen, M.J., Wernstedt, C., Alitalo, K. and Claesson-Welsh, L. 2003. Ligand-induced Vascular Endothelial Growth Factor Receptor-3 (VEGFR-3) Heterodimerization with VEGFR-2 in Primary Lymphatic Endothelial Cells Regulates Tyrosine Phosphorylation Sites. *Journal of Biological Chemistry*. **278**(42), pp.40973–40979.
- Donnem, T., Hu, J., Ferguson, M., Adighibe, O., Snell, C., Harris, A.L., Gatter, K.C. and Pezzella, F. 2013. Vessel co-option in primary human tumors and metastases: an obstacle to effective anti-angiogenic treatment? *Cancer medicine*. **2**(4), pp.427–36.
- Draffin, J.E., McFarlane, S., Hill, A., Johnston, P.G. and Waugh, D.J.J. 2004. CD44 Potentiates the Adherence of Metastatic Prostate and Breast Cancer Cells to Bone Marrow Endothelial Cells. *Cancer Research*. **64**(16), pp.5702–5711.
- DuBridge, R.B., Tang, P., Hsia, H.C., Leong, P.M., Miller, J.H. and Calos, M.P. 1987. Analysis of mutation in human cells by using an Epstein-Barr virus shuttle system. *Molecular and cellular biology*. **7**(1), pp.379–87.
- Dufies, M., Nollet, M., Ambrosetti, D., Traboulsi, W., Viotti, J., Borchiellini, D., Grépin, R., Parola, J., Giuliano, S., Helley-Russick, D., Bensalah, K., Ravaud, A., Bernhard, J.-C., Schiappa, R., Bardin, N., Dignat-George, F., Rioux-Leclercq, N., Oudard, S., Négrier, S., Ferrero, J.-M., Chamorey, E., Blot-Chabaud, M. and Pagès, G. 2018. Soluble CD146 is a predictive marker of pejorative evolution and of sunitinib efficacy in clear cell renal cell carcinoma. *Theranostics*. **8**(9), pp.2447–2458.
- Dufour, E.M., Deroche, A., Bae, Y. and Muller, W.A. 2008. CD99 is essential for leukocyte diapedesis in vivo. *Cell communication & adhesion*. **15**(4), pp.351–63.
- Ebnet, K. 2017. Junctional Adhesion Molecules (JAMs): Cell Adhesion Receptors With Pleiotropic Functions in Cell Physiology and Development. *Physiological Reviews*. **97**(4), pp.1529–1554.
- Eden, S., Rohatgi, R., Podtelejnikov, A. V., Mann, M. and Kirschner, M.W. 2002. Mechanism of regulation of WAVE1-induced actin nucleation by Rac1 and Nck. *Nature*. **418**(6899), pp.790–793.
- Edlund, K., Lindskog, C., Saito, A., Berglund, A., Pontén, F., Göransson-Kultima, H., Isaksson, A., Jirstrom, K., Planck, M., Johansson, L., Lambe, M., Holmberg, L., Nyberg, F., Ekman, S., Bergqvist, M., Landelius, P., Lamberg, K., Botling, J., Östman, A. and Micke, P. 2012. CD99 is a novel prognostic stromal marker in non-small cell lung cancer. *International Journal of Cancer*. **131**(10), pp.2264–2273.
- Ehrlich, P.E. 1885. Das Sauerstoff-Bedurfnis des Organismus. *Eine Farbenanalytische Studie*. Ph.D. thesis. **Herschwarl**(Berlin), pp.69–72.
- Ellenbroek, S.I.J. and Collard, J.G. 2007. Rho GTPases: functions and association with cancer. *Clinical & Experimental Metastasis*. **24**(8), pp.657–672.
- Ellis, N.A., Tippet, P., Petty, A., Reid, M., Weller, P.A., Ye, T.Z., German, J., Goodfellow, P.N., Thomas, S. and Banting, G. 1994. PBDX is the XG blood

- group gene. *Nature Genetics*. **8**(3), pp.285–290.
- Engelhardt, B. and Ransohoff, R.M. 2012. Capture, crawl, cross: the T cell code to breach the blood–brain barriers. *Trends in Immunology*. **33**(12), pp.579–589.
- Engelhardt, B., Vestweber, D., Hallmann, R. and Schulz, M. 1997. E- and P-selectin are not involved in the recruitment of inflammatory cells across the blood-brain barrier in experimental autoimmune encephalomyelitis. *Blood*. **90**(11), pp.4459–72.
- Er, E.E., Valiente, M., Ganesh, K., Zou, Y., Agrawal, S., Hu, J., Griscom, B., Rosenblum, M., Boire, A., Brogi, E., Giancotti, F.G., Schachner, M., Malladi, S. and Massagué, J. 2018. Pericyte-like spreading by disseminated cancer cells activates YAP and MRTF for metastatic colonization. *Nature Cell Biology*. **20**(8), pp.966–978.
- Evani, S.J., Prabhu, R.G., Gnanaruban, V., Finol, E.A. and Ramasubramanian, A.K. 2013. Monocytes mediate metastatic breast tumor cell adhesion to endothelium under flow. *FASEB journal : official publication of the Federation of American Societies for Experimental Biology*. **27**(8), pp.3017–29.
- Falchetti, M.L., Mongiardi, M.P., Fiorenzo, P., Petrucci, G., Pierconti, F., D’Agnano, I., D’Alessandris, G., Alessandri, G., Gelati, M., Ricci-Vitiani, L., Maira, G., Larocca, L.M., Levi, A. and Pallini, R. 2008. Inhibition of telomerase in the endothelial cells disrupts tumor angiogenesis in glioblastoma xenografts. *International Journal of Cancer*. **122**(6), pp.1236–1242.
- Fazakas, C., Wilhelm, I., Nagyósz, P., Farkas, A.E., Haskó, J., Molnár, J., Bauer, H., Bauer, H.-C., Ayaydin, F., Dung, N.T.K., Siklós, L. and Krizbai, I.A. 2011. Transmigration of Melanoma Cells through the Blood-Brain Barrier: Role of Endothelial Tight Junctions and Melanoma-Released Serine Proteases G. J. Guillemin, ed. *PLoS ONE*. **6**(6), p.e20758.
- Feoktistov, I., Goldstein, A.E. and Biaggioni, I. 2000. Cyclic AMP and protein kinase A stimulate Cdc42: role of A(2) adenosine receptors in human mast cells. *Molecular pharmacology*. **58**(5), pp.903–10.
- Feoktistova, M., Geserick, P. and Leverkus, M. 2016. Crystal Violet Assay for Determining Viability of Cultured Cells. *Cold Spring Harbor Protocols*. **2016**(4), pdb.prot087379.
- Ferrara, N. 2004. Vascular Endothelial Growth Factor: Basic Science and Clinical Progress. *Endocrine Reviews*. **25**(4), pp.581–611.
- Ferrara, N., Gerber, H.-P. and LeCouter, J. 2003. The biology of VEGF and its receptors. *Nature Medicine*. **9**(6), pp.669–676.
- Ferrara, N. and Henzel, W.J. 1989. Pituitary follicular cells secrete a novel heparin-binding growth factor specific for vascular endothelial cells. *Biochemical and biophysical research communications*. **161**(2), pp.851–8.
- Fidler, I.J. 1970. Metastasis: quantitative analysis of distribution and fate of tumor emboli labeled with <sup>125</sup>I-5-iodo-2'-deoxyuridine. *Journal of the National Cancer Institute*. **45**(4), pp.773–82.
- Fidler, I.J. and Kripke, M.L. 1977. Metastasis results from preexisting variant cells within a malignant tumor. *Science (New York, N.Y.)*. **197**(4306), pp.893–5.
- Fina, L., Molgaard, H. V, Robertson, D., Bradley, N.J., Monaghan, P., Delia, D., Sutherland, D.R., Baker, M.A. and Greaves, M.F. 1990. Expression of the CD34 gene in vascular endothelial cells. *Blood*. **75**(12), pp.2417–26.
- Finger, E.B., Purl, K.D., Alon, R., Lawrence, M.B., von Andrian, U.H. and Springer, T.A. 1996. Adhesion through L-selectin requires a threshold hydrodynamic shear. *Nature*. **379**(6562), pp.266–269.
- Finlay, C.A., Hinds, P.W. and Levine, A.J. 1989. The p53 proto-oncogene can act as a suppressor of transformation. *Cell*. **57**(7), pp.1083–93.
- Finlay, C.A., Hinds, P.W., Tan, T.H., Eliyahu, D., Oren, M. and Levine, A.J. 1988. Activating mutations for transformation by p53 produce a gene product that forms an hsc70-p53 complex with an altered half-life. *Molecular and cellular biology*. **8**(2), pp.531–9.

- Fischer, S., Nishio, M., Peters, S.C., Tschernatsch, M., Walberer, M., Weidemann, S., Heidenreich, R., Couraud, P.O., Weksler, B.B., Romero, I.A., Gerriets, T. and Preissner, K.T. 2009. Signaling mechanism of extracellular RNA in endothelial cells. *The FASEB Journal*. **23**(7), pp.2100–2109.
- Flamme, I., Frölich, T. and Risau, W. 1997. Molecular mechanisms of vasculogenesis and embryonic angiogenesis. *Journal of Cellular Physiology*. **173**(2), pp.206–210.
- Flanagan, K., Fitzgerald, K., Baker, J., Regnstrom, K., Gardai, S., Bard, F., Mocchi, S., Seto, P., You, M., Larochelle, C., Prat, A., Chow, S., Li, L., Vandeventer, C., Zago, W., Lorenzana, C., Nishioka, C., Hoffman, J., Botelho, R., Willits, C., Tanaka, K., Johnston, J. and Yednock, T. 2012. Laminin-411 Is a Vascular Ligand for MCAM and Facilitates TH17 Cell Entry into the CNS S. G. Meuth, ed. *PLoS ONE*. **7**(7), p.e40443.
- Fogh, J., Fogh, J.M. and Orfeo, T. 1977. One hundred and twenty-seven cultured human tumor cell lines producing tumors in nude mice. *Journal of the National Cancer Institute*. **59**(1), pp.221–6.
- Follain, G., Osmani, N., Azevedo, A.S., Allio, G., Mercier, L., Karreman, M.A., Solecki, G., Garcia León, M.J., Lefebvre, O., Fekonja, N., Hille, C., Chabannes, V., Dollé, G., Metivet, T., Hovsepian, F. Der, Prudhomme, C., Pichot, A., Paul, N., Carapito, R., Bahram, S., Ruthensteiner, B., Kemmling, A., Siemonsen, S., Schneider, T., Fiehler, J., Glatzel, M., Winkler, F., Schwab, Y., Pantel, K., Harlepp, S. and Goetz, J.G. 2018. Hemodynamic Forces Tune the Arrest, Adhesion, and Extravasation of Circulating Tumor Cells. *Developmental Cell*. **45**(1), p.33–52.e12.
- Fong, G.-H., Rossant, J., Gertsenstein, M. and Breitman, M.L. 1995. Role of the Flt-1 receptor tyrosine kinase in regulating the assembly of vascular endothelium. *Nature*. **376**(6535), pp.66–70.
- Freeman, J.L., Abo, A. and Lambeth, J.D. 1996. Rac &quot;insert region&quot; is a novel effector region that is implicated in the activation of NADPH oxidase, but not PAK65. *The Journal of biological chemistry*. **271**(33), pp.19794–801.
- Frisch, S.M. and Ruoslahti, E. 1997. Integrins and anoikis. *Current opinion in cell biology*. **9**(5), pp.701–6.
- Fröhlich, C., Klitgaard, M., Noer, J.B., Kotsch, A., Nehammer, C., Kronqvist, P., Berthelsen, J., Blobel, C., Kveiborg, M., Albrechtsen, R. and Wewer, U.M. 2013. ADAM12 is expressed in the tumour vasculature and mediates ectodomain shedding of several membrane-anchored endothelial proteins. *Biochemical Journal*. **452**(1), pp.97–109.
- Fuh, G., Li, B., Crowley, C., Cunningham, B. and Wells, J.A. 1998. Requirements for binding and signaling of the kinase domain receptor for vascular endothelial growth factor. *The Journal of biological chemistry*. **273**(18), pp.11197–204.
- Fujio, Y. and Walsh, K. 1999. Akt mediates cytoprotection of endothelial cells by vascular endothelial growth factor in an anchorage-dependent manner. *The Journal of biological chemistry*. **274**(23), pp.16349–54.
- Furuse, M., Hirase, T., Itoh, M., Nagafuchi, A., Yonemura, S., Tsukita, S. and Tsukita, S. 1993. Occludin: a novel integral membrane protein localizing at tight junctions. *The Journal of cell biology*. **123**(6 Pt 2), pp.1777–88.
- Garcia, S., Dalès, J.-P., Charafe-Jauffret, E., Carpentier-Meunier, S., Andrac-Meyer, L., Jacquemier, J., Andonian, C., Lavaut, M.-N., Allasia, C., Bonnier, P. and Charpin, C. 2007. Poor prognosis in breast carcinomas correlates with increased expression of targetable CD146 and c-Met and with proteomic basal-like phenotype. *Human Pathology*. **38**(6), pp.830–841.
- Gasic, G.J., Gasic, T.B. and Stewart, C.C. 1968. Antimetastatic effects associated with platelet reduction. *Proceedings of the National Academy of Sciences of the United States of America*. **61**(1), pp.46–52.
- Gastl, G., Spizzo, G., Obrist, P., Dünser, M. and Mikuz, G. 2000. Ep-CAM overexpression in breast cancer as a predictor of survival. *The Lancet*.

- 356(9246), pp.1981–1982.
- Geng, Y., Yeh, K., Takatani, T. and King, M.R. 2012. Three to Tango: MUC1 as a Ligand for Both E-Selectin and ICAM-1 in the Breast Cancer Metastatic Cascade. *Frontiers in Oncology*. **2**.
- Gertler, F. and Condeelis, J. 2011. Metastasis: tumor cells becoming MENAcing. *Trends in Cell Biology*. **21**(2), pp.81–90.
- Geudens, I. and Gerhardt, H. 2011. Coordinating cell behaviour during blood vessel formation. *Development*. **138**(21), pp.4569–4583.
- Ghajar, C.M., Peinado, H., Mori, H., Matei, I.R., Evason, K.J., Brazier, H., Almeida, D., Koller, A., Hajjar, K.A., Stainier, D.Y.R., Chen, E.I., Lyden, D. and Bissell, M.J. 2013. The perivascular niche regulates breast tumour dormancy. *Nature cell biology*. **15**(7), pp.807–17.
- Gille, H., Kowalski, J., Yu, L., Chen, H., Pisabarro, M.T., Davis-Smyth, T. and Ferrara, N. 2000. A repressor sequence in the juxtamembrane domain of Flt-1 (VEGFR-1) constitutively inhibits vascular endothelial growth factor-dependent phosphatidylinositol 3'-kinase activation and endothelial cell migration. *The EMBO Journal*. **19**(15), pp.4064–4073.
- González-Mariscal, L., Betanzos, A., Nava, P. and Jaramillo, B.E. 2003. Tight junction proteins. *Progress in biophysics and molecular biology*. **81**(1), pp.1–44.
- Goodfellow, P.J., Darling, S.M., Thomas, N.S. and Goodfellow, P.N. 1986. A pseudoautosomal gene in man. *Science (New York, N.Y.)*. **234**(4777), pp.740–3.
- Goswami, D., März, S., Li, Y.-T., Artz, A., Schäfer, K., Seelige, R., Pacheco-Blanco, M., Jing, D., Bixel, M.G., Araki, M., Araki, K., Yamamura, K.-I. and Vestweber, D. 2017. Endothelial CD99 supports arrest of mouse neutrophils in venules and binds to neutrophil PILRs. *Blood*. **129**(13), pp.1811–1822.
- Graesser, D., Solowiej, A., Bruckner, M., Osterweil, E., Juedes, A., Davis, S., Ruddle, N.H., Engelhardt, B. and Madri, J.A. 2002. Altered vascular permeability and early onset of experimental autoimmune encephalomyelitis in PECAM-1-deficient mice. *Journal of Clinical Investigation*. **109**(3), pp.383–392.
- Guevara, N. V., Kim, H.-S., Antonova, E.I. and Chan, L. 1999. The absence of p53 accelerates atherosclerosis by increasing cell proliferation in vivo. *Nature Medicine*. **5**(3), pp.335–339.
- van der Gun, B.T.F., Melchers, L.J., Ruiters, M.H.J., de Leij, L.F.M.H., McLaughlin, P.M.J. and Rots, M.G. 2010. EpCAM in carcinogenesis: the good, the bad or the ugly. *Carcinogenesis*. **31**(11), pp.1913–1921.
- Guo, W. and Giancotti, F.G. 2004. Integrin signalling during tumour progression. *Nature Reviews Molecular Cell Biology*. **5**(10), pp.816–826.
- Gupta, G.P. and Massagué, J. 2006. Cancer metastasis: building a framework. *Cell*. **127**(4), pp.679–95.
- Gupta, G.P., Nguyen, D.X., Chiang, A.C., Bos, P.D., Kim, J.Y., Nadal, C., Gomis, R.R., Manova-Todorova, K. and Massagué, J. 2007. Mediators of vascular remodelling co-opted for sequential steps in lung metastasis. *Nature*. **446**(7137), pp.765–770.
- Hahn, J.H., Kim, M.K., Choi, E.Y., Kim, S.H., Sohn, H.W., Ham, D.I., Chung, D.H., Kim, T.J., Lee, W.J., Park, C.K., Ree, H.J. and Park, S.H. 1997. CD99 (MIC2) regulates the LFA-1/ICAM-1-mediated adhesion of lymphocytes, and its gene encodes both positive and negative regulators of cellular adhesion. *Journal of immunology (Baltimore, Md. : 1950)*. **159**(5), pp.2250–8.
- Hall, A. 1998. Rho GTPases and the actin cytoskeleton. *Science (New York, N.Y.)*. **279**(5350), pp.509–14.
- Hanahan, D. and Folkman, J. 1996. Patterns and emerging mechanisms of the angiogenic switch during tumorigenesis. *Cell*. **86**(3), pp.353–64.
- Hanahan, D. and Weinberg, R.A. 2011. Hallmarks of Cancer: The Next Generation.

- Cell*. **144**(5), pp.646–674.
- Hanahan, D. and Weinberg, R.A. 2000. The hallmarks of cancer. *Cell*. **100**(1), pp.57–70.
- Haqqani, A.S., Delaney, C.E., Tremblay, T.-L., Sodja, C., Sandhu, J.K. and Stanimirovic, D.B. 2013. Method for isolation and molecular characterization of extracellular microvesicles released from brain endothelial cells. *Fluids and Barriers of the CNS*. **10**(1), p.4.
- Harper, K.L., Sosa, M.S., Entenberg, D., Hosseini, H., Cheung, J.F., Nobre, R., Avivar-Valderas, A., Nagi, C., Girnius, N., Davis, R.J., Farias, E.F., Condeelis, J., Klein, C.A. and Aguirre-Ghiso, J.A. 2016. Mechanism of early dissemination and metastasis in Her2+ mammary cancer. *Nature*. **540**(7634), pp.588–592.
- Haupt, Y., Maya, R., Kazaz, A. and Oren, M. 1997. Mdm2 promotes the rapid degradation of p53. *Nature*. **387**(6630), pp.296–299.
- Hawkins, B.T. and Davis, T.P. 2005. The Blood-Brain Barrier/Neurovascular Unit in Health and Disease. *Pharmacological Reviews*. **57**(2), pp.173–185.
- Heemskerk, N., van Rijssel, J. and van Buul, J.D. 2014. Rho-GTPase signaling in leukocyte extravasation: an endothelial point of view. *Cell adhesion & migration*. **8**(2), pp.67–75.
- Heo, K.-S., Chang, E., Le, N.-T., Cushman, H., Yeh, E.T.H., Fujiwara, K. and Abe, J. 2013. De-SUMOylation Enzyme of Sentrin/SUMO-Specific Protease 2 Regulates Disturbed Flow-Induced SUMOylation of ERK5 and p53 that Leads to Endothelial Dysfunction and Atherosclerosis. *Circulation Research*. **112**(6), pp.911–923.
- Herbert, S.P. and Stainier, D.Y.R. 2011. Molecular control of endothelial cell behaviour during blood vessel morphogenesis. *Nature Reviews Molecular Cell Biology*. **12**(9), pp.551–564.
- Hinds, P., Finlay, C. and Levine, A.J. 1989. Mutation is required to activate the p53 gene for cooperation with the ras oncogene and transformation. *Journal of virology*. **63**(2), pp.739–46.
- Hoeben, A., Landuyt, B., Highley, M.S., Wildiers, H., Van Oosterom, A.T. and De Bruijn, E.A. 2004. Vascular Endothelial Growth Factor and Angiogenesis. *Pharmacological Reviews*. **56**(4), pp.549–580.
- Holmgren, L., O'Reilly, M.S. and Folkman, J. 1995. Dormancy of micrometastases: balanced proliferation and apoptosis in the presence of angiogenesis suppression. *Nature medicine*. **1**(2), pp.149–53.
- Holmqvist, K., Cross, M.J., Rolny, C., Hägerkvist, R., Rahimi, N., Matsumoto, T., Claesson-Welsh, L. and Welsh, M. 2004. The Adaptor Protein Shb Binds to Tyrosine 1175 in Vascular Endothelial Growth Factor (VEGF) Receptor-2 and Regulates VEGF-dependent Cellular Migration. *Journal of Biological Chemistry*. **279**(21), pp.22267–22275.
- Honda, R., Tanaka, H. and Yasuda, H. 1997. Oncoprotein MDM2 is a ubiquitin ligase E3 for tumor suppressor p53. *FEBS letters*. **420**(1), pp.25–7.
- Horm, T.M. and Schroeder, J.A. 2013. MUC1 and metastatic cancer: expression, function and therapeutic targeting. *Cell adhesion & migration*. **7**(2), pp.187–98.
- Hoshino, A., Costa-Silva, B., Shen, T.-L., Rodrigues, G., Hashimoto, A., Tesic Mark, M., Molina, H., Kohsaka, S., Di Giannatale, A., Ceder, S., Singh, S., Williams, C., Soplop, N., Uryu, K., Pharmed, L., King, T., Bojmar, L., Davies, A.E., Ararso, Y., Zhang, T., Zhang, H., Hernandez, J., Weiss, J.M., Dumont-Cole, V.D., Kramer, K., Wexler, L.H., Narendran, A., Schwartz, G.K., Healey, J.H., Sandstrom, P., Jørgen Labori, K., Kure, E.H., Grandgenett, P.M., Hollingsworth, M.A., de Sousa, M., Kaur, S., Jain, M., Mallya, K., Batra, S.K., Jarnagin, W.R., Brady, M.S., Fodstad, O., Muller, V., Pantel, K., Minn, A.J., Bissell, M.J., Garcia, B.A., Kang, Y., Rajasekhar, V.K., Ghajar, C.M., Matei, I., Peinado, H., Bromberg, J. and Lyden, D. 2015. Tumour exosome integrins determine organotropic metastasis. *Nature*. **527**(7578), pp.329–335.
- Hosseini, H., Obradović, M.M.S., Hoffmann, M., Harper, K.L., Sosa, M.S., Werner-

- Klein, M., Nanduri, L.K., Werno, C., Ehrl, C., Maneck, M., Patwary, N., Haunschild, G., Gužvić, M., Reimelt, C., Grauvogl, M., Eichner, N., Weber, F., Hartkopf, A.D., Taran, F.-A., Brucker, S.Y., Fehm, T., Rack, B., Buchholz, S., Spang, R., Meister, G., Aguirre-Ghiso, J.A. and Klein, C.A. 2016. Early dissemination seeds metastasis in breast cancer. *Nature*. **540**(7634), pp.552–558.
- Houck, K.A., Ferrara, N., Winer, J., Cachianes, G., Li, B. and Leung, D.W. 1991. The Vascular Endothelial Growth Factor Family: Identification of a Fourth Molecular Species and Characterization of Alternative Splicing of RNA. *Molecular Endocrinology*. **5**(12), pp.1806–1814.
- Huang, B., Krafft, P.R., Ma, Q., Rolland, W.B., Caner, B., Lekic, T., Manaenko, A., Le, M., Tang, J. and Zhang, J.H. 2012. Fibroblast growth factors preserve blood–brain barrier integrity through RhoA inhibition after intracerebral hemorrhage in mice. *Neurobiology of Disease*. **46**(1), pp.204–214.
- Huang, R.-L., Teo, Z., Chong, H.C., Zhu, P., Tan, M.J., Tan, C.K., Lam, C.R.I., Sng, M.K., Leong, D.T.W., Tan, S.M., Kersten, S., Ding, J.L., Li, H.Y. and Tan, N.S. 2011. ANGPTL4 modulates vascular junction integrity by integrin signaling and disruption of intercellular VE-cadherin and claudin-5 clusters. *Blood*. **118**(14), pp.3990–4002.
- Hupe, M., Li, M.X., Kneitz, S., Davydova, D., Yokota, C., Kele, J., Hot, B., Stenman, J.M. and Gessler, M. 2017. Gene expression profiles of brain endothelial cells during embryonic development at bulk and single-cell levels. *Science signaling*. **10**(487), p.eaag2476.
- Imbert, A.-M., Garulli, C., Choquet, E., Koubi, M., Aurrand-Lions, M. and Chabannon, C. 2012. CD146 expression in human breast cancer cell lines induces phenotypic and functional changes observed in Epithelial to Mesenchymal Transition. *PloS one*. **7**(8), p.e43752.
- Infanger, D.W., Cho, Y., Lopez, B.S., Mohanan, S., Liu, S.C., Gursel, D., Boockvar, J.A. and Fischbach, C. 2013. Glioblastoma stem cells are regulated by interleukin-8 signaling in a tumoral perivascular niche. *Cancer research*. **73**(23), pp.7079–89.
- Ito, N., Wernstedt, C., Engström, U. and Claesson-Welsh, L. 1998. Identification of vascular endothelial growth factor receptor-1 tyrosine phosphorylation sites and binding of SH2 domain-containing molecules. *The Journal of biological chemistry*. **273**(36), pp.23410–8.
- Iyer, S., Ferreri, D.M., DeCocco, N.C., Minnear, F.L. and Vincent, P.A. 2004. VE-cadherin-p120 interaction is required for maintenance of endothelial barrier function. *American journal of physiology. Lung cellular and molecular physiology*. **286**(6), pp.L1143-53.
- Jain, R.K. 2003. Molecular regulation of vessel maturation. *Nature Medicine*. **9**(6), pp.685–693.
- Jakobsson, L., Franco, C.A., Bentley, K., Collins, R.T., Ponsioen, B., Aspalter, I.M., Rosewell, I., Busse, M., Thurston, G., Medvinsky, A., Schulte-Merker, S. and Gerhardt, H. 2010. Endothelial cells dynamically compete for the tip cell position during angiogenic sprouting. *Nature Cell Biology*. **12**(10), pp.943–953.
- Jatoi, I., Hilsenbeck, S.G., Clark, G.M. and Osborne, C.K. 1999. Significance of Axillary Lymph Node Metastasis in Primary Breast Cancer. *Journal of Clinical Oncology*. **17**(8), pp.2334–2334.
- Jeon, J.S., Bersini, S., Gilardi, M., Dubini, G., Charest, J.L., Moretti, M. and Kamm, R.D. 2015. Human 3D vascularized organotypic microfluidic assays to study breast cancer cell extravasation. *Proceedings of the National Academy of Sciences of the United States of America*. **112**(1), pp.214–9.
- Jiang, T., Zhuang, J., Duan, H., Luo, Y., Zeng, Q., Fan, K., Yan, H., Lu, D., Ye, Z., Hao, J., Feng, J., Yang, D. and Yan, X. 2012. CD146 is a coreceptor for VEGFR-2 in tumor angiogenesis. *Blood*. **120**(11), pp.2330–2339.
- Jin, Y., Liu, Y., Lin, Q., Li, J., Druso, J.E., Antonyak, M.A., Meininger, C.J., Zhang,

- S.L., Dostal, D.E., Guan, J.-L., Cerione, R.A. and Peng, X. 2013. Deletion of Cdc42 Enhances ADAM17-Mediated Vascular Endothelial Growth Factor Receptor 2 Shedding and Impairs Vascular Endothelial Cell Survival and Vasculogenesis. *Molecular and Cellular Biology*. **33**(21), pp.4181–4197.
- Jouve, N., Bachelier, R., Despoix, N., Blin, M.G., Matinzadeh, M.K., Poitevin, S., Aurrand-Lions, M., Fallague, K., Bardin, N., Blot-Chaubaud, M., Vely, F., Dignat-George, F. and Leroyer, A.S. 2015. CD146 mediates VEGF-induced melanoma cell extravasation through FAK activation. *International Journal of Cancer*. **137**(1), pp.50–60.
- Joyce, J.A. and Pollard, J.W. 2009. Microenvironmental regulation of metastasis. *Nature Reviews Cancer*. **9**(4), pp.239–252.
- JuanYin, J., Tracy, K., Zhang, L., Munasinghe, J., Shapiro, E., Koretsky, A. and Kelly, K. 2009. Noninvasive imaging of the functional effects of anti-VEGF therapy on tumor cell extravasation and regional blood volume in an experimental brain metastasis model. *Clinical & Experimental Metastasis*. **26**(5), pp.403–414.
- Junttila, M.R. and Evan, G.I. 2009. p53 — a Jack of all trades but master of none. *Nature Reviews Cancer*. **9**(11), pp.821–829.
- Kaighn, M.E., Narayan, K.S., Ohnuki, Y., Lechner, J.F. and Jones, L.W. 1979. Establishment and characterization of a human prostatic carcinoma cell line (PC-3). *Investigative urology*. **17**(1), pp.16–23.
- Kalluri, R. and Weinberg, R.A. 2009. The basics of epithelial-mesenchymal transition. *The Journal of clinical investigation*. **119**(6), pp.1420–8.
- Kang, Y., Siegel, P.M., Shu, W., Drobnjak, M., Kakonen, S.M., Cordón-Cardo, C., Guise, T.A. and Massagué, J. 2003. A multigenic program mediating breast cancer metastasis to bone. *Cancer Cell*. **3**(6), pp.537–549.
- Kastan, M.B., Zhan, Q., El-Deiry, W.S., Carrier, F., Jacks, T., Walsh, W. V., Plunkett, B.S., Vogelstein, B. and Fornace, A.J. 1992. A mammalian cell cycle checkpoint pathway utilizing p53 and GADD45 is defective in ataxia-telangiectasia. *Cell*. **71**(4), pp.587–597.
- Kastenhuber, E.R. and Lowe, S.W. 2017. Putting p53 in Context. *Cell*. **170**(6), pp.1062–1078.
- Kendall, R.L. and Thomas, K.A. 1993. Inhibition of vascular endothelial cell growth factor activity by an endogenously encoded soluble receptor. *Proceedings of the National Academy of Sciences of the United States of America*. **90**(22), pp.10705–9.
- Khaitan, D., Sankpal, U.T., Weksler, B., Meister, E.A., Romero, I.A., Couraud, P.-O. and Ningaraj, N.S. 2009. Role of KCNMA1 gene in breast cancer invasion and metastasis to brain. *BMC Cancer*. **9**(1), p.258.
- Khuon, S., Liang, L., Dettman, R.W., Sporn, P.H.S., Wysolmerski, R.B. and Chew, T.-L. 2010. Myosin light chain kinase mediates transcellular intravasation of breast cancer cells through the underlying endothelial cells: a three-dimensional FRET study. *Journal of Cell Science*. **123**(3), pp.431–440.
- Kienast, Y., von Baumgarten, L., Fuhrmann, M., Klinkert, W.E.F., Goldbrunner, R., Herms, J. and Winkler, F. 2010. Real-time imaging reveals the single steps of brain metastasis formation. *Nature Medicine*. **16**(1), pp.116–122.
- Kim, A.S., Kakalis, L.T., Abdul-Manan, N., Liu, G.A. and Rosen, M.K. 2000. Autoinhibition and activation mechanisms of the Wiskott–Aldrich syndrome protein. *Nature*. **404**(6774), pp.151–158.
- Kim, K.-J., Kwon, S.-H., Yun, J.-H., Jeong, H.-S., Kim, H.-R., Lee, E.H., Ye, S.-K. and Cho, C.-H. 2017. STAT3 activation in endothelial cells is important for tumor metastasis via increased cell adhesion molecule expression. *Oncogene*. **36**(39), pp.5445–5459.
- Kim, Y.J., Borsig, L., Varki, N.M. and Varki, A. 1998. P-selectin deficiency attenuates tumor growth and metastasis. *Proceedings of the National Academy of Sciences of the United States of America*. **95**(16), pp.9325–30.

- Koch, S., Tugues, S., Li, X., Gualandi, L. and Claesson-Welsh, L. 2011. Signal transduction by vascular endothelial growth factor receptors. *Biochemical Journal*. **437**(2), pp.169–183.
- Köhler, S., Ullrich, S., Richter, U. and Schumacher, U. 2010. E-/P-selectins and colon carcinoma metastasis: first in vivo evidence for their crucial role in a clinically relevant model of spontaneous metastasis formation in the lung. *British Journal of Cancer*. **102**(3), pp.602–609.
- Kouklis, P., Konstantoulaki, M., Vogel, S., Broman, M. and Malik, A.B. 2004. Cdc42 Regulates the Restoration of Endothelial Barrier Function. *Circulation Research*. **94**(2), pp.159–166.
- Krause, G., Winkler, L., Mueller, S.L., Haseloff, R.F., Piontek, J. and Blasig, I.E. 2008. Structure and function of claudins. *Biochimica et Biophysica Acta (BBA) - Biomembranes*. **1778**(3), pp.631–645.
- Krishnan, S., Szabo, E., Burghardt, I., Frei, K., Tabatabai, G. and Weller, M. 2015. Modulation of cerebral endothelial cell function by TGF- $\beta$  in glioblastoma: VEGF-dependent angiogenesis versus endothelial mesenchymal transition. *Oncotarget*. **6**(26), pp.22480–95.
- de Kruijff, I., Timmermans, A., den Bakker, M., Trapman-Jansen, A., Foekens, R., Meijer-Van Gelder, M., Oomen-de Hoop, E., Smid, M., Hollestelle, A., van Deurzen, C., Foekens, J., Martens, J. and Sleijfer, S. 2018. The Prevalence of CD146 Expression in Breast Cancer Subtypes and Its Relation to Outcome. *Cancers*. **10**(5), p.134.
- Kruiswijk, F., Labuschagne, C.F. and Vousden, K.H. 2015. p53 in survival, death and metabolic health: a lifeguard with a licence to kill. *Nature Reviews Molecular Cell Biology*. **16**(7), pp.393–405.
- Kubbutat, M.H.G., Jones, S.N. and Vousden, K.H. 1997. Regulation of p53 stability by Mdm2. *Nature*. **387**(6630), pp.299–303.
- Kukk, E., Lymboussaki, A., Taira, S., Kaipainen, A., Jeltsch, M., Joukov, V. and Alitalo, K. 1996. VEGF-C receptor binding and pattern of expression with VEGFR-3 suggests a role in lymphatic vascular development. *Development (Cambridge, England)*. **122**(12), pp.3829–37.
- Kumar, A., Kim, C.-S., Hoffman, T.A., Naqvi, A., DeRicco, J., Jung, S.-B., Lin, Z., Jain, M.K. and Irani, K. 2011. p53 Impairs Endothelial Function by Transcriptionally Repressing Kruppel-Like Factor 2. *Arteriosclerosis, Thrombosis, and Vascular Biology*. **31**(1), pp.133–141.
- Kunkel, E.J. and Ley, K. 1996. Distinct phenotype of E-selectin-deficient mice. E-selectin is required for slow leukocyte rolling in vivo. *Circulation research*. **79**(6), pp.1196–204.
- Kurokawa, K., Itoh, R.E., Yoshizaki, H., Nakamura, Y.O.T. and Matsuda, M. 2004. Coactivation of Rac1 and Cdc42 at lamellipodia and membrane ruffles induced by epidermal growth factor. *Molecular biology of the cell*. **15**(3), pp.1003–10.
- Labelle, M., Begum, S. and Hynes, R.O. 2011. Direct Signaling between Platelets and Cancer Cells Induces an Epithelial-Mesenchymal-Like Transition and Promotes Metastasis. *Cancer Cell*. **20**(5), pp.576–590.
- Lamallice, L., Houle, F. and Huot, J. 2006. Phosphorylation of Tyr<sup>1214</sup> within VEGFR-2 Triggers the Recruitment of Nck and Activation of Fyn Leading to SAPK2/p38 Activation and Endothelial Cell Migration in Response to VEGF. *Journal of Biological Chemistry*. **281**(45), pp.34009–34020.
- Lambert, A.W., Pattabiraman, D.R. and Weinberg, R.A. 2017. Emerging Biological Principles of Metastasis. *Cell*. **168**(4), pp.670–691.
- Lampugnani, M.G. 2012. Endothelial cell-to-cell junctions: adhesion and signaling in physiology and pathology. *Cold Spring Harbor perspectives in medicine*. **2**(10).
- Lampugnani, M.G., Orsenigo, F., Gagliani, M.C., Tacchetti, C. and Dejana, E. 2006. Vascular endothelial cadherin controls VEGFR-2 internalization and signaling from intracellular compartments. *The Journal of cell biology*. **174**(4), pp.593–

604.

- Lampugnani, M.G., Resnati, M., Raiteri, M., Pigott, R., Pisacane, A., Houen, G., Ruco, L.P. and Dejana, E. 1992. A novel endothelial-specific membrane protein is a marker of cell-cell contacts. *The Journal of cell biology*. **118**(6), pp.1511–22.
- Lánczky, A., Nagy, Á., Bottai, G., Munkácsy, G., Szabó, A., Santarpia, L. and Györfy, B. 2016. miRpower: a web-tool to validate survival-associated miRNAs utilizing expression data from 2178 breast cancer patients. *Breast Cancer Research and Treatment*. **160**(3), pp.439–446.
- Lane, D.P. 1992. p53, guardian of the genome. *Nature*. **358**(6381), pp.15–16.
- LANE, D.P. and CRAWFORD, L. V. 1979. T antigen is bound to a host protein in SY40-transformed cells. *Nature*. **278**(5701), pp.261–263.
- Lawrence, M.B., Kansas, G.S., Kunkel, E.J. and Ley, K. 1997. Threshold levels of fluid shear promote leukocyte adhesion through selectins (CD62L,P,E). *The Journal of cell biology*. **136**(3), pp.717–27.
- Lee, H.-J., Kim, E., Jee, B., Hahn, J.-H., Han, K., Jung, K.C., Park, S.H. and Lee, H. 2002. Functional involvement of src and focal adhesion kinase in a CD99 splice variant-induced motility of human breast cancer cells. *Experimental & molecular medicine*. **34**(3), pp.177–83.
- Lee, K.-J., Kim, Y., Yoo, Y.H., Kim, M.-S., Lee, S.-H., Kim, C.-G., Park, K., Jeoung, D., Lee, H., Ko, I.Y. and Hahn, J.-H. 2017. CD99-Derived Agonist Ligands Inhibit Fibronectin-Induced Activation of  $\beta$ 1 Integrin through the Protein Kinase A/SHP2/Extracellular Signal-Regulated Kinase/PTPN12/Focal Adhesion Kinase Signaling Pathway. *Molecular and Cellular Biology*. **37**(14).
- Lee, K.J., Yoo, Y.H., Kim, M.S., Yadav, B.K., Kim, Y., Lim, D., Hwangbo, C., Moon, K.W., Kim, D., Jeoung, D., Lee, H., Lee, J.-H. and Hahn, J.-H. 2015. CD99 inhibits CD98-mediated  $\beta$ 1 integrin signaling through SHP2-mediated FAK dephosphorylation. *Experimental Cell Research*. **336**(2), pp.211–222.
- Lee, S.-W., Kim, W.J., Choi, Y.K., Song, H.S., Son, M.J., Gelman, I.H., Kim, Y.-J. and Kim, K.-W. 2003. SSeCKS regulates angiogenesis and tight junction formation in blood-brain barrier. *Nature Medicine*. **9**(7), pp.900–906.
- Lehmann, J.M., Riethmüller, G. and Johnson, J.P. 1989. MUC18, a marker of tumor progression in human melanoma, shows sequence similarity to the neural cell adhesion molecules of the immunoglobulin superfamily. *Proceedings of the National Academy of Sciences of the United States of America*. **86**(24), pp.9891–5.
- Lerosey, I., Pizon, V., Tavitian, A. and de Gunzburg, J. 1991. The cAMP-dependent protein kinase phosphorylates the rap1 protein in vitro as well as in intact fibroblasts, but not the closely related rap2 protein. *Biochemical and Biophysical Research Communications*. **175**(2), pp.430–436.
- Leung, T., Chen, X.Q., Manser, E. and Lim, L. 1996. The p160 RhoA-binding kinase ROK alpha is a member of a kinase family and is involved in the reorganization of the cytoskeleton. *Molecular and cellular biology*. **16**(10), pp.5313–27.
- Levine, A.J. 2009. The common mechanisms of transformation by the small DNA tumor viruses: The inactivation of tumor suppressor gene products: p53. *Virology*. **384**(2), pp.285–293.
- Ley, K., Laudanna, C., Cybulsky, M.I. and Nourshargh, S. 2007. Getting to the site of inflammation: the leukocyte adhesion cascade updated. *Nature Reviews Immunology*. **7**(9), pp.678–689.
- Li, B., Zhao, W.-D., Tan, Z.-M., Fang, W.-G., Zhu, L. and Chen, Y.-H. 2006. Involvement of Rho/ROCK signalling in small cell lung cancer migration through human brain microvascular endothelial cells. *FEBS Letters*. **580**(17), pp.4252–4260.
- Liao, F., Huynh, H.K., Eiroa, A., Greene, T., Polizzi, E. and Muller, W.A. 1995. Migration of monocytes across endothelium and passage through extracellular

- matrix involve separate molecular domains of PECAM-1. *The Journal of experimental medicine*. **182**(5), pp.1337–43.
- Lilyestrom, W., Klein, M.G., Zhang, R., Joachimiak, A. and Chen, X.S. 2006. Crystal structure of SV40 large T-antigen bound to p53: interplay between a viral oncoprotein and a cellular tumor suppressor. *Genes & Development*. **20**(17), p.2373.
- Linzer, D.I.H. and Levine, A.J. 1979. Characterization of a 54K Dalton cellular SV40 tumor antigen present in SV40-transformed cells and uninfected embryonal carcinoma cells. *Cell*. **17**(1), pp.43–52.
- Liu, N., Ding, D., Hao, W., Yang, F., Wu, X., Wang, M., Xu, X., Ju, Z., Liu, J.-P., Song, Z., Shay, J.W., Guo, Y. and Cong, Y.-S. 2016. hTERT promotes tumor angiogenesis by activating VEGF via interactions with the Sp1 transcription factor. *Nucleic Acids Research*. **44**(18), pp.8693–8703.
- Liu, Y., Elf, S.E., Miyata, Y., Sashida, G., Liu, Y., Huang, G., Di Giandomenico, S., Lee, J.M., Deblasio, A., Menendez, S., Antipin, J., Reva, B., Koff, A. and Nimer, S.D. 2009. p53 regulates hematopoietic stem cell quiescence. *Cell stem cell*. **4**(1), pp.37–48.
- Livak, K.J. and Schmittgen, T.D. 2001. Analysis of Relative Gene Expression Data Using Real-Time Quantitative PCR and the 2- $\Delta\Delta$ CT Method. *Methods*. **25**(4), pp.402–408.
- Llombart-Bosch, A., Machado, I., Navarro, S., Bertoni, F., Bacchini, P., Alberghini, M., Karzeladze, A., Savelov, N., Petrov, S., Alvarado-Cabrero, I., Mihaila, D., Terrier, P., Lopez-Guerrero, J.A. and Picci, P. 2009. Histological heterogeneity of Ewing's sarcoma/PNET: an immunohistochemical analysis of 415 genetically confirmed cases with clinical support. *Virchows Archiv*. **455**(5), pp.397–411.
- Lorger, M. and Felding-Habermann, B. 2010. Capturing changes in the brain microenvironment during initial steps of breast cancer brain metastasis. *The American journal of pathology*. **176**(6), pp.2958–71.
- Lou, O., Alcaide, P., Luscinskas, F.W. and Muller, W.A. 2007. CD99 is a key mediator of the transendothelial migration of neutrophils. *Journal of immunology (Baltimore, Md. : 1950)*. **178**(2), pp.1136–43.
- Ludes-Meyers, J.H., Subler, M.A., Shivakumar, C. V, Munoz, R.M., Jiang, P., Bigger, J.E., Brown, D.R., Deb, S.P. and Deb, S. 1996. Transcriptional activation of the human epidermal growth factor receptor promoter by human p53. *Molecular and cellular biology*. **16**(11), pp.6009–19.
- Luissint, A.-C., Federici, C., Guillonneau, F., Chrétien, F., Camoin, L., Glacial, F., Ganeshamoorthy, K. and Couraud, P.-O. 2012. Guanine nucleotide-binding protein Gai2: a new partner of claudin-5 that regulates tight junction integrity in human brain endothelial cells. *Journal of cerebral blood flow and metabolism : official journal of the International Society of Cerebral Blood Flow and Metabolism*. **32**(5), pp.860–73.
- Ma, L., Rohatgi, R. and Kirschner, M.W. 1998. The Arp2/3 complex mediates actin polymerization induced by the small GTP-binding protein Cdc42. *Proceedings of the National Academy of Sciences of the United States of America*. **95**(26), pp.15362–7.
- Machesky, L.M. and Insall, R.H. 1998. Scar1 and the related Wiskott-Aldrich syndrome protein, WASP, regulate the actin cytoskeleton through the Arp2/3 complex. *Current biology : CB*. **8**(25), pp.1347–56.
- Madsen, C.D. and Sahai, E. 2010. Cancer dissemination--lessons from leukocytes. *Developmental cell*. **19**(1), pp.13–26.
- Makinen, T., Veikkola, T., Mustjoki, S., Karpanen, T., Catimel, B., Nice, E.C., Wise, L., Mercer, A., Kowalski, H., Kerjaschki, D., Stacker, S.A., Achen, M.G. and Alitalo, K. 2001. Isolated lymphatic endothelial cells transduce growth, survival

- and migratory signals via the VEGF-C/D receptor VEGFR-3. *The EMBO Journal*. **20**(17), pp.4762–4773.
- Mamdouh, Z., Mikhailov, A. and Muller, W.A. 2009. Transcellular migration of leukocytes is mediated by the endothelial lateral border recycling compartment. *The Journal of Experimental Medicine*. **206**(12), pp.2795–2808.
- Manara, M.C., Pasello, M. and Scotlandi, K. 2018. CD99: A Cell Surface Protein with an Oncojanus Role in Tumors. *Genes*. **9**(3), p.159.
- Manara, M.C., Terracciano, M., Mancarella, C., Sciandra, M., Guerzoni, C., Pasello, M., Grilli, A., Zini, N., Picci, P., Colombo, M.P., Morrione, A., Scotlandi, K., Manara, M.C., Terracciano, M., Mancarella, C., Sciandra, M., Guerzoni, C., Pasello, M., Grilli, A., Zini, N., Picci, P., Colombo, M.P., Morrione, A. and Scotlandi, K. 2016. CD99 triggering induces methuosis of Ewing sarcoma cells through IGF-1R/RAS/Rac1 signaling. *Oncotarget*. **7**(48), pp.79925–79942.
- Mani, S.A., Guo, W., Liao, M.-J., Eaton, E.N., Ayyanan, A., Zhou, A.Y., Brooks, M., Reinhard, F., Zhang, C.C., Shipitsin, M., Campbell, L.L., Polyak, K., Brisken, C., Yang, J. and Weinberg, R.A. 2008. The Epithelial-Mesenchymal Transition Generates Cells with Properties of Stem Cells. *Cell*. **133**(4), pp.704–715.
- Mansour, A.A., Gonçalves, J.T., Bloyd, C.W., Li, H., Fernandes, S., Quang, D., Johnston, S., Parylak, S.L., Jin, X. and Gage, F.H. 2018. An in vivo model of functional and vascularized human brain organoids. *Nature Biotechnology*. **36**(5), pp.432–441.
- Masson-Gadais, B., Houle, F., Laferrière, J. and Huot, J. 2003. Integrin alphavbeta3, requirement for VEGFR2-mediated activation of SAPK2/p38 and for Hsp90-dependent phosphorylation of focal adhesion kinase in endothelial cells activated by VEGF. *Cell stress & chaperones*. **8**(1), pp.37–52.
- McCull, B.K., Baldwin, M.E., Roufail, S., Freeman, C., Moritz, R.L., Simpson, R.J., Alitalo, K., Stacker, S.A. and Achen, M.G. 2003. Plasmin activates the lymphangiogenic growth factors VEGF-C and VEGF-D. *The Journal of experimental medicine*. **198**(6), pp.863–8.
- McFarlane, S., Coulter, J.A., Tibbits, P., O'Grady, A., McFarlane, C., Montgomery, N., Hill, A., McCarthy, H.O., Young, L.S., Kay, E.W., Isacke, C.M. and Waugh, D.J.J. 2015. CD44 increases the efficiency of distant metastasis of breast cancer. *Oncotarget*. **6**(13), pp.11465–76.
- Meadows, K.N., Bryant, P. and Pumiglia, K. 2001. Vascular Endothelial Growth Factor Induction of the Angiogenic Phenotype Requires Ras Activation. *Journal of Biological Chemistry*. **276**(52), pp.49289–49298.
- Meadows, S.M., Salanga, M.C. and Krieg, P.A. 2009. Kruppel-like factor 2 cooperates with the ETS family protein ERG to activate Flk1 expression during vascular development. *Development*. **136**(7), pp.1115–1125.
- Melnikova, V.O., Balasubramanian, K., Villares, G.J., Dobroff, A.S., Zigler, M., Wang, H., Petersson, F., Price, J.E., Schroit, A., Prieto, V.G., Hung, M.-C. and Bar-Eli, M. 2009. Crosstalk between protease-activated receptor 1 and platelet-activating factor receptor regulates melanoma cell adhesion molecule (MCAM/MUC18) expression and melanoma metastasis. *The Journal of biological chemistry*. **284**(42), pp.28845–55.
- Mercer, J. and Bennett, M. 2006. The Role of p53 in Atherosclerosis. *Cell Cycle*. **5**(17), pp.1907–1909.
- Miki, H., Miura, K. and Takenawa, T. 1996. N-WASP, a novel actin-depolymerizing protein, regulates the cortical cytoskeletal rearrangement in a PIP2-dependent manner downstream of tyrosine kinases. *The EMBO journal*. **15**(19), pp.5326–35.
- Miki, H., Sasaki, T., Takai, Y. and Takenawa, T. 1998. Induction of filopodium formation by a WASP-related actin-depolymerizing protein N-WASP. *Nature*. **391**(6662), pp.93–96.
- Milanezi, F., Pereira, E.M., Ferreira, F. V, Leitão, D. and Schmitt, F.C. 2001. CD99/MIC-2 surface protein expression in breast carcinomas. *Histopathology*.

**39**(6), pp.578–83.

- Millauer, B., Wizigmann-Voos, S., Schnürch, H., Martinez, R., Møller, N.P., Risau, W. and Ullrich, A. 1993. High affinity VEGF binding and developmental expression suggest Flk-1 as a major regulator of vasculogenesis and angiogenesis. *Cell*. **72**(6), pp.835–46.
- Minamino, T. and Komuro, I. 2007. Vascular Cell Senescence. *Circulation Research*. **100**(1), pp.15–26.
- Minn, A.J., Gupta, G.P., Siegel, P.M., Bos, P.D., Shu, W., Giri, D.D., Viale, A., Olshen, A.B., Gerald, W.L. and Massagué, J. 2005. Genes that mediate breast cancer metastasis to lung. *Nature*. **436**(7050), pp.518–524.
- Mishra, R., Thorat, D., Soundararajan, G., Pradhan, S.J., Chakraborty, G., Lohite, K., Karnik, S. and Kundu, G.C. 2015a. Semaphorin 3A upregulates FOXO 3a-dependent MelCAM expression leading to attenuation of breast tumor growth and angiogenesis. *Oncogene*. **34**(12), pp.1584–1595.
- Mishra, R., Thorat, D., Soundararajan, G., Pradhan, S.J., Chakraborty, G., Lohite, K., Karnik, S. and Kundu, G.C. 2015b. Semaphorin 3A upregulates FOXO 3a-dependent MelCAM expression leading to attenuation of breast tumor growth and angiogenesis. *Oncogene*. **34**(12), pp.1584–1595.
- Miyauchi, H., Minamino, T., Tateno, K., Kunieda, T., Toko, H. and Komuro, I. 2004. Akt negatively regulates the in vitro lifespan of human endothelial cells via a p53/p21-dependent pathway. *The EMBO journal*. **23**(1), pp.212–20.
- Mochida, G.H., Ganesh, V.S., Felie, J.M., Gleason, D., Hill, R.S., Clapham, K.R., Rakiec, D., Tan, W.-H., Akawi, N., Al-Saffar, M., Partlow, J.N., Tinschert, S., Barkovich, A.J., Ali, B., Al-Gazali, L. and Walsh, C.A. 2010. A Homozygous Mutation in the Tight-Junction Protein JAM3 Causes Hemorrhagic Destruction of the Brain, Subependymal Calcification, and Congenital Cataracts. *The American Journal of Human Genetics*. **87**(6), pp.882–889.
- Montagne, A., Zhao, Z. and Zlokovic, B. V 2017. Alzheimer's disease: A matter of blood-brain barrier dysfunction? *The Journal of experimental medicine*. **214**(11), pp.3151–3169.
- Morita, K., Sasaki, H., Furuse, M. and Tsukita, S. 1999. Endothelial claudin: claudin-5/TMVCF constitutes tight junction strands in endothelial cells. *The Journal of cell biology*. **147**(1), pp.185–94.
- Moriya, J., Minamino, T., Tateno, K., Okada, S., Uemura, A., Shimizu, I., Yokoyama, M., Nojima, A., Okada, M., Koga, H. and Komuro, I. 2010. Inhibition of Semaphorin As a Novel Strategy for Therapeutic Angiogenesis. *Circulation Research*. **106**(2), pp.391–398.
- Muller, W.A. 1995. The role of PECAM-1 (CD31) in leukocyte emigration: studies in vitro and in vivo. *Journal of leukocyte biology*. **57**(4), pp.523–8.
- Muller, W.A., Weigl, S.A., Deng, X. and Phillips, D.M. 1993. PECAM-1 is required for transendothelial migration of leukocytes. *The Journal of experimental medicine*. **178**(2), pp.449–60.
- Nakamura, F. and Goshima, Y. 2013. Structural and Functional Relation of Neuropilins.
- Nath, S. and Mukherjee, P. 2014. MUC1: a multifaceted oncoprotein with a key role in cancer progression. *Trends in molecular medicine*. **20**(6), pp.332–42.
- Nayak, L., Lee, E.Q. and Wen, P.Y. 2012. Epidemiology of Brain Metastases. *Current Oncology Reports*. **14**(1), pp.48–54.
- Nayak, L., Lin, Z. and Jain, M.K. 2011. "Go with the flow": how Krüppel-like factor 2 regulates the vasoprotective effects of shear stress. *Antioxidants & redox signaling*. **15**(5), pp.1449–61.
- Nelson, W.J. and Nusse, R. 2004. Convergence of Wnt, beta-catenin, and cadherin pathways. *Science (New York, N.Y.)*. **303**(5663), pp.1483–7.
- Nieswandt, B., Hafner, M., Echtenacher, B. and Männel, D.N. 1999. Lysis of tumor cells by natural killer cells in mice is impeded by platelets. *Cancer research*. **59**(6), pp.1295–300.

- Nitta, T., Hata, M., Gotoh, S., Seo, Y., Sasaki, H., Hashimoto, N., Furuse, M. and Tsukita, S. 2003. Size-selective loosening of the blood-brain barrier in claudin-5-deficient mice. *The Journal of Cell Biology*. **161**(3), pp.653–660.
- O'Driscoll, M.C., Daly, S.B., Urquhart, J.E., Black, G.C.M., Pilz, D.T., Brockmann, K., McEntagart, M., Abdel-Salam, G., Zaki, M., Wolf, N.I., Ladda, R.L., Sell, S., D'Arrigo, S., Squier, W., Dobyns, W.B., Livingston, J.H. and Crow, Y.J. 2010. Recessive Mutations in the Gene Encoding the Tight Junction Protein Occludin Cause Band-like Calcification with Simplified Gyration and Polymicrogyria. *The American Journal of Human Genetics*. **87**(3), pp.354–364.
- Ocaña, O.H., Córcoles, R., Fabra, Á., Moreno-Bueno, G., Acloque, H., Vega, S., Barrallo-Gimeno, A., Cano, A. and Nieto, M.A. 2012. Metastatic Colonization Requires the Repression of the Epithelial-Mesenchymal Transition Inducer Prrx1. *Cancer Cell*. **22**(6), pp.709–724.
- Ohtsuki, S., Ikeda, C., Uchida, Y., Sakamoto, Y., Miller, F., Glacial, F., Declèves, X., Scherrmann, J.-M., Couraud, P.-O., Kubo, Y., Tachikawa, M. and Terasaki, T. 2013a. Quantitative Targeted Absolute Proteomic Analysis of Transporters, Receptors and Junction Proteins for Validation of Human Cerebral Microvascular Endothelial Cell Line hCMEC/D3 as a Human Blood–Brain Barrier Model. *Molecular Pharmaceutics*. **10**(1), pp.289–296.
- Ohtsuki, S., Ikeda, C., Uchida, Y., Sakamoto, Y., Miller, F., Glacial, F., Declèves, X., Scherrmann, J.-M., Couraud, P.-O., Kubo, Y., Tachikawa, M. and Terasaki, T. 2013b. Quantitative Targeted Absolute Proteomic Analysis of Transporters, Receptors and Junction Proteins for Validation of Human Cerebral Microvascular Endothelial Cell Line hCMEC/D3 as a Human Blood–Brain Barrier Model. *Molecular Pharmaceutics*. **10**(1), pp.289–296.
- Oka, S., Uramoto, H., Chikaishi, Y. and Tanaka, F. 2012. The expression of CD146 predicts a poor overall survival in patients with adenocarcinoma of the lung. *Anticancer research*. **32**(3), pp.861–4.
- Olivier, M., Eeles, R., Hollstein, M., Khan, M.A., Harris, C.C. and Hainaut, P. 2002. The IARC TP53 database: New online mutation analysis and recommendations to users. *Human Mutation*. **19**(6), pp.607–614.
- Olson, M.F. and Sahai, E. 2009. The actin cytoskeleton in cancer cell motility. *Clinical & Experimental Metastasis*. **26**(4), pp.273–287.
- Olsson, A.-K., Dimberg, A., Kreuger, J. and Claesson-Welsh, L. 2006. VEGF receptor signalling ? in control of vascular function. *Nature Reviews Molecular Cell Biology*. **7**(5), pp.359–371.
- Onken, M.D., Li, J. and Cooper, J.A. 2014. Uveal Melanoma Cells Utilize a Novel Route for Transendothelial Migration A. T. Slominski, ed. *PLoS ONE*. **9**(12), p.e115472.
- Osaki, T., Sivathanu, V. and Kamm, R.D. 2018. Vascularized microfluidic organ-chips for drug screening, disease models and tissue engineering. *Current Opinion in Biotechnology*. **52**, pp.116–123.
- Osawa, M., Masuda, M., Kusano, K. and Fujiwara, K. 2002. Evidence for a role of platelet endothelial cell adhesion molecule-1 in endothelial cell mechanosignal transduction. *The Journal of Cell Biology*. **158**(4), pp.773–785.
- Osta, W.A., Chen, Y., Mikhitarian, K., Mitas, M., Salem, M., Hannun, Y.A., Cole, D.J. and Gillanders, W.E. 2004. EpCAM Is Overexpressed in Breast Cancer and Is a Potential Target for Breast Cancer Gene Therapy. *Cancer Research*. **64**(16), pp.5818–5824.
- Ouhtit, A., Abdraboh, M.E., Hollenbach, A.D., Zayed, H. and Raj, M.H.G. 2017. CD146, a novel target of CD44-signaling, suppresses breast tumor cell invasion. *Cell communication and signaling : CCS*. **15**(1), p.45.
- Padua, D., Zhang, X.H.-F., Wang, Q., Nadal, C., Gerald, W.L., Gomis, R.R. and Massagué, J. 2008. TGFbeta primes breast tumors for lung metastasis seeding through angiopoietin-like 4. *Cell*. **133**(1), pp.66–77.
- Paget, S. 1889. THE DISTRIBUTION OF SECONDARY GROWTHS IN CANCER

- OF THE BREAST. *The Lancet*. **133**(3421), pp.571–573.
- Paku, S., Döme, B., Tóth, R. and Timár, J. 2000. Organ-specificity of the extravasation process: an ultrastructural study. *Clinical & experimental metastasis*. **18**(6), pp.481–92.
- Pal, S., Datta, K. and Mukhopadhyay, D. 2001. Central Role of p53 on Regulation of Vascular Permeability Factor/Vascular Endothelial Growth Factor (VPF/VEGF) Expression in Mammary Carcinoma. *Cancer Research*. **61**(18), pp.6952–6957.
- Palmieri, D., Bronder, J.L., Herring, J.M., Yoneda, T., Weil, R.J., Stark, A.M., Kurek, R., Vega-Valle, E., Feigenbaum, L., Halverson, D., Vortmeyer, A.O., Steinberg, S.M., Aldape, K. and Steeg, P.S. 2007. Her-2 overexpression increases the metastatic outgrowth of breast cancer cells in the brain. *Cancer research*. **67**(9), pp.4190–8.
- Pardridge, W.M. 2005. The blood-brain barrier: bottleneck in brain drug development. *NeuroRx: the journal of the American Society for Experimental NeuroTherapeutics*. **2**(1), pp.3–14.
- Park, H.J., Ban, Y.L., Byun, D., Park, S.H. and Jung, K.C. 2010. Interaction between the mouse homologue of CD99 and its ligand PILR as a mechanism of T cell receptor-independent thymocyte apoptosis. *Experimental and Molecular Medicine*. **42**(5), p.353.
- Park, S.H., Shin, Y.K., Suh, Y.H., Park, W.S., Ban, Y.L., Choi, H.-S., Park, H.J. and Jung, K.C. 2005. Rapid divergency of rodent CD99 orthologs: Implications for the evolution of the pseudoautosomal region. *Gene*. **353**(2), pp.177–188.
- Parsons, J.T., Horwitz, A.R. and Schwartz, M.A. 2010. Cell adhesion: integrating cytoskeletal dynamics and cellular tension. *Nature reviews. Molecular cell biology*. **11**(9), pp.633–43.
- Paterson, H.F., Self, A.J., Garrett, M.D., Just, I., Aktories, K. and Hall, A. 1990. Microinjection of recombinant p21rho induces rapid changes in cell morphology. *The Journal of cell biology*. **111**(3), pp.1001–7.
- Pfister, N.T., Fomin, V., Regunath, K., Zhou, J.Y., Zhou, W., Silwal-Pandit, L., Freed-Pastor, W.A., Laptenko, O., Neo, S.P., Bargonetti, J., Hoque, M., Tian, B., Gunaratne, J., Engebraaten, O., Manley, J.L., Børresen-Dale, A.-L., Neilsen, P.M. and Prives, C. 2015. Mutant p53 cooperates with the SWI/SNF chromatin remodeling complex to regulate *VEGFR2* in breast cancer cells. *Genes & Development*. **29**(12), pp.1298–1315.
- Piali, L., Hammel, P., Uherek, C., Bachmann, F., Gisler, R.H., Dunon, D. and Imhof, B.A. 1995. CD31/PECAM-1 is a ligand for alpha v beta 3 integrin involved in adhesion of leukocytes to endothelium. *The Journal of cell biology*. **130**(2), pp.451–60.
- Piera-Velazquez, S., Li, Z. and Jimenez, S.A. 2011. Role of endothelial-mesenchymal transition (EndoMT) in the pathogenesis of fibrotic disorders. *The American journal of pathology*. **179**(3), pp.1074–80.
- Plein, A., Fantin, A., Denti, L., Pollard, J.W. and Ruhrberg, C. 2018. Erythromyeloid progenitors contribute endothelial cells to blood vessels. *Nature*. **562**(7726), pp.223–228.
- Pliyev, B.K., Shepelev, A. V. and Ivanova, A. V. 2013. Role of the adhesion molecule CD99 in platelet-neutrophil interactions. *European Journal of Haematology*. **91**(5), pp.456–461.
- Plouët, J., Schilling, J. and Gospodarowicz, D. 1989. Isolation and characterization of a newly identified endothelial cell mitogen produced by AtT-20 cells. *The EMBO journal*. **8**(12), pp.3801–6.
- Potente, M., Gerhardt, H. and Carmeliet, P. 2011. Basic and therapeutic aspects of angiogenesis. *Cell*. **146**(6), pp.873–87.
- Prahst, C., Héroult, M., Lanahan, A.A., Uziel, N., Kessler, O., Shraga-Heled, N., Simons, M., Neufeld, G. and Augustin, H.G. 2008. Neuropilin-1-VEGFR-2 Complexing Requires the PDZ-binding Domain of Neuropilin-1. *Journal of*

- Biological Chemistry*. **283**(37), pp.25110–25114.
- Prasad, V.V. and Gopalan, R.O. 2015. Continued use of MDA-MB-435, a melanoma cell line, as a model for human breast cancer, even in year, 2014. *npj Breast Cancer*. **1**(1), p.15002.
- Presta, M., Dell’Era, P., Mitola, S., Moroni, E., Ronca, R. and Rusnati, M. 2005. Fibroblast growth factor/fibroblast growth factor receptor system in angiogenesis. *Cytokine & Growth Factor Reviews*. **16**(2), pp.159–178.
- Public Health England 2014. Cancer outcome metrics.
- Quail, D.F. and Joyce, J.A. 2013. Microenvironmental regulation of tumor progression and metastasis. *Nature medicine*. **19**(11), pp.1423–37.
- Rakha, E.A., El-Sayed, M.E., Green, A.R., Lee, A.H.S., Robertson, J.F. and Ellis, I.O. 2007. Prognostic markers in triple-negative breast cancer. *Cancer*. **109**(1), pp.25–32.
- Ramchandran, R., Mehta, D., Vogel, S.M., Mirza, M.K., Kouklis, P. and Malik, A.B. 2008. Critical role of Cdc42 in mediating endothelial barrier protection in vivo. *American journal of physiology. Lung cellular and molecular physiology*. **295**(2), pp.L363-9.
- Rane, C.K. and Minden, A. 2014. P21 activated kinases: structure, regulation, and functions. *Small GTPases*. **5**.
- Ravi, R., Mookerjee, B., Bhujwalla, Z.M., Sutter, C.H., Artemov, D., Zeng, Q., Dillehay, L.E., Madan, A., Semenza, G.L. and Bedi, A. 2000. Regulation of tumor angiogenesis by p53-induced degradation of hypoxia-inducible factor 1 $\alpha$ . *Genes & development*. **14**(1), pp.34–44.
- Regimbald, L.H., Pilarski, L.M., Longenecker, B.M., Reddish, M.A., Zimmermann, G. and Hugh, J.C. 1996. The Breast Mucin MUC1 as a Novel Adhesion Ligand for Endothelial Intercellular Adhesion Molecule 1 in Breast Cancer. *Cancer Research*. **56**(18), pp.4244–4249.
- Reymond, N., d’Água, B.B. and Ridley, A.J. 2013a. Crossing the endothelial barrier during metastasis. *Nature Reviews Cancer*. **13**(12), pp.858–870.
- Reymond, N., d’Água, B.B. and Ridley, A.J. 2013b. Crossing the endothelial barrier during metastasis. *Nature Reviews Cancer*. **13**(12), pp.858–870.
- Reymond, N., Im, J.H., Garg, R., Vega, F.M., Borda d’Água, B., Riou, P., Cox, S., Valderrama, F., Muschel, R.J. and Ridley, A.J. 2012. Cdc42 promotes transendothelial migration of cancer cells through  $\beta$ 1 integrin. *The Journal of cell biology*. **199**(4), pp.653–68.
- Reymond, N., Imbert, A.-M., Devilard, E., Fabre, S., Chabannon, C., Xerri, L., Farnarier, C., Cantoni, C., Bottino, C., Moretta, A., Dubreuil, P. and Lopez, M. 2004. DNAM-1 and PVR Regulate Monocyte Migration through Endothelial Junctions. *The Journal of Experimental Medicine*. **199**(10), pp.1331–1341.
- Rezaei, M., Cao, J., Friedrich, K., Kemper, B., Brendel, O., Grosser, M., Adrian, M., Baretton, G., Breier, G. and Schnittler, H.-J. 2018. The expression of VE-cadherin in breast cancer cells modulates cell dynamics as a function of tumor differentiation and promotes tumor–endothelial cell interactions. *Histochemistry and Cell Biology*. **149**(1), pp.15–30.
- Ridley, A.J. 2001. Rho family proteins: coordinating cell responses. *Trends in cell biology*. **11**(12), pp.471–7.
- Ridley, A.J. 2015. Rho GTPase signalling in cell migration. *Current opinion in cell biology*. **36**, pp.103–12.
- Ridley, A.J., Paterson, H.F., Johnston, C.L., Diekmann, D. and Hall, A. 1992. The small GTP-binding protein rac regulates growth factor-induced membrane ruffling. *Cell*. **70**(3), pp.401–10.
- Rohatgi, R., Ma, L., Miki, H., Lopez, M., Kirchhausen, T., Takenawa, T. and Kirschner, M.W. 1999. The Interaction between N-WASP and the Arp2/3 Complex Links Cdc42-Dependent Signals to Actin Assembly. *Cell*. **97**(2), pp.221–231.
- Rojas, A.M., Fuentes, G., Rausell, A. and Valencia, A. 2012. The Ras protein

- superfamily: evolutionary tree and role of conserved amino acids. *The Journal of cell biology*. **196**(2), pp.189–201.
- Rosso, A., Balsamo, A., Gambino, R., Dentelli, P., Falcioni, R., Cassader, M., Pegoraro, L., Pagano, G. and Brizzi, M.F. 2006. p53 Mediates the accelerated onset of senescence of endothelial progenitor cells in diabetes. *The Journal of biological chemistry*. **281**(7), pp.4339–47.
- Rubin, L.L. and Staddon, J.M. 1999. THE CELL BIOLOGY OF THE BLOOD-BRAIN BARRIER. *Annual Review of Neuroscience*. **22**(1), pp.11–28.
- Saitou, M., Furuse, M., Sasaki, H., Schulzke, J.D., Fromm, M., Takano, H., Noda, T. and Tsukita, S. 2000. Complex phenotype of mice lacking occludin, a component of tight junction strands. W. J. Nelson, ed. *Molecular biology of the cell*. **11**(12), pp.4131–42.
- Sakurai, A., Doçi, C.L., Doci, C. and Gutkind, J.S. 2012. Semaphorin signaling in angiogenesis, lymphangiogenesis and cancer. *Cell research*. **22**(1), pp.23–32.
- Sakurai, Y., Ohgimoto, K., Kataoka, Y., Yoshida, N. and Shibuya, M. 2005. Essential role of Flk-1 (VEGF receptor 2) tyrosine residue 1173 in vasculogenesis in mice. *Proceedings of the National Academy of Sciences*. **102**(4), pp.1076–1081.
- Sano, M., Minamino, T., Toko, H., Miyauchi, H., Orimo, M., Qin, Y., Akazawa, H., Tateno, K., Kayama, Y., Harada, M., Shimizu, I., Asahara, T., Hamada, H., Tomita, S., Molkentin, J.D., Zou, Y. and Komuro, I. 2007. p53-induced inhibition of Hif-1 causes cardiac dysfunction during pressure overload. *Nature*. **446**(7134), pp.444–448.
- Saunders, A., Macosko, E.Z., Wysoker, A., Goldman, M., Krienen, F.M., de Rivera, H., Bien, E., Baum, M., Bortolin, L., Wang, S., Goeva, A., Nemes, J., Kamitaki, N., Brumbaugh, S., Kulp, D. and McCarroll, S.A. 2018. Molecular Diversity and Specializations among the Cells of the Adult Mouse Brain. *Cell*. **174**(4), p.1015–1030.e16.
- Schenkel, A.R., Mamdouh, Z., Chen, X., Liebman, R.M. and Muller, W.A. 2002. CD99 plays a major role in the migration of monocytes through endothelial junctions. *Nature Immunology*. **3**(2), pp.143–150.
- Schlesinger, M. and Bendas, G. 2015. Vascular cell adhesion molecule-1 (VCAM-1)-An increasing insight into its role in tumorigenicity and metastasis. *International Journal of Cancer*. **136**(11), pp.2504–2514.
- Secchiero, P., Corallini, F., Gonelli, A., Dell'Eva, R., Vitale, M., Capitani, S., Albin, A. and Zauli, G. 2007. Antiangiogenic Activity of the MDM2 Antagonist Nutlin-3. *Circulation Research*. **100**(1), pp.61–69.
- Senger, D.R., Galli, S.J., Dvorak, A.M., Perruzzi, C.A., Harvey, V.S. and Dvorak, H.F. 1983. Tumor cells secrete a vascular permeability factor that promotes accumulation of ascites fluid. *Science (New York, N.Y.)*. **219**(4587), pp.983–5.
- Seol, H.J., Chang, J.H., Yamamoto, J., Romagnuolo, R., Suh, Y., Weeks, A., Agnihotri, S., Smith, C.A. and Rutka, J.T. 2012. Overexpression of CD99 Increases the Migration and Invasiveness of Human Malignant Glioma Cells. *Genes & Cancer*. **3**(9–10), pp.535–549.
- Shalaby, F., Rossant, J., Yamaguchi, T.P., Gertsenstein, M., Wu, X.-F., Breitman, M.L. and Schuh, A.C. 1995. Failure of blood-island formation and vasculogenesis in Flk-1-deficient mice. *Nature*. **376**(6535), pp.62–66.
- Sheldon, H., Heikamp, E., Turley, H., Dragovic, R., Thomas, P., Oon, C.E., Leek, R., Edelmann, M., Kessler, B., Sainson, R.C.A., Sargent, I., Li, J.-L. and Harris, A.L. 2010. New mechanism for Notch signaling to endothelium at a distance by Delta-like 4 incorporation into exosomes. *Blood*. **116**(13), pp.2385–2394.
- Shen, B., Delaney, M.K. and Du, X. 2012. Inside-out, outside-in, and inside-outside-in: G protein signaling in integrin-mediated cell adhesion, spreading, and retraction. *Current opinion in cell biology*. **24**(5), pp.600–6.
- Shibuya, M., Yamaguchi, S., Yamane, A., Ikeda, T., Tojo, A., Matsushima, H. and

- Sato, M. 1990. Nucleotide sequence and expression of a novel human receptor-type tyrosine kinase gene (flt) closely related to the fms family. *Oncogene*. **5**(4), pp.519–24.
- Shieh, S.Y., Ahn, J., Tamai, K., Taya, Y. and Prives, C. 2000. The human homologs of checkpoint kinases Chk1 and Cds1 (Chk2) phosphorylate p53 at multiple DNA damage-inducible sites. *Genes & development*. **14**(3), pp.289–300.
- Shih, L.M., Hsu, M.Y., Palazzo, J.P. and Herlyn, M. 1997. The cell-cell adhesion receptor Mel-CAM acts as a tumor suppressor in breast carcinoma. *The American journal of pathology*. **151**(3), pp.745–51.
- Shinkai, A., Ito, M., Anazawa, H., Yamaguchi, S., Shitara, K. and Shibuya, M. 1998. Mapping of the sites involved in ligand association and dissociation at the extracellular domain of the kinase insert domain-containing receptor for vascular endothelial growth factor. *The Journal of biological chemistry*. **273**(47), pp.31283–8.
- Shiomi, T. and Okada, Y. 2003. MT1-MMP and MMP-7 in invasion and metastasis of human cancers. *Cancer and Metastasis Reviews*. **22**(2/3), pp.145–152.
- Shweiki, D., Itin, A., Soffer, D. and Keshet, E. 1992. Vascular endothelial growth factor induced by hypoxia may mediate hypoxia-initiated angiogenesis. *Nature*. **359**(6398), pp.843–845.
- Siemerink, M.J., Klaassen, I., Vogels, I.M.C., Griffioen, A.W., Van Noorden, C.J.F. and Schlingemann, R.O. 2012. CD34 marks angiogenic tip cells in human vascular endothelial cell cultures. *Angiogenesis*. **15**(1), pp.151–163.
- Smith, M.J., Goodfellow, P.J. and Goodfellow, P.N. 1993. The genomic organisation of the human pseudoautosomal gene *MIC2* and the detection of a related locus. *Human Molecular Genetics*. **2**(4), pp.417–422.
- Sohn, H.W., Shin, Y.K., Lee, I.S., Bae, Y.M., Suh, Y.H., Kim, M.K., Kim, T.J., Jung, K.C., Park, W.S., Park, C.S., Chung, D.H., Ahn, K., Kim, I.S., Ko, Y.H., Bang, Y.J., Kim, C.W. and Park, S.H. 2001. CD99 regulates the transport of MHC class I molecules from the Golgi complex to the cell surface. *Journal of immunology (Baltimore, Md. : 1950)*. **166**(2), pp.787–94.
- Soker, S., Takashima, S., Miao, H.Q., Neufeld, G. and Klagsbrun, M. 1998. Neuropilin-1 is expressed by endothelial and tumor cells as an isoform-specific receptor for vascular endothelial growth factor. *Cell*. **92**(6), pp.735–45.
- Soldi, R., Mitola, S., Strasly, M., Defilippi, P., Tarone, G. and Bussolino, F. 1999. Role of  $\alpha\beta 3$  integrin in the activation of vascular endothelial growth factor receptor-2. *The EMBO Journal*. **18**(4), pp.882–892.
- Sosa, M.S., Bragado, P. and Aguirre-Ghiso, J.A. 2014. Mechanisms of disseminated cancer cell dormancy: an awakening field. *Nature Reviews Cancer*. **14**(9), pp.611–622.
- Soule, H.D., Vazquez, J., Long, A., Albert, S. and Brennan, M. 1973. A human cell line from a pleural effusion derived from a breast carcinoma. *Journal of the National Cancer Institute*. **51**(5), pp.1409–16.
- St Hill, C.A. 2011. Interactions between endothelial selectins and cancer cells regulate metastasis. *Frontiers in bioscience (Landmark edition)*. **16**, pp.3233–51.
- Staehelin, L.A. 1974. Structure and function of intercellular junctions. *International review of cytology*. **39**, pp.191–283.
- Stengel, K. and Zheng, Y. 2011. Cdc42 in oncogenic transformation, invasion, and tumorigenesis. *Cellular Signalling*. **23**(9), pp.1415–1423.
- Stoletov, K., Kato, H., Zardoujian, E., Kelber, J., Yang, J., Shattil, S. and Klemke, R. 2010. Visualizing extravasation dynamics of metastatic tumor cells. *Journal of cell science*. **123**(Pt 13), pp.2332–41.
- Strilic, B. and Offermanns, S. 2017. Intravascular Survival and Extravasation of Tumor Cells. *Cancer Cell*. **32**(3), pp.282–293.
- Strilic, B., Yang, L., Albarrán-Juárez, J., Wachsmuth, L., Han, K., Müller, U.C.,

- Pasparakis, M. and Offermanns, S. 2016. Tumour-cell-induced endothelial cell necroptosis via death receptor 6 promotes metastasis. *Nature*. **536**(7615), pp.215–218.
- Suh, Y.H., Shin, Y.K., Kook, M.-C., Oh, K.I., Park, W.S., Kim, S.H., Lee, I.-S., Park, H.J., Huh, T.-L. and Park, S.H. 2003. Cloning, genomic organization, alternative transcripts and expression analysis of CD99L2, a novel paralog of human CD99, and identification of evolutionary conserved motifs. *Gene*. **307**, pp.63–76.
- Sullivan, D.P., Seidman, M.A. and Muller, W.A. 2013. Poliovirus receptor (CD155) regulates a step in transendothelial migration between PECAM and CD99. *The American journal of pathology*. **182**(3), pp.1031–42.
- Tabernero, J. 2007. The role of VEGF and EGFR inhibition: implications for combining anti-VEGF and anti-EGFR agents. *Molecular cancer research : MCR*. **5**(3), pp.203–20.
- Tabouret, E., Chinot, O., Metellus, P., Tallet, A., Viens, P. and Gonçalves, A. 2012. Recent trends in epidemiology of brain metastases: an overview. *Anticancer research*. **32**(11), pp.4655–62.
- Taddei, A., Giampietro, C., Conti, A., Orsenigo, F., Breviario, F., Pirazzoli, V., Potente, M., Daly, C., Dimmeler, S. and Dejana, E. 2008. Endothelial adherens junctions control tight junctions by VE-cadherin-mediated upregulation of claudin-5. *Nature Cell Biology*. **10**(8), pp.923–934.
- Takabe, W., Alberts-Grill, N. and Jo, H. 2011. Disturbed flow: p53 SUMOylation in the turnover of endothelial cells. *The Journal of cell biology*. **193**(5), pp.805–7.
- Takahashi, K., Nakanishi, H., Miyahara, M., Mandai, K., Satoh, K., Satoh, A., Nishioka, H., Aoki, J., Nomoto, A., Mizoguchi, A. and Takai, Y. 1999. Nectin/PRR: an immunoglobulin-like cell adhesion molecule recruited to cadherin-based adherens junctions through interaction with Afadin, a PDZ domain-containing protein. *The Journal of cell biology*. **145**(3), pp.539–49.
- Talmadge, J.E., Meyers, K.M., Prieur, D.J. and Starkey, J.R. 1980. Role of NK cells in tumour growth and metastasis in beige mice. *Nature*. **284**(5757), pp.622–4.
- Tampaki, E.C., Tampakis, A., Nonni, A., Kontzoglou, K., Patsouris, E. and Kouraklis, G. 2017. Nestin and cluster of differentiation 146 expression in breast cancer: Predicting early recurrence by targeting metastasis? *Tumor Biology*. **39**(3), p.101042831769118.
- Tarin, D., Price, J.E., Kettlewell, M.G., Souter, R.G., Vass, A.C. and Crossley, B. 1984. Mechanisms of human tumor metastasis studied in patients with peritoneovenous shunts. *Cancer research*. **44**(8), pp.3584–92.
- Thiery, J.P. 2002. Epithelial–mesenchymal transitions in tumour progression. *Nature Reviews Cancer*. **2**(6), pp.442–454.
- Thiery, J.P., Acloque, H., Huang, R.Y.J. and Nieto, M.A. 2009. Epithelial-Mesenchymal Transitions in Development and Disease. *Cell*. **139**(5), pp.871–890.
- Tichet, M., Prod'Homme, V., Fenouille, N., Ambrosetti, D., Mallavialle, A., Cerezo, M., Ohanna, M., Audebert, S., Rocchi, S., Giaccherio, D., Boukari, F., Allegra, M., Chambard, J.-C., Lacour, J.-P., Michiels, J.-F., Borg, J.-P., Deckert, M. and Tartare-Deckert, S. 2015. Tumour-derived SPARC drives vascular permeability and extravasation through endothelial VCAM1 signalling to promote metastasis. *Nature Communications*. **6**(1), p.6993.
- Tischer, E., Mitchell, R., Hartman, T., Silva, M., Gospodarowicz, D., Fiddes, J.C. and Abraham, J.A. 1991. The human gene for vascular endothelial growth factor. Multiple protein forms are encoded through alternative exon splicing. *The Journal of biological chemistry*. **266**(18), pp.11947–54.
- Torzicky, M., Viznerova, P., Richter, S., Strobl, H., Scheinecker, C., Foedinger, D. and Riedl, E. 2012. Platelet Endothelial Cell Adhesion Molecule-1 (PECAM-1/CD31) and CD99 Are Critical in Lymphatic Transmigration of Human Dendritic Cells. *Journal of Investigative Dermatology*. **132**(4), pp.1149–1157.

- Tremblay, P.-L., Auger, F.A. and Huot, J. 2006. Regulation of transendothelial migration of colon cancer cells by E-selectin-mediated activation of p38 and ERK MAP kinases. *Oncogene*. **25**(50), pp.6563–6573.
- Tremmel, M., Matzke, A., Albrecht, I., Laib, A.M., Olaku, V., Ballmer-Hofer, K., Christofori, G., Héroult, M., Augustin, H.G., Ponta, H. and Orian-Rousseau, V. 2009. A CD44v6 peptide reveals a role of CD44 in VEGFR-2 signaling and angiogenesis. *Blood*. **114**(25), pp.5236–44.
- Tsai, J.H., Donaher, J.L., Murphy, D.A., Chau, S. and Yang, J. 2012. Spatiotemporal Regulation of Epithelial-Mesenchymal Transition Is Essential for Squamous Cell Carcinoma Metastasis. *Cancer Cell*. **22**(6), pp.725–736.
- Tsukada, Y., Fouad, A., Pickren, J.W. and Lane, W.W. 1983. Central nervous system metastasis from breast carcinoma autopsy study. *Cancer*. **52**(12), pp.2349–2354.
- Tsukita, S., Furuse, M. and Itoh, M. 2001. Multifunctional strands in tight junctions. *Nature Reviews Molecular Cell Biology*. **2**(4), pp.285–293.
- Tu, T., Gao, Q., Luo, Y., Chen, J., Lu, D., Feng, J., Yang, D., Song, L. and Yan, X. 2013. CD146 deletion in the nervous system impairs appetite, locomotor activity and spatial learning in mice. *PLoS one*. **8**(9), p.e74124.
- Tzima, E., Irani-Tehrani, M., Kiosses, W.B., Dejana, E., Schultz, D.A., Engelhardt, B., Cao, G., DeLisser, H. and Schwartz, M.A. 2005. A mechanosensory complex that mediates the endothelial cell response to fluid shear stress. *Nature*. **437**(7057), pp.426–431.
- Ubil, E., Duan, J., Pillai, I.C.L., Rosa-Garrido, M., Wu, Y., Bargiacchi, F., Lu, Y., Stanbouly, S., Huang, J., Rojas, M., Vondriska, T.M., Stefani, E. and Deb, A. 2014. Mesenchymal–endothelial transition contributes to cardiac neovascularization. *Nature*. **514**(7524), pp.585–590.
- Urias, Ú., Marie, S.K.N., Uno, M., da Silva, R., Evagelinellis, M.M., Caballero, O.L., Stevenson, B.J., Silva, W.A., Simpson, A.J. and Oba-Shinjo, S.M. 2014. CD99 is upregulated in placenta and astrocytomas with a differential subcellular distribution according to the malignancy stage. *Journal of Neuro-Oncology*. **119**(1), pp.59–70.
- Vajkoczy, P., Laschinger, M. and Engelhardt, B. 2001.  $\alpha$ 4-integrin-VCAM-1 binding mediates G protein-independent capture of encephalitogenic T cell blasts to CNS white matter microvessels. *Journal of Clinical Investigation*. **108**(4), pp.557–565.
- De Val, S. and Black, B.L. 2009. Transcriptional control of endothelial cell development. *Developmental cell*. **16**(2), pp.180–95.
- Valastyan, S. and Weinberg, R.A. 2011. Tumor Metastasis: Molecular Insights and Evolving Paradigms. *Cell*. **147**(2), pp.275–292.
- Vanlandewijck, M., He, L., Mäe, M.A., Andrae, J., Ando, K., Del Gaudio, F., Nahar, K., Lebouvier, T., Laviña, B., Gouveia, L., Sun, Y., Raschperger, E., Räsänen, M., Zarb, Y., Mochizuki, N., Keller, A., Lendahl, U. and Betsholtz, C. 2018. A molecular atlas of cell types and zonation in the brain vasculature. *Nature*. **554**(7693), pp.475–480.
- Vetter, I.R. and Wittinghofer, A. 2001. The Guanine Nucleotide-Binding Switch in Three Dimensions. *Science*. **294**(5545), pp.1299–1304.
- Voura, E.B., Chen, N. and Siu, C.H. 2000. Platelet-endothelial cell adhesion molecule-1 (CD31) redistributes from the endothelial junction and is not required for the transendothelial migration of melanoma cells. *Clinical & experimental metastasis*. **18**(6), pp.527–32.
- Vousden, K.H. 2002. Activation of the p53 tumor suppressor protein. *Biochimica et biophysica acta*. **1602**(1), pp.47–59.
- Waltenberger, J., Mayr, U., Pentz, S. and Hombach, V. 1996. Functional upregulation of the vascular endothelial growth factor receptor KDR by hypoxia. *Circulation*. **94**(7), pp.1647–54.
- Wang, D., Müller, S., Amin, A.R.M.R., Huang, D., Su, L., Hu, Z., Rahman, M.A.,

- Nannapaneni, S., Koenig, L., Chen, Z., Tighiouart, M., Shin, D.M. and Chen, Z.G. 2012. The pivotal role of integrin  $\beta 1$  in metastasis of head and neck squamous cell carcinoma. *Clinical cancer research : an official journal of the American Association for Cancer Research*. **18**(17), pp.4589–99.
- Wang, W., Goswami, S., Sahai, E., Wyckoff, J.B., Segall, J.E. and Condeelis, J.S. 2005. Tumor cells caught in the act of invading: their strategy for enhanced cell motility. *Trends in Cell Biology*. **15**(3), pp.138–145.
- Watanabe, H., Ishibashi, K., Mano, H., Kitamoto, S., Sato, N., Hoshiba, K., Kato, M., Matsuzawa, F., Takeuchi, Y., Shirai, T., Ishikawa, S., Morioka, Y., Imagawa, T., Sakaguchi, K., Yonezawa, S., Kon, S. and Fujita, Y. 2018. Mutant p53-Expressing Cells Undergo Necroptosis via Cell Competition with the Neighboring Normal Epithelial Cells. *Cell Reports*. **23**(13), pp.3721–3729.
- Watson, R.L., Buck, J., Levin, L.R., Winger, R.C., Wang, J., Arase, H. and Muller, W.A. 2015. Endothelial CD99 signals through soluble adenylyl cyclase and PKA to regulate leukocyte transendothelial migration. *The Journal of experimental medicine*. **212**(7), pp.1021–41.
- Weber, M.R., Zuka, M., Loriger, M., Tschan, M., Torbett, B.E., Zijlstra, A., Quigley, J.P., Staffin, K., Eliceiri, B.P., Krueger, J.S., Marchese, P., Ruggeri, Z.M. and Felding, B.H. 2016. Activated tumor cell integrin  $\alpha \beta 3$  cooperates with platelets to promote extravasation and metastasis from the blood stream. *Thrombosis research*. **140 Suppl 1**(Suppl 1), pp.S27-36.
- Weis, S., Cui, J., Barnes, L. and Cheresch, D. 2004. Endothelial barrier disruption by VEGF-mediated Src activity potentiates tumor cell extravasation and metastasis. *The Journal of cell biology*. **167**(2), pp.223–9.
- Weiss, L. 1992. Biomechanical interactions of cancer cells with the microvasculature during hematogenous metastasis. *Cancer metastasis reviews*. **11**(3–4), pp.227–35.
- Weksler, B., Romero, I.A. and Couraud, P.-O. 2013. The hCMEC/D3 cell line as a model of the human blood brain barrier. *Fluids and barriers of the CNS*. **10**(1), p.16.
- Weksler, B.B., Subileau, E.A., Perrière, N., Charneau, P., Holloway, K., Leveque, M., Tricoire-Leignel, H., Nicotra, A., Bourdoulous, S., Turowski, P., Male, D.K., Roux, F., Greenwood, J., Romero, I.A. and Couraud, P.O. 2005. Blood-brain barrier-specific properties of a human adult brain endothelial cell line. *The FASEB Journal*. **19**(13), pp.1872–1874.
- van Wetering, S., van den Berk, N., van Buul, J.D., Mul, F.P.J., Lommerse, I., Mous, R., Klooster, J.-P. ten, Zwaginga, J.-J. and Hordijk, P.L. 2003. VCAM-1-mediated Rac signaling controls endothelial cell-cell contacts and leukocyte transmigration. *American Journal of Physiology-Cell Physiology*. **285**(2), pp.C343–C352.
- Whitaker, G.B., Limberg, B.J. and Rosenbaum, J.S. 2001. Vascular Endothelial Growth Factor Receptor-2 and Neuropilin-1 Form a Receptor Complex That Is Responsible for the Differential Signaling Potency of VEGF<sub>165</sub> and VEGF<sub>121</sub>. *Journal of Biological Chemistry*. **276**(27), pp.25520–25531.
- White, R. (Macmillan C.S. n.d. [https://www.macmillan.org.uk/\\_images/exploring-healthcare-cost-implications-cancer-stage\\_tcm9-307202.pdf](https://www.macmillan.org.uk/_images/exploring-healthcare-cost-implications-cancer-stage_tcm9-307202.pdf)).
- Wieland, E., Rodriguez-Vita, J., Liebler, S.S., Mogler, C., Moll, I., Herberich, S.E., Espinet, E., Herpel, E., Menuchin, A., Chang-Claude, J., Hoffmeister, M., Gebhardt, C., Brenner, H., Trumpp, A., Siebel, C.W., Hecker, M., Utikal, J., Sprinzak, D. and Fischer, A. 2017. Endothelial Notch1 Activity Facilitates Metastasis. *Cancer cell*. **31**(3), pp.355–367.
- Wilkerson, A.E., Glasgow, M.A. and Hiatt, K.M. 2006. Immunoreactivity of CD99 in invasive malignant melanoma. *Journal of Cutaneous Pathology*. **33**(10), pp.663–666.
- Wolburg, H. and Lippoldt, A. 2002. Tight junctions of the blood-brain barrier: development, composition and regulation. *Vascular pharmacology*. **38**(6),

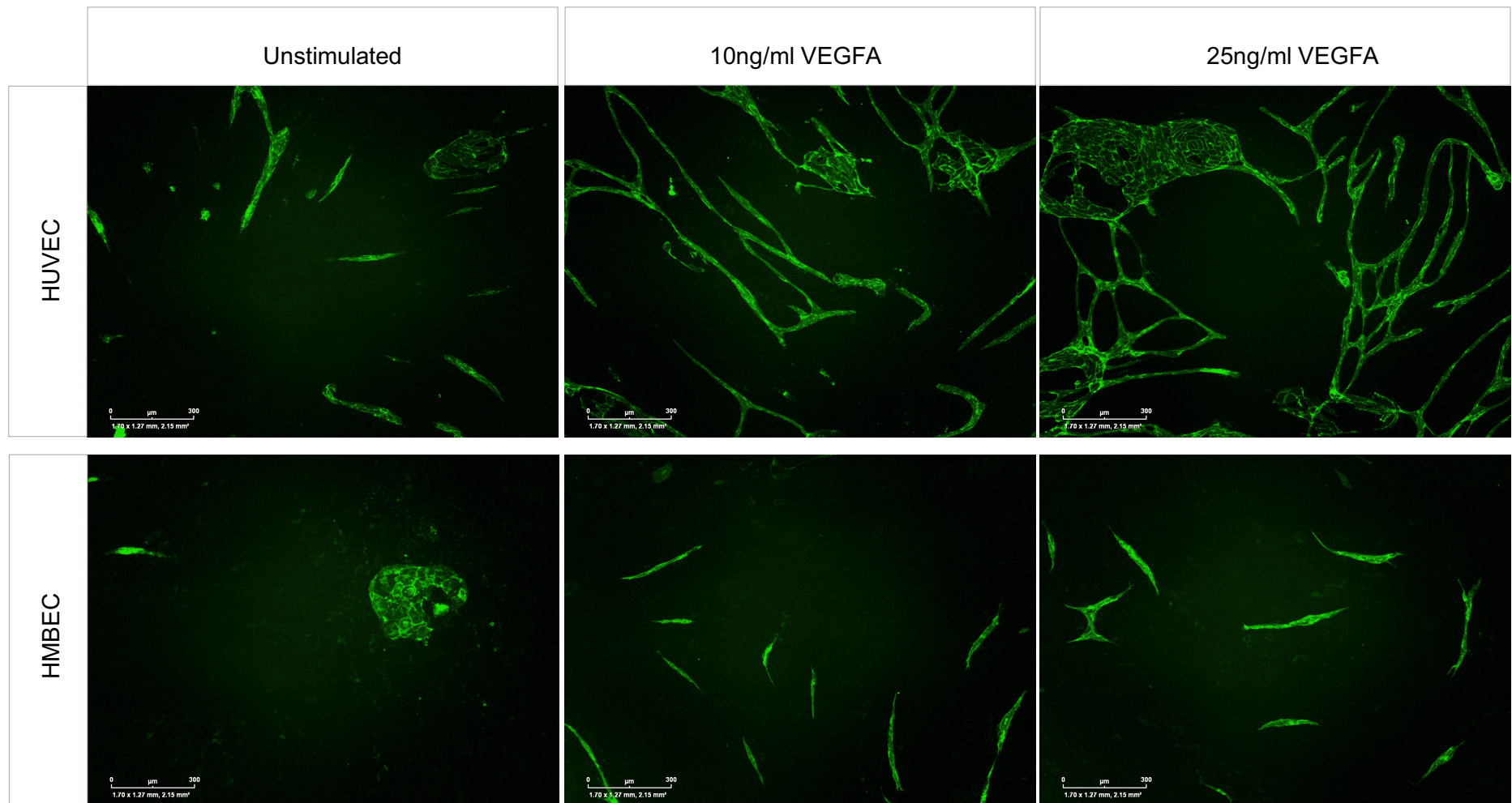
pp.323–37.

- Wolf, M.J., Hoos, A., Bauer, J., Boettcher, S., Knust, M., Weber, A., Simonavicius, N., Schneider, C., Lang, M., Stürzl, M., Croner, R.S., Konrad, A., Manz, M.G., Moch, H., Aguzzi, A., van Loo, G., Pasparakis, M., Prinz, M., Borsig, L. and Heikenwalder, M. 2012. Endothelial CCR2 signaling induced by colon carcinoma cells enables extravasation via the JAK2-Stat5 and p38MAPK pathway. *Cancer cell*. **22**(1), pp.91–105.
- Wu, K., Fukuda, K., Xing, F., Zhang, Y., Sharma, S., Liu, Y., Chan, M.D., Zhou, X., Qasem, S.A., Pochampally, R., Mo, Y.-Y. and Watabe, K. 2015. Roles of the Cyclooxygenase 2 Matrix Metalloproteinase 1 Pathway in Brain Metastasis of Breast Cancer. *Journal of Biological Chemistry*. **290**(15), pp.9842–9854.
- Wu, X., Bayle, J.H., Olson, D. and Levine, A.J. 1993. The p53-mdm-2 autoregulatory feedback loop. *Genes & development*. **7**(7A), pp.1126–32.
- Xie, S., Luca, M., Huang, S., Gutman, M., Reich, R., Johnson, J.P. and Bar-Eli, M. 1997. Expression of MCAM/MUC18 by human melanoma cells leads to increased tumor growth and metastasis. *Cancer research*. **57**(11), pp.2295–303.
- Yang, J., Mani, S.A., Donaher, J.L., Ramaswamy, S., Itzykson, R.A., Come, C., Savagner, P., Gitelman, I., Richardson, A. and Weinberg, R.A. 2004. Twist, a master regulator of morphogenesis, plays an essential role in tumor metastasis. *Cell*. **117**(7), pp.927–39.
- Yilmaz, M. and Christofori, G. 2009. EMT, the cytoskeleton, and cancer cell invasion. *Cancer and Metastasis Reviews*. **28**(1–2), pp.15–33.
- Yoneda, T., Williams, P.J., Hiraga, T., Niewolna, M. and Nishimura, R. 2001. A Bone-Seeking Clone Exhibits Different Biological Properties from the MDA-MB-231 Parental Human Breast Cancer Cells and a Brain-Seeking Clone In Vivo and In Vitro. *Journal of Bone and Mineral Research*. **16**(8), pp.1486–1495.
- Yurchenco, P.D., Cheng, Y.S. and Colognato, H. 1992. Laminin forms an independent network in basement membranes. *The Journal of cell biology*. **117**(5), pp.1119–33.
- Zabouo, G., Imbert, A.-M., Jacquemier, J., Finetti, P., Moreau, T., Esterni, B., Birnbaum, D., Bertucci, F. and Chabannon, C. 2009. CD146 expression is associated with a poor prognosis in human breast tumors and with enhanced motility in breast cancer cell lines. *Breast Cancer Research*. **11**(1), p.R1.
- Zen, K., Liu, D.-Q., Guo, Y.-L., Wang, C., Shan, J., Fang, M., Zhang, C.-Y. and Liu, Y. 2008. CD44v4 Is a Major E-Selectin Ligand that Mediates Breast Cancer Cell Transendothelial Migration J. P. R. O. Orgel, ed. *PLoS ONE*. **3**(3), p.e1826.
- Zeng, G., Cai, S. and Wu, G.-J. 2011. Up-regulation of METCAM/MUC18 promotes motility, invasion, and tumorigenesis of human breast cancer cells. *BMC Cancer*. **11**(1), p.113.
- Zeng, P., Li, H., Lu, P.-H., Zhou, L.-N., Tang, M., Liu, C.-Y. and Chen, M.-B. 2017. Prognostic value of CD146 in solid tumor: A Systematic Review and Meta-analysis. *Scientific Reports*. **7**(1), p.4223.
- Zeng, Q., Li, W., Lu, D., Wu, Z., Duan, H., Luo, Y., Feng, J., Yang, D., Fu, L. and Yan, X. 2012. CD146, an epithelial-mesenchymal transition inducer, is associated with triple-negative breast cancer. *Proceedings of the National Academy of Sciences*. **109**(4), pp.1127–1132.
- Zou, Y., Li, J., Ma, H., Jiang, H., Yuan, J., Gong, H., Liang, Y., Guan, A., Wu, J., Li, L., Zhou, N., Niu, Y., Sun, A., Nakai, A., Wang, P., Takano, H., Komuro, I. and Ge, J. 2011. Heat shock transcription factor 1 protects heart after pressure overload through promoting myocardial angiogenesis in male mice. *Journal of Molecular and Cellular Cardiology*. **51**(5), pp.821–829.
- Zovein, A.C., Luque, A., Turlo, K.A., Hofmann, J.J., Yee, K.M., Becker, M.S., Fassler, R., Mellman, I., Lane, T.F. and Iruela-Arispe, M.L. 2010. Beta1

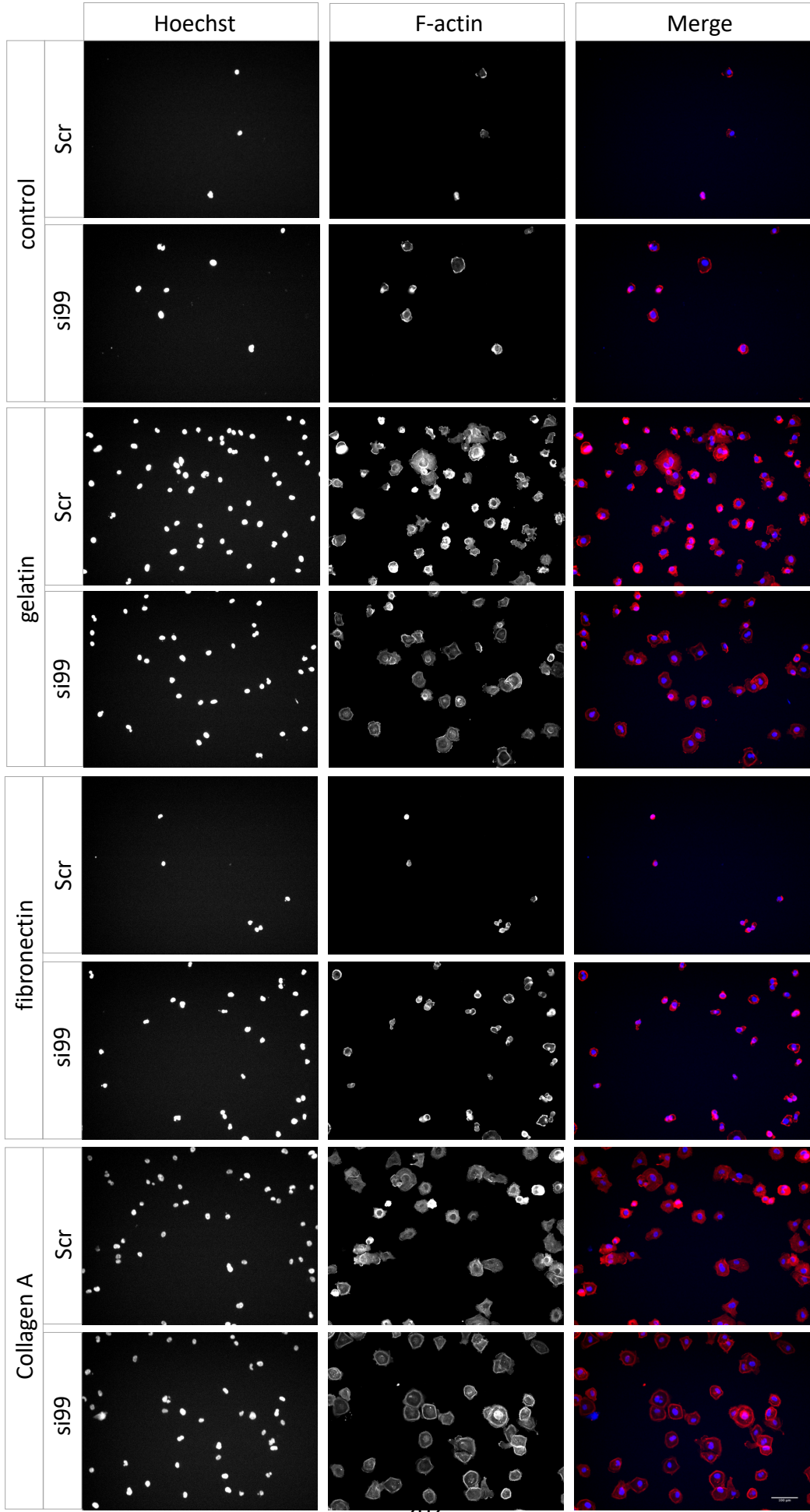
integrin establishes endothelial cell polarity and arteriolar lumen formation via a Par3-dependent mechanism. *Developmental cell*. **18**(1), pp.39–51.

Zucchini, C., Manara, M.C., Pinca, R.S., De Sanctis, P., Guerzoni, C., Sciandra, M., Lollini, P.-L., Cenacchi, G., Picci, P., Valvassori, L. and Scotlandi, K. 2014. CD99 suppresses osteosarcoma cell migration through inhibition of ROCK2 activity. *Oncogene*. **33**(15), pp.1912–1921.

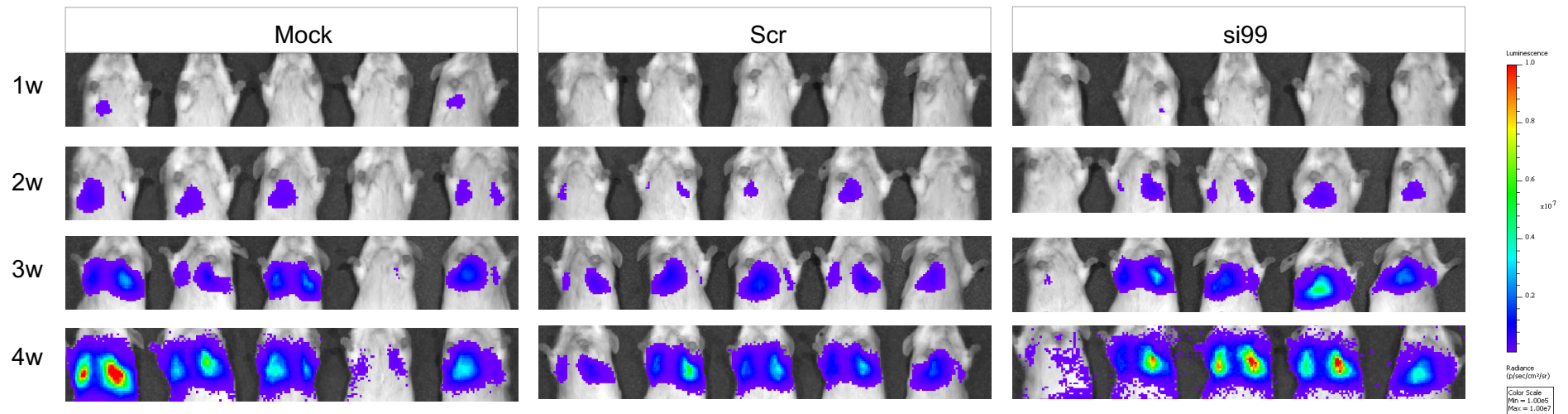
## Appendix



**Appendix. Figure 1. HMBEC exhibit poor angiogenic function. A,** HUVEC and HMBEC cells were grown upon a feeder layer of immortalised human dermal fibroblasts (HDF) for 9 days. Cocultures were supplemented with either control media, or media supplemented with 10 or 25ng/ml VEGFA. Cocultures were subsequently fixed in 4% PFA and stained with anti-CD31 and imaged on an Incucyte microscopy platform. Scale bar: 300µm.



**Appendix. Figure 2. Actin reorganisation upon adhesion to ECM substrates is regulated by CD99.** 72 hours following transfection MDA-231 cells treated with control scrambled or CD99 siRNA were seeded to 96 well plates coated in gelatin, fibronectin and Collagen type 1. After 30 minutes of adhesion, non-adherent cells were washed away with PBS and adherent cells were fixed in 4% PFA. Cells were then permeabilised and stained for F-actin and nuclear stain with Hoechst and imaged used high content Perkin Elmer Operetta microscope. Scale bar: 100µm.



**Appendix. Figure . CD99 suppresses metastatic dissemination of breast cancer in vivo.** Luciferase expressing MDA-231 cells were transfected with scramble control or CD99 siRNA or Mock treatment for 72h before tail-vein injection of  $5 \times 10^5$  cells. BLI was performed weekly to monitor metastatic burden within the lungs and mice were culled at week 4 before symptoms were shown in mice.

